

School of Civil and Mechanical Engineering

**Development of Recycled tyre-bale and Recycled tyre Crumb Sandwich
Panels**

Abdul Basir Awan

**This thesis is presented for the Degree of
Doctor of Philosophy
of
Curtin University**

April 2022

Declaration

To the best of my knowledge and belief, this thesis contains no material previously published by any other person except where due acknowledgement has been made.

This thesis contains no material which has been accepted for the award of any other degree or diploma in any university.

Signature: (Abdul Basir Awan)

Date: 28/04/2022

Copyright

I warrant that I have obtained, where necessary, permission from the copyright owners to use any third-party copyright material reproduced in the thesis (e.g., questionnaires, artwork, unpublished letters), or to use any of my own published work (e.g., journal articles) in which the copyright is held by another party (e.g., publisher, co-authors).

Signature: (Abdul Basir Awan)

Date: 28/04/2022

Dedication

I would like to dedicate my thesis to my parents for their incredible support, constant prayers and endless love!

To my beloved wife and both sons!

To my all siblings!

ABSTRACT

A standard tyre has a life cycle of around four years and each year billions of tyres complete their designed service life across the globe. Thus, used tyres pile up rapidly in a short period of time. Generally, these tyres are disposed of in numerous ways such as dumping in landfill, stockpiling, retreading, and for fuel and energy extraction purposes. Lack of appropriate disposal practices usually lead to several environmental risks like leaching of toxic chemicals, fire and ideal sites for the growth of vermin and insects. In addition, they are source of greenhouse gasses emissions when consumed by burning. Due to massive volume of waste tyres around the world, it is critical to look for practical alternatives to reuse/recycle waste tyres. In civil engineering, the waste tyres are usually recycled as a modifier in asphalt mix or as a replacement of coarse or fine aggregate in concrete mixture. At present, the percentage of recycling waste tyres is negligible. Therefore, this research adopted a novel idea of recycling waste tyres in precast concrete sandwich panels as core material. The research investigated the use of waste tyres in two distinct ways; (a) recycled tyre-bale sandwich panels and (b) recycled tyre crumb sandwich panels.

In first phase of this research, a recycled tyre-bale consisted of minimum hundred used tyres is manufactured as per British Standards Institution PAS108:2007 specifications and used as core in precast concrete sandwich panels. This phase of research was based on a series of laboratory experiments and finite element numerical simulations to study the structural response of recycled tyre sandwich panel. The sandwich walls consisted of 650mm thick recycled tyre-bale as core and sandwiched between two 125mm thick reinforced concrete walls. The structural response was evaluated by externally applying different types of static loads such as compression, flexural bending and punching shear. Subsequently, finite element-based 3D numerical models were developed in ABAQUS and validated against experimental results to analyse the ultimate structural capacities and to predict the concrete damage.

In the second phase of this research, a newly proposed recycled tyre crumb sandwich panels (CRSPs) were developed. This panel consisted of two 40 mm thick reinforced concrete wythes and a 20 mm thick recycled tyre crumb core. The comparative assessment was conducted against two other precast concrete panels namely precast solid concrete panel (SCP) and polystyrene sandwich panel (FSP) in terms of deflections (vertical and out-of-plane displacements), strain variations, critical failure load and concrete damage behaviour. The

investigations included a series of laboratory experiments and finite element numerical simulations to investigate the structural response and to capture the associated damage in the concrete wythes. The research mainly focussed on flexural bending, impact resistance and concrete crushing under compression. Furthermore, the numerical models were developed in ABAQUS and validated against test results. In the end, it was found that recycled tyre crumb sandwich panel showed significant resistance against flexural bending, compression and impact loading. In flexural bending, partial composite behaviour was observed in all sandwich panels and the average flexural strength of CRSP was 6.54% higher than the FSP. In this case, the failure was governed by flexural cracks. In uni-axial compression, crumb rubber panel resisted 93% of the average ultimate axial load of SCP, where the failure was governed by the crushing of concrete due to low slenderness ratio. Similarly, the use of crumb rubber as a core material decreased the midspan deflection by 78% and 44% when compared to SCP and FSP against impact load. Also, the concrete damage in all sandwich panels was less severe than the SCP. Therefore, the proposed panel can be employed as a structural and non-structural member in the construction projects. The effect of using steel fibres as alternative reinforcement to the structural behaviour of recycled tyre crumb sandwich panel was also evaluated and benchmarked with that containing traditional steel mesh reinforcement. Similar behaviour in terms of concrete failure at ultimate load, deflection and strain variations was also observed between the two reinforcing types.

ACKNOWLEDGEMENTS

My amazing journey to pursue PhD kicked off in the end of year 2018, which unfolded an amazing chapter of my life beholding memories, challenges, success and celebrations. I am extremely thankful to Almighty Allah for giving me the incredible vigour to achieve this imperative milestone in my life. I also want to express my utmost gratitude for everyone who contributed towards my Ph.D., wholeheartedly in any provided capacity.

I would like to express my sincere gratitude to all the thesis committee members; Dr. Abhijit Mukherjee, Dr. Faiz Shaikh, Dr. Prabir Sarker and Dr. Wensu Chen for their advice and incessant support throughout the journey. First and foremost, my utmost gratitude to my thesis supervisor Professor Faiz Shaikh for providing me with a fantastic opportunity to work on this research project. Dr. Faiz started his guidance since the day I received my confirmation of enrolment and scholarship offer letter, his assistance continued and proved to be a beacon light directing my Ph.D. During my PhD tenure, I found him extremely humble, compassionate, and kind. My dream of pursuing PhD could not have been possible without his indefatigable support. I have never felt stressed out on any single occasion. This was only possible due to my supervisor support and advice. He has always been available and responded promptly to my queries. Today, I can proudly say that I learnt a lot from his professional skills and strong academic knowledge. I am appreciative for his precious time to review the draft manuscripts before submission to the scientific journals. My acknowledgements to the anonymous reviewers for their positive feedbacks and recommendations to improve the quality of the research work which is now part of the thesis.

I am thankful to Dr. Abhijit Mukherjee and Dr. Prabir Sarker, Dr. Wensu Chen for providing positive feedback and suggestions during the milestones. I would like to express my appreciation to Dr. Xihong and Chong Chen for their support and guidance during the impact testing. I am incredibly thankful to Dr. Mussad Zahir Khan for introducing me to my thesis supervisor, encouraging me to pursue PhD and he also supported me in settling down in Australia during my early days. His continuing support and help are ineffable.

I am grateful to the Tyre Stewardship Australia for supporting this research project through award/grant number CRT-10757. I take this opportunity to acknowledge Curtin University, Australia for offering me the financial support through Curtin International Postgraduate Research Scholarship and Research Stipend Scholarship to pursue Ph.D. degree.

I would also like to extend a heartfelt thanks to technical operations coordinator Mr. Mark Whittaker in reviewing the associated risk assessment and coordinating the test setups at multiple occasions. Exclusive acknowledgement is extended to all the lab technicians in Civil Engineering Laboratory including Mr. Kevin Reilly, Mr. Ashely Hughes, Mr. Darren Isaac, Mr. Leon Forgas, Mr. Gary Woodward and Dr. Arnie Bredin for their assistance in preparing, casting and testing of the panels. I am indebted to Ms. Cheryl Cheng for helping me in procuring the strain gauges and other relevant material.

Ultimately, a big shout out to my lovely family including my mother, father, siblings for their relentless inspiration and affection during this time. I would like to express my supreme appreciation towards the love of my life, Amna Ayub for sacrificing her dream job and traveling to Australia to support me in my studies and offering continual motivation to complete my Ph.D. in time. Without her sacrifices, this journey would have been impossible. I also wish to express my sincere love for my little angles, Arshmaan Awan and Suleiman Awan, who are true blessings without them it would have been very hard to survive through pandemic.

LIST OF PUBLICATIONS AND WORK PREPARED FOR PUBLICATION

The list of published papers and work prepared for publication, with the full bibliographic citations in the order they appear in the thesis, are listed below.

Chapter 2

Awan, Abdul & Shaikh, Faiz (2020). Structural behaviour of tyre-bale sandwich wall under axial load. Structures, 31, 792-804. DOI: <https://doi.org/10.1016/j.istruc.2021.02.037>.

Chapter 3

Awan, Abdul & Shaikh, Faiz (2021). Experimental and numerical study on structural behaviour of tyre-bale sandwich wall under different loading conditions. Australian Journal of Structural Engineering, 22(4), 299-316. DOI: <https://doi.org/10.1080/13287982.2021.1970699>

Chapter 4

Awan, Abdul & Shaikh, Faiz (2021). Structural behaviour of recycled tire crumb rubber sandwich panel in flexural bending. Structural Concrete, 22(6), 3602-3619. DOI: <https://doi.org/10.1002/suco.202100356>

Chapter 5

Awan, Abdul & Shaikh, Faiz (2021). Compressive behaviour of precast concrete sandwich panels containing recycled tyre crumb rubber core. Structural Concrete. DOI: <https://doi.org/10.1002/suco.202100470>

LIST OF ADDITIONAL PUBLICATION

Awan, Abdul & Shaikh, Faiz (2022). Numerical simulation of structural behaviour of tyre-bale sandwich wall at elevated temperatures. (*under review*)

Authorship Attribution

Paper 1 “Structural behaviour of tyre-bale sandwich wall under axial load”

The contribution of authors is listed below:

	Conception and Design	Testing including Setup and Instrumentation	Analysis and Discussion	Finite Element Modeling	Manuscript
Author 1 Abdul Basir Awan	80%	80%	80%	80%	80%
<p>Author 1 Acknowledgement.</p> <p>I acknowledge that these represent my contribution to the above research output, and I have approved the final version.</p>					
Author 2 Faiz Shaikh	20%	20%	20%	20%	20%
<p>Author 2 Acknowledgement.</p> <p>I acknowledge that these represent my contribution to the above research output, and I have approved the final version.</p>					
<p>Note: Co-Author Faiz Shaikh was responsible for funding.</p>					

Authorship Attribution

Paper 2 “Experimental and numerical study on structural behaviour of tyre-bale sandwich wall under different loading conditions”

The contribution of authors is listed below:

	Conception and Design	Testing including Setup and Instrumentation	Analysis and Discussion	Finite Element Modeling	Manuscript
Author 1 Abdul Basir Awan	80%	80%	80%	80%	80%
<p>Author 1 Acknowledgement.</p> <p>I acknowledge that these represent my contribution to the above research output, and I have approved the final version.</p>					
Author 2 Faiz Shaikh	20%	20%	20%	20%	20%
<p>Author 2 Acknowledgement.</p> <p>I acknowledge that these represent my contribution to the above research output, and I have approved the final version.</p>					
<p>Note: Co-Author Faiz Shaikh was responsible for funding.</p>					

Authorship Attribution

Paper 3 “Structural behaviour of recycled tire crumb rubber sandwich panel in flexural bending”

The contribution of authors is listed below:

	Conception and Design	Testing including Setup and Instrumentation	Analysis and Discussion	Finite Element Modeling	Manuscript
Author 1 Abdul Basir Awan	80%	80%	80%	80%	80%
Author 1 Acknowledgement. I acknowledge that these represent my contribution to the above research output, and I have approved the final version.					
Author 2 Faiz Shaikh	20%	20%	20%	20%	20%
Author 2 Acknowledgement. I acknowledge that these represent my contribution to the above research output, and I have approved the final version.					
Note: Co-Author Faiz Shaikh was responsible for funding.					

Authorship Attribution

Paper 4 “Compressive behaviour of precast concrete sandwich panels containing recycled tyre crumb rubber core”

The contribution of authors is listed below:

	Conception and Design	Testing including Setup and Instrumentation	Analysis and Discussion	Finite Element Modeling	Manuscript
Author 1 Abdul Basir Awan	80%	80%	80%	80%	80%
<p>Author 1 Acknowledgement.</p> <p>I acknowledge that these represent my contribution to the above research output, and I have approved the final version.</p>					
Author 2 Faiz Shaikh	20%	20%	20%	20%	20%
<p>Author 2 Acknowledgement.</p> <p>I acknowledge that these represent my contribution to the above research output, and I have approved the final version.</p>					
<p>Note: Co-Author Faiz Shaikh was responsible for funding.</p>					

STATEMENT OF CONTRIBUTION OF CO-AUTHOR

Assoc. Prof. Faiz Shaikh primarily conceived the idea of this research project. As a principal investigator, Prof. Faiz Shaikh guided thoroughly in identifying the research scope and objectives. The research works reported in this thesis were primarily conducted by the first author (Abdul Basir Awan) including the literature review, design of test setups, instrumentation, casting of all panels, performing the laboratory experiments, interpretation and analysis of results, development of finite element models and writing the manuscripts. In addition, Prof. Faiz Shaikh provided continuous finances through Tyre Stewardship Australia, Grant/ Award number: CRT-10757 for performing all the experimental tests in structure lab at Curtin University. Also, Prof. Faiz Shaikh provided additional financial support for the purchase of sensors, load spreader, rolling pins and construction material for recycled tyre crumb sandwich panels. Lomwest enterprise Pty Ltd. provided recycled tyre-bale sandwich concrete panels in this study. Based on the experimental findings, the manuscripts were written by the first author (Abdul Basir Awan) which were later reviewed and edited by the co-author (Prof. Faiz Shaikh) before submission to the journals.

Chapter 6

The author (Abdul Basir Awan) designed the test setup for the experimental study in thorough discussion with Prof. Faiz Shaikh and Prof. Xihong Zhang. The candidate performed the low-velocity impact test under the supervision of Prof Xihong Zhang. Chong Chen assisted in conducting the test and collecting the data. The first author (Abdul Basir Awan) analysed the results and wrote the manuscript which was later reviewed by Prof. Faiz Shaikh.

Table of Contents

CHAPTER 1 INTRODUCTION AND LITERATURE REVIEW	1
1.1 Research Background.....	1
1.2 Civil Engineering Applications of Waste Tyres	3
1.3 Problem Statement and Research Significance	6
1.3.1 Recycled tyre-bale sandwich panel.....	6
1.3.2 Recycled tyre crumb sandwich panel	7
1.4 Objectives and Scope of the Research	7
1.5 Thesis Outline and Structure	8
1.6 References	11
CHAPTER 2 STRUCTURAL BEHAVIOUR OF TYRE-BALE SANDWICH WALL UNDER AXIAL LOAD	15
2.1 Abstract	15
2.2 Introduction	15
2.3 State-of-the-art	16
2.4 Experimental program.....	17
2.4.1 Test scenarios.....	17
2.4.2 Manufacturing of tyre-bale	17
2.4.3 Casting of tyre-bale sandwich wall.....	20
2.4.4 Instrumentation.....	21
2.4.5 Test setup.....	22
2.5 Finite element modelling.....	23
2.5.1 Material modelling	23
2.5.2 Assembly of parts and interaction.....	24
2.5.3 Loading and boundary conditions.....	24
2.6 Results and discussion.....	25
2.6.1 Ultimate load capacity and load vs vertical deflection behaviour	25
2.6.2 Load vs lateral deflection behaviour	27
2.6.3 Strain Variations.....	30
2.6.4 Failure mode and cracking pattern.....	31
2.7 Finite element analysis (FEA) results	33
2.8 Theoretical load capacity of walls.....	34
2.9 Conclusion.....	36
2.10 References	38

CHAPTER 3 EXPERIMENTAL AND NUMERICAL STUDY ON STRUCTURAL BEHAVIOUR OF TYRE-BALE SANDWICH WALL UNDER DIFFERENT LOADING CONDITIONS.....40

3.1 Abstract40

3.2 Introduction40

3.3 Experimental program.....42

 3.3.1 Tyre-bale manufacturing and construction phase43

 3.3.2 Instrumentation.....45

 3.3.3 Test setup.....47

3.4 Results and discussion.....48

 3.4.1 Experimental results 48

 3.4.2 Compressibility in tyre-bale.....48

 3.4.3 Concrete Damage and cracks formation51

 3.4.4 Vertical deflection.....52

 3.4.5 Strain variations.....55

 3.4.6 Assessment of composite behaviour56

3.5 Numerical analysis57

 3.5.1 Finite element modeling of tyre-bale sandwich wall.....57

 3.5.2 Finite element analysis.....59

 3.5.3 Validation of material model59

 3.5.4 Validation of load and boundary conditions61

 3.5.5 Punching shear strength and failure mechanism.....62

3.6 Flexural strength prediction using yield line theory.....64

3.7 Conclusion.....66

3.8 References68

CHPATER 4 STRUCTURAL BEHAVIOUR OF RECYCLE TYRE CRUMB RUBBER SANDWICH PANEL IN FLEXURAL BENDING70

4.1 Abstract70

4.2 Introduction70

4.3 Experimental Program.....73

 4.3.1 Material Properties76

 4.3.2 Formwork and Panel Casting.....80

 4.3.3 Instrumentation.....81

 4.3.4 Test setup.....81

4.4 Results and discussion.....83

 4.4.1 Load-deflection at mid-span (LD-4).....83

4.4.2	Strain distribution.....	85
4.4.3	Composite behaviour of sandwich panels.....	88
4.4.4	Formation of cracks.....	91
	92
4.5	Finite Element Analysis	92
4.5.1	Material Properties.....	92
4.5.2	Assembly and Interaction properties	93
4.5.3	Loading and boundary conditions.....	94
4.5.4	Validation of model.....	95
4.5.5	FE Analysis Discussion	95
4.6	Conclusion.....	97
4.7	Reference.....	99

CHAPTER 5 COMPRESSIVE BEHAVIOUR OF PRECAST CONCRETE SANDWICH PANELS CONTAINING RECYCLED TYRE CRUMB CORE.....102

5.1	Abstract	102
5.2	Introduction	102
5.3	Experimental work	104
5.3.1	Geometric details of specimen.....	104
5.3.2	Casting of specimen.....	107
5.3.3	Material properties.....	108
5.3.4	Instrumentation.....	112
5.3.5	Assembly of test setup	114
5.4	Results and discussion.....	115
5.4.1	Load – deflection behaviour	115
5.4.2	Lateral displacement.....	116
5.4.3	Strain distribution in PCSPs.....	118
5.4.4	Concrete damage pattern.....	121
5.5	Finite Element Analysis (FEA).....	123
5.5.1	Material properties.....	123
5.5.2	Assembly method and interaction techniques.....	126
5.5.3	Model constraints.....	126
5.5.4	Validation of FE model.....	126
5.5.5	Discussion on FE model	127
5.6	Design axial capacity of precast concrete panels	129
5.7	Conclusions	131

5.8	References	132
CHAPTER 6 BEHAVIOUR OF RECYCLED TYRE CRUMB SANDWICH PANEL UNDER LOW-VELOCITY IMPACT TEST		
135		
6.1	Abstract	135
6.2	Introduction	135
6.3	Research Significance	136
6.4	Experimental Program.....	137
6.4.1	Specimen and geometric details.....	137
6.4.2	Material details.....	138
6.4.3	Test setup.....	140
6.4.4	Instrumentation.....	141
6.5	Results and discussion.....	142
6.5.1	Impact force and deflection time-history.....	142
6.5.2	Strain time-history variation	144
6.5.3	Impact energy.....	146
6.5.4	Damage behaviour.....	146
6.6	Conclusion.....	150
6.7	References	152
CHAPTER 7 STRUCTURAL BEHAVIOUR OF STEEL FIBRES REINFORCED CONCRETE SANDWICH PANEL CONTAINING RECYCLED TYRE CRUMB CORE UNDER DIFFERENT LOADINGS		
154		
7.1	Abstract	154
7.2	Introduction	154
7.3	Experimental Program.....	156
7.3.1	Geometric properties.....	156
7.3.2	Material properties.....	157
7.3.3	Specimen casting.....	159
7.4	Flexural bending.....	160
7.4.1	Test setup.....	160
7.4.2	Instrumentation.....	161
7.5	Uni-axial compression test.....	161
7.5.1	Test setup.....	161
7.5.2	Instrumentation.....	162
7.6	Results and discussions	163
7.6.1	Flexural bending - load-deflection behaviour.....	163
7.6.2	Strain distribution.....	165

7.6.3	Failure mode.....	166
7.6.4	Degree of composite action	167
7.7	Uni-axial compression.....	168
7.7.1	Load deflection behaviour	168
7.7.2	Out-of-plane displacement.....	169
7.7.3	Strain distribution.....	170
7.7.4	Failure mode.....	171
7.8	Conclusion.....	172
7.9	Reference.....	174
8.	CHAPTER 8 CONCLUSIONS AND RECOMMENDATIONS	177
8.1	Summary	177
8.2	Recycled tyre-bale sandwich panels	177
8.3	Recycled tyre crumb sandwich panels	178
8.4	Recommendation for Future Work	180

LIST OF FIGURES

Figure 1-1 Different stages in life cycle of a standard tyre.....	1
Figure 1-2 Domestic disposal of waste tyres in Australia	3
Figure 1-3 Thesis outline and structure	10
Figure 2-1 Actual test setup and instrumentation for compression testing under reaction frame (a) load applied on tyre-bale, (b) load applied on one concrete wall and (c) load applied on both concrete walls	18
Figure 2-2 Cut steel wires in the tyre-bale simulating severe corrosion during service life ...	19
Figure 2-3 Typical tyre-bale made of used tyres	20
Figure 2-4 Dimensions and details of sandwich wall	20
Figure 2-5 Test setup and instrumentation – location of LVDTs	21
Figure 2-6 Instrumentation – location of strain gauges	22
Figure 2-7 Typical finite element model of sandwich wall	24
Figure 2-8 Load-vertical deflection of tyre-bale under compression load (test-1).....	26
Figure 2-9 Comparison of load-vertical deflection of tyre-bale sandwich wall	26
Figure 2-10 Load-lateral deflection of tyre-bale sandwich wall under different loading conditions.....	28
Figure 2-11 Lateral deflection at top of sandwich wall under compression load.....	29
Figure 2-12 Variation in lateral deflection along the wall height of test-2.....	29
Figure 2-13 Variations in lateral deflections along the wall height of test-3.....	30
Figure 2-14 Strain variations in tyre-bale sandwich wall (a) SH1 (b) SH2 (c) SV1	31
Figure 2-15 Failure behaviour in tyre-bale sandwich wall	32
Figure 2-16 Concrete compression damage of tyre-bale sandwich wall in FEM under compression load (test-3).....	33
Figure 2-17 Comparison of load-deflection behaviour from experiment (test-3) and FEM ...	34
Figure 3-1 Details of tyre-bale sandwich wall	44
Figure 3-2 Test setup and Instrumentation - front elevation.....	45
Figure 3-3 Instrumentation – location of LVDTs – plan	46
Figure 3-4 Instrumentation – location of strain gauges	46
Figure 3-5 Flexural bending test setup.....	47
Figure 3-6 Vertical deflection of wall-1 at mid span a) rear side b) front side.....	49
Figure 3-7 Vertical deflection of wall-2 at mid span a) rear side b) front side.....	50
Figure 3-8 Crack pattern in bottom concrete wall during experimental testing	51

Figure 3-9 Ultimate load versus vertical deflection at mid-span (front-side).....	52
Figure 3-10 Deflected profile of tyre-bale sandwich wall-1 (a) front side (b) rear side.....	53
Figure 3-11 Deflected profile of tyre-bale sandwich wall-2 (a) front side (b) rear side.....	54
Figure 3-12 Strain distribution in bottom concrete wall (a) wall-1 at mid-span (b) wall-2 between applied loads and support	55
Figure 3-13 Finite element model of tyre-bale sandwich wall	58
Figure 3-14 Failure mode of tyre-bale sandwich wall in FEA (a) Crack at 13.68 kN (b) collapse at ultimate load.....	60
Figure 3-15 Development of flexural cracks in bottom concrete wall at various stages of loading – view from bottom.....	60
Figure 3-16 Load deflection of tyre-bale sandwich wall from experiment and FEA	61
Figure 3-17 FE model of two-way concrete slab.....	61
Figure 3-18 Failure mode of two-way concrete slab (a) Failure mode obtained in Ju experiment (b) Final failure mode and crack pattern of bottom concrete surface in FEA (c) Crack at 165KN in FEA (d) Final failure mode and crack pattern in 3D	63
Figure 3-19 Failure mode in tyre-bale sandwich wall under punching load (a) Crack pattern in 3D (b) view from the bottom	64
Figure 3-20 Yield line pattern in bottom concrete wall	64
Figure 3-21 Deflected shape at failure and formation of plastic hinges	65
Figure 4-1 Details of solid concrete panel	74
Figure 4-2 Details of precast concrete sandwich panel	74
Figure 4-3 Crumb rubber used as core material.....	75
Figure 4-4 Recycled tyre crumb with steel reinforcement.....	75
Figure 4-5 Recycled tyre crumb properties (a) Tensile strength (b) Stress-strain curve in uniaxial tensile test.....	78
Figure 4-6 Recycled tyre crumb properties (a) Compressive strength (b) Stress-strain in uniaxial compression	79
Figure 4-7 (a) Timber formwork and location of core material (b) Final finish after pouring SCC	80
Figure 4-8 Instrumentation: Arrangement of LVDTs for specimen.....	81
Figure 4-9 Instrumentation: Arrangement of strain gauges on concrete surface and reinforcement	82
Figure 4-10 Test setup: Arrangement of four-point bending for all specimen	83
Figure 4-11 Load-deflection at mid-span (LD-4)	84

Figure 4-12 Load versus vertical deflection along the span for CRSP-II.....	85
Figure 4-13 Strain distribution at mid-span in concrete top surface (SG1) and bottom surface (SG2) in SCP-I.....	86
Figure 4-14 Strain distribution at mid-span in concrete wyth and reinforcement in FSP-II ...	86
Figure 4-15 Strain distribution at mid-span in concrete wyth and reinforcement in CRSP-II	87
Figure 4-16 Strain variation along panel thickness in CRSP-II at different loading points	88
Figure 4-17 Ultimate strength approach to gauge degree of composition in sandwich panels	89
Figure 4-18 Failure and crack pattern at end of test (a) SCP (b) FSP (c) CRSP	92
Figure 4-19 Numerical model of CRSP showing loading and boundary conditions.....	94
Figure 4-20 Load versus vertical deflection at mid-span for CRSP	95
Figure 4-21 Concrete damage (a) 3D crack pattern on the bottom concrete wyth of CRSP at ultimate load (b) 2D crack pattern of CRSP at ultimate load	96
Figure 4-22 Deformed shape of numerical model of CRSP at ultimate load	97
Figure 5-1 Geometric details of solid concrete panel	105
Figure 5-2 Geometric details of precast concrete sandwich panels.....	105
Figure 5-3 Recycle tyre crumb sheet	106
Figure 5-4 Steel mesh (SL81) and recycle tyre crumb rubber sheet with reinforcement details	106
Figure 5-5 Formwork and casting of all concrete panels.....	107
Figure 5-6 Ultimate tensile strength of four specimen of recycle tyre crumb core	110
Figure 5-7 Tensile behaviour of recycle tyre crumb core.....	110
Figure 5-8 Compressive strength of five specimen of recycle tyre crumb core at strain value of 87.5%	111
Figure 5-9 Compressive behaviour of recycle tyre crumb core.....	112
Figure 5-10 Instrumentation - Positioning of LVDTs	113
Figure 5-11 Instrumentation and test configuration – strain gauges on back side of concrete wythe.....	113
Figure 5-12 Strain gauges positioning on concrete surface at back and front face and on reinforcement mesh.....	114
Figure 5-13 Structural performance of all precast concrete panels - load vs vertical deflection (LV-7).	116
Figure 5-14 Structural performance of all precast concrete panels – load vs lateral deflection (LV-1)	118

Figure 5-15 Lateral defections (LV1 to LV6) along the height of the panel at different loading phases (CRPN-I)	118
Figure 5-16 Strain distribution on concrete surfaces (S-1 to S-4) and in reinforcement (S-5 to S-8) in FPN-I.....	119
Figure 5-17 Strain distribution in CRPN-I on concrete surfaces (S-1 to S-4) and in reinforcement (S-5 to S-8)	120
Figure 5-18 Strain variations along the thickness of panel (CRPN-I) at 550mm height at different phases of loading	121
Figure 5-19 Final failure modes in panels (a) Solid concrete panel (b) Crumb sandwich panel (c) Foam sandwich panel	123
Figure 5-20 Concrete compressive behaviour (a) Stress-inelastic strain relationship (b) Compressive damage parameters.....	125
Figure 5-21 Concrete tensile behaviour (a) Tensile stress-cracking strain relationship (b) tensile damage parameters	125
Figure 5-22 3D FE model of CRPN with constraints	127
Figure 5-23 Axial performance of FEM and experimental test of CRPN	128
Figure 5-24 Concrete failure mechanism in compression in CRPN.....	128
Figure 5-25 Concrete failure in compression predicted by FEA in CRPN.....	129
Figure 6-1 Geometric details of solid concrete panel	137
Figure 6-2 Geometric details of concrete sandwich panel.....	138
Figure 6-3 Impact test setup and instrumentation.....	141
Figure 6-4 Impact force time-history of all panels	142
Figure 6-5 Displacement time-history of all panels at midspan	143
Figure 6-6 Strain distribution time-history of FSP	145
Figure 6-7 Strain distribution time-history of CRSP	145
Figure 6-8 Failure mode against impact at different time intervals (a) SCP (b) FSP (c) CRSP	148
Figure 6-9 Ultimate failure against impact (a) SCP (b) FSP (c) CRSP.....	150
Figure 7-1 Geometric details of precast concrete sandwich panel	156
Figure 7-2 Concrete cylinder of SFRC taken at time of casting.....	157
Figure 7-3 Material testing - concrete compressive strength.....	158
Figure 7-4 Formwork and casting of panels	159
Figure 7-5 Flexural bending test setup.....	160

Figure 7-6 Instrumentation of flexural bending test – location of LVDTs and strain gauges	161
Figure 7-7 Uni-axial compression test setup	162
Figure 7-8 Instrumentation of compression test – location of LVDTs	163
Figure 7-9 Load-deflection response of both panels at midspan (L3)	164
Figure 7-10 Load-deflection response of panel-II along the span	164
Figure 7-11 Strain variations in the panel at the top and bottom concrete surface.....	165
Figure 7-12 Concrete damage - flexural failure in the panel	166
Figure 7-13 Degree of composite action – cross section of the panel	167
Figure 7-14 Load-deflection response of both panels in uni-axial compression (L7).....	169
Figure 7-15 Out-of-plane displacement along the height of the panel	170
Figure 7-16 Strain variation in the panel under compression	171
Figure 7-17 Concrete damage under compression at ultimate failure	171

LIST OF TABLES

Table 1-1 Dimensions and mass of reference tyre-bale (PAS108:2007).....	4
Table 1-2 Engineering properties of all tyre-bales (PAS108:2007)	4
Table 1-3 Summary of tyre-bale civil engineering projects	5
Table 2-1 Engineering properties of tyre-bale	19
Table 2-2 Properties of concrete and reinforced steel	23
Table 2-3 Concrete damaged plasticity parameters	23
Table 2-4 Summary of test results in compression loading.....	29
Table 2-5 Ultimate failure loads of experimental and FEM of sandwich wall.....	34
Table 2-6 Comparison of ultimate failure load.....	36
Table 3-1 Existing tyre-bale applications in different projects.....	41
Table 3-2 Engineering properties of tyre-bale (PAS 108:2007).....	43
Table 3-3 Properties of concrete and reinforced steel	44
Table 3-4 Summary of experimental results in flexural bending	52
Table 3-5 Assessment of composite behaviour for both specimens	57
Table 3-6 Concrete damage plasticity parameters used in FEA	58
Table 3-7 Ultimate load and vertical deflection from experiment and FEA	59
Table 3-8 Input parameters for 30 MPa concrete slab under punching shear load.....	62
Table 3-9 Ultimate load comparison of concrete slab	62
Table 3-10 Load prediction trials using yield line theory.....	66
Table 4-1 Thermal conductivity of few commonly used materials	72
Table 4-2 Mix design proportions for 50 MPa SCC.....	76
Table 4-3 Tests performed on SCC and detail of results	76
Table 4-4 Properties of 50 MPa SCC at 28 days	77
Table 4-5 Mechanical properties of recycled tyre crumb in uniaxial compressive and tensile testing.....	78
Table 4-6 Properties of steel reinforcement and shear connector.....	80
Table 4-7 Summary of experimental test results in terms of load, moment and deflection	85
Table 4-8 Composite action of all sandwich panels at elastic and ultimate stage	91
Table 4-9 Concrete Damage Parameters of 50MPa SCC used in FEA	93
Table 4-10 Material properties for concrete compression and tension behaviour.....	93
Table 4-11 Comparison of ultimate load for experimental and FEA	95
Table 5-1 Mix proportion of SCC.....	108

Table 5-2 Consistency tests for SCC and results	108
Table 5-3 Material properties of SCC.....	109
Table 5-4 Material properties of steel mesh (SL81) and shear connectors.....	109
Table 5-5 Material properties of recycle tyre crumb rubber.....	111
Table 5-6 Summary of experimental test results in terms of initial cracking and ultimate load	116
Table 5-7 Concrete damage parameters for SCC	124
Table 5-8 Comparison of ultimate load for experimental and FEA (CRPN)	127
Table 5-9 Design axial load (kN) of PCSPs calculated by existing equations	130
Table 6-1 Details of mix design and proportion for SCC of 50 MPa.....	139
Table 6-2 Relevant test for SCC along with results and acceptable ranges.....	139
Table 6-3 Properties of 50 MPa SCC	139
Table 6-4 Engineering properties of 8mm and 6mm diameter steel.....	140
Table 6-5 Recycled tyre crumb properties in uni-axial compression and tension.....	140
Table 6-6 Summary of impact forces and displacements of all panels.....	144
Table 7-1 Details of mix design and proportion for SFRC.....	157
Table 7-2 Properties of 35 MPa SFRC	158
Table 7-3 Properties of steel fibres	158
Table 7-4 Recycled tyre crumb properties in uni-axial compression and tension.....	159
Table 7-5 Degree of composite action at initial stiffness stage	168

NOTATION

a = shear span length

A_c = the gross area of section

A_{sc} = total area of longitudinal reinforcement

b = overall width of cross section

Δ = mid-span deflection

e = eccentricity of the load measured perpendicular to the plane of the wall

e_a = an additional eccentricity taken as $(H_{we})^2/2500t_w$

ϵ = eccentricity

E = modulus of elasticity of concrete

f_{b0}/f_{c0} = Initial biaxial/uniaxial ratio

f'_c = compressive strength of concrete

f_{cu} = the compressive strength of concrete

f_t = tensile strength of concrete

f_y = the tensile strength of steel

g = gravitational constant

h = overall depth of cross section

h_1 = depth of top concrete wythe

h_2 = depth of bottom concrete wythe

H = the vertical distance between supports; or height

\emptyset = factor taking into account curvature, including second order effects of creep

I_C = composite moment of inertia

I_E = experimental moment of inertia

I_{NC} = non-composite moment of inertia

$k = 0.8$ for wall brace top and bottom against lateral translation and restrained against rotation
at one or both ends

K_1 = degree of composite action at initial stiffness stage

K_2 = degree of composite action at ultimate stage

K_c = ratio of the second stress invariant on the tensile meridian, $q_{(TM)}$, to that on the compressive meridian, $q_{(CM)}$, at initial yield for any given value of the pressure invariant such that the maximum principal stress is negative

L = clear span length

m = mass

N_u = ultimate load per unit length of wall

N_{RD} = axial load of wall

η = effective length factor, 1.0 for compressive strength of concrete at 28 days $\leq 50\text{MPa}$

P = load acting on specimen

P_C = load due to composite action

P_E = experimental load

P_{NC} = load due to non-composite action

P_u = the ultimate load

ν = Poisson's ratio

t = the overall thickness of member

t_w = thickness of the wall

μ = viscosity parameter

v = velocity

Φ = the strength of reduction factor (0.7 for reinforced member)

ψ = dilation angle

ABBREVIATIONS

AS	= Australian Standards
ASTM	= American Society for Testing and Materials
BSI	= British Standards Institution
CDP	= Concrete Damage Plasticity
CRSP	= Crumb Sandwich Panel
CRPN	= Crumb Sandwich Panel
CN	= Cyanoacrylate
C3D8R	= eight node brick elements with reduced integration
EBS	= Ecological Building System
FEA	= Finite Element Analysis
FEM	= Finite Element Modeling
FSP	= Foam Sandwich Panel
FPN	= Foam Sandwich Panel
L1	= Linear Variable Displacement Transducer
LD	= Linear Variable Displacement Transducer
LVDT	= Linear Variable Displacement Transducer
LV	= Linear Variable Displacement Transducer
MDI	= Methyl Diphenyl Diisocyanate
PCSPs	= Precast Concrete Sandwich Panels
PE	= Plastic Strain
PVC	= Polyvinyl Chloride
PAS	= Publicly Available Specification
RP	= Reference Point
SFRC	= Steel Fibre Reinforced Concrete

S1	= Strain Gauge
SCP	= Solid Concrete Panel
SPN	= Solid Concrete Panel
SH	= Strain Gauge in Horizontal direction
SG	= Strain Gauge
SV	= Strain Gauge in Vertical direction
SL	= Steel Mesh
T3D2	= Two nodes three-dimensional truss element
U _X	= Displacement in x-axis
U _Y	= Displacement in y-axis
U _Z	= Displacement in z-axis
U _{XR}	= Rotation about x-axis
U _{YR}	= Rotation about x-axis
U _{ZR}	= Rotation about x-axis
UB	= Universal Beam

CHAPTER 1 INTRODUCTION AND LITERATURE REVIEW

1.1 Research Background

Each year approximately 1.6 billion tyres are manufactured globally, in which one billion tyres reach their designed service life (Goldstein, 2020). In US, nearly 300 million tyres are disposed of in an annual year (USTMA, 2020). Similarly, around 50 million tyres are discarded every year in Australia (WMR, 2016). After reaching the design life, discarded tyres are used in a number of ways including recovery in the form of fuel, dumping, stockpiling, salvaging useful material and retreading. The various phases involved in the life cycle of a tyre from production till disposal are shown in Figure 1-1.

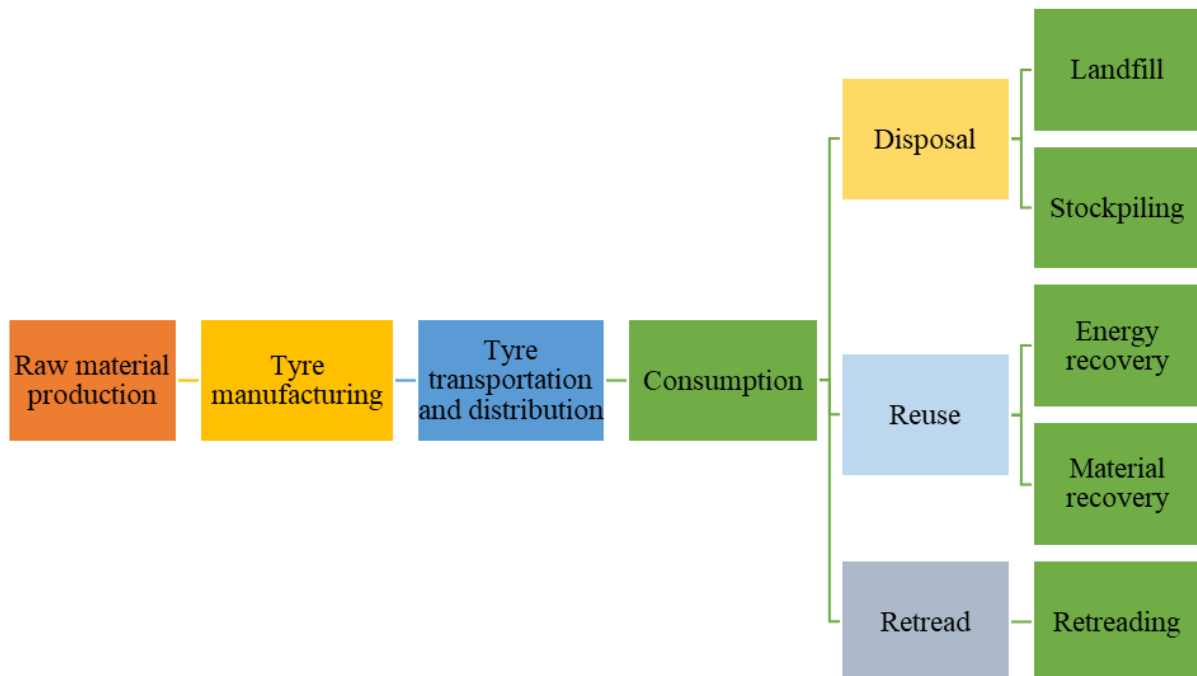


Figure 1-1 Different stages in life cycle of a standard tyre

A standard tyre is a non-biodegradable and has a service life of approximately four years. Waste tyres become primary source of health as well as environmental hazards if appropriate means of disposal are not implemented. Every year, there is an exponential increase in automobiles that generates large number of waste tyres in short period of time. Hence, large chunk of waste tyres is stored by stockpiling or dumping in unlicensed landfill. The illegal dumping of waste tyres can lead to pollution, leaching, fire and breeding places for the growth of mosquitoes. Similarly, tyres can also harm the atmosphere when dispose of by burning and result in toxic fumes.

Tyres are made up of combustible material and burning of waste tyres can produce extremely high temperatures for a long period of time. Similarly, tyre fires cause destruction to the surrounding area and extremely hard to control. The air quality and visibility of the area are also affected due to the release of toxic gases (Mohajerani et al., 2020). In year 2012, 1.3 million waste tyres were burned in Iowa city, USA. As a result, harmful gases were released and affected the health of millions of people living in nearby area (Singh et al., 2015). The investigations revealed that substantial amount of sulphur dioxide, several polycyclic aromatic hydrocarbons (PAH), carcinogenic and mutagenic pollutants were detected in the air (Downard et al., 2015).

Waste tyres are source of leachate and contain highly toxic chemicals which can pollute land, ground water and can also cause severe damage to human health. The leaching of waste tyres produces manganese and iron (Downs et al., 1996). The illegal dumping sites storing waste tyres are key source of leaching and poses a significant threat to the environment and the surrounding areas (Turner & Rice, 2010).

Waste tyres become an ideal breeding place for the growth of mosquitoes and vermin due to accumulation of water inside the tyres. As a result of this, various kinds of insects and viruses are produced and subsequently, spread by the mosquitoes and vermin. It was found that mosquito species namely *Aedes aegypti* and complex *Culex pipiens* L grow in waste tyre water and cause viral diseases such as meningitis, dengue and yellow fever. These types of diseases possess critical hazard to human well-being (Rubio et al., 2011).

Waste tyres are currently used in extraction of oil, energy, retreading and in civil engineering applications. To extract oil from tyres, a process known as pyrolysis is applied. It is basically the thermal decomposition of the organic components of the tyres either in the absence of oxygen into smaller molecules of oil, gas and low-grade carbon black. The oil obtained this way can be used in heavy generators, boiler heater, steel industry and cement factory. A negligible percentage of waste tyres are treated this way. As oil produced through pyrolysis needs to have a compatible price when comparing with the low prices of traditional fuel (Hossain et al., 2000).

For energy recovery, the waste tyres are burned for fuel in cement furnaces, paper industry, steam generators and power plants. According to a report published by an environment body (Brindley et al., 2012), in year 2009 less than 1% waste tyres were used for energy recovery in Australia. Similarly, another method of reclaiming the waste tyre is retreading. It is a process

in which the old used tyres are refurbished by replacing the tread. A study found that this practice is rapidly becoming obsolete in USA due to the latest technologies adopted in the manufacturing of new tyres (Hossain et al., 2000).

1.2 Civil Engineering Applications of Waste Tyres

Civil engineering applications of waste tyres were negligible in the past, which got attention of researchers in 1960s due to abundance of waste tyres every year and the urge for recycling the waste material. Civil engineering projects utilise whole waste tyres in the construction of barriers, earth retaining structures, erosion control structures and shoreline protection. Also, waste tyres are shredded and processed into rubber crumb or chips with varying sizes normally ranging from 50 mm to 100 mm. They are typically used as a replacement material in concrete, bitumen, asphalt and on playground and sporting tracks. The exceptional properties of waste tyres such as drainage, durability, compressibility, insulation and low density forced researchers to investigate the practical applications in civil engineering.

Figure 1-2 illustrates the disposal of waste tyres in Australia. It is evident that only a small portion of waste tyres that is 3.3% were brought to licensed landfill. The percentage for civil engineering applications and recycling were limited to 5.8% and 10.2% respectively. The explanation of low percentage associated with recycling may be the small financial worth of waste tyres, transportation cost and pricey recycling equipment (WAGLA, 2012).

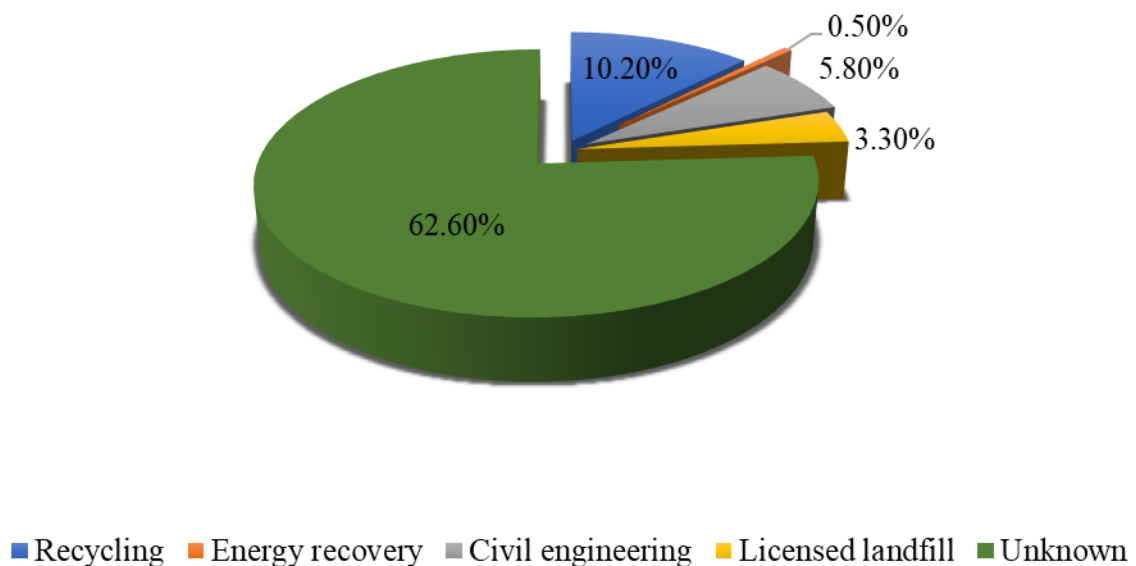


Figure 1-2 Domestic disposal of waste tyres in Australia (WAGLA, 2012)

Consequently, the management of waste tyres has become a point of concern in the absence of an organized recycling structure. With growing attention regarding climate change, the agencies around the globe are also taking strict measures to control the illegal dumping and stockpiling of waste tyres. This clearly highlights that sustainable means for disposal of waste tyres are needed.

Whole waste tyres are generally recycled in the form of bales in USA, Indonesia, Austria and Australia. Use of whole waste tyres in the form of tyre-bales offer several advantages such as cheap maintenance cost, low-cost baler and less manufacturing time. The compact shape of tyres-bale does not accumulate water and therefore, not considered a hazard to the environment. Similarly, the low surface area, absence of air and density of tyre-bale eliminates the possibility of fire risk. The storage and transportation of tyre-bales becomes easy because of reduced volume size (Hossain et al., 2000).

The waste and resources action programme (WRAP) in coordination with the British Standards Institution (BSI) developed a specification (PAS108:2007) for the standard construction of tyre-bales. The specification is a comprehensive guideline on the dimensions, engineering properties, behaviour and disposal options for tyre-bale (BSI, 2007). The tyre-bale is made of minimum 100 used tyres, compressed by applying a force of 600 kN in a baler machine. The waste tyres are stacked in herring-bone form, providing capping tyres both at top and bottom. Five steel tie wires of diameter 4 mm, with tensile strength ranging from 1500 MPa to 1700 MPa, are used to wrap the tyres together. Table 1-1 and 1-2 illustrates the geometric and engineering properties of tyre-bale. Table 1-3 presents the summary of few civil engineering projects in which tyre-bale was used.

Table 1-1 Dimensions and mass of reference tyre-bale (PAS108:2007)

Property	Length (m)	Width (m)	Depth (m)	Volume (m ³)	Mass (kg)
Value(s)	1.33 (+0.08/-0.06)	1.55 (± 0.07)	0.83 (± 0.04)	1.70 (+0.24/-0.15)	810 (±35)

Table 1-2 Engineering properties of all tyre-bales (PAS108:2007)

Property	Value (s)
Nominal mass density	470 kg/m ³ (± 50 kg/m ³)
True mass density	500 kg/m ³ (± 70 kg/m ³)
Porosity	62 % (± 5 %)

Shear strength: angle of inter-bale friction, ϕ	35° to 36°
Stiffness	800 MPa to 1000 MPa
Total creep (35 months)	Up to 1.1%
Permeability through depth	0.1 m/s to 0.2 m/s
Permeability through length	0.02 m/s to 0.04 m/s

Table 1-3 Summary of tyre-bale civil engineering projects

Project	Location	Use
A-21 motorway	Bedford, England	Construction of embankment structure
Tampere western ring road	Tampere, Finland	Lightweight fill in embankment ramp
Interstate highway (I-30)	Fort Worth, USA	Slope stabilization and repair
Road foundation in Chautauqua County	New York, USA	Subgrade replacement for roads over soft ground
B-871 road foundation	Sutherland, Scotland	Road foundation on soft soil
Retaining wall projects in Winston and Hillsboro	New Mexico, USA	Tyre-bale gravity retaining walls

Similarly, waste tyres are shredded in form of large sized tyre shreds, tyre chips, crumb rubber and fine-grained rubber. Tyre chips are shredded in two phases; In first phase, 460 - 300 mm long and 230 - 100 mm wide rubber fragments are used a coarse aggregate replacement whereas in second phase, a rubber size of 76 – 13 mm are manufactured. Crumb rubber is used as a replacement of fine aggregate and particle size ranges from 4.75 mm to 0.075 mm. Fine-grained rubber is also used as a replacement of very fine aggregate with particle size varies between 0.5 mm 0.075 mm (Ganjian et al., 2009).

Crumb rubber when used in concrete provides low stiffness (Gheni et al., 2019), high flexibility (Elchalakani, 2015), thermal conductivity ranges between 0.1 and 0.25W/mK (Fraile-Garcia et al., 2018) and improved sound insulation (Corredor-Bedoya et al., 2017). However, several research studies highlighted that use of crumb rubber in concrete mix significantly affects compressive strength (da Silva et al., 2015), elastic modulus (Murugan et al., 2015), flexural strength (Fernández-Ruiz et al., 2018), (Jokar et al., 2019) and tensile strength (Hesami et al., 2016) due to poor bonding at interfacial transition zone between concrete mix and crumb rubber (Rivas-Vázquez et al., 2015). Subsequently, number of attempts has been made to

improve the mechanical properties of crumb rubber concrete by pre-treating (Raffoul et al., 2016) or use of additives (Carroll & Helminger, 2016) but no significant techniques have been reported. Youssf (Youssf et al., 2019) reported that all treatment techniques used to improve mechanical properties of crumb rubber concrete made negligible contribution and therefore, researchers should rely on reduced strength when comparing to traditional mix of concrete. Contrarily, the use of crumb rubber concrete in structural members offers advantages like light in weight, smaller crack width and better structural response against seismic loading (Xu et al., 2020), fire (Xu et al., 2018) and fatigue (Han et al., 2016).

1.3 Problem Statement and Research Significance

1.3.1 Recycled tyre-bale sandwich panel

In the past, recycled tyres have successfully been used in the form of tyre-bale in ground improvement, subgrade replacement and embankment repair owing to its lightweight and excellent permeability. The mechanical properties of tyre-bale have been investigated for highway (Freilich & Zornberg, 2009) and geotechnical applications (Duda & Siwowski, 2021). The research focussed on compressibility, characteristics of tyre-bale including elastic modulus, Poisson's ratio, shear strength, creep and stiffness degradation under cyclic loading. The stiffness degradation was evaluated as a resilient value i.e. the difference between maximum and minimum deformations. After 10,000 cycles of loading over a period 400 minutes, no stiffness degradation was reported in any sample. Similarly, the coefficient of creep for one year was 0.0039 (Duda & Siwowski, 2021). The use of tyre-bales improved embankment strength and durability and reduced vertical settlement (Mohajerani et al., 2020). In addition, the use of tyre-bales in highway and geotechnical applications promoted environmental sustainability by reducing the demand for concrete and steel and lowered greenhouse gas emissions.

Despite showing excellent technical properties and mechanical behaviour in highway and geotechnical applications, the use of tyre-bales in structural engineering has been negligible. It was learnt through a comprehensive literature review that the structural behaviour of tyre-bale in precast concrete sandwich panels (PCSPs) has never been investigated. It is due to this fact the construction industry is hesitant to use tyre-bale in structural engineering applications.

1.3.2 Recycled tyre crumb sandwich panel

Sandwich panels are widely used in the manufacturing of automotive, aerospace and reinforced concrete structures. In the construction industry, a typical precast concrete sandwich panel (PCSPs) consists of two outer wythes and a core. A wyth is usually made up of reinforced concrete or steel sheet whereas core is an insulation material like foam, balsa wood or corrugated sheet. Previously, numerous research studies have been carried out to explore the possibility of using different core materials like corrugated sheets (Rejab & Cantwell, 2013; Wadley et al., 2013; Zhang et al., 2016), honeycomb cores (Davalos et al., 2001; Qi et al., 2017; Xie et al., 2020), foam concrete core (Flores-Johnson & Li, 2012), truss core (Kazemahvazi et al., 2009; Kazemahvazi & Zenkert, 2009) and foam (A. Amran, Rashid, Raizal, Hejazi, Farzad, Safiee, 2016; R. Amran, Farzad, Azizi, Safiee, Ali, 2016; Amran et al., 2016; Benayoune et al., 2006; Benayoune et al., 2008; Gara et al., 2012; Khalil et al., 2014; Metelli et al., 2011; Mohamad et al., 2017).

At present, the information considering the use of recycled tyre crumb as a core material in PCSPs is not available or has not been fully investigated. However, the use of recycled tyre crumb rubber in sandwich panels can add benefits like low thermal conductivity, high sound insulation, high impact resistance, elimination of low compressive strength problems and low energy utilization. Additionally, the building construction industry contributes nearly one-third of all greenhouse gas emissions and recycling huge quantities of discarded tyres in the form of recycled tyre crumb core material in PCSPs could significantly reduce toxic emissions and alleviate environmental hazards.

1.4 Objectives and Scope of the Research

The main objective of this thesis is to investigate the structural performance in context of ultimate load capacity, deformations, strain variations and mode of failure of recycled tyre-bale and recycled tyre crumb sandwich panels under different static and dynamic loadings. Additional objectives include the development of engineering guidelines for reliable design of sandwich panels for any structural engineering applications. The specific objectives of this research are as followed:

- a. To investigate analytically and experimentally the structural behaviour of recycled tyre-bale sandwich panels under uni-axial loading including the

compressibility of tyre-bale, effect of eccentric loading and effect of severe corrosion condition of tyre-bale's tie-wires.

- b. To investigate analytically and experimentally the flexural bending behaviour of recycled tyre-bale sandwich panel under four-point and punching shear load including the degree of composite action.
- c. To investigate analytically and experimentally the structural behaviour of recycled tyre crumb sandwich panels under flexural bending including the degree of composite action.
- d. To investigate analytically and experimentally the structural behaviour of recycled tyre crumb sandwich panels under uni-axial compression load and validity of theoretical expression.
- e. To investigate the low-velocity impact behaviour of recycled tyre crumb sandwich panels under drop weight.
- f. To investigate the structural behaviour of precast steel fibre reinforced concrete sandwich panel containing recycled tyre crumb core under static loadings in context of flexural bending and uni-axial compression.

1.5 Thesis Outline and Structure

The thesis comprised of eight chapters and is compiled using author's journal publications according to Curtin University HDR guidelines and rules. The body of the thesis consists of Chapter 2 to Chapter 7, whereas Chapter 8 presents the recommendations and future studies. Each chapter begins with a comprehensive literature review particularly linked with the individual research objective, followed by geometric details, test setup, instrumentation, results and discussion and culminates with conclusion. Figure 1-3 illustrates the thesis outline and structure.

Chapter 2 includes the structural behaviour of recycled tyre-bale sandwich panel in uni-axial compression. The results obtained through experimental testing are compared with existing empirical equations proposed by various international building codes. A finite element modelling (FEM) is developed in ABAQUS through concrete damage plasticity model to simulate the structural behaviour of sandwich panel.

- Chapter 3** describes the structural behaviour of tyre-bale sandwich panel under flexural bending in terms of ultimate load capacity, deflection, concrete damage in tension and failure mechanism. A FEM is developed and validated with the experimental results and later, used to predict the punching shear load and crack patterns.
- Chapter 4** explains the structural behaviour of innovative precast concrete sandwich panel, in which recycled tyres are used for the first time as crumb rubber core. The degree of composite action was assessed in terms of initial stiffness and ultimate strength. The research also proposed a 3D FE model for recycled tyre crumb rubber sandwich panel to study the analytical behaviour in flexure bending. CDP model was implemented to simulate concrete damage in compression and tension.
- Chapter 5** explores the structural response of recycled tyre crumb rubber sandwich panel in uni-axial compression. This study compares the performance of commonly used precast concrete panels like solid concrete panel and foam (expanded polystyrene) sandwich panel with recycle tyre crumb rubber sandwich panel in terms of axial load capacity, deflections, strain distribution and mode of failure.
- Chapter 6** presents the low-velocity impact behaviour of precast concrete sandwich panels containing recycle tyre crumb. This study compares the structural response of recycled tyre crumb rubber sandwich panel with solid concrete panel and foam concrete sandwich panel against impact. The impact test was carried out by dropping a weight from 2m height to generate sufficient impact energy, which can cause ultimate failure in all specimens.
- Chapter 7** covers the structural response of steel fibre reinforced concrete sandwich panels containing recycled tyre crumb rubber as core in flexural bending and uni-axial compression. A series of lab experiments carried out to examine the ultimate strength capacity, deformations, strain variations in concrete and mode of failure. In the end, the degree of composite action is assessed in flexural bending through stiffness method in elastic stage.

Chapter 8 summarizes the significant contribution of this research and include recommendations for further research studies.

Note: The term “sandwich wall” used in Chapter 2 and 3 is similar as “sandwich panel”. Also, “Crumb rubber” used in Chapter 4 and 5 is same as “Crumb”.

Chapter 2 – 5 includes author’s journal publications that are reproduced. In the thesis, the geometric and material details may appear more than once in different chapters, which readers may like to read separately. The copyright agreements between the author and the respective journals are attached in Appendix - I.

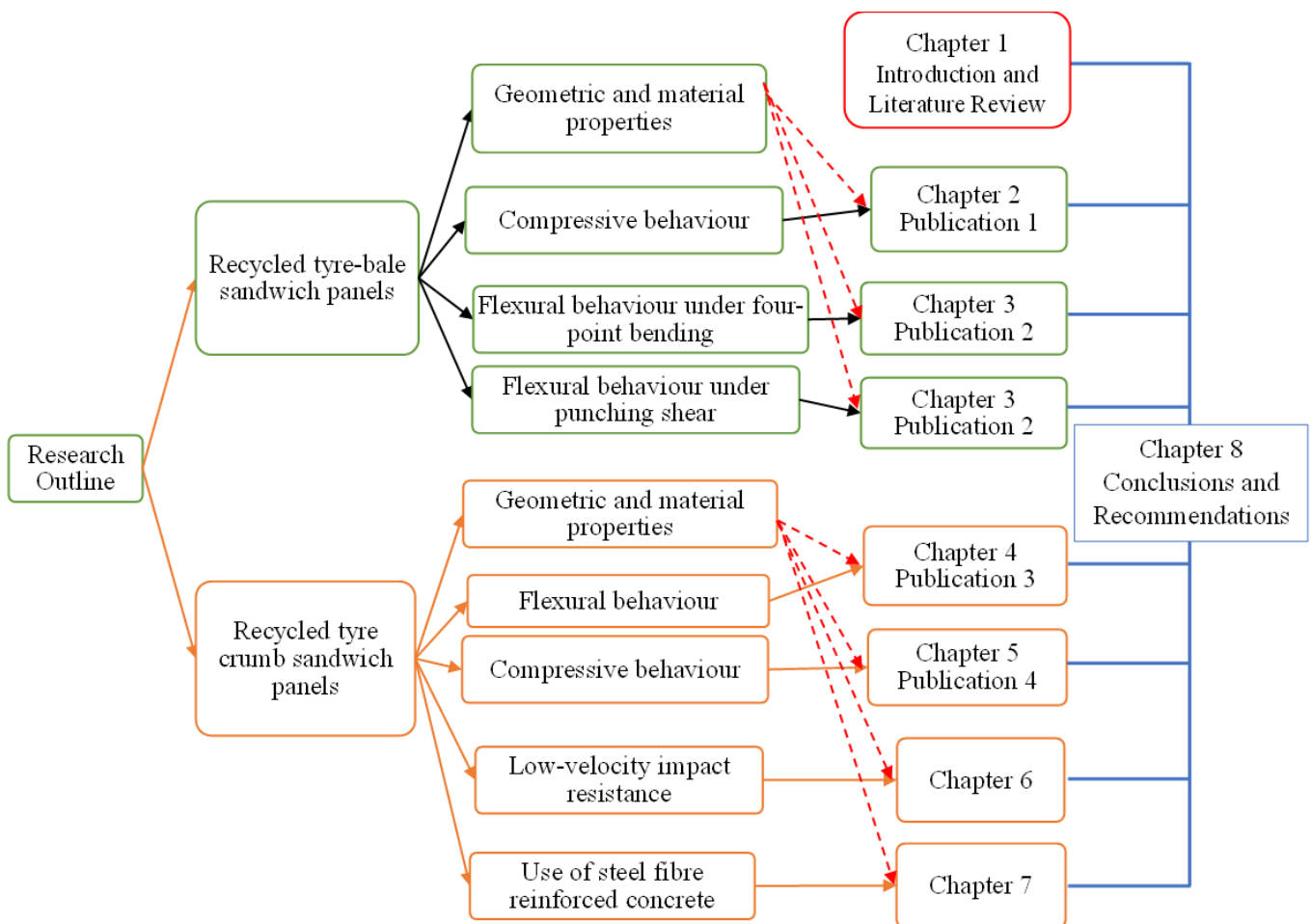


Figure 1-3 Thesis outline and structure

1.6 References

- Amran, A., Rashid, Raizal, Hejazi, Farzad, Safiee. (2016). Structural behavior of axially loaded precast foamed concrete sandwich panels. *Construction and Building Materials*, 107, 307-320.
- Amran, R., Farzad, Azizi, Safiee, Ali. (2016). Structural Behavior Of Precast Foamed Concrete Sandwich Panel Subjected To Vertical In-Plane Shear Loading. In: Zenodo.
- Amran, Y. H. M., Rashid, R. S. M., Hejazi, F., Safiee, N. A., & Ali, A. A. A. (2016). Response of precast foamed concrete sandwich panels to flexural loading. *Journal of Building Engineering*, 7, 143-158.
- Benayoune, A., Samad, A. A. A., Trikha, D. N., Abang Ali, A. A., & Ashrabov, A. A. (2006). Structural behaviour of eccentrically loaded precast sandwich panels. *Construction and Building Materials*, 20(9), 713-724.
- Benayoune, A., Samad, A. A. A., Trikha, D. N., Ali, A. A. A., & Ellinna, S. H. M. (2008). Flexural behaviour of pre-cast concrete sandwich composite panel – Experimental and theoretical investigations. *Construction and Building Materials*, 22(4), 580-592.
- Brindley, Mountjoy, & Mountjoy. (2012). Study into domestic and international fate of end-of-life tyres (AA003649-RO1-19).
- BSI. (2007). Specification for the production of tyre bales for use in construction. In PAS 108:2007. London, UK.
- Carroll, J. C., & Helminger, N. (2016). Fresh and Hardened Properties of Fiber-Reinforced Rubber Concrete. *Journal of Materials in Civil Engineering*, 28(7), 04016027.
- Corredor-Bedoya, A. C., Zoppi, R. A., & Serpa, A. L. (2017). Composites of scrap tire rubber particles and adhesive mortar – Noise insulation potential. *Cement and Concrete Composites*, 82, 45-66.
- da Silva, F. M., Gachet Barbosa, L. A., Lintz, R. C. C., & Jacintho, A. E. P. G. A. (2015). Investigation on the properties of concrete tactile paving blocks made with recycled tire rubber. *Construction and Building Materials*, 91, 71-79.
- Davalos, J. F., Qiao, P., Frank Xu, X., Robinson, J., & Barth, K. E. (2001). Modeling and characterization of fiber-reinforced plastic honeycomb sandwich panels for highway bridge applications. *Composite Structures*, 52(3), 441-452.
- Downard, J., Singh, A., Bullard, R., Jayarathne, T., Rathnayake, C. M., Simmons, D. L., Wels, B. R., Spak, S. N., Peters, T., & Beardsley, D. (2015). Uncontrolled combustion of shredded tires in a landfill–Part 1: Characterization of gaseous and particulate emissions. *Atmospheric Environment*, 104, 195-204.
- Downs, L. A., Humphrey, D. N., Katz, L. E., & Rock, C. A. (1996). Water quality effects of using tire chips below the groundwater table in Civil Engineering, University of Maine].
- Duda, A., & Siwowski, T. (2021). Experimental Determination of Mechanical Properties of Waste Tyre Bales Used for Geotechnical Applications. *Materials*, 14(12), 3310.
- Elchalakani, M. (2015). High strength rubberized concrete containing silica fume for the construction of sustainable road side barriers. *Structures*, 1, 20-38.

- Fernández-Ruiz, M. A., Gil-Martín, L. M., Carbonell-Márquez, J. F., & Hernández-Montes, E. (2018). Epoxy resin and ground tyre rubber replacement for cement in concrete: Compressive behaviour and durability properties. *Construction and Building Materials*, 173, 49-57.
- Flores-Johnson, E. A., & Li, Q. M. (2012). Structural behaviour of composite sandwich panels with plain and fibre-reinforced foamed concrete cores and corrugated steel faces. *Composite Structures*, 94(5), 1555-1563.
- Fraile-Garcia, E., Ferreiro-Cabello, J., Mendivil-Giro, M., & Vicente-Navarro, A. S. (2018). Thermal behaviour of hollow blocks and bricks made of concrete doped with waste tyre rubber. *Construction and Building Materials*, 176, 193-200.
- Freilich, & Zornberg. (2009). *Mechanical Properties of Tire Bales for Highway Applications [Technical Report2019]*.
- Ganjian, E., Khorami, M., & Maghsoudi, A. A. (2009). Scrap-tyre-rubber replacement for aggregate and filler in concrete. *Construction and Building Materials*, 23(5), 1828-1836.
- Gara, F., Ragni, L., Roia, D., & Dezi, L. (2012). Experimental tests and numerical modelling of wall sandwich panels. *Engineering Structures*, 37, 193-204.
- Gheni, A. A., Alghazali, H. H., ElGawady, M. A., Myers, J. J., & Feys, D. (2019). Durability properties of cleaner cement mortar with by-products of tire recycling. *Journal of Cleaner Production*, 213, 1135-1146.
- Goldstein. (2020). *Global Tire Recycling Market Analysis 2025: Opportunity, Demand, Growth And Forecast 2017-2025 (Industry Research Outlook, Issue)*.
- Han, Wang Y-H, Xu J, & Y, X. (2016). Fatigue behavior of stud shear connectors in steel and recycled tyre rubber-filled concrete composite beams. *Steel and Composite Structures*, 22(2), 353-368.
- Hesami, S., Salehi Hikouei, I., & Emadi, S. A. A. (2016). Mechanical behavior of self-compacting concrete pavements incorporating recycled tire rubber crumb and reinforced with polypropylene fiber. *Journal of Cleaner Production*, 133, 228-234.
- Hossain, Priyantha W, & Jayawickrama. (2000). *Use of whole Tyres in Earth retaining structures (0-1876)*.
- Jokar, F., Khorram, M., Karimi, G., & Hataf, N. (2019). Experimental investigation of mechanical properties of crumbed rubber concrete containing natural zeolite. *Construction and Building Materials*, 208, 651-658.
- Kazemahvazi, S., Tanner, D., & Zenkert, D. (2009). Corrugated all-composite sandwich structures. Part 2: Failure mechanisms and experimental programme. *Composites Science and Technology*, 69(7), 920-925.
- Kazemahvazi, S., & Zenkert, D. (2009). Corrugated all-composite sandwich structures. Part 1: Modeling. *Composites Science and Technology*, 69(7), 913-919.
- Khalil, A., Abdul Samad, A., & Goh, W. (2014). Structural Behavior of Precast Lightweight Foam Concrete Sandwich Panel with Double Shear Truss Connectors under Flexural Load. *ISRN Civil Engineering*, 2014(1).

- Metelli, G., Bettini, N., & Plizzari, G. (2011). Experimental and numerical studies on the behaviour of concrete sandwich panels. *European Journal of Environmental and Civil Engineering*, 15(10), 1465-1481.
- Mohajerani, A., Burnett, L., Smith, J. V., Markovski, S., Rodwell, G., Rahman, M. T., Kurmus, H., Mirzababaei, M., Arulrajah, A., Horpibulsuk, S., & Maghool, F. (2020). Recycling waste rubber tyres in construction materials and associated environmental considerations: A review. *Resources, Conservation and Recycling*, 155, 104679.
- Mohamad, N., Goh, W. I., Abdullah, R., Samad, A. A. A., Mendis, P., & Sofi, M. (2017). Structural performance of FCS wall subjected to axial load. *Construction and Building Materials*, 134, 185-198.
- Murugan, Natarajan, & C. (2015, 2015//). Investigation of the Behaviour of Concrete Containing Waste Tire Crumb Rubber. *Advances in Structural Engineering*, New Delhi.
- Qi, C., Remennikov, A., Pei, L.-Z., Yang, S., Yu, Z.-H., & Ngo, T. D. (2017). Impact and close-in blast response of auxetic honeycomb-cored sandwich panels: Experimental tests and numerical simulations. *Composite Structures*, 180, 161-178.
- Raffoul, S., Garcia, R., Pilakoutas, K., Guadagnini, M., & Medina, N. F. (2016). Optimisation of rubberised concrete with high rubber content: An experimental investigation. *Construction and Building Materials*, 124, 391-404.
- Rejab, M. R. M., & Cantwell, W. J. (2013). The mechanical behaviour of corrugated-core sandwich panels. *Composites Part B: Engineering*, 47, 267-277.
- Rivas-Vázquez, L. P., Suárez-Orduña, R., Hernández-Torres, J., & Aquino-Bolaños, E. (2015). Effect of the surface treatment of recycled rubber on the mechanical strength of composite concrete/rubber. *Materials and Structures*, 48(9), 2809-2814.
- Rubio, A., Cardo, M. V., & Vezzani, D. (2011). Tire-breeding mosquitoes of public health importance along an urbanisation gradient in Buenos Aires, Argentina. *Memórias do Instituto Oswaldo Cruz*, 106(6), 678-684.
- Singh, A., Spak, S. N., Stone, E. A., Downard, J., Bullard, R. L., Pooley, M., Kastle, P. A., Mainprize, M. W., Wichman, M. D., & Peters, T. M. (2015). Uncontrolled combustion of shredded tires in a landfill—Part 2: Population exposure, public health response, and an air quality index for urban fires. *Atmospheric Environment*, 104, 273-283.
- Turner, A., & Rice, L. (2010). Toxicity of tire wear particle leachate to the marine macroalga, *Ulva lactuca*. *Environmental Pollution*, 158(12), 3650-3654.
- USTMA. (2020). Scrap tire markets. Retrieved 12/04 from <https://www.ustires.org/scrap-tire-markets>
- Wadley, H. N. G., Dharmasena, K. P., O'Masta, M. R., & Wetzel, J. J. (2013). Impact response of aluminum corrugated core sandwich panels. *International Journal of Impact Engineering*, 62, 114-128.
- End-of-life Tyre Management in Australia, 12 (2012).
- WMR. (2016, 02 August 2016). A rubbery problem – the Australian scrap tyre management challenge. Prime Creative Media. Retrieved 15 Nov from

Xie, S., Feng, Z., Zhou, H., & Wang, D. (2020). Three-point bending behavior of Nomex honeycomb sandwich panels: Experiment and simulation. *Mechanics of Advanced Materials and Structures*, 1-15.

Xu, J., Fu, Z., Han, Q., Lacidogna, G., & Carpinteri, A. (2018). Micro-cracking monitoring and fracture evaluation for crumb rubber concrete based on acoustic emission techniques. *Structural Health Monitoring*, 17(4), 946-958.

Xu, J., Yao, Z., Yang, G., & Han, Q. (2020). Research on crumb rubber concrete: From a multi-scale review. *Construction and Building Materials*, 232, 117282.

Youssf, O., Hassanli, R., Mills, J. E., Skinner, W., Ma, X., Zhuge, Y., Roychand, R., & Gravina, R. (2019). Influence of Mixing Procedures, Rubber Treatment, and Fibre Additives on Rubcrete Performance. *Journal of Composites Science*, 3(2), 41.

Zhang, P., Cheng, Y., Liu, J., Li, Y., Zhang, C., Hou, H., & Wang, C. (2016). Experimental study on the dynamic response of foam-filled corrugated core sandwich panels subjected to air blast loading. *Composites Part B: Engineering*, 105, 67-81.

CHAPTER 2 STRUCTURAL BEHAVIOUR OF TYRE-BALE SANDWICH WALL UNDER AXIAL LOAD

2.1 Abstract

This paper presents structural behaviour of tyre-bale sandwich wall that is made of two outer reinforced concrete walls and tyre-bale as core material. The thickness of tyre-bale and each concrete wall is 650mm and 125mm respectively. The concrete walls are reinforced with 6mm diameter steel bars in each direction. Four sandwich walls were casted and tested on full scale under different compression loadings. In the first test, the axial load was applied directly to the tyre-bale to investigate the tyre-bale compressibility. The effect of eccentric loading was studied in the second test by applying the compression load on one concrete wall. In the third test, load was applied simultaneously on both concrete walls and finally, the fourth compression test was conducted by cutting-off the tie wires to simulate the severe corrosion conditions. The structural behaviour of sandwich wall is discussed in terms of ultimate load, vertical and lateral deflections, strain distribution and failure mechanism. In addition, the change in structural behaviour of sandwich wall under the effect of severe corrosion is presented. A significant reduction in structural capacity of sandwich wall was observed, when simulating corrosion conditions. Finite element modeling (FEM) of the sandwich wall was conducted in ABAQUS to simulate the damage of concrete in compression using concrete damage plasticity model. The difference in experimental and FEM results was found to be 15%. Furthermore, the experimental peak loads are compared with the existing empirical equations, which provided conservative design values to estimate the ultimate design load of sandwich wall.

2.2 Introduction

Australia generates around 50 million waste tyres each year. It is alarming to report that only a negligible percentage is recycled (WMR, 2016). In year 2010, 17.6% used tyres were exported, while 82.4% were locally retained in which about 10.2% were recycled, 5.8% were used in civil engineering applications, 3.3% landed in authorised landfill, 0.5% were used in energy generation and 60% of used tyres were missing (Brindley et al., 2012). Owing to a limited percentage used in recycling, the remaining used tyres become source of environmental and health hazards such as fire, leaching and breeding place for mosquitoes leading to health issues. Tyre fires, in Australia, not only damage valuable property but also produce toxic fumes causing

health risks. Similarly, mosquitoes breeding in trapped water inside tyres spread dangerous diseases. Therefore, it is imperative to encourage the reuse of used tyres to alleviate associated dangers. The used tyres are presently reprocessed in rethreading, recycle/reuse, rubber crumb and fuel for energy generation. In civil engineering applications, the used tyres are recycled either in the form of crumb rubber in asphalt mix or aggregate replacement in cement concrete. The use of crumb rubber in cement concrete offers different advantages like improved ductility, light-weight, impact resistance and great sound and thermal insulation (Yazdi et al., 2015). However, its use in structural applications is limited due to reduction in strength. Many researchers have suggested pre-treatment methods to improve the structural performance of crumb rubber cement concrete (Huang et al., 2013; Li et al., 2019; Li et al., 1998; Onuaguluchi & Panesar, 2014; Segre & Joekes, 2000). After deliberate research, some useful applications of waste tyres in construction of house and as retaining structures are reported as follows.

2.3 State-of-the-art

Gagnepain (Gagnepain, 2017) came up with an innovative idea of building a house using tyre-bales instead of masonry walls. Each bale was around 152cm x 152cm x 76.2cm high, with 80 to 120 fully compact tyres and weighed approximately one ton. The bales were stacked to the desired height. After placing the bales, they were either covered with a reinforced concrete bond beam all around or by applying shotcrete. The tyre-bales with an R-value of 45 along with concrete served as thermal mass to keep the temperature of interior comfortable and consequently eliminated the further addition of insulation. It also resulted in reduced construction cost. The article lacks technical information on the structural properties of tyre-bale walls like flexural, shear and axial strength, type of bonding between tyre-bales and concrete, etc.

Ecological Building System (EBS) in Texas, USA developed a structural wall using tyre-bale as core and was named as “Eco-Bloc”. The core is enclosed completely in concrete from all directions. This system can be used as retaining wall, border wall, wing wall or for controlling soil erosion. The innovative use of tyre-bale in replacing the concrete, reduced the overall cost by 52% (Hossain et al., 2000). Balcioglu manufactured sandwich panels containing ground waste tyres particles as core having thickness of 4mm, 8mm and 12mm. The core material was prepared by grinding the waste tyres in three particle sizes of 1mm, 2mm and 4mm and then, mixing with cobalt and Methyl-Ethyl-Ketone Peroxide. Jute fiber woven fabric was used in preparation of outer walls. The panels were tested under three-point loading and shear

resistance. In findings, the sample with fine rubber particles showed better bending and shear resistance to loading. The flexural strength of panel decreased with increase in core thickness. The author proposed the use of such sandwich panels only for medium level or lesser loadings (Balcioglu, 2018).

This paper introduces an innovative tyre-bale reinforced concrete sandwich wall system where whole tyres in form of a bale are used as core. These bales are manufactured as per PAS 108:2007 specifications (BSI, 2007). The results of tyre-bale reinforced concrete sandwich walls, subjected to compression loading, are discussed in terms of ultimate failure load, vertical and lateral displacement, strain variations and failure behaviour. The effect of severe corrosion of tie wires in tyre-bale on the axial load capacity and structural behaviour of sandwich wall is also investigated. In the end, the ultimate failure load of the sandwich walls is compared with the empirical equations proposed by various design codes. A 3D finite element model (FEM) is developed in ABAQUS and validated with experimental results. The validation of material model was evaluated by comparing the concrete damage in compression and plotting load-deflection curve of experimental test and FEM.

2.4 Experimental program

2.4.1 Test scenarios

In order to evaluate the structural strength of tyre-bale sandwich wall, four types of loading scenarios were considered. In the first case (Test-1), vertical line load was applied directly on the tyre-bale through a rigid steel beam (see Figure. 2-1a). In the second case (Test-2), the same line load was applied on one concrete wall to simulate the eccentric loading condition (see Figure. 2-1b). In the third load case (Test-3), the line load was applied simultaneously on both concrete walls of the sandwich wall (see Figure. 2-1c), while the fourth case (Test-4) was similar to the third case in every aspect except the tie wires were cut to simulate the rupturing of wires under severe corrosion (Figure. 2-2). One sandwich wall was tested for each loading scenario.

2.4.2 Manufacturing of tyre-bale

The tyre-bale is made of minimum 100 used tyres, compressed by applying a force of 600 kN in a baler machine as per PAS108:2007 specifications (BSI, 2007). The waste tyres are stacked in herring-bone form, providing capping tyres both at top and bottom. Five steel tie wires of diameter 4 mm, with tensile strength ranging from 1500 MPa to 1700 MPa, are used to wrap

the tyres together. The tyre-bale dimensions are 1270 x 1480 x 650 mm and a typical tyre-bale is shown in Figure 2-3. Table 2-1 shows the engineering properties of tyre-bale and tie-wires.



(a)



(b)



(c)

Figure 2-1 Actual test setup and instrumentation for compression testing under reaction frame (a) load applied on tyre-bale, (b) load applied on one concrete wall (eccentric loading) and (c) load applied on both concrete walls

Table 2-1 Engineering properties of tyre-bale

Material	Nominal density (kg/m ³)	True density (kg/m ³)	Young Modulus (MPa)	Poisson's Ratio (ν)
Tyre-bale	470 (± 50)	500 (± 70)	800 – 1000	0.3
Tie-wires	-	7800	200,000	0.3

The sandwich wall studied in this research consist of two outer reinforced concrete walls and a tyre-bale core. Each concrete wall is reinforced with steel wires of diameter 6 mm in both longitudinal and lateral directions and spaced at 100 mm centre-to-centre (Figure. 2-4). A concrete cover of about 50 mm is provided in both concrete walls. There are four M12 bolts used as shear connectors and drilled in both sides of tyre-bale with 75 mm protrusion in order to improve bond strength between tyre-bale and concrete walls. Furthermore, the undulating surface of tyre-bale provides additional bonding between two surfaces.



Figure 2-2 Cut steel wires in the tyre-bale simulating severe corrosion during service life



Figure 2-3 Typical tyre-bale made of used tyres

2.4.3 Casting of tyre-bale sandwich wall

During casting of sandwich wall, the formwork is first placed flat on ground with reinforcement mesh and concrete is poured through mixer in the formwork. In next stage, the tyre-bale is horizontally immersed by crane to allow strong bond between concrete and tyre-bale. This procedure last till concrete is completely hardened. In last stage, the tyre-bale is flipped, and similar practice is followed to cast the other side of concrete wall. The material properties of hardened concrete were measured by testing three concrete specimens, which were obtained by drilling core samples through the concrete sandwich wall. The sandwich wall is 1470 mm high and 1770 mm wide. The average thickness of each concrete wall is 125 mm and tyre-bale core is 650 mm (Figure. 2-4). A variation in concrete thickness was noticed after placing tyre-bale in concrete mix, as tyre-bale displaced concrete volume due to self-weight. The overall

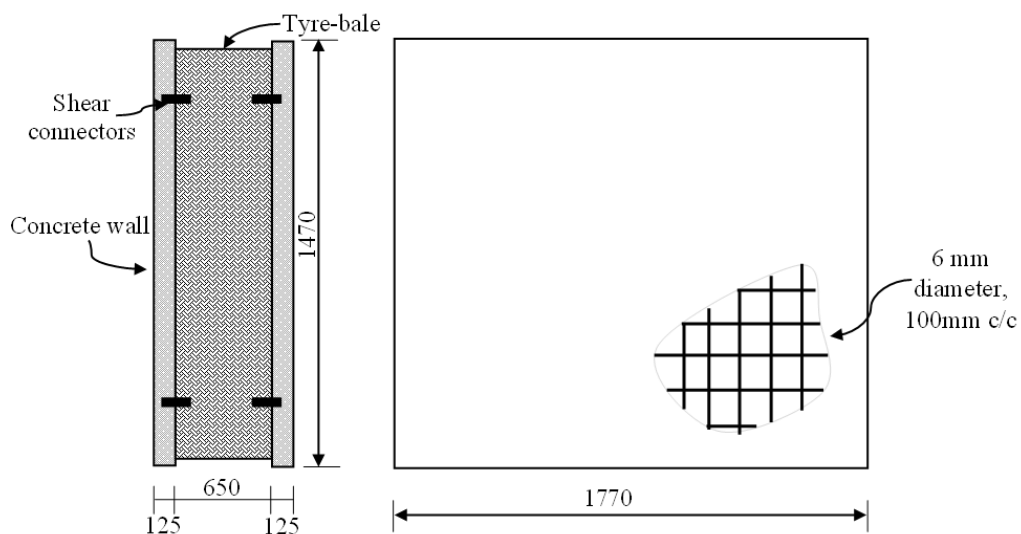


Figure 2-4 Dimensions and details of sandwich wall (all dimensions are in mm)

dimensions of the tyre-bale are shorter than the concrete walls to facilitate easy handling and transportation.

2.4.4 Instrumentation

Linear variable differential transformer (LVDT) and strain gauges were used to measure deflections and strains in sandwich wall. A total of seven LVDTs with stroke length of 100 mm were used on both concrete walls, in which three LVDTs were placed in horizontal position on each side to record the lateral deflections and one LVDT was used vertically to measure the vertical deflection (Figure. 2-5). The electrical strain gauges with a gauge length of 60 mm, gauge resistance of 120Ω and gauge factor of $2.08 \pm 1\%$ were used on concrete wall surface to measure the strain variations along the width and height of the sandwich wall. Three strain gauges were used in horizontal position while other three were arranged vertically on each concrete wall (Figure. 2-6). The concrete surface was prepared before installation of strain gauges by removing dust, sanding the surface and wiping thoroughly with acetone. The strain gauges were attached firmly to the concrete surface using CNE adhesive and lead wires were secured using tape.

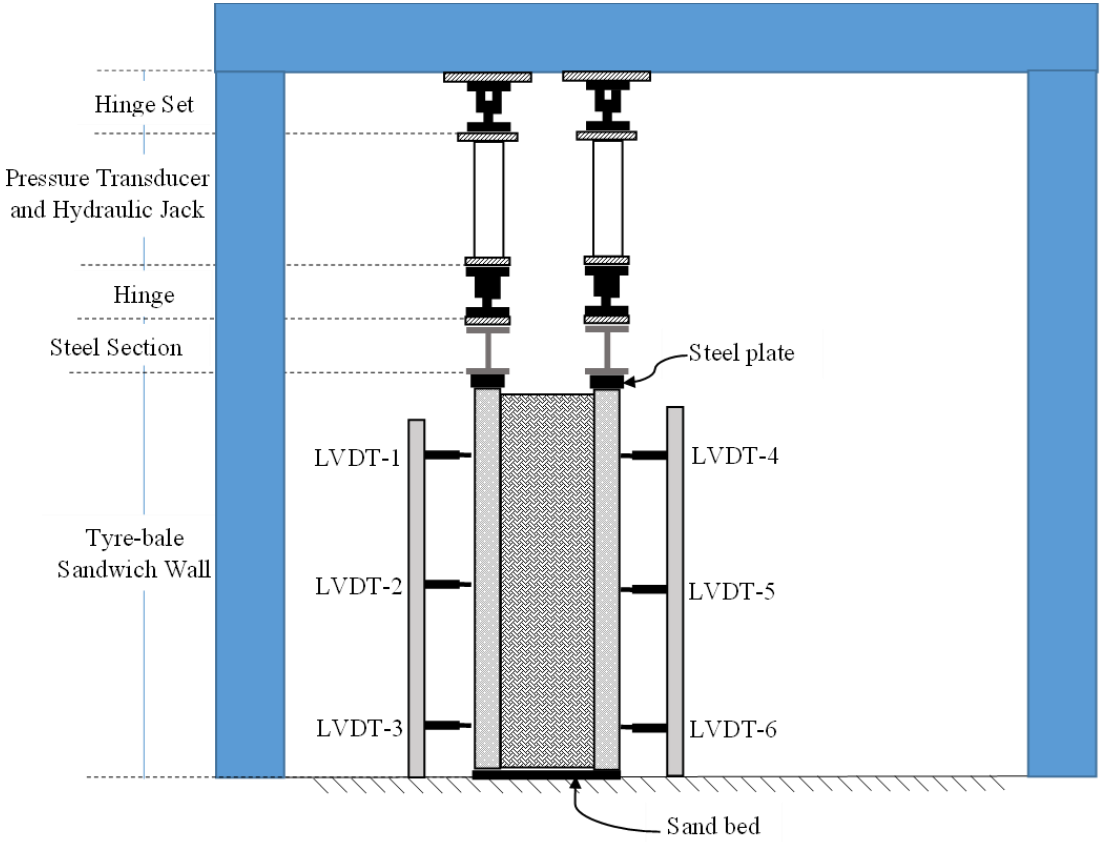


Figure 2-5 Test setup and instrumentation – location of LVDTs (sectional view)

2.4.5 Test setup

All sandwich walls were tested in compression using a 4000 kN capacity reaction frame. The test setup was built using 500 kN steel hinges, 550 kN hydraulic jacks (SPX RD5518) double-acting, hydraulic pump and modified universal beam (UB-460 steel section). The top steel hinge was attached to 25 mm thick plate, which was secured firmly to the reaction frame. The hydraulic jacks were attached to steel hinges at both ends to allow free movement in both directions and to avoid any kind of damage to hydraulic cylinder. The steel beam was specially modified for the compression test by welding an additional 12.5 mm thick plate at top flange and adding 25 mm thick stiffeners to apply a load of 1500 kN. A 50 mm thick and 900 mm long steel plate was used to transfer the load from steel beam to the sandwich wall as shown in Figure 2-5.

A 100 mm thick sand bed was laid on the test floor under the sandwich wall in order to provide a level surface. The top surface of the sandwich wall was levelled by applying plaster of Paris. All LVDTs and strain gauges were securely attached to data logger (HBM - Quantum X) to monitor deformations and strain variations during the test. The load was applied centrally to 900 mm length of the wall due to restricted load capacity of the testing frame. A preliminary load of 30 kN was applied in order to inspect the working of all LVDTs and strain gauges. The load was gradually increased till noticeable cracks appeared on the surface of the concrete wall. Actual test setup of sandwich walls under compression loading is shown in Figures 2-1 and 2-2.

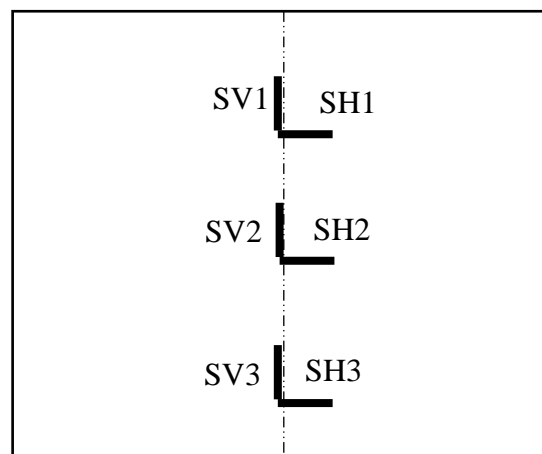


Figure 2-6 Instrumentation – location of strain gauges (elevation view)

2.5 Finite element modelling

2.5.1 Material modelling

Finite element analysis was conducted to understand the failure behaviour of sandwich wall and to evaluate the ultimate load capacity, when the load is applied on both concrete walls (Test-3). For this purpose, ABAQUS software was used to simulate the tyre-bale sandwich wall. The material model for steel reinforcement is simulated using elastic modulus (E) and Poisson ratio (μ) in linear elastic region, whereas non-linear behaviour is defined using yield stress and plastic strain. There was no plastic deformation observed during experimentation in tyre-bale. Therefore, only linear elastic parameters were defined for tyre-bale. However, tyre-bale was modelled as solid element in order to simplify the analysis and to facilitate a 3D trial model. This approach was previously adopted by Duda in investigating backfill (made of tyre-bales) pressure on bridge abutment (Duda & Siwowski, 2020). The linear elastic behaviour of concrete is adopted using modulus of elasticity and Poisson ratio. ABAQUS offers three constitutive model to simulate non-linear behaviour of concrete (a) brittle cracking concrete model (b) concrete smeared cracking model and (c) concrete damage plasticity. In this analysis, the concept of Concrete Damage Plasticity (CDP) is used to simulate the concrete plastic behaviour. It is an effective in-built tool for simulating the damage of concrete in compression and tension. The associated parameters like dilation angle, eccentricity, initial biaxial/uniaxial ratio, K_c and viscosity are obtained from previous research on concrete and are presented in Table 2-3 (Esfahani et al., 2017). The parameters like stress, inelastic strain and damage required in compression and tensile behaviour during the analysis were approximated for similar compressive strength of concrete. The material properties of tyre-bale, concrete and steel bars used in the analysis are presented in Tables 2-1 and 2-2.

Table 2-2 Properties of concrete and reinforced steel

Materials	Density (Kg/m ³)	Compressive strength (f^c) (MPa)	Ultimate tensile strength (MPa)	Modulus of Elasticity (MPa)	Poisson's Ratio (ν)
Concrete	2443	13.3	-	12000	0.20
Steel bar (6 mm)	7800	-	574	200,000	0.30

Table 2-3 Concrete damaged plasticity parameters

Dilation Angle	Eccentricity	Initial biaxial/uniaxial ratio (f_{b0}/f_{c0})	K	Viscosity
30°	0.1	1.16	0.67	0.00001

2.5.2 Assembly of parts and interaction

All individual members of the sandwich wall like concrete wall, 6mm steel reinforcement and tyre-bale were built independently as 3D deformable type in “parts” section of standard/explicit model database. The concrete wall and tyre-bale were joined together in “assembly” section by using “face-to-face” option. The steel rebar is placed inside the concrete element at 50 mm from the edges to provide appropriate concrete cover using “translate” and “rotate instance”. The remaining rebars were reproduced using pattern technique. In interaction section, embedding technique was applied to obtain appropriate bonding between concrete and rebars. The perfect bonding was assumed between tyre-bale and concrete wall surface to avoid sliding between surfaces and was obtained using “tie technique” in constraint section.

2.5.3 Loading and boundary conditions

The model consists of two steps; initial and static (general). The bottom end of both concrete walls was constraint against any translation and rotation ($U_x=U_y=U_z=U_{RX}=U_{RY}=U_{RZ}=0$), while the top end of concrete walls could only translate in vertical direction ($U_x=U_z=0$). The displacement control method was adopted to apply the displacement load on the top of concrete walls through a steel plate. These steel plates were defined as rigid bodies and assigned “reference point” in centre to extract the load. Several mesh sizes were used repetitively to obtain the convergence of the ultimate load in accordance with experimental test results. Figure 2-7 shows 3D model, interactions scheme, boundary conditions and applied load. The FEM simulated the ultimate failure load, failure mode,

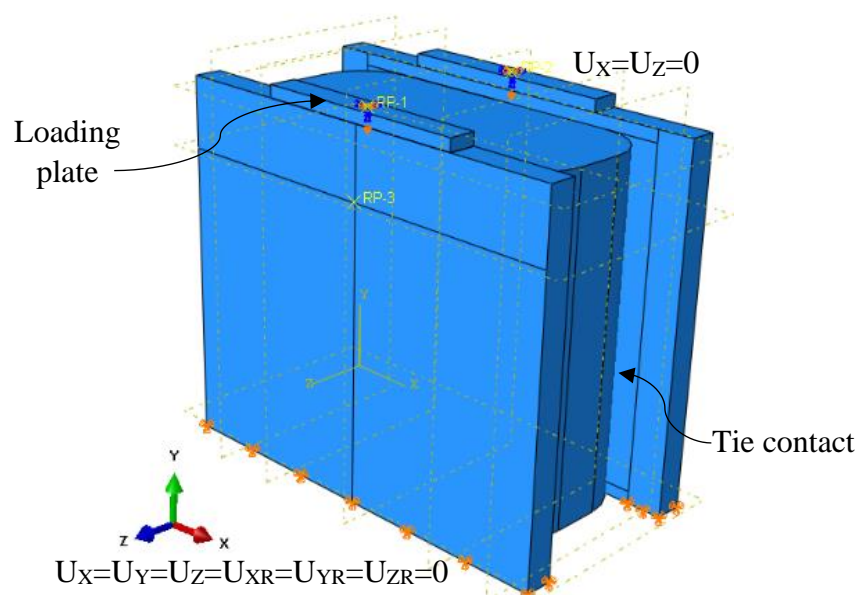


Figure 2-7 Typical finite element model of sandwich wall

concrete damage and deflections. The validation of FEM of sandwich wall was initially performed using the experimental test results of test-3. The ultimate load and vertical deflection obtained from simulation were compared with the experimental test results.

2.6 Results and discussion

2.6.1 Ultimate load capacity and load vs vertical deflection behaviour

In first compression test (Test-1), three hydraulic jacks, each with a capacity of 550 kN, were used to apply the load directly onto the core (tyre-bale). The initial vertical deflection at each end of tyre-bale is recorded using LVDTs. The maximum compression load and deformation in tyre-bale were significant in designing the remaining three compression tests. It was initially planned to apply the load on entire width of sandwich wall in all compression tests but later, the remaining three tests were modified due to compressible nature of tyre-bale since failure was expected only in concrete walls. It is pertinent to highlight that during the entire experiment, no failure was observed in tyre-bale and on increasing the load, the tyre-bale deformed in a ductile manner. The deformations became large on a small increase in applied load. A maximum vertical deflection of 234.9 mm was recorded on applying a load of 237 kN. Additional deformation could not be recorded due to limited travel of LVDT's stroke length. However, the tyre-bale deformed in non-linear elastic manner throughout the test. Upon unloading, it reverted back as shown in Figure. 2-8(a) and no damage was observed in the tyre-bale or tie-wires. This behaviour also signified the benefit of recycling the tyre-bale when sandwich wall reaches its end of service life. Figure 2-8(b) shows the comparison of the deflections at each bank of tyre-bale which indicates variable compressibility of the tyre-bale at both ends. This also resulted in tilting of load spreader during the test at one end. Therefore, the test was ended to avoid bending of cylinder in hydraulic jacks. After first test, it became obvious to apply the load on concrete walls in order to study the ultimate failure mode of sandwich wall.

In second compression test (Test-2), an initial testing load was applied on single concrete wall to allow the settlement of sand bed underneath. After initial adjustment, the load was continuously increased till failure. Elastic linear behaviour is observed before the initiation of first crack, which started to appear at around 950 kN (78% of ultimate load). The load-deflection curve became non-linear after the cracks opened up and ultimately the sandwich wall failed by crushing at a load of 1215 kN. The cracks appeared under both ends of steel loading plate, propagated straight down around 200 mm and moved toward the centre of the

wall. During the test, few hairline cracks have also been seen propagating towards the wall ends. A sudden and brittle failure was noticed in concrete wall. On failure, it was observed that the concrete wall held a strong bond with tyre-bale and prevented the concrete wall from falling over.

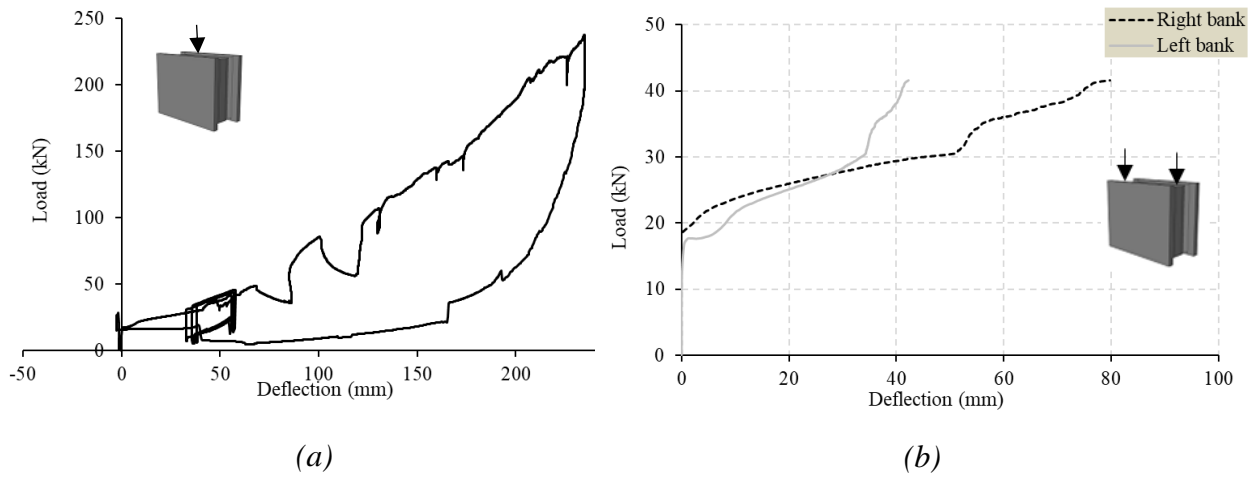


Figure 2-8 Load-vertical deflection of tyre-bale under compression load (test-1)

(a) centre of tyre-bale (b) each end of tyre-bale

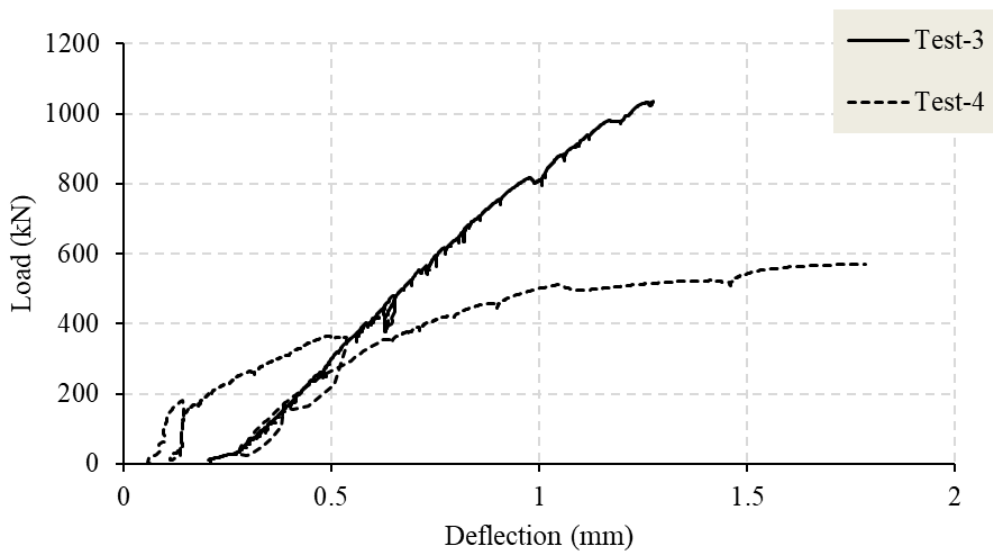


Figure 2-9 Comparison of load-vertical deflection of tyre-bale sandwich wall

In third compression test (Test-3), the load was applied on both concrete walls simultaneously. The load-deflection curve was linear elastic before appearance of first crack at 978.5 kN (94.6 % of ultimate load). The wall failed suddenly in a brittle fashion at an ultimate load of about 1034 kN. The failure and crack pattern were similar to single wall loading but failed at about 85% of ultimate failure load of single wall loading (Test-2). The difference in ultimate failure load may be attributed to number of reasons; (a) variations in concrete wall thickness, occurred as tyre-bale displaced fresh concrete during casting phase (b) variations in depth of tyre-bale projected inside the concrete wall, as it is practically impossible to keep the bonding depth similar during concrete casting.

In fourth compression test (Test-4), all tie wires were cut off manually to simulate the rupturing of wires due to severe corrosion. The aim of this test was to investigate the change in ultimate load capacity and failure mode of sandwich wall. Figure 2-9 presents a comparison of load-deflection for test-3 and test-4. The ultimate strength of sandwich wall was considerably affected and reduced to 45% of the ultimate load of Test-3 and failed at about 569.56 kN. Therefore, it is concluded that tie wires provided additional strength to the overall structural capacity of wall by holding tyre-bale and both concrete walls together. However, the mode of failure and crack patterns remained the same. The sandwich wall became unstable on reaching the ultimate failure load during the test. The load-deflection curve of test-4 illustrates constant increase in vertical deformation after reaching the peak load, which indicates continuous unstable response of sandwich wall. The comparison of results from test-3 and test-4 illustrates a significant drop in strength, when all tie-wires were cut-off. This means tie-wires along with shear connectors are assisting in smooth transfer of load from concrete wall to tyre-bale. However, in order to evaluate the precise role of shear connectors, it is recommended to conduct shear test on sandwich wall, in future. The summary of maximum load, deflections and failure pattern of each compression test is reported in Table 2-4.

2.6.2 Load vs lateral deflection behaviour

The lateral deflections were recorded along the height of sandwich wall at three locations (Figure 2-5). Figure 2-10 shows comparison of lateral deflections measured at 285mm from top of sandwich wall. In test-2, when load was gradually increased, the sandwich wall adjusted itself initially and the increase in deflection was proportional to the applied load. However, after the appearance of first crack, the specimen started to deflect in-elastically resulting in large deflection. A maximum deflection of 9.75 mm was recorded in test-2 at failure.

Subsequently, in test-3 when load was applied on both walls, a similar trend was witnessed at early stage of loading, however, on reaching the ultimate load, the wall failed in a brittle fashion by deflecting 3.52 mm in lateral direction. In test-4, a maximum deflection of 9.41mm was recorded at failure. The sandwich wall in test-4 shows large deflection values due to instability of specimen and therefore, was unable to take high load.

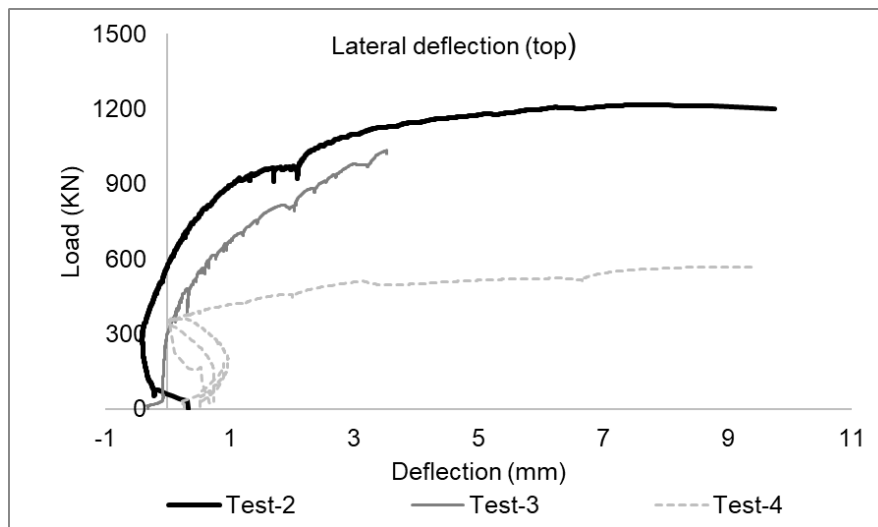


Figure 2-10 Load-lateral deflection of tyre-bale sandwich wall under different loading conditions

Figures 2-11(a-b) illustrates comparison of lateral deflection on either side of sandwich wall, which indicates that both concrete walls in test-3 and test-4 deflected simultaneously during the application of load. The maximum lateral deflection of 9.41 mm is recorded in specimen, where corrosion is simulated by cutting the tie-wires (Test-4). The lateral deflections of the wall along the height are presented in Figures. 2-12 and 2-13 at different loading stages. Figure 2-12 shows the variations in lateral deflection of the sandwich wall in test-2, whereas Figure 2-13 shows the lateral deflections of test-3. The wall deflected in a similar fashion in both test and maximum lateral deflection is recorded before the specimen failed near the top. As there was no deformation below mid height of wall during the experimental test, therefore a decrease in values can be seen towards bottom. The maximum lateral deflection recorded in single wall loading (Test-2) is higher than both walls loading (Test-3).

Table 2-4 Summary of test results in compression loading

Test	Loading condition	Ultimate load (kN)	Vertical deflection (mm)	Lateral deflection (mm)	Failure Mode
Test 1	Compression load on core (tyre-bale)	237.61	234.9	-	No failure in tyre-bale and tie-wires. Slight de-bonding of tyre-bale from concrete wall
Test 2	Compression load on single concrete wall	1215	8.57	9.75	Crack and sliding of concrete at top under loading beam
Test 3	Compression load on both concrete walls	1034	1.27	3.52	Crack and sliding of concrete at top under loading beam
Test 4	Compression load on both concrete walls (tie-wires cut)	569.56	1.78	9.41	Cracks and sliding of concrete at top under loading beam

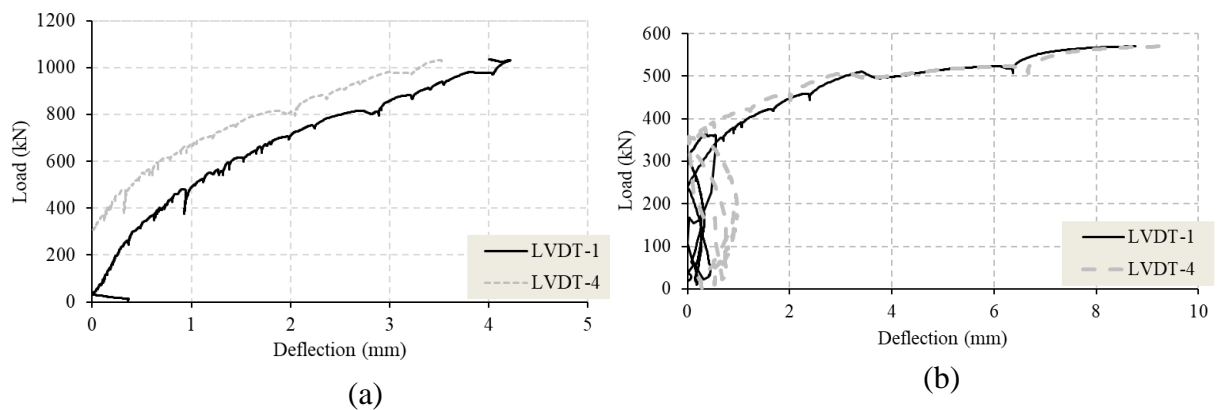


Figure 2-11 Lateral deflection at top of sandwich wall under compression load

(a) test-3 (b) test-

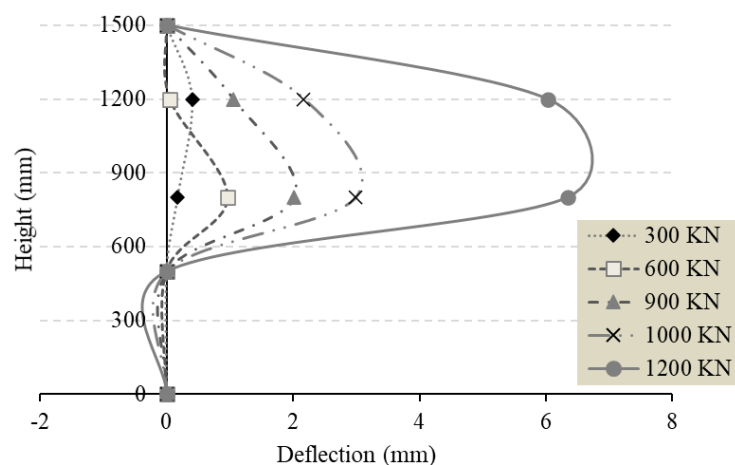


Figure 2-12 Variation in lateral deflection along the wall height of test-2

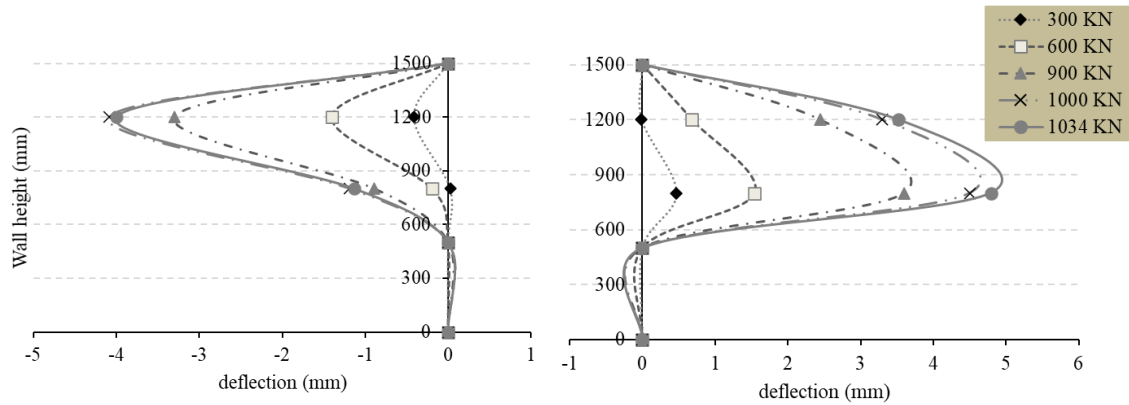


Figure 2-13 Variations in lateral deflections along the wall height of test-3

2.6.3 Strain Variations

The strain gauges were primarily placed in horizontal and vertical direction at top, mid and bottom of both walls as shown in Figure 2-6. After the second compression test (Test-2), it was observed that the failure occurred near the top end of the sandwich wall, therefore, the position of all strain gauges was adjusted. Two strain gauges (SH1 and SH2) were placed horizontally under the loading plate to capture strain variation under both ends whereas, one vertical strain gauge (SV1) was placed at the centre of wall.

Figure 2-14 shows the uniform variations in strain on the surface of concrete wall at different loading (Test-3 and Test-4). The solid line represents the specimen when both concrete walls (Test-3) were subjected to compression loading, whereas the dashed lines represent corrosion condition (Test-4). The negative and positive values of strains indicate the compression and tension on the concrete surface. The strains measured in concrete wall (Test-4) were very small ranges from 0.0001 to 0.0002 and much lower than the strain in both walls (Test-3) ranges from 0.0005 to 0.0025. The strain values remain proportional to the applied load and increased while increasing the load. After the appearance of first cracks, both curves become non-linear but still remain proportional to the load, eventually causing the failure. The strain values in SH2 and SV1 shows that specimen was in pure compression, whereas the early strain values indicated that SH1 was initially under compression in both walls but at later stage in both walls went under tension. This could be due to the variation in application of load, which exerted extra pressure at one end and eventually lead to appearance of cracks discretely. These cracks also travelled inward through the entire cross-section of the wall. All the specimens failed by concrete crushing near the top. Furthermore, it is concluded that cutting tie-wires in a tyre-bale

sandwich wall changed the strain variations and decreased the structural resistance of the wall. Thus, the behaviour near the failure load becomes sudden and unpredictable.

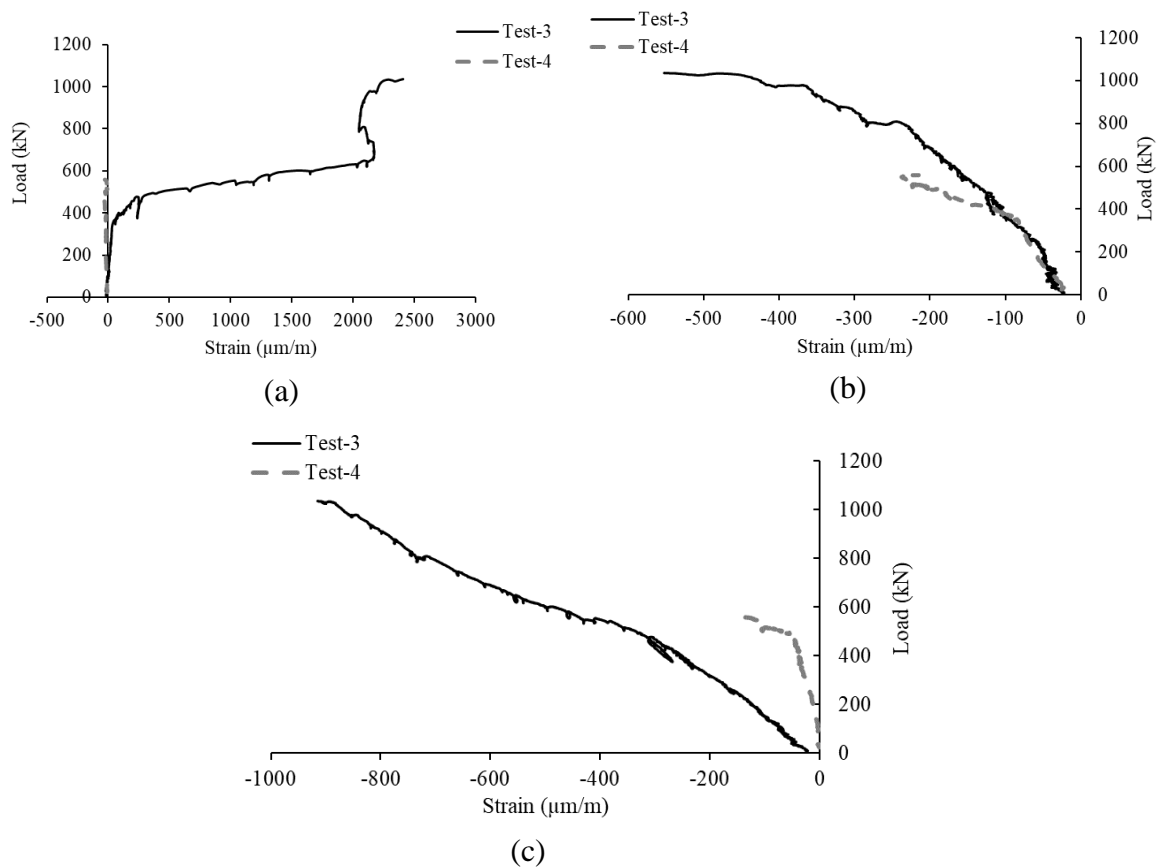


Figure 2-14 Strain variations in tyre-bale sandwich wall (a) SH1 (b) SH2 (c) SV1

2.6.4 Failure mode and cracking pattern

All sandwich walls failed below the loading plate. It is observed that the failure mode remained same in all specimens regardless of loading conditions. However, the wall strength reduced significantly on cutting all tie-wires wrapped around the tyre-bale. The integration of tyre-bale as a single unit was compromised and the sandwich wall behaved like two independent concrete walls connected together through a weak link and failed at much lower load.

During the test, all specimen initiated micro-cracks under the loading plate and failed by concrete crushing and sliding at the top. Figure 2-15 shows the actual failure of sandwich wall specimens. Since all the specimens were short and have the similar slenderness (height to thickness ratio of 12), no buckling failure was observed. The tyre-bale provided a continuous support to the inner side of both concrete wall and prevented from buckling failure. The cross-section of the wall fully contributed in resisting the applied load. The cracks pattern were initially small but started to widen up on approaching the failure load. Since, the loading was

applied to 900 mm length, which caused stress concentration under the ends of loading plate and forced the concrete to slide down by shearing. In the end, slight de-bonding between tyre-bale and concrete walls was observed, which lead to the conclusion that the undulating surface of tyre-bale may have provided enough adhesion before the failure.

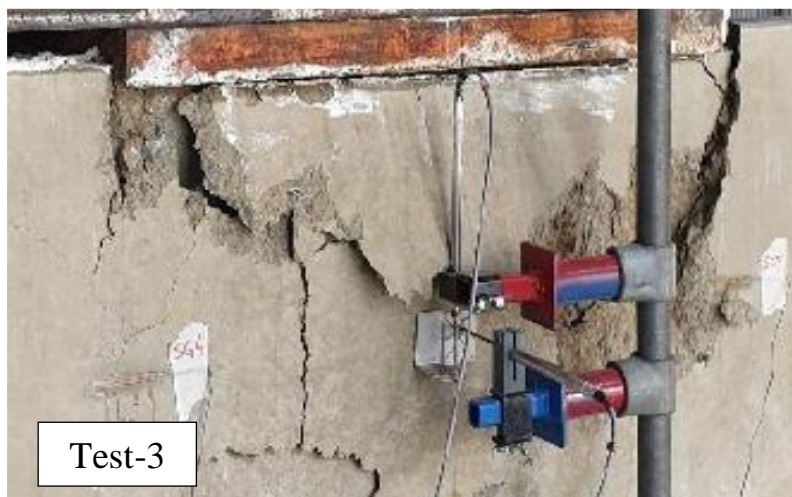


Figure 2-15 Failure behaviour in tyre-bale sandwich wall

2.7 Finite element analysis (FEA) results

The FEA analysis was conducted in two phases (a) validation of material model (b) application of compression load on full length of wall. In first phase, each concrete wall and tyre-bale was modelled using brick elements of C3D8R with mesh size of 25 mm and 80 mm respectively. The steel reinforcement was defined using two-noded 3D deformable truss element (T3D2). The mesh sensitivity analysis was performed to reduce the error and obtain the convergence of results with experimental values. The model was initially validated with the experimental results of test-3 by comparing load-deflection curve and concrete damage in compression (dc). The concrete damage in compression predicted by FE model related well with the actual failure witness in lab. Figure. 2-16 shows the failure of concrete wall in compression obtained at the end of analysis.

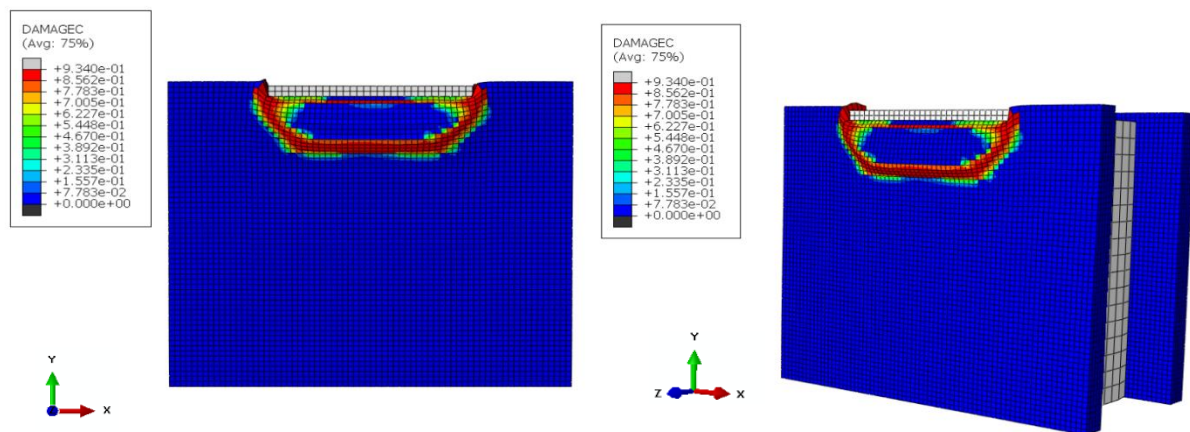


Figure 2-16 Concrete compression damage of tyre-bale sandwich wall in FEM under compression load (test-3)

The comparison of load-deflection of test-3 and FEM is presented in Figure 2-17. The behaviour of FEM model is linearly elastic at primary stage and converges with the experimental results approximately at 1034 kN. However, the load keeps on increasing and ultimately, fails at maximum load of 1190.22 kN. The FEA failure load is higher by approximately 15% than the value measured during experimental testing. The difference in ultimate load could be due to (a) variation in concrete strength, (b) non-linear behaviour of material and (c) complex nature of bonding between concrete and tyre-bale. However, FE model was still able to capture a comparable concrete compression damage. The failure load and displacement obtained from FEA and the experimental results are presented in Table 2-5.

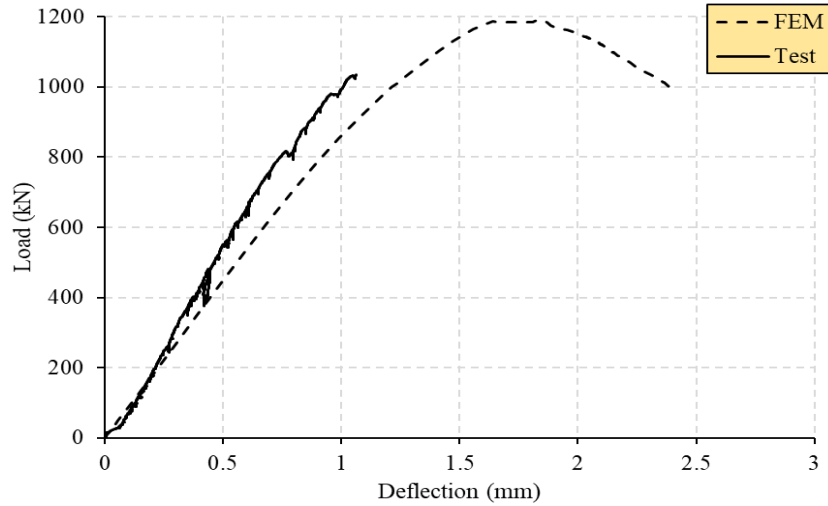


Figure 2-17 Comparison of load-deflection behaviour from experiment (test-3) and FEM

In next phase of analysis, the compression load was applied on the entire length of concrete wall to obtain ultimate load capacity and concrete compression damage. Figure 18 reflects the damage in concrete wall when complete length and cross section of sandwich wall is subjected to compression load. The model predicted the cracking of concrete wall in horizontal direction (along x-axis) and concrete crushing near top. The initiation of inclined crack pattern is symmetric from both ends of sandwich wall and propagating towards the centre. This type of failure is common in precast concrete panels, when subjected to axial loading. The results and crack pattern have been discussed in detail by previous researchers (Amran, 2016; Gara et al., 2012; Mohamad et al., 2017). The ultimate failure load of 1743.18 kN was recorded during the analysis and was terminated after load started to drop.

Table 2-5 Ultimate failure loads of experimental and FEM of sandwich wall

Wall Specimen	FEM		Experiment		Difference (%)
	Failure load (kN)	Displacement (mm)	Failure load (kN)	Displacement (mm)	
Test-3	1190.22	1.84	1034	1.27	15.10

2.8 Theoretical load capacity of walls

The ultimate load capacity of sandwich wall in compression is also computed using existing empirical models for comparison purposes. There are several models available in international concrete codes to determine the axial load capacity of solid concrete wall. The concrete wall can be either designed using the empirical equations for concrete wall or design as a column

depending upon the code requirements. The equations commonly used for design of concrete wall are listed below;

First, the simplified equation found in Australian standard AS3600:2018 for calculating the design load per unit length of a braced wall under compression (AS3600, 2018):

$$N_u = (t_w - 1.2e - 2e_a) 0.6 f'_c$$

where,

N_u = ultimate load per unit length of wall

t_w = thickness of the wall

e = eccentricity of the load measured perpendicular to the plane of the wall

e_a = an additional eccentricity taken as $(H_{we})^2 / 2500 t_w$

f'_c = compressive strength of concrete

According to American concrete institute (ACI), the equation used for estimating the design load of solid wall is (ACI, 1992):

$$P_u = 0.55 \Phi f_{cu} A_c [1 - (kH/32t)^2]$$

where,

P_u = the ultimate load

Φ = the strength of reduction factor (0.7 for reinforced member)

f_{cu} = the compressive strength of concrete

A_c = the gross area of section

$k = 0.8$ for wall brace top and bottom against lateral translation and restrained against rotation at one or both ends

H = the vertical distance between supports; or height

t = the overall thickness of member

British standard institutions (BSI) also provides an empirical equation to calculate the design load for short braced concrete walls (BSI, 1997) :

$$P_u = 0.35 f_{cu} A_c + 0.67 f_y A_{scf}$$

where,

f_y = the tensile strength of steel

A_{sc} = total area of longitudinal reinforcement

The equation for assessing the axial load of reinforced concrete wall is also stated in Euro code 2 (BSI, 2004):

$$N_{Rd} = \phi (\eta f_{cu} b h)$$

where,

N_{RD} =axial load of wall

ϕ =factor taking into account curvature, including second order effects of creep

η =effective length factor, 1.0 for compressive strength of concrete at 28 days $\leq 50\text{MPa}$

b =overall width of cross section

h =overall depth of cross section

Table 2-6 shows the axial design load of solid concrete wall using the existing code equations. ACI and BS codes yield very conservative values of axial design load and the estimated values are less than 46.80% and 47.8% of the experimental results. The axial design load calculated using AS equation gives close estimation but about 17% lower than the experimental value, whereas Eurocode overestimates the design strength of concrete wall. The possible reason behind the difference in ultimate load could be that these design equations generally imply safety factor to incorporate irregularities in material property and geometric nonlinearity. Therefore, these empirical equations may not accurately predict the ultimate design capacity of sandwich wall, however, may be used to get a safe design estimate of load.

Table 2-6 Comparison of ultimate failure load

Axial Capacity (kN)	Experiment	FEM	AS	ACI	BS	Eurocode
	1034	1190.22	857.25	550.06	539.76	1428.75

2.9 Conclusion

An innovative idea of using waste tyres was introduced in this paper. The tyres were recycled to form a tyre-bale according to BSI PAS108:2007. Four reinforced concrete sandwich walls were casted using tyre-bale as core material and tested in different compression loadings to understand the structural behaviour. The results were reported in terms of ultimate failure load, lateral and vertical deflections, strain variations and failure modes. The results obtained through experimental testing were compared with existing empirical equations proposed by various codes. Finite element modelling (FEM) was also performed in ABAQUS through concrete damage plasticity model to simulate the structural behaviour of sandwich wall. A

difference of 15% between FEM and experimental values were recorded due to various reasons. The following important findings of this research are summarized:

- The tyre-bale behaved in non-linear elastic manner and showed no sign of damage upon loading and unloading. This behaviour highlights the significance of reusing/recycling the tyre-bale, when sandwich walls reach their end of life.
- The tyre-bale sandwich wall may be employed as a structural and non-structural member, where the expected axial load (surcharge) remains below 1000 kN.
- Tie-wires holding the tyre-bale played an important role in increasing the axial resistance of sandwich wall. In case, these tie-wires are affected by severe corrosion, the axial strength of sandwich wall reduces significantly. In this study, a drop of about 55% in axial strength was recorded, when these wires were cut off to simulate the corrosion conditions. Therefore, it is imperative to employ traditional methods in protecting the tie-wires against corrosion.
- The undulating surface of tyre-bale significantly increased the bond strength between concrete wall and tyre-bale and stayed intact before the failure. Only a slight de-bonding was observed after the failure.
- The existing empirical equations used to calculate the axial design strength of concrete wall provide conservative failure load. Therefore, these equations may only be used to estimate the failure load of concrete walls.
- It is strongly suggested to perform additional research in order to understand the structural behaviour of tyre-bale sandwich wall subjected to other loading condition e.g., flexural loading, lateral loading, impact loading and shear loading etc.

2.10 References

- ACI. (1992). Requirements for Reinforced Concrete (ACI 318-89) (Revised 1992) and Commentary-ACI 318-89(Revised 1992). In Building Code Michigan.
- Amran, A., Rashid, Raizal, Hejazi, Farzad, Safiee. (2016). Structural behavior of axially loaded precast foamed concrete sandwich panels. *Construction and Building Materials*, 107, 307-320.
- AS3600. (2018). Concrete Structures AS3600:2018. In AS3600:2018. Sydney.
- Balcıoğlu, H. (2018). Flexural Behaviours of Sandwich Composites produced using Recycled and Natural Material.
- Brindley, Mountjoy, & Mountjoy. (2012). Study into domestic and international fate of end-of-life tyres (AA003649-RO1-19).
- BSI. (1997). Structural Use of Concrete BS8110 BS8110-1. In BS 8110-1:1997. London.
- BSI. (2004). Design of Concrete Structures- Part 1-1 General Rules and rules for buildings. In BS EN1992-1-1:2004. London.
- BSI. (2007). Specification for the production of tyre bales for use in construction. In PAS 108:2007. London, UK.
- Duda, A., & Siwowski, T. (2020). Pressure evaluation of bridge abutment backfill made of waste tyre bales and shreds: Experimental and numerical study. *Transportation Geotechnics*, 24, 100366.
- Esfahani, Hejazi, Vaghei, Jaafar, Karimzade, & Keyhan. (2017). Simplified Damage Plasticity Model for Concrete. *Structural Engineering International*, 27, 68-78.
- Gagnepain, J. (2017). Build Your Own Low-Cost, Earth-Friendly, High-Efficiency Home. Retrieved 20 Nov from http://www.dirtcheapbuilder.com/Articles/Tire_Bale_Home.htm
- Gara, F., Ragni, L., Roia, D., & Dezi, L. (2012). Experimental tests and numerical modelling of wall sandwich panels. *Engineering Structures*, 37, 193-204.
- Hossain, Priyantha W, & Jayawickrama. (2000). Use of whole Tyres in Earth retaining structures (0-1876).
- Huang, B., Shu, X., & Cao, J. (2013). A two-staged surface treatment to improve properties of rubber modified cement composites. *Construction and Building Materials*, 40(Complete), 270-274.
- Li, Y., Zhang, S., Wang, R., & Dang, F. (2019). Potential use of waste tire rubber as aggregate in cement concrete – A comprehensive review. *Construction and Building Materials*, 225, 1183-1201.
- Li, Z., Li, F., & Li, J. S. L. (1998). Properties of concrete incorporating rubber tyre particles. *Magazine of Concrete Research*, 50(4), 297-304.
- Mohamad, N., Goh, W. I., Abdullah, R., Samad, A. A. A., Mendis, P., & Sofi, M. (2017). Structural performance of FCS wall subjected to axial load. *Construction and Building Materials*, 134, 185-198.

Onuaguluchi, O., & Panesar, D. K. (2014). Hardened properties of concrete mixtures containing pre-coated crumb rubber and silica fume. *Journal of Cleaner Production*, 82(Complete), 125-131.

Segre, N., & Joeke, I. (2000). Use of tire rubber particles as addition to cement paste. *Cement and Concrete Research*, 30(9), 1421-1425.

WMR. (2016, 02 August 2016). A rubbery problem – the Australian scrap tyre management challenge. Prime Creative Media. Retrieved 15 Nov from <https://wastemanagementreview.com.au/a-rubbery-problem/>

Yazdi, J. Yang, L. Yihui, & Su, H. (2015). A review on application of waste tire in concrete. *International Journal of Civil and Environmental Engineering*, 9(12), 1656-1661.

CHAPTER 3 EXPERIMENTAL AND NUMERICAL STUDY ON STRUCTURAL BEHAVIOUR OF TYRE-BALE SANDWICH WALL UNDER DIFFERENT LOADING CONDITIONS

3.1 Abstract

This study presents the structural behaviour of tyre-bale sandwich wall under four-point bending and punching shear load. The research entails two stages; (a) full-scale experimental testing and (b) and numerical analysis of a 3D finite element modeling (FEM). In the first stage, two tyre-bale sandwich walls were tested experimentally in flexural bending to investigate the structural behaviour in terms of ultimate load, vertical deflection, strain distribution on the concrete surface, deflected profile, crack pattern and tyre-bale compressibility. The second stage consisted of three phases; (a) validation of the material model and assembly of different parts by comparing load-deflection curve and concrete damage in tension (b) calibration of punching shear load and boundary conditions using previous experimental research data and (c) study of ultimate load and failure mode under punching shear in tyre-bale sandwich wall. The results of the proposed 3D FEM model showed good agreement with experimental work and accurately predicted the failure mechanism. The calibrated model can be used in the future to further investigate the factors effecting the structural behaviour of tyre-bale sandwich walls under different loading conditions. Finally, the strength of reinforced concrete member was confirmed using yield line theory, which showed a fair agreement with the experimental values.

3.2 Introduction

Waste tyres are usually reprocessed in form of rethreading, recycling, energy recovery and in numerous civil engineering applications like slope stabilization, road embankments and noise reduction barrier (Hylands & Shulman, 2003). The whole used tyres are frequently wrapped together using a baler machine to form a tyre-bale. These tyre-bales have been used in highway projects as a fill material owing to the ease of manufacturing tyre-bale (Freilich & Zornberg, 2009). Table 3-1 shows the summary of tyre-bale applications in various projects completed in the USA and UK. Moreover, British standards institution (BSI) published comprehensive specifications for the construction of tyre-bale in PAS 108:2007, which aimed at standardizing the construction process and provided standard dimensions for a typical tyre-bale. Numerous research studies on the use of tyre-bale in the construction of retaining wall system, highway noise abatement barriers, impact barriers, erosion control and wing walls can be found in the

literature (Ayrilmis et al., 2009; Garga & O'Shaughnessy, 2000; Keleştemur, 2010; Keller & Gordon, 1990; M. A. Yazdi, 2015; Shu & Huang, 2014; W. & A., 2006; W. Prikryl et al., 2005; Yazdi et al., 2015).

Table 3-1 Existing tyre-bale applications in different projects

Tyre-bale use	Location	Project	Year	Reference
Road foundation	Highland Council, Scotland	Road construction	2002	(Freilich & Zornberg, 2009)
Subgrade construction	Chautauqua County, New York	Road construction	2003	
Embankment construction and slope stabilization	Fort Worth, Texas	IH 30 embankment repair	2005	
Fill material	Mountain Home, Arkansas	Dam construction	2001	
Retaining wall	US550, New Mexico	Gravity retaining wall	-	
Soil erosion control	Carlsbad, New Mexico	Pecos River in lake Carlsbad	1997	(Keller & Gordon, 1990)
Structural wall	Cypress, Texas	Structural concrete building product	-	

In structural engineering, tyre-bale can be used as a core material enclosed between reinforced concrete walls to form a tyre-bale sandwich wall. These walls can be employed as blast resistant walls, roadside barriers, retaining walls, border walls and wing walls for rivers and dams. Ecological building system in Texas, USA manufactured different sizes of reinforced concrete units using tyre-bale as core material. Two types were developed i.e. reinforced concrete units for structural applications and unreinforced units for non-structural applications. It was mentioned that each unit contains at least one ton of recycled tyres, which displaces around 72% of concrete volume (compare to the solid concrete wall) and therefore reduces the overall

cost at around 52% (Hossain et al., 2000). Furthermore, when the sandwich wall reaches its service life, the tyre-bale can be recycled by replacing the concrete walls. The article however lacks engineering and technical details about the structural response of the member under different loadings. After a comprehensive literature review, it was established that the concept of using tyre-bale for structural purposes has not been fully investigated.

The structural use of tyre-bale sandwich wall is still limited worldwide due to the lack of research on the technical properties and the mechanical behaviour, which ultimately led to study the structural efficiency of tyre-bale sandwich wall. The axial response of tyre-bale sandwich wall was investigated in previous research study (Awan & Shaikh, 2021). In addition, when these walls are employed as retaining walls in order to stabilize the soil, they are primarily subjected to flexural bending. Similarly, various tying techniques (like soil nailing) are used to secure the walls against overturning with reinforcing steel and bearing plate, which normally applies punching load on the structural member. Therefore, it is significant to explore the structural response of these walls under both flexural bending and punching loading. This research will also guide professional engineers and industrial experts to enhance the use of sandwich wall for civil engineering projects.

In this study, two tyre-bale sandwich walls were manufactured and tested experimentally to study the ultimate failure load, vertical deflection, failure mode, cracks propagation and strain variations. The experimental setup was specially designed to conduct large scale flexural testing on the walls. The tyre-bale sandwich wall was modelled in finite element software ABAQUS and validated with experimental results. A good agreement of results was found. Since, it was not possible to apply punching shear load due to limitation of lab equipment, therefore FEM was conducted to understand the structural behaviour under punching shear load. For this purpose, validation of loading and boundary conditions was performed. Afterwards, these calibrated loading condition and constraints were applied to numerical model of tyre-bale sandwich wall to study the structural response under punching shear load in terms of ultimate load, concrete damage in tension and crack pattern.

3.3 Experimental program

The tyre-bale sandwich wall consists of three parts: two outer reinforced concrete walls, the core containing tyre-bale and shear connectors.

- a. *Reinforced concrete wall.* Each reinforced concrete wall is 125 mm thick and reinforced with 6 mm diameter bar in both horizontal and vertical directions. The

centre-to-centre spacing of reinforced bar is 100 mm and have a concrete cover of 50 mm. The density of concrete is 2443 kg/m³.

- b. *Tyre-bale*. The typical dimensions of a tyre-bale varies such as length (1270 - 1410) x width (1480 – 1520) x depth (790 -870) mm³. The tyre-bale consisted of minimum 100 used tyres, compressed together using a baler machine. All bales were manufactured according to British Standard Institution (BSI), PAS108:2007 specification and pertinent technical details can be found in the reference (Institution, 2007). The tyre-bale was wrapped together using five 4 mm diameter stainless steel tie-wires. The technical properties of tyre-bale and tie-wires are provided in Table 3-2.
- c. *Shear connectors (M12 bolts)*. In order to strengthen the bond between reinforced concrete wall and tyre-bale, four M12 bolts were used on each side. The tyre-bale was equally dividing in four parts and the bolt was placed at the centre of each part. The bolt-head was deeply immersed in the concrete wall whereas, the threaded end was screwed directly into tyre-bale.

Table 3-2 Engineering properties of tyre-bale as per BSI PAS 108:2007

Material	Nominal density (kg/m ³)	True density (kg/m ³)	Young modulus (MPa)	Poisson's ratio (ν)
Tyre-bale	470 (±50)	500 (±70)	800 – 1000	0.3
Tie-wires	-	7800	200,000	0.3

3.3.1 Tyre-bale manufacturing and construction phase

Initially, the tyre-bale was manufactured by placing capping tyres in a horizontal position at the bottom. The tyres were filled in herring-bone arrangement in baler machine up to the top. In the second stage, compression load was directly applied to the tyres to generate space for the addition of remaining tyres. The process was repeated until the mandatory length was achieved. Lastly, the capping tyres were placed on the top. At the end, the tyre-bale was wrapped with five evenly spaced tie-wires. The nominal density of each tyre-bale is usually greater than 420 kg/m³.

Subsequently, the next phase entails the construction of tyre-bale sandwich wall. The reinforcement mesh was placed in the formwork by providing adequate concrete cover and fresh concrete was poured. The concrete was thoroughly vibrated to eliminate air voids. One side of tyre-bale was immersed in the fresh concrete with the help of a crane. This practice lasted until the concrete has hardened. The second concrete wall was manufactured by

removing and flipping over the tyre-bale and following the similar practice. The material properties of concrete were obtained by drilling the core in each wall and later testing the samples in the lab as shown in Table 3-3. The overall size of tyre-bale sandwich wall is 1770 x 1470 x 900 mm³ (Figure 3-1).

Table 3-3 Properties of concrete and reinforced steel

Materials	Density (kg/m ³)	Compressive strength (MPa)	Ultimate tensile strength (MPa)	Elastic modulus (GPa)	Poisson's ratio (ν)
Concrete	2443	13.3	-	12	0.20
Steel bar (6 mm)	7800	-	574	200	0.30

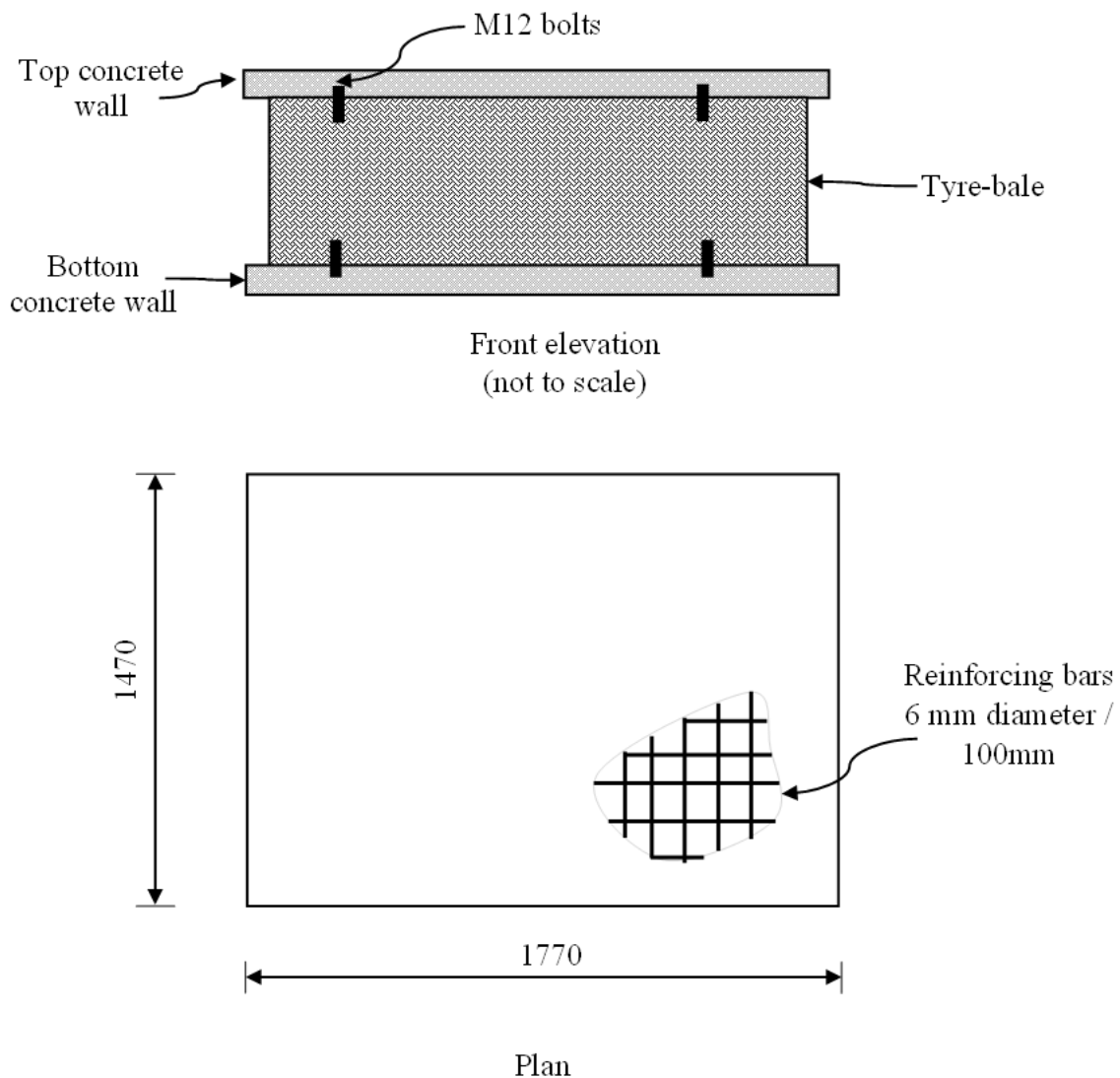


Figure 3-1 Details of tyre-bale sandwich wall (all dimensions are in mm)

3.3.2 Instrumentation

The vertical deflection and strain distribution was measured using linear voltage differential transformer (LVDT) and strain gauges respectively. A total of nine LVDTs with 100 mm travel length were used as shown in Figure 3-2. Six LVDTs were positioned on the bottom concrete wall to record the vertical deflections in the centre (LVDT-2 and 5) and under each applied load at the front and rear side (LVDT-1, 3, 4 and 6) respectively. This arrangement of LVDTs later assisted in generating the deflected shape of the sandwich wall. In order to measure the compressibility of tyre-bale along the width, three LVDTs (LVDT 7-9) were placed on the top of concrete wall in the centre (Figure 3-3).

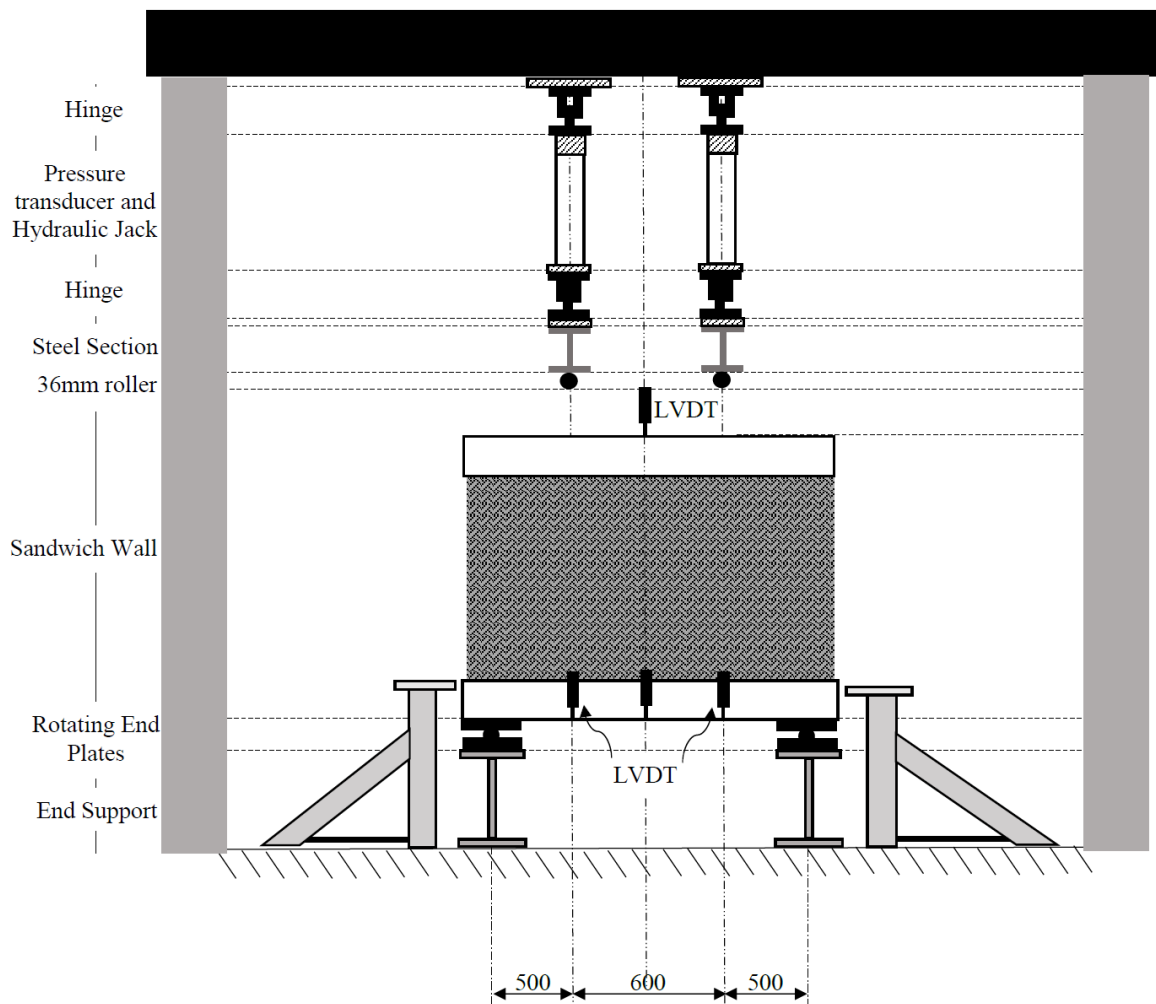


Figure 3-2 Test setup and Instrumentation - front elevation (all dimensions are in mm)

The strain distribution was recorded using the electrical strain gauge of 60 mm length, gauge resistance of 120Ω and gauge factor of $2.08 \pm 1\%$. As, the sandwich wall was expected to fail in flexural bending, therefore, the strain gauges were used only on the bottom concrete wall. Five strain gauges were used along the length and width of bottom concrete wall, in which three strain gauges were evenly placed at the centre along the width while the other two strain gauges were placed between the support and applied load (Figure 3-4). In order to provide a level surface for recording vertical deflections, L-shaped aluminium angles were attached to the bottom concrete wall with glue. The concrete surface was also prepared for attaching the strain gauges by removing dust, sanding and wiping with acetone. CNE adhesive was used to bond the strain gauges tightly with the concrete surface by removing air voids.

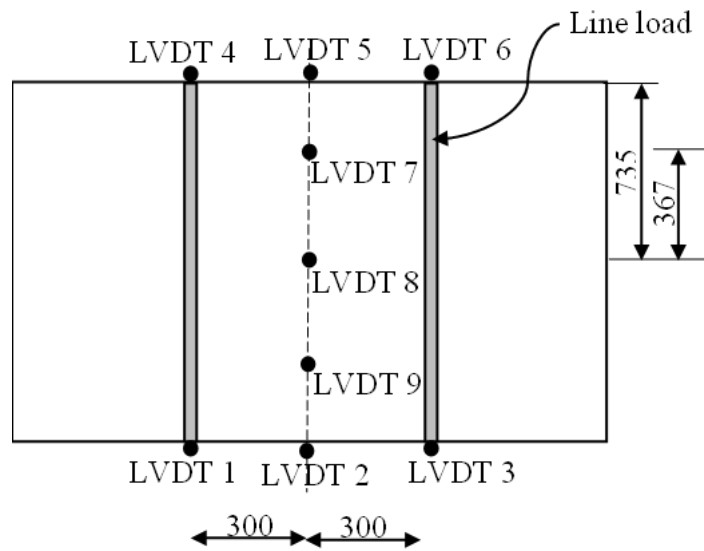


Figure 3-3 Instrumentation – location of LVDTs – plan (all dimensions are in mm)

Note: LVDT 1-6 on bottom concrete wall and LVDT 7-9 on top concrete wall

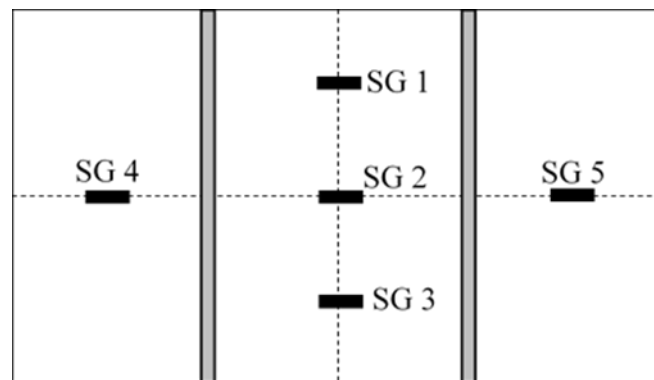


Figure 3-4 Instrumentation – location of strain gauges (all strain gauges are placed on bottom concrete wall)

3.3.3 Test setup

Two specimens were tested in flexural bending using a reaction frame of 4000 kN. The setup was built using four hydraulic jacks (SPX RD5518) double –acting hydraulic pump, two 1500 kN steel load spreader (UB-460) attached with 36 mm diameter round bars, rotating steel plates and steel hinges. Two hydraulic jacks were used on each bank to apply a line load on the sandwich wall; where the bottom end of the hydraulic jack was attached to steel load spreader through a steel hinge, while the top end was secured with the reaction frame by another steel hinge. The load spreader was attached with 36 mm diameter round bar through 25 mm thick steel plates in order to provide a smooth contact between the surfaces and avoid shear damage to the surface of top concrete wall. The steel sections were positioned on the flat ground at each end to provide support to the sandwich wall. The rotating steel plates were welded on top of these steel section to restrict translation in all directions and allowing the rotational degree of freedom around z-axis only. In order to safeguard against sudden failure, extra supports were also placed on both ends as shown in Figure 3-2. The distance between the load spreader was kept 600 mm while the distance between load spreader and pin support was 500 mm on each side. The width of rotating plates was 100 mm.

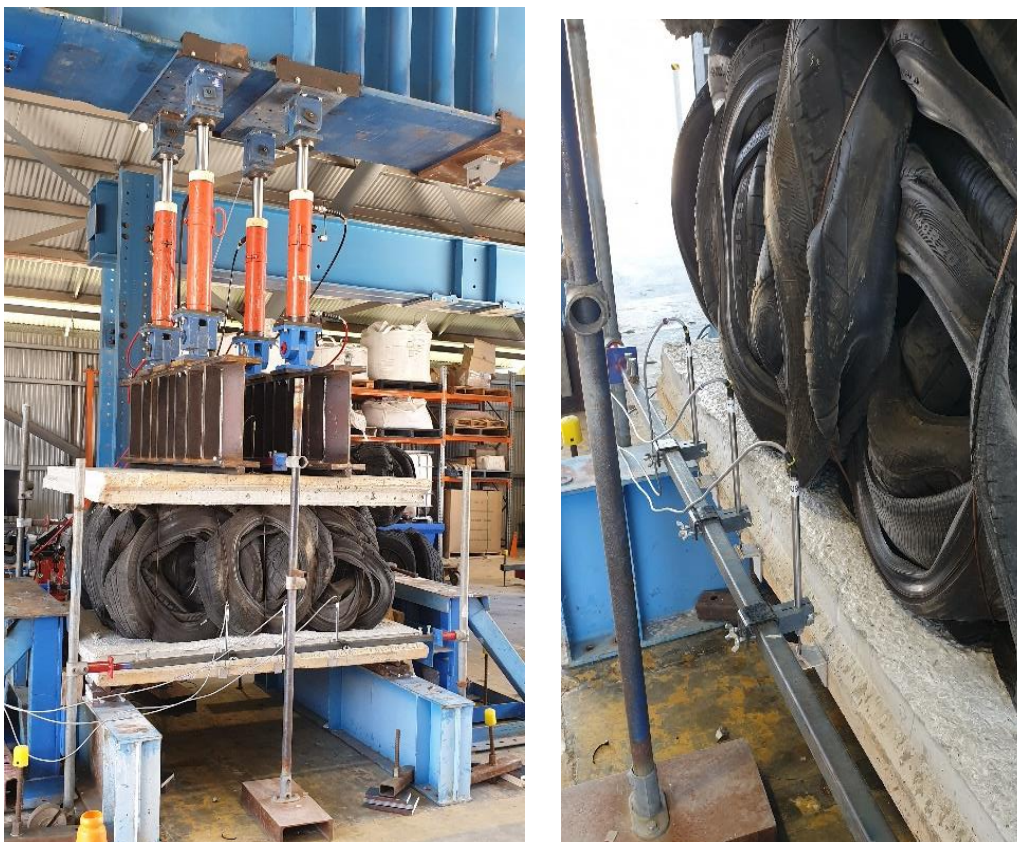


Figure 3-5 Flexural bending test setup

The sandwich wall was placed in a horizontal position using a fork-lift machine. All the dimensions were accurately measured and marked to ensure the sandwich wall was positioned centrally in the middle of test setup. All LVDTs and electrical strain gauges were attached as shown in Figure 3-4. An initial load of 3 kN was applied on the sandwich wall to check the working of all instruments. After the initial checking, the load was gradually increased till the failure and the test data was recorded and stored in the data logger (HBM – Quantum X). The real flexure bending test setup build in lab is illustrated in Figure 3-5. During the testing, the specimen was regularly checked and marked for the visible cracks.

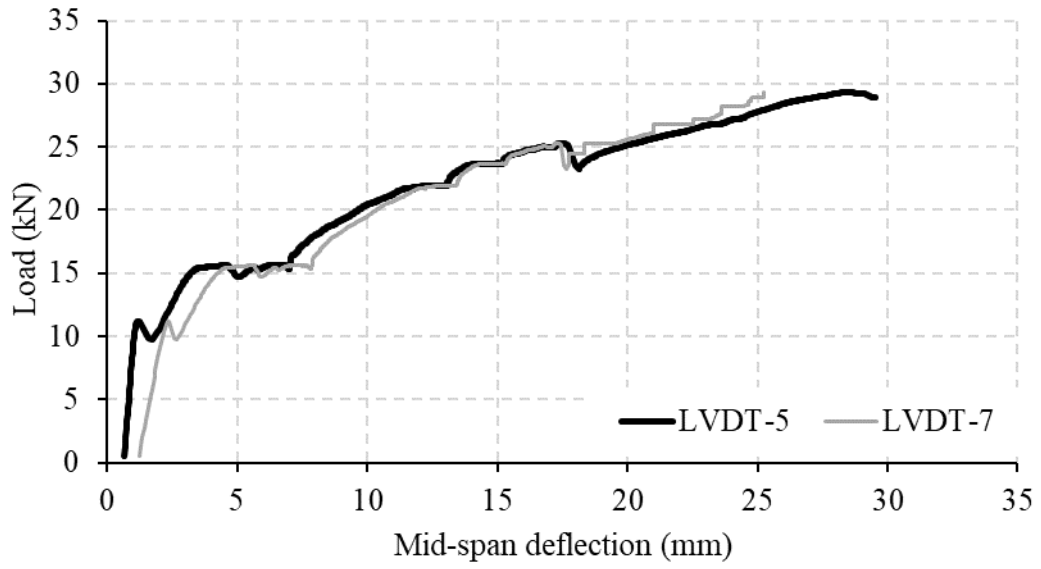
3.4 Results and discussion

3.4.1 Experimental results

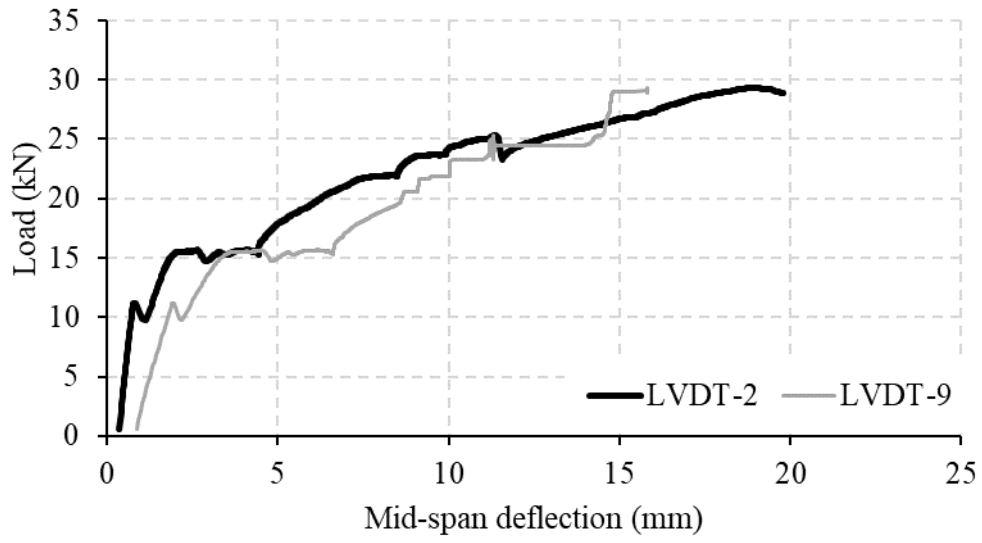
Two sandwich walls were tested in four-point bending. The structural behaviour is elaborated in the following sections by discussing ultimate failure load, vertical deflections at centre and under the applied load, deflected profile, strain distribution on the surface of bottom concrete wall and failure in terms of formation of cracks.

3.4.2 Compressibility in tyre-bale

Figures 3-6 and 3-7 compare the deflections recorded in the centre of both sandwich walls. LVDT-2 and LVDT-5 measured deflections in the bottom concrete wall (dark line) whereas, LVDT-7 and LVDT-9 recorded the deflections in top concrete wall in the centre (grey line). The top and bottom concrete walls deflected simultaneously before the propagation of cracks and a similar response was recorded on load-deflection curve. The first crack appeared in the bottom concrete wall, which started to deflect independently as illustrated in Figures 3-7 and 3-8. However, a negligible difference in vertical deflections between the top and bottom concrete wall indicates that tyre-bale experienced insignificant compression at such a low load during the test and behaved almost like a solid stiff body. A maximum deflection of 25.25 mm was recorded in top concrete wall, whereas bottom concrete wall deflected up to 29.52 mm. The line load applied on the top concrete wall directly transferred to the tyre-bale and ultimately, applied an area load to bottom concrete wall. A difference of 9.76 mm in vertical deflection was recorded at LVDT-2 (front-side) and LVDT-5 (rear-side) proves that non-uniform load was applied on bottom concrete wall, which resulted in deflection variations across the width of wall.

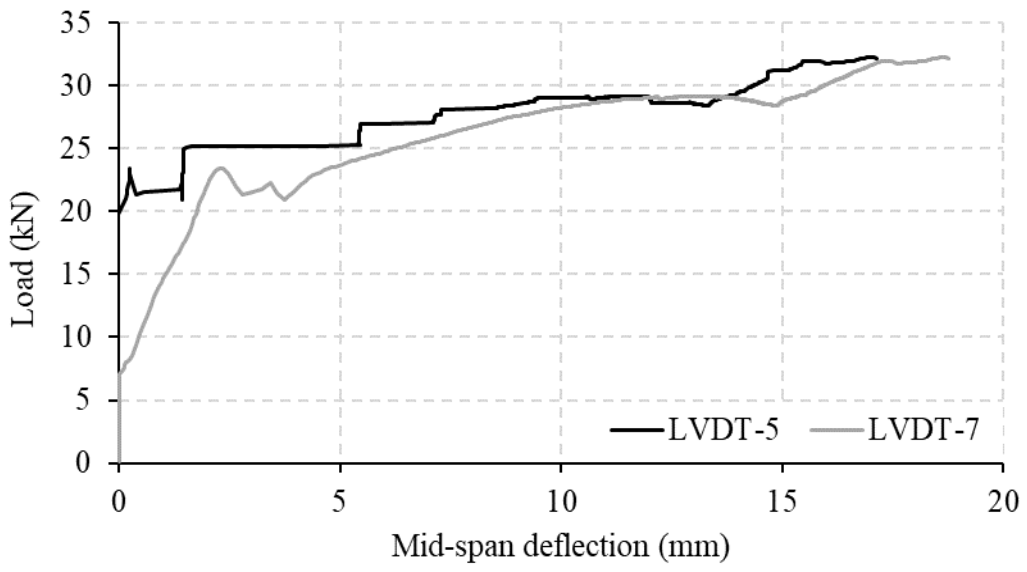


(a)

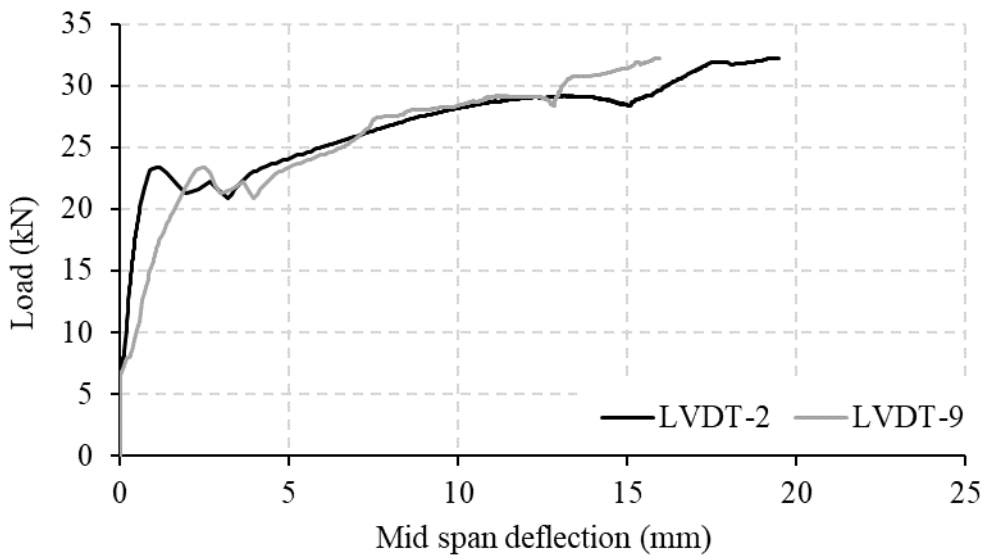


(b)

Figure 3-6 Vertical deflection of wall-1 at mid span a) rear side b) front side



(a)



(b)

Figure 3-7 Vertical deflection of wall-2 at mid span a) rear side b) front side

3.4.3 Concrete Damage and cracks formation

It is vital to highlight that the bottom concrete wall was carefully inspected for the development of any hairline cracks under self-weight of tyre-bale and top concrete wall before starting the test. The self-weight of tyre-bale and the top concrete wall generated an area load of 6.13 kN/m^2 . After visual inspection, no visible cracks were seen on the surface of the bottom concrete wall before the testing. During the experimental testing, it was observed that there was no damage in the top concrete wall as the entire concrete wall was thoroughly supported on the tyre-bale and acted as load distribution member whereas, the bottom concrete wall failed in tension and behaved similar to a solid reinforced concrete slab. The failure started by the initiation of flexural cracks between the applied loads (maximum moment area). These cracks travelled vertically through the entire depth of the bottom concrete wall towards tyre-bale and, along the width of the bottom concrete wall parallel to the supports. The entire depth of the bottom concrete wall contributed in resisting the applied load. The development and pattern of cracks are similar to the solid concrete slabs as reported by Ahmad et al (Ahmad et al., 2017). However, no failure was witnessed in the tyre-bale and tie-wires. The actual failure and crack pattern in the bottom concrete wall can be seen in Figure 3-8 taken before the removal of specimen from the reaction frame.



Figure 3-8 Crack pattern in bottom concrete wall during experimental testing

3.4.4 Vertical deflection

Figure 3-9 shows the load-deflection curve of both sandwich walls measured at mid-span of the bottom concrete wall. The specimen initially behaved linearly up to 10.85 kN and 9.41 kN respectively and started to deflect non-linearly on the appearance of initial cracks. As the crack size widened up, the large deflections were recorded at mid-span on a slight increase in applied load. The maximum vertical deflections of 19.76 mm and 19.48 mm were recorded by LVDT-2 (front-side) near the failure. These large deflections depict a flexural failure in the bottom concrete wall, where the reinforcement usually yields before the failure and prevent the structural member from brittle failure. The post-cracking behaviour of the bottom concrete wall revealed that the wall continued to resist the applied load even after the appearance of the first crack, exhibiting ductile failure on reaching the ultimate load. The variation in structural behaviour of both walls could be due to the undulating surface of tyre-bale and inconsistent depth between tyre-bale and concrete. Table 3-4 presents a summary of first cracking load, cracking moment, failure load, ultimate moment and failure mode in tyre-bale sandwich wall.

Table 3-4 Summary of experimental results in flexural bending

Specimen	Cracking load (kN)	Cracking moment (kN-m)	Ultimate load (kN)	Ultimate moment (kN-m)	Failure
Wall-1	10.85	5.425	32.16	16.08	Flexural cracks in bottom concrete wall
Wall-2	9.41	4.705	28.86	14.43	

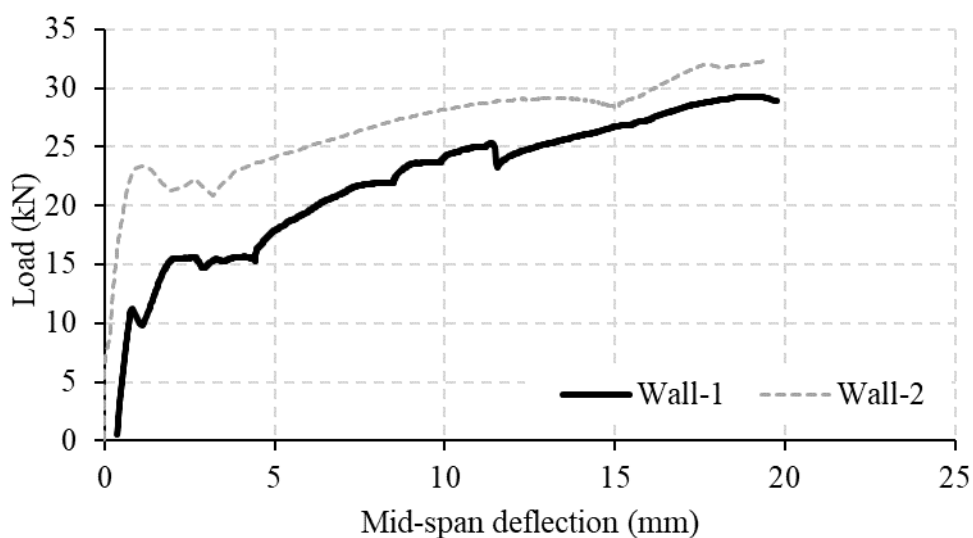
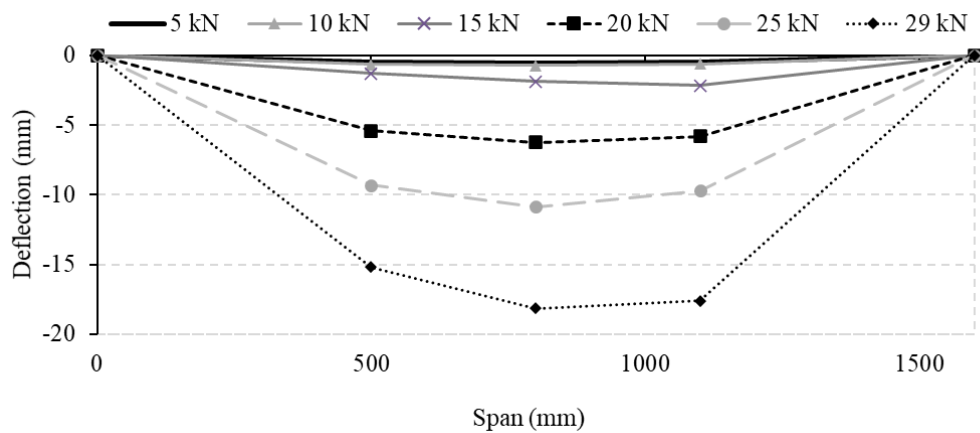
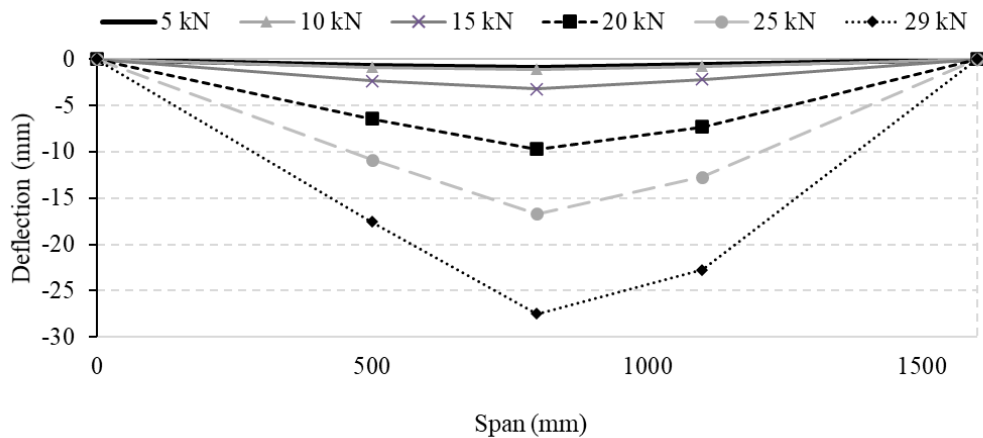


Figure 3-9 Ultimate load versus vertical deflection at mid-span (front-side)

Figures 3-10 and 3-11 illustrate the deflected shape of the sandwich wall plotted at different loading stages. It is worth noticing that the wall did not experience significant deflection at the early stage of loading however, a major increase is witnessed as the applied load started to approach the failure. The maximum vertical deflection of 18.15 mm and 12.55 mm occurred at the mid-span (front-side) just before the failure. The deformed shape of the bottom concrete wall demonstrates that the vertical deflection is not symmetric along the span in either sandwich wall and even varies along the width from front face to back.



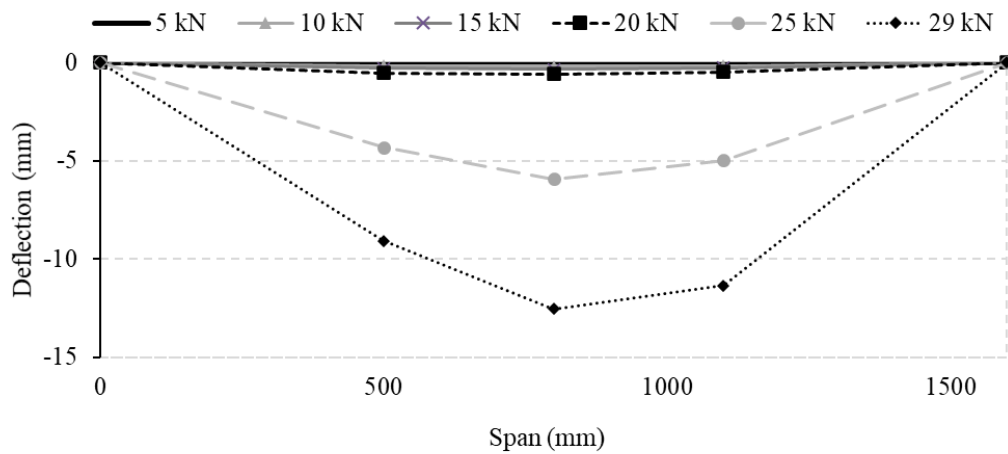
(a)



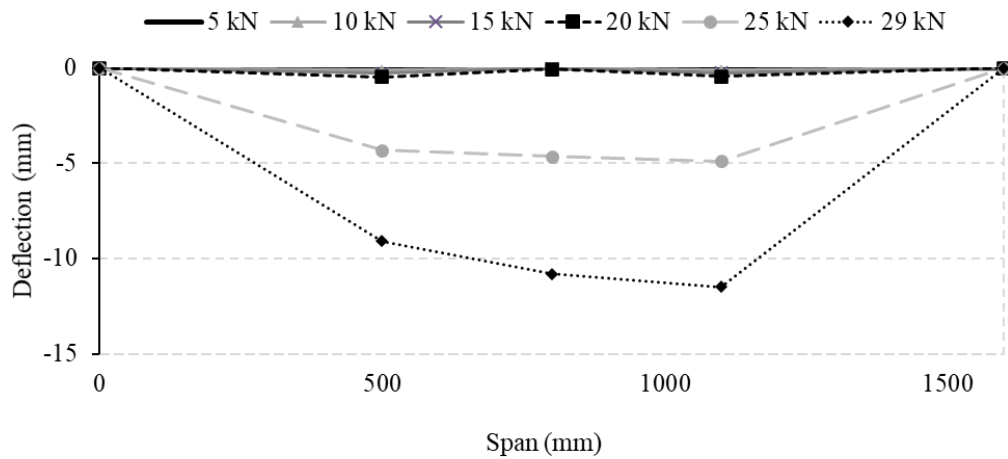
(b)

Figure 3-10 Deflected profile of tyre-bale sandwich wall-1 (a) front side (b) rear side

As per Australian standards (AS3600, 2018), the total deflection in slabs and beams under working loads should not exceed span/ 250 in order to alleviate damage to the structure. For structural members in transferring loads, the deflection should not exceed span/ 500. The vertical deflection in both specimens measured before the appearance of the first crack is below the deflection limits, which reveals that both specimens performed reasonably.



(a)



(b)

Figure 3-11 Deflected profile of tyre-bale sandwich wall-2 (a) front side (b) rear side

3.4.5 Strain variations

As anticipated, there was no failure in the top concrete wall during the entire test therefore, Figure 3-12 illustrates the strain variations for the bottom concrete wall. The positive sign displays the tensile strain while the compression strain in the member is shown in negative. The bottom concrete wall initially developed stresses, which are proportional to tensile strain and on increasing the applied load, the increase in strain led to the development of flexural cracks in the bottom concrete wall. The strain increased rapidly during the loading and damaged the strain gauges i.e. SG-1 in wall-1 and SG-4 in wall-2. Therefore, the unexpected higher values recorded by these strain gauges were deleted after detecting damage in them. The maximum values of tensile strain were measured in SG-1 (mid-span) in wall-1 as shown in Figure 3-12(a) and SG-4 and SG-5 (between load and support) in wall-2 in Figure 3-12(b).

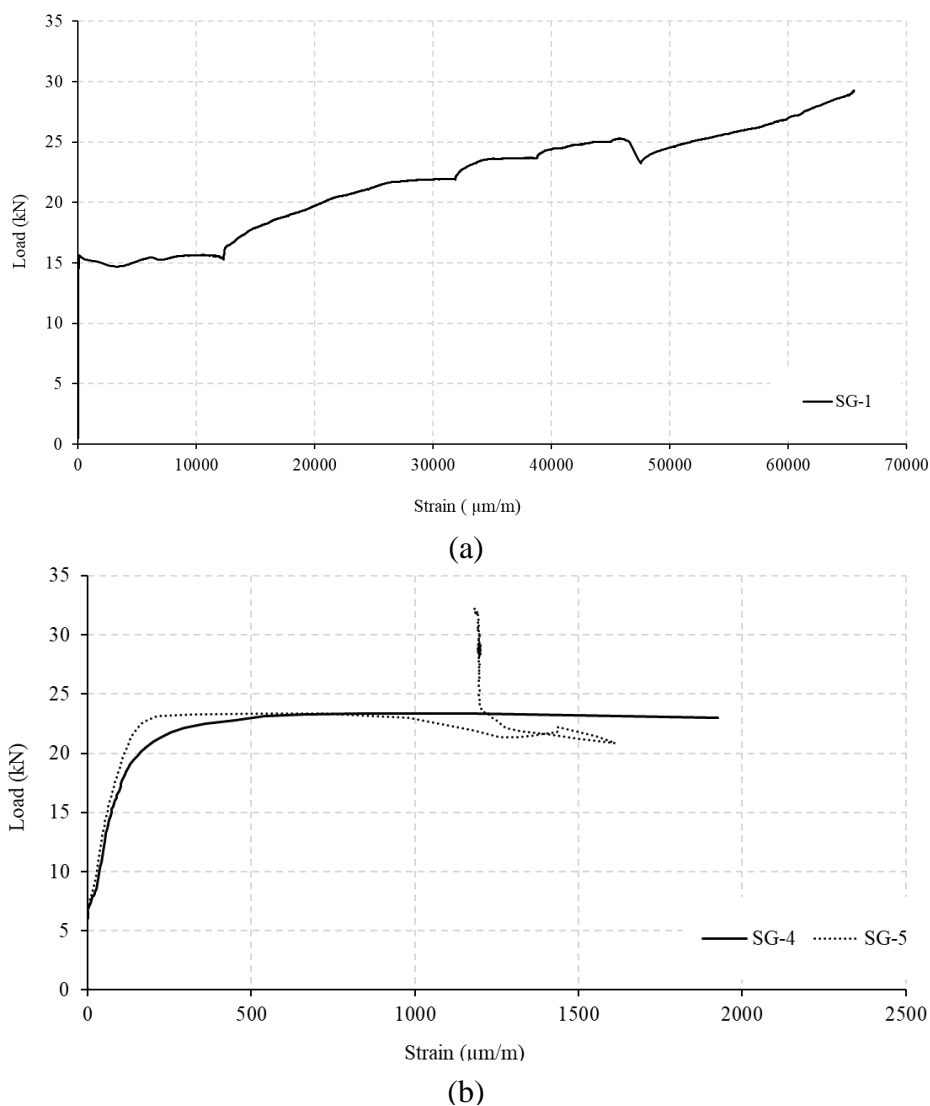


Figure 3-12 Strain distribution in bottom concrete wall (a) wall-1 at mid-span (b) wall-2 between applied loads and support

The strain recorded at five points shows dissimilar crack propagation in both walls. In wall-1, the maximum strain of 0.065 occurred at mid span, whereas wall-2 had a maximum strain of 0.0019 and 0.0016 between support and applied load. It is therefore established that the undulating surface of tyre-bale applied non-uniform pressure on the bottom concrete wall, which led to the formation of different crack patterns in both walls. However, both walls developed flexural cracks between the applied loads i.e. maximum moment area.

3.4.6 Assessment of composite behaviour

The degree of composite behaviour was evaluated at the elastic stage using cracking load and deflections whereas the strength method was adopted at the ultimate stage. At linear stage, the degree of composite action (K_1) was calculated using following equation (1), in which I_E is the experimental moment of inertia, I_C is theoretical moment of inertia of fully composite action and I_{NC} is theoretical moment of inertia of non-composite action. The experimental moment of inertia was calculated using equation (2).

$$K_1 = \frac{I_E - I_{NC}}{I_C - I_{NC}} \quad - \quad (1)$$

$$I_E = \frac{Pa}{24E_C\Delta} (3L^2 - 4a^2) \quad - \quad (2)$$

where, P = load acting on specimen, a= shear span length, L= clear span length, E= modulus of elasticity of concrete and Δ = mid-span deflection, as shown in figure 3-2.

At the ultimate stage, the theoretical fully composite (P_C) and non-composite (P_{NC}) loads were calculated using Benayoune (Benayoune et al., 2008) approach. When the specimen was considered fully composite, both concrete walls acted as one structural member to resist the applied loads, whereas, in a non-composite approach, the flexural strength of each concrete wall was calculated separately. The percentage of composite action (K_2) at ultimate load is given by equation 3.

$$K_2 = \frac{P_E - P_{NC}}{P_C - P_{NC}} \quad - \quad (3)$$

The theoretical load calculated for fully composite and non-composite action are 265 kN and 29.44 kN respectively. Table 3-5 shows the summary of the percentage of composite action at linear and the ultimate stage. The tyre-bale sandwich wall is in the initial stage of development and lack refined research. The composite action was initially expected to be achieved through M12 bolts and tie wires. However, a negligible percentage of composite action was witnessed

in both specimens, which indicates that flexural stresses were only resisted by the bottom concrete wall and M12 bolts were unable to contribute effectively in transferring stresses. Therefore, it is recommended to improve the composite action of tyre-bale sandwich wall by employing the latest techniques.

Table 3-5 Assessment of composite behaviour for both specimens

Specimen	Stiffness method				Strength method	
	Cracking load (kN)	Deflection (mm)	I_E (10^7 mm^4)	K_1 (%)	Ultimate load (kN)	K_2 (%)
Wall-1	10.85	0.205	61.3	0.486	32.16	1.15
Wall-2	9.41	0.161	67.7	0.681	28.86	-0.106

3.5 Numerical analysis

3.5.1 Finite element modeling of tyre-bale sandwich wall

The finite element modeling was performed in commercially available software “ABAQUS/CAE 6.14-5” in standard/explicit model to investigate the structural behaviour of tyre-bale sandwich wall. The vertical deflection at mid-point and ultimate failure load was observed during the analysis to obtain concrete damage similar to experimental testing.

Primarily, all the individual members were built separately as a 3D deformable solid body in parts section in x-y plane and extruded along z-direction. Linear elastic behaviour of concrete was assigned using modulus of elasticity ($E = 12 \text{ GPa}$) and Poisson ratio ($\mu = 0.2$). The non-linear behaviour of concrete was defined using the plasticity model in concrete damage plasticity (CDP). The input parameters used in this study were dilation angle, eccentricity, f_{b0}/f_{c0} , K and viscosity parameter (Table 3-6), where compression behaviour and tensile behaviour was modelled using yield stress, inelastic strain and damage parameters. The parameters used in numerical simulation of concrete were obtained from previous research (I. Goh et al., 2016). For steel, the input parameters for the linear elastic region were elastic modulus ($E = 200 \text{ GPa}$) and Poisson ratio ($\mu=0.3$) while the non-linear region was defined using yield stress and plastic strain. The input parameters for tyre-bale were elastic modulus ($E = 500 \text{ MPa}$) and Poisson ratio ($\mu = 0.3$) (Freilich & Zornberg, 2009).

After defining parts and material properties, all parts were assembled together using rotation and translation method in the assembly section (Figure 3-13). The step module consisted of initial and static, general. The tyre-bale and concrete wall surface was connected using the tie technique, whereas the reinforcement mesh was arranged inside the concrete and bonded using

embedded region. The supports were assigned as rigid bodies and connected with the concrete wall using tie technique. A vertical displacement was applied on the top concrete wall in y-direction ($U_x=U_z=U_{RY}=0$), whereas the supports were only allowed to rotate around z-direction i.e. $U_x=U_y=U_z=U_{RX}=U_{RY}=0$. In order to minimize the analysis time and the number of elements, only half model was generated and the symmetry boundary conditions (z-symm) were applied in x-y plane. However, the results were plotted for the full model after the completion of analysis.

Table 3-6 Concrete damage plasticity parameters used in FEA

Dilation Angle	Eccentricity	Initial biaxial/uniaxial ratio (f_{b0}/f_{c0})	K	Viscosity parameter
27°	0.1	1.16	0.67	0

Both concrete walls and tyre-bale were defined as homogenous sections using C3D8R with a mesh size of 20 mm and 50 mm respectively. During the experimentation, tyre-bale experienced insignificant compression on low load (failure load of 32 kN) and transferred the entire load to the bottom concrete wall. No deformation in terms of expansion was witnessed in the tyre-bale and almost behaved like a solid stiff body. A load of 668 kN to 2668 kN is reported in the literature to produce significant deformations (Freilich & Zornberg, 2009). In order to study the crack pattern in the bottom concrete wall, special field output was requested for concrete damage in tension. The convergence of results were obtained by comparing the load-deflection curve for both experimental testing and numerical analysis.

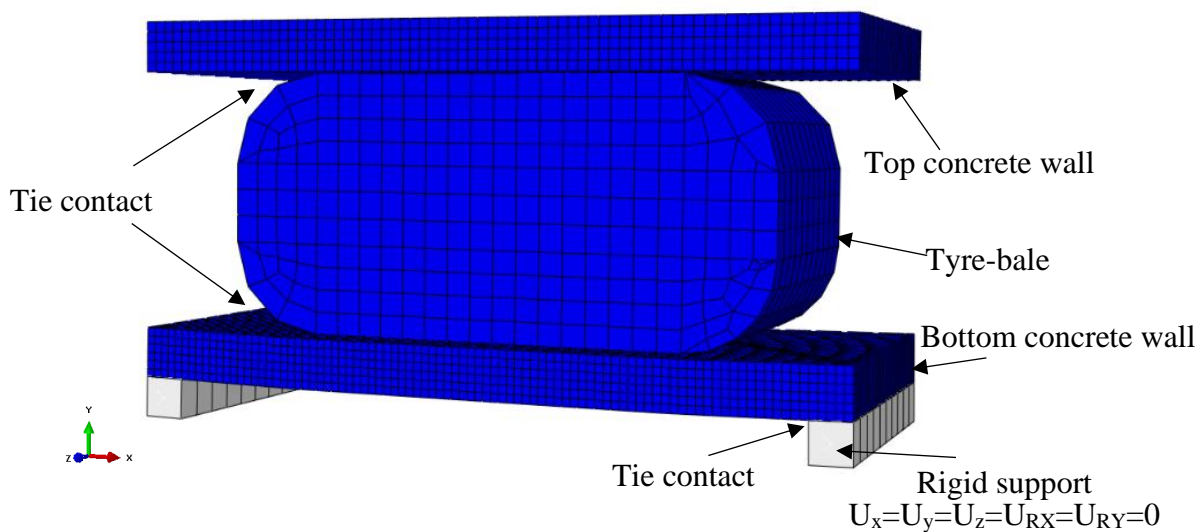


Figure 3-13 Finite element model of tyre-bale sandwich wall

3.5.2 Finite element analysis

The aim of conducting 3D FEM analysis was to investigate the structural response of sandwich wall under punching shear load. Therefore, two stages of validation were conducted in this research. First validation was done to check the performance of FE model in terms of material model and assembling of structural members. In this stage, the model was validated by comparing load-deflection curve and the material damage as obtained during experimental testing. Second validation was mandatory to define the appropriate loading and type of boundary conditions. This step was completed by comparing the ultimate load and failure mode. After the conclusion of both stages, punching load was finally applied to the tyre-bale sandwich wall.

3.5.3 Validation of material model

The FEA model of the tyre-bale sandwich wall predicted comparable damage of concrete in tension in the bottom wall by the initiation of flexural cracks through the complete depth and also travelled across the width. Table 3-7 presents a comparison of ultimate load and vertical deflection obtained in experimental testing and FEA.

Table 3-7 Ultimate load and vertical deflection from experiment and FEA

Experimental results		FEA results		$\% = \frac{P_{FEA} - P_{EXP}}{P_{EXP}} \times 100$
Ultimate load (kN)	deflection (mm)	Ultimate load (kN)	deflection (mm)	
32.16	19.84	33.92	19.92	5.47 %

The initial crack appeared at a load of 13.68 kN as shown in Figure 3-14 (a), slightly higher than the experimental load, which may be attributed to smooth contact between tyre-bale and concrete, assumed during the analysis. Figure 3-14 (b) shows ultimate failure mode of tyre-bale sandwich wall after completion of simulation, in which PE represents maximum principal plastic strain in the concrete in tension. The flexural failure of bottom concrete wall is presented in Figure 3-15. Furthermore, Figure 3-16 shows the response of FEA model compared to experimental load-deflection curve and illustrates that the FEA results were within the acceptable limits, which is 5.47%. The difference in results may be attributed to complex nature of bonding and uneven surface of the tyre-bale, which is a challenging task to simulate.

The calibrated FE model deformed linear elastically like experimental specimen (wall-2) at early stage and resisted a high load as compared to experimental values. After reaching the peak load, the model started to deform non-linearly due to loss of flexural stiffness and produced large deflection. During the analysis, no failure either in compression or tension was observed in the top concrete wall. Furthermore, the comparison of load-deflection curve of FEM with experimental results shows that the FE model closely captured the flexural response of the structural member.

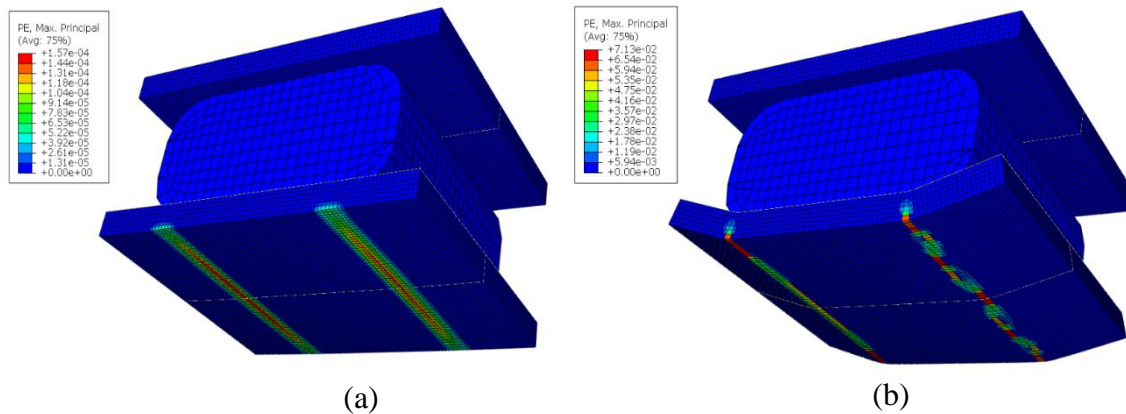


Figure 3-14 Failure mode of tyre-bale sandwich wall in FEA (a) Crack at 13.68 kN (b) collapse at ultimate load

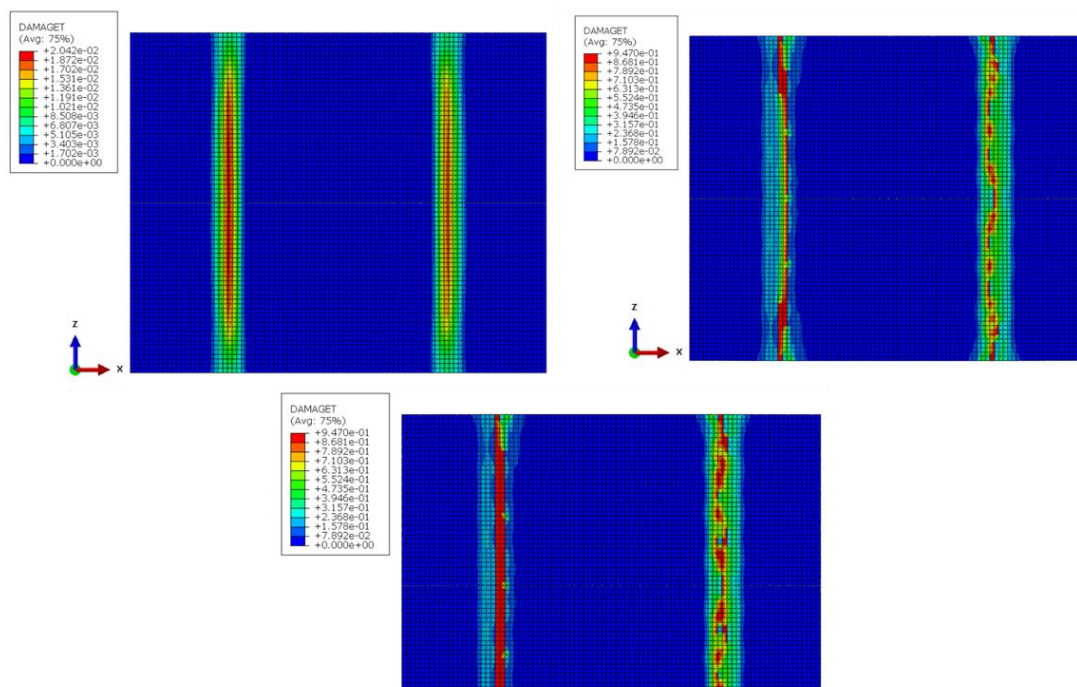


Figure 3-15 Development of flexural cracks in bottom concrete wall at various stages of loading – view from bottom

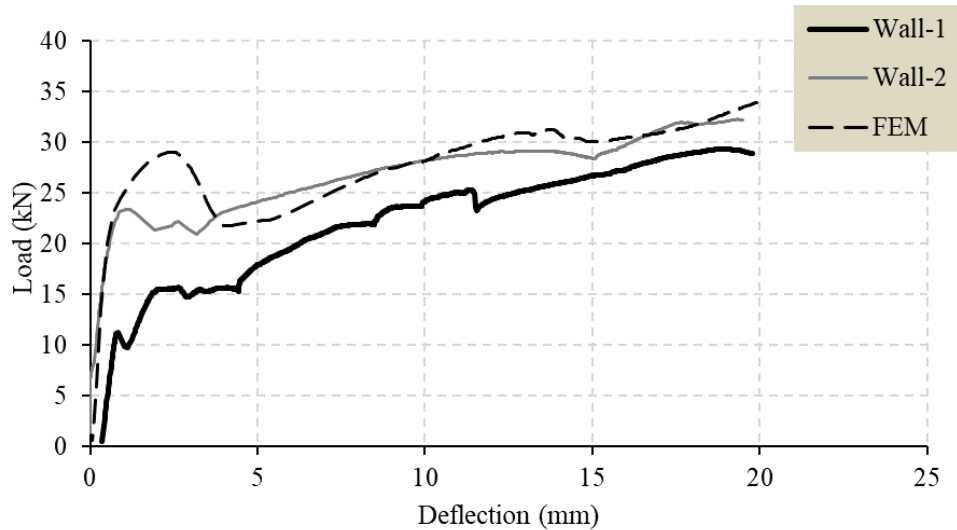


Figure 3-16 Load deflection of tyre-bale sandwich wall from experiment and FEA

3.5.4 Validation of load and boundary conditions

Ju studied the punching shear behaviour of concrete slabs using steel bars as control specimen and glass fibre reinforced polymer bars as alternative replacement (Ju et al., 2018). This research was selected for the validation of loading and boundary conditions. Figure 3-17 shows the assembly of FE model, punching load and boundary conditions. The input parameters used in the concrete damage plasticity model for 30 MPa concrete were obtained from Esfahani and are presented in Table 3-8 (Esfahani et al., 2017).

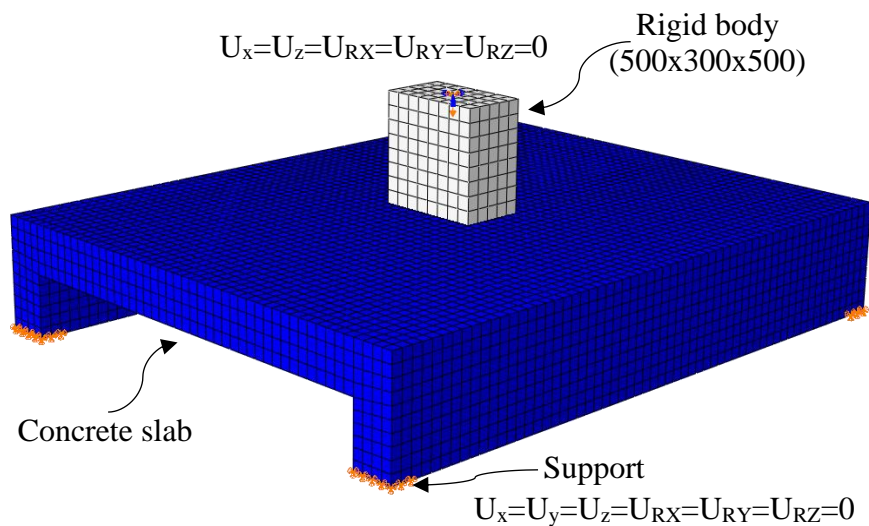


Figure 3-17 FE model of two-way concrete slab

Table 3-8 Input parameters for 30 MPa concrete slab under punching shear load

Dilation Angle	Eccentricity	Initial biaxial/uniaxial ratio (f_{b0}/f_{c0})	K	Viscosity parameter
31°	0.1	1.16	0.67	0

The validation was achieved by comparing the ultimate load and failure mechanism obtained from the simulation of FE model with the experimental results. The comparison of the ultimate load is presented in Table 3-9, which confirms a good agreement of 5.88%. The failure mechanism of two-way concrete slab from the experiment was compared with FEA simulation in Figure 3-18 (a) and (b). Failure mode obtained in FEA accurately predicted the development of radial cracks underneath the loading plate along with propagation of few longitudinal cracks as described in experimental research.

Table 3-9 Ultimate load comparison of concrete slab

Initial cracking load (kN)		Ultimate load (kN)		$\% = \frac{P_{FEA} - P_{EXP}}{P_{EXP}} \times 100$
Experimental Ju	FEA	Experimental Ju	FEA	
150	165	355	375.89	5.88 %

3.5.5 Punching shear strength and failure mechanism

After the validation phase, the punching shear load was applied on the tyre-bale sandwich wall to investigate the response of FE model with regard to ultimate load and failure mode. For this purpose, a reference point was defined on the rigid body to apply vertical displacement in the y-axis. The analysis was terminated on reaching the desired deflection. The failure output was obtained through tensile damage i.e. DAMAGE-T. Figure 3-19 (a) shows tensile failure in a 3D model of the sandwich wall observed at maximum load whereas, Figure 3-19 (b) shows the bottom view of failure in the sandwich wall. The initial cracking begins in plasticity model (using concrete damage plasticity), where maximum principal plastic strain becomes positive. In this analysis, the initial cracks started to appear on the face of the bottom concrete wall at around 21.9 kN and propagated in transverse direction along the width of the wall. After the termination of analysis, it was observed that the tensile reinforcement in the longitudinal direction has yielded right below the edges of the tyre-bale. A maximum load of 44.58 kN load was recorded at the failure. The simulation recorded a ductile failure. It is significant to mention that the propagation of cracks is similar to flexural bending in which longitudinal cracks

dominated the failure mode. Therefore, it is deduced that the punching shear load has not altered the failure mechanism except that a higher load caused the collapse. In addition, no cracking or damage was observed in the top concrete wall.

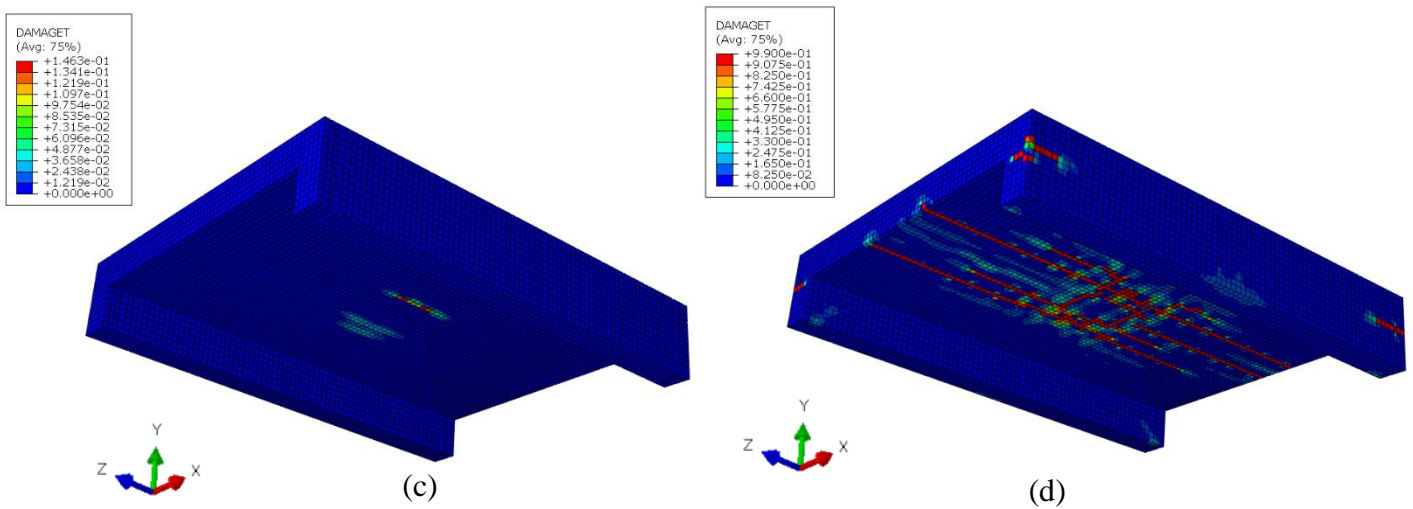
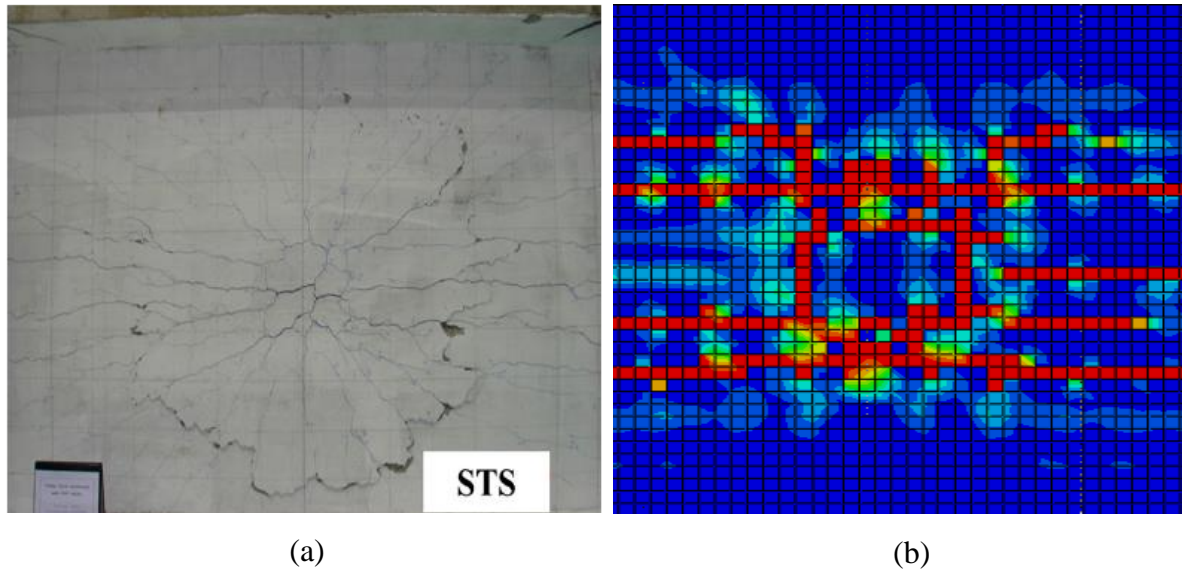


Figure 3-18 Failure mode of two-way concrete slab (a) Failure mode obtained in Ju experiment (b) Final failure mode and crack pattern of bottom concrete surface in FEA (c) Crack at 165KN in FEA (d) Final failure mode and crack pattern in 3D

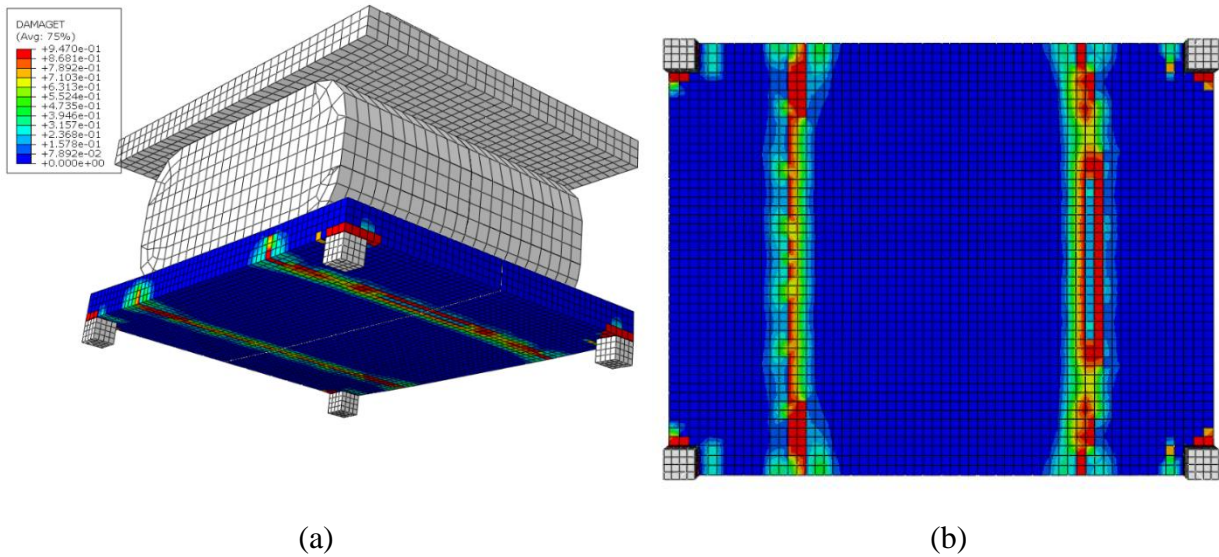


Figure 3-19 Failure mode in tyre-bale sandwich wall under punching load (a) Crack pattern in 3D (b) view from the bottom

3.6 Flexural strength prediction using yield line theory

This section aimed at estimating a theoretical ultimate load, which may cause a collapse in the bottom concrete wall. Since, the bottom wall failed in a ductile manner by yielding of tensile reinforcement therefore, yield line theory for reinforced concrete slab was employed to calculate the ultimate load (Kennedy & Goodchild, 2004). The bottom concrete wall failed in flexure by developing two crack lines called “yield lines” parallel to the support as shown in Figure 3-20. A typical collapse mechanism carrying a uniformly distributed load of tyre-bale and top concrete wall is shown in Figure 3-21.

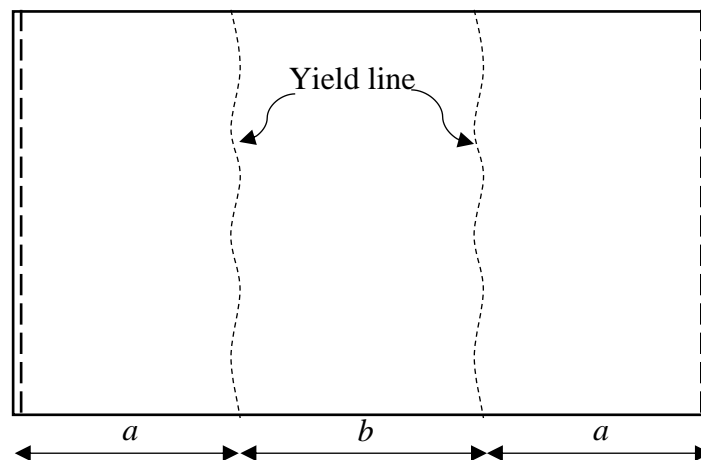


Figure 3-20 Yield line pattern in bottom concrete wall

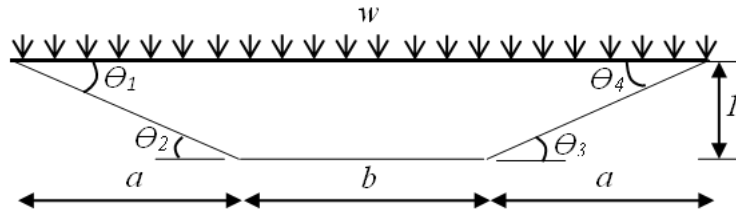


Figure 3-21 Deflected shape at failure and formation of plastic hinges

In order to estimate the ultimate load, virtual work analysis approach was adopted, in which external work done by applied load causing vertical deflection is equal to internal work done by slab by rotating at yield lines and accommodating induced deflections. A rectangular slab is simply supported along two sides and is isotropically reinforced. A unit deflection is assumed at the centre of the member.

External work done by load “w” is the sum of load times the displacement and equal to

$$\sum w \cdot \delta = w \times \left(\frac{l}{2} \times a\right) \times 2 + w \times b \times l$$

$$wal + wbl = wl (a+b)$$

The rotations at the hinges are calculated in terms of unit deflection

$$\theta_1 = \theta_2 = \frac{l}{a}$$

$$\theta_3 = \theta_4 = \frac{l}{a}$$

The internal work is the sum of moments times their rotation angles:

$$\sum M \cdot \theta = m \times \frac{l}{a} \times l + m \times \frac{l}{a} \times l = \frac{2m}{a} l$$

Equating the external and internal work:

$$\sum w \cdot \delta = \sum M \cdot \theta$$

$$w (a+b) \times l = \frac{2m}{a} l$$

$$\text{Also, } b = 1.6 - 2a$$

The resisting moment calculated by moment equation of reinforced concrete slab is 5.85 kN-m.

$$M_u = \phi \cdot M_n = A_s \cdot f_y (d - a/2)$$

where, M_n = nominal moment of member

A_s = area of steel bars

f_y = yield strength of steel bars

d = effective depth

a = depth of whitney stress block = $A_s \cdot f_y / 0.85f_c \cdot b$

Table 3-10 shows set of various trials performed in order to calculate the flexural strength of the bottom concrete wall. The load obtained by yield line method was added to the self-weight of tyre-bale and the top concrete wall to obtain the total load. Hence, the combine self-weight of tyre-bale and top concrete wall is 9.01 kN/m. The final strength predicted by yield line theory ranges from 23.18 KN to 26.86 kN, which provided a fair agreement. Since, the load fluctuates with the position of yield lines therefore, it is critical to determine the accurate location of plastic hinges. However, the method is capable of predicting the flexural strength of concrete members, if precise collapse mechanism is known.

Table 3-10 Load prediction trials using yield line theory

Trial	a	b	Moment, m (kN-m)	w (kN/m)	w_{self} (kN/m)	Total weight (kN/m)	$w \cdot l/2$ (kN)
1	0.7	0.2	5.85	18.28	9.01	27.28	23.18
2	0.65	0.3	5.85	18.57	9.01	27.57	23.43
3	0.60	0.4	5.85	18.94	9.01	27.94	23.75
4	0.55	0.5	5.85	19.5	9.01	28.5	24.22
5	0.50	0.6	5.85	20.25	9.01	29.25	24.87
6	0.45	0.70	5.85	21.27	9.01	30.27	25.73
7	0.40	0.80	5.85	22.60	9.01	31.60	26.86

3.7 Conclusion

This research study investigated the structural behaviour of tyre-bale sandwich wall under flexural bending in terms of ultimate load, vertical deflection, concrete damage in tension and failure mechanism. Finite element modelling was performed for predicting the punching shear load and crack patterns. The material model and assembly of members was first calibrated using experimental results and later, validation of punching load and boundary conditions were performed using previous research on two-way concrete slab. The results of FE analysis in both calibrations showed good agreement. The summary of important findings are as follows:

- (a) The difference in vertical deflection recorded at mid-span of the top and bottom concrete wall revealed that tyre-bale displayed negligible compressibility at low load. Subsequently, no failure was observed in the tyre-bale and tie-wires.

- (b) Both specimens displayed flexural failure in the bottom concrete wall. The flexural cracks were developed between the applied loads and travelled through the depth and width of bottom concrete wall. The vertical deflection measured before the initiation of first crack was within the defined limits of span/250 as per Australian standards. But, a significant increase in vertical deflection was recorded on reaching the failure load. However, no crack/failure was witnessed in the top concrete wall.
- (c) The structural behaviour of tyre-bale sandwich wall under the punching shear load is similar to flexural bending and generated similar crack lines in transverse direction along width. In this analysis, maximum punching load of 44.58 kN and the yielding of tensile longitudinal reinforcement was predicted by the simulation.
- (d) The FE analysis conducted to validate the material model, punching shear load and boundary conditions, showed a good agreement between experimental results and ABAQUS simulation. The FE tool has been successfully employed to predict the structural behaviour of tyre-bale sandwich wall under the punching shear. This also highlights the significance of FEA for research studies that cannot be performed in laboratory due to limitations. The proposed model can be used for futuristic studies in determining the factors affecting the flexural and punching shear strength of the tyre-bale sandwich wall.
- (e) The theoretical flexural strength of the bottom concrete wall was calculated using the yield line theory, which showed strength variation ranging from 13.6% to 31.6% when compared with mean experimental results.
- (f) The degree of composite action was evaluated at the elastic stage by initial stiffness and at the ultimate stage by the strength method. The analysis showed poor composite action. Therefore, it is recommended to employ the latest techniques to improve the degree of composite action in the tyre-bale sandwich wall.

3.8 References

- Ahmad, H., Hashim, M. H. M., Bakar, A. A., Hamzah, S. H., & Rahman, F. A. (2017). Flexural strength and behaviour of SFRSCC ribbed slab under four point bending. *AIP Conference Proceedings*, 1903(1), 020014.
- AS3600. (2018). *Concrete Structures AS3600:2018*. In AS3600:2018. Sydney.
- Awan, A. B., & Shaikh, F. U. A. (2021). Structural behaviour of tyre-bale sandwich wall under axial load. *Structures*, 31, 792-804.
- Ayrilmis, N., Buyuksari, U., & Avci, E. (2009). Utilization of waste tire rubber in manufacture of oriented strandboard. *Waste Management*, 29(9), 2553-2557.
- Benayoune, A., Samad, A. A. A., Trikha, D. N., Ali, A. A. A., & Ellinna, S. H. M. (2008). Flexural behaviour of pre-cast concrete sandwich composite panel – Experimental and theoretical investigations. *Construction and Building Materials*, 22(4), 580-592.
- Esfahani, Hejazi, Vaghei, Jaafar, Karimzade, & Keyhan. (2017). Simplified Damage Plasticity Model for Concrete. *Structural Engineering International*, 27, 68-78.
- Freilich, & Zornberg. (2009). *Mechanical Properties of Tire Bales for Highway Applications [Technical Report2019]*.
- Garga, V. K., & O'Shaughnessy, V. (2000). Tire-reinforced earthfill. Part 1: Construction of a test fill, performance, and retaining wall design. *Canadian Geotechnical Journal*, 37(1), 75-96.
- Hossain, Priyantha W, & Jayawickrama. (2000). Use of whole Tyres in Earth retaining structures (0-1876).
- Hylands, K. N., & Shulman, D. V. (2003). *Civil engineering applications of tyres*.
- I. Goh, W., Mohamad, N., Abdullah, R., & A. Samad, A. A. (2016). Finite Element Analysis of Precast Lightweight Foamed Concrete Sandwich Panel Subjected to Axial Compression. *Journal of Computer Science & Computational Mathematics*, 6(1), 1-9.
- Institution, B. S. (2007). *Specification for the production of tyre bales for use in construction*. In PAS 108:2007. United Kingdom.
- Ju, M., Park, K., & Park, C. (2018). Punching Shear Behavior of Two-Way Concrete Slabs Reinforced with Glass-Fiber-Reinforced Polymer (GFRP) Bars. *Polymers*, 10(8), 893.
- Keleştemur, O. (2010). Utilization of waste vehicle tires in concrete and its effect on the corrosion behavior of reinforcing steels. *International Journal of Minerals, Metallurgy, and Materials*, 17(3), 363-370.
- Keller, & Gordon. (1990). *Retaining Forest Roads*. Civil Engineering (Reston): engineered design and construction, 60(12), 50-50.
- Kennedy, G., & Goodchild, C. H. (2004). *Practical yield line design*. The concrete centre.
- M. A. Yazdi, J. Y., L. Yihui, H. Su. (2015). A review on application of waste tire in Concrete. *International Journal of Civil and Environmental Engineering*, 9(12), 1656-1661.

Shu, X., & Huang, B. (2014). Recycling of waste tire rubber in asphalt and portland cement concrete: An overview. *Construction and Building Materials*, 67(PB), 217-224.

W., B. M., & A., Y. (2006). Use of waste tyre bales to construct a flood embankment. *Proceedings of the Institute of Civil Engineering*,

W. Prikryl, and, R. W., & Winter, M. G. (2005). Slope failure repair using tyre bales at Interstate Highway 30, Tarrant County, Texas, USA. *Quarterly Journal of Engineering Geology and Hydrogeology*, 38, 377-386.

Yazdi, J. Yang, L. Yihui, & Su, H. (2015). A review on application of waste tire in concrete. *International Journal of Civil and Environmental Engineering*, 9(12), 1656-1661.

CHAPTER 4 STRUCTURAL BEHAVIOUR OF RECYCLE TYRE CRUMB RUBBER SANDWICH PANEL IN FLEXURAL BENDING

4.1 Abstract

This study presents the first phase of research, in which recycle tyre crumb rubber is used as core in precast concrete sandwich panels. The proposed sandwich panel offers sustainable reuse of waste tyres and improved structural efficiency by utilization of natural properties of rubber like high flexibility, thermal and sound insulation. Three type of panels namely solid concrete panel, foam (polystyrene) sandwich panel and recycle tyre crumb rubber sandwich panel are prepared and cast using 50MPa self-compacting concrete. A core thickness of 20mm is provided as insulation in sandwich panels. A total of six specimens having 1100mm length, 500mm width and 100mm thickness are tested in flexural bending under four-point loading. The structural performance of crumb rubber sandwich panel is compared against foam panel and solid concrete panel in terms of initial crack load, vertical deflection, critical peak load, strain distribution on concrete surface and in reinforcement, crack pattern, degree of composite action and deformed shape. Moreover, initial stiffness method at elastic stage and ultimate strength method at failure is implemented to gauge the percentage of composite behaviour in sandwich panels. Both approaches predicted partial composite behaviour in all specimens of sandwich panel. The research analysis demonstrated encouraging results in terms of flexural behaviour for crumb rubber sandwich panel and feasibility of using it as a structural member in construction industry. The numerical analysis was performed in commercially available software “ABAQUS” in standard/explicit model using in-built concrete damage plasticity model (CDP). The proposed model is developed as a potential tool for future studies on crumb rubber sandwich panels. The validation phase predicted a good agreement between experimentation and numerical results.

4.2 Introduction

Every year millions of tyres complete their design service life and typically disposed off through recycling, energy recovery, civil engineering applications or dumping in landfill. In civil engineering applications, whole waste tyres are recycled by compressing in a baler machine to produce tyre-bales, which are used as embankment fill, road foundations, retaining walls, slope protection, drainage or barriers (Winter et al., 2005). Waste tyres are also mechanically grinded in varying sizes to yield powder, chip, granular and fibres. These are

typically utilized as cement (Fernández-Ruiz et al., 2018), fine (Girskas & Nagrockienė, 2017), (Ismail et al., 2017), (Mohammed & Adamu, 2018) or coarse (Mishra & Panda, 2015), (Alsaif et al., 2018) aggregate replacement in concrete mix or as modifier in the construction of asphalt pavements. Crumb rubber when used in concrete provides low stiffness (Gheni et al., 2019), high flexibility (Elchalakani, 2015), thermal conductivity ranges between 0.1 and 0.25 W/mK (Fraile-Garcia et al., 2018) and improved sound insulation (Corredor-Bedoya et al., 2017). However, several research studies highlighted that use of crumb rubber in concrete mix significantly affects compressive strength (da Silva et al., 2015), elastic modulus (Murugan et al., 2015), flexural strength (Fernández-Ruiz et al., 2018), (Jokar et al., 2019) and tensile strength (Hesami et al., 2016) due to poor bonding at interfacial transition zone between concrete mix and crumb rubber (Rivas-Vázquez et al., 2015). Subsequently, number of attempts has been made to improve the mechanical properties of crumb rubber concrete by pre-treating (Raffoul et al., 2016) or use of additives (Carroll & Helminger, 2016) but no significant techniques have been reported. Youssf (Youssf et al., 2019) reported that all treatment techniques used to improve mechanical properties of crumb rubber concrete made negligible contribution and therefore, researchers should rely on reduced strength when comparing to traditional mix of concrete. Contrarily, the use of crumb rubber concrete in structural members offers advantages like light in weight, smaller crack width and better structural response against seismic loading (Xu et al., 2020), fire (Xu et al., 2018) and fatigue (Han et al., 2016). It is deduced that all existing research studies mainly focussed on the use of crumb rubber as a replacement of aggregates in concrete mixture and hardly any application in sandwich panels have been reported. Therefore, it is compelling to investigate the use of recycle tyre crumb rubber in precast concrete sandwich panels.

Precast concrete sandwich panel (PCSP) system is widely used to build residential, commercial and industrial buildings. The system consists of two high strength concrete layers called “wythes” and an insulated material called “core”. The core is inserted between two outer wythes and is usually a low strength material used to reduce thermal conductivity. Several materials like plastic, stiff foam, polystyrene (expanded or extruded), polyurethane and phenolic foam have been used as insulation core materials. The thermal resistance of various materials and surfaces is available in PCI design handbook (Handbook, 2007). Table 4-1 lists thermal conductivity of few common materials. Currently, polystyrene is used in construction industry owing to its low cost, light-weight and low water absorption (Bida et al., 2018). Another important element of sandwich panel is shear connector, which are added in sandwich panels to attain composite behaviour. A sandwich panel may be classified as fully-composite,

partially-composite or non-composite panel based on the stiffness and strength of shear connectors (Colombo et al., 2015). A composite action allows complete transfer of shear loads between two wythes, whereas in non-composite action, both wythes act independently and there is no transfer of shear loads. A partial-composite action happens, when any percentage (between 0-100%) of fully-composite shear load is transferred. In recent years, numerous research studies have been conducted to refine the structural and thermal efficiency of PCSP and can be found in literature (Benayoune et al., 2007; Benayoune et al., 2006; Ekenel, 2014; Gara et al., 2012; I. Goh et al., 2016; Joseph et al., 2017; Khalil et al., 2014; Ma, 2014; Mohamad et al., 2017; Mugahed Amran et al., 2016; Naito et al., 2012; Pessiki & Mlynarczyk, 2003).

Table 4-1 Thermal conductivity of few commonly used materials

Materials	Thermal conductivity, k (W/m-k) at 25 °C
Brickwork	0.6 - 1.0
Concrete, stone	1.7
Glass	1.05
Polystyrene	0.1 - 0.15
Rubber, natural	0.13
Timber	0.14 – 0.19
Vacuum	0

It is reported that approximately 56 million tyres are abandoned every year in Australia. These waste tyres are usually dumped at various landfill locations across the country and are major cause of health and environmental hazards. Therefore, by providing alternative means of reusing waste tyres will assist in alleviating these harmful environmental impacts. Crumb rubber is generally obtained through recycling waste tyres and offers numerous advantages like light in weight, better at impact absorption and insulation against heat and sound (Dębska et al., 2019). Han et al. investigated the use of crumb rubber blends in noise reduction on highways (Han et al., 2008) and found that these barriers showed better performance in terms of sound absorption than concrete barriers. Piti (Sukontasukkul, 2009) explored the use of crumb rubber in precast concrete panel and reported that replacing fine aggregate with crumb rubber improved the thermal and sound properties. Balcioglu (Balcioglu, 2018) manufactured composite sandwich panels using waste tyres as core material and jute fibre woven-fabric as wythes. The panels were tested on small scale under three-point loading and shear resistance. In findings, the sample with fine rubber particles showed better bending and shear resistance to loading. The strength of panel is decreased with increase in core thickness. The author

proposed use of such sandwich panels only for medium level or lesser loadings. All the previous research studies were mainly conducted on the use of crumb rubber in concrete mix. Hence, utilization of crumb rubber as core material has never been explored. Therefore, this research adopted an innovative idea of using crumb rubber as an insulation material for precast concrete sandwich panels and expected to address existing impediments in following ways:

- (a) Will eliminate problem of reduced compressive strength when crumb rubber is used directly in traditional concrete,
- (b) Will overcome inefficient bonding issues between crumb rubber particles and cement mix in interfacial transition zone,
- (c) Will entirely wipe out pre-treatment of crumb rubber or use of additives typically employed to improve mechanical properties.
- (d) Will alleviate harmful environmental impacts by recycling of waste tyres and promote sustainability.

As, the practice of using recycle tyre crumb rubber as core material in PCSP has never been tried earlier, therefore, the main objective of this paper is to introduce crumb rubber as a new core material and compare the structural behaviour of crumb rubber sandwich panel with foam sandwich panel and solid concrete panel in terms of ultimate load, mid-span deflection, strain variations and mode of failure. In the study, all specimens were tested experimentally in four-point bending and a numerical model was developed using ABAQUS for crumb rubber sandwich panel to predict its behaviour in flexure.

4.3 Experimental Program

In this research, three type of panels i.e. (a) solid concrete panel (b) foam sandwich panel and (c) crumb rubber sandwich panel were designed, manufactured and tested in four-point bending. Total six specimens were cast and tested, in which two specimens were tested for each type of panel. The typical size of panel was 1100 x 500 x 100 mm³. The details are explained as below: -

Solid Concrete Panel (SCP): The panel is cast using self-compacting concrete (SCC) and reinforced with 8mm diameter deformed bars in both directions with a minimum concrete cover of 25mm. The reinforcement is evenly spaced at 100mm centre-to-centre as shown in Figure 4-1. This panel comprises of only one steel mesh.

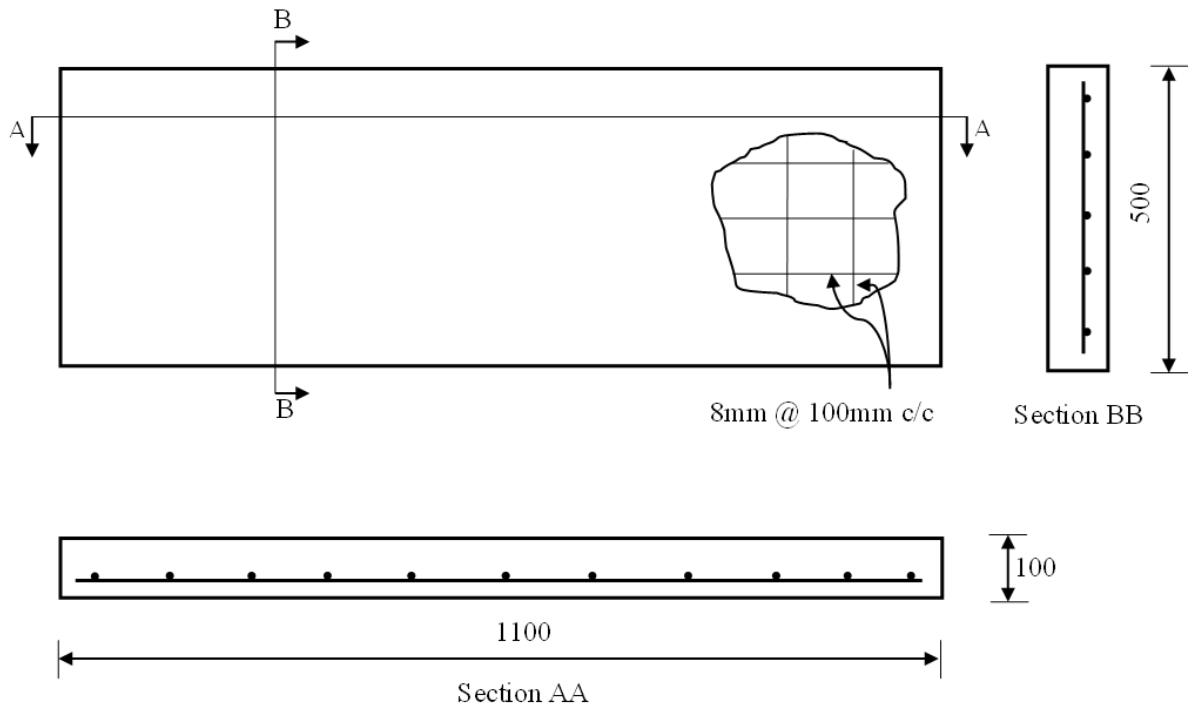


Figure 4-1 Details of solid concrete panel (All dimensions are in mm)

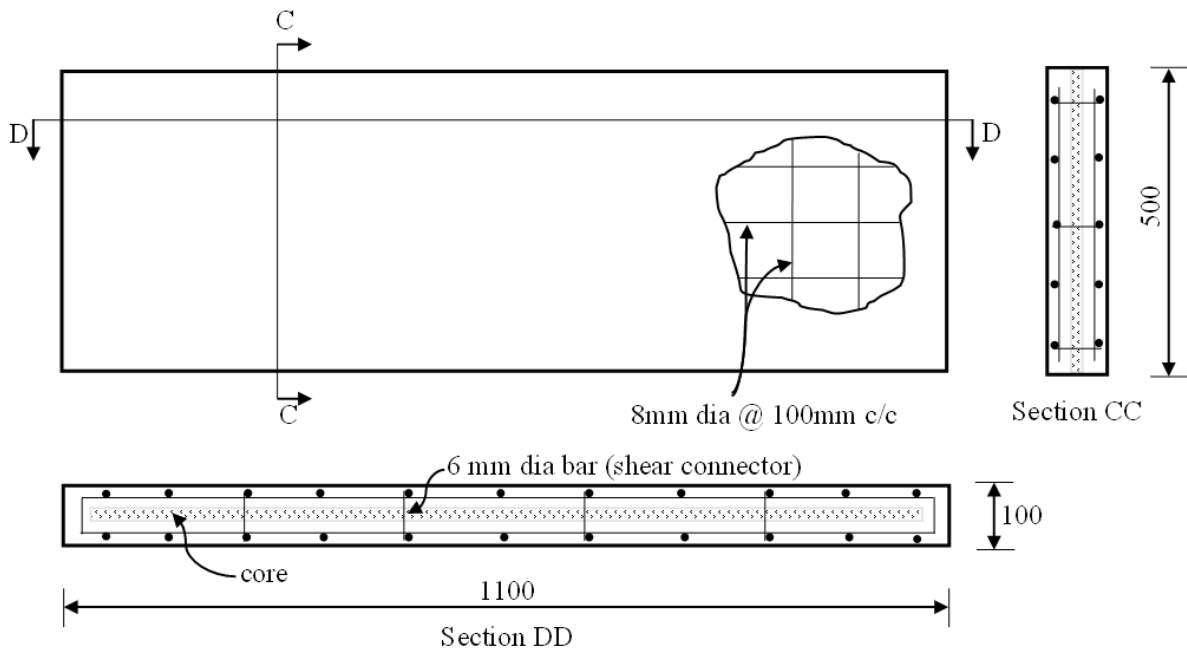


Figure 4-2 Details of precast concrete sandwich panel (All dimensions are in mm)

Foam Sandwich Panel (FSP): The panel consist of two 40mm thick concrete wythes and 20mm thick polystyrene core as shown in Figure 4-2. Each concrete wythe is reinforced with 8mm diameter deformed bars steel mesh. The reinforced meshes are connected orthogonally by 6mm diameter shear connectors. The properties of polystyrene were obtained from respective manufacturer. The density typically ranges from 28 - 45 kg/m³, elastic modulus between 1090-2900 MPa and Poisson's ratio of 0.2-0.4.



Figure 4-3 Crumb rubber used as core material

Crumb Rubber Sandwich Panel (CRSP): This sandwich panel is similar in size and configuration to FSP except that the core material is replaced with recycle tyre crumb rubber as shown in Figure 4-3. The recycle tyre crumb rubber sheets are readily available in commercial warehouse in 1000 mm x 1000 mm x 20 mm size and are locally procured. According to manufacturer, Methylene diphenyl diisocyanate (MDI) polyurethane is used as rubber binder, which is a methyl based harmless product. The procedure for binding crumb rubber is available online (Huntsman, 2021). The typical recycle tyre crumb rubber frame with reinforcement mesh and shear connectors is illustrated in Figure 4-4.

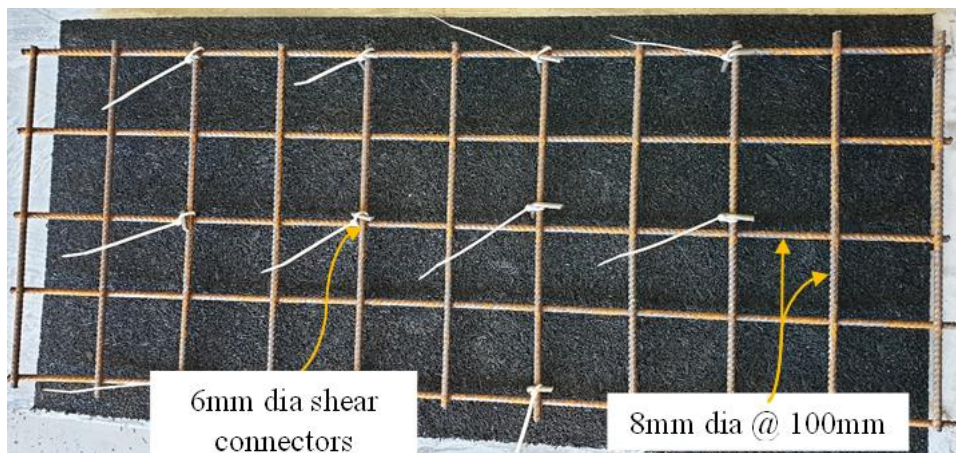


Figure 4-4 Recycled tyre crumb with steel reinforcement

4.3.1 Material Properties

Self-compacting concrete (SCC)

The self-compacting concrete, deformed bars, round bars, polystyrene and recycle tyre crumb rubber were used for the construction of panels. The constituents and respective proportions used in mix design to obtain 50MPa SCC are listed in Table 4-2. In order to determine workability of SCC, slump flow test, T₅₀₀, V-funnel test, J-ring and U-box test were conducted at time of pouring fresh concrete to formwork. Based on test results obtained in Table 4-3, it is evident that all values were within the acceptable range for SCC. The material properties of SCC, as defined in Table 4-4, were measured by testing cylinder specimen of 100 mm x 200 mm for compressive strength, elastic modulus and Poisson ratio at 28 days.

Table 4-2 Mix design proportions for 50 MPa SCC

Mix Constituent	Proportion
Cement Type GP, kg/m ³	291
Cement Type LH, GGBS, kg/m ³	194
Aggregate, 10mm, kg/m ³	788
Dust, kg/m ³	207
Coarse Sand, kg/m ³	307
Fine Sand, kg/m ³	419
Admixture-1 Retarder N (Type Re Retarder), ml/m ³	728
Admixture-2 Viscocrete10 (Type HWRRe), ml/m ³	2910
Admixture-3 Flow 15 (Type HWRRe), ml/m ³	970
Water, L	190

Table 4-3 Tests performed on SCC and detail of results

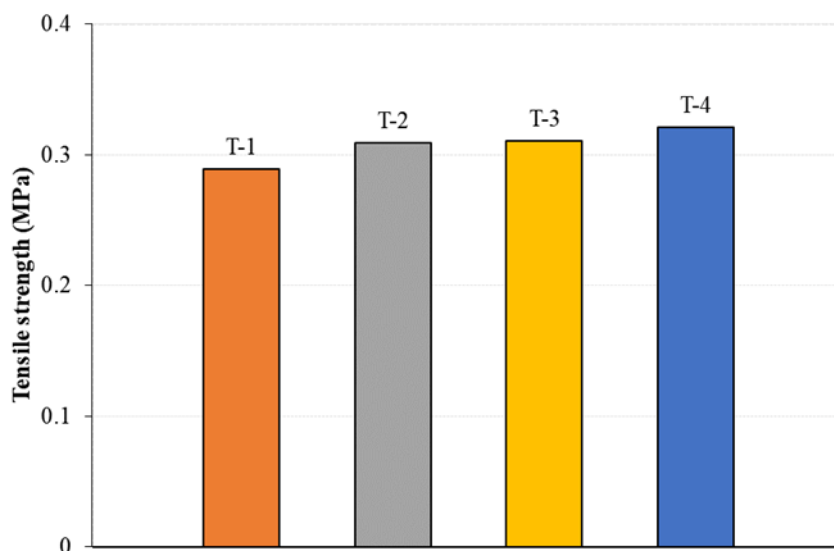
Method	Unit	Results	Acceptable range
Slump flow	mm	750	650-800
T ₅₀₀ slump flow	sec	5	2-5
V-funnel	sec	8	6-12
J-ring	mm	8	0-10
U-box (h ₂ -h ₁)	mm	1	0-30

Table 4-4 Properties of 50 MPa SCC at 28 days

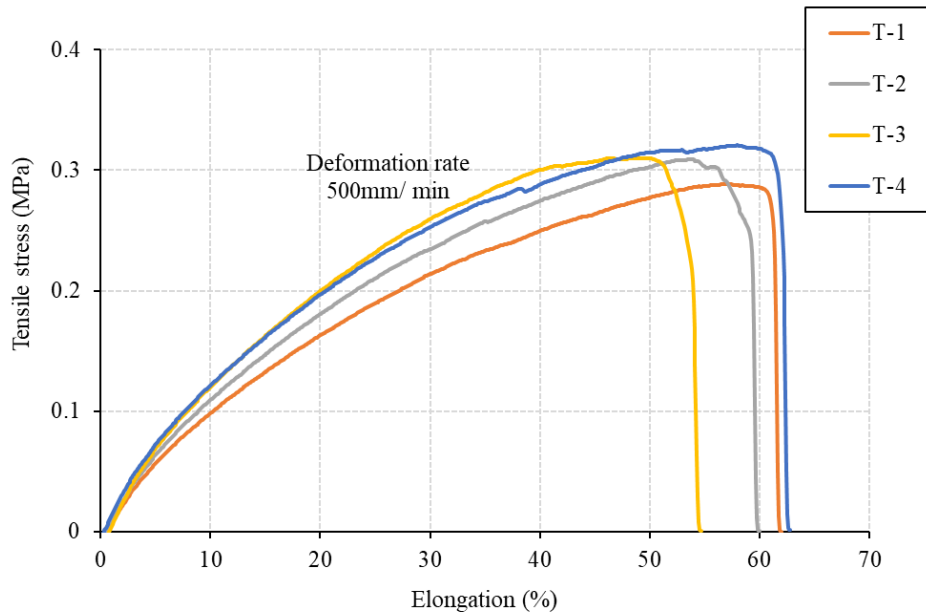
Properties	SCC
Density (kg/m ³)	2506
f_c' (MPa)	50
f_t (MPa)	4.07
Modulus of elasticity (MPa)	28000
Poisson's ratio(ν)	0.3

Recycled tyre crumb

The properties of recycled tyre crumb were investigated by performing two types of tests on different specimen (a) uniaxial tensile test and (b) uniaxial compression test. In uniaxial tensile test, five specimens of 200 mm x 50 mm x 20 mm were tested according to ASTM D412 on a universal testing machine (Schimadzu, 50kN). The load was applied at constant rate of 500mm/min till failure. All specimens initially deformed elastically and ultimately failed in rupture. The tensile strength and elongation were determined by averaging the test data from four specimens, as presented in Figures 4-5(a) and 4-5(b). The data from one specimen was discarded being an outlier.



(a)



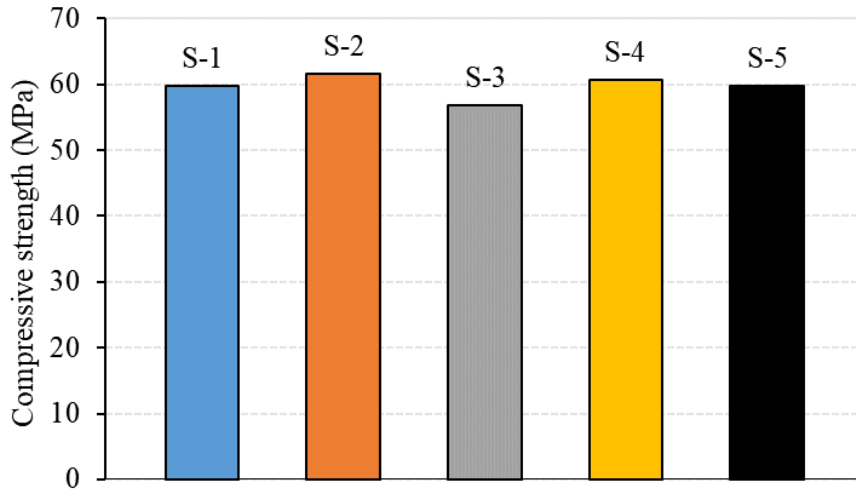
(b)

Figure 4-5 Recycled tyre crumb properties (a) Tensile strength (b) Stress-strain curve in uniaxial tensile test

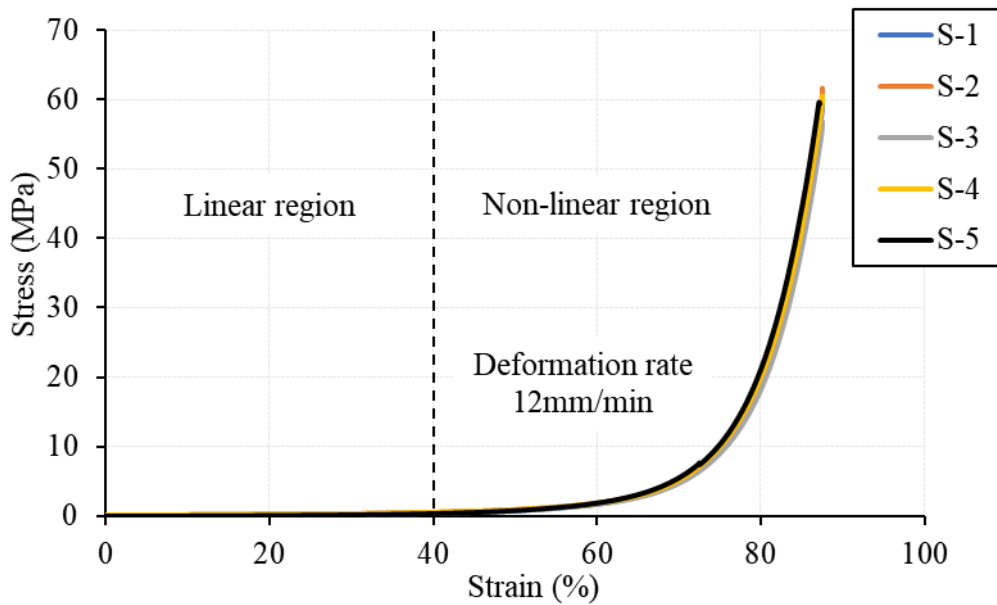
Similarly, uniaxial compression test was conducted on five specimens, as illustrated in Figure 4-6(a), with a thickness of 20 mm in accordance with ASTM D575 on universal testing machine (Schimadzu, 50kN). A uniform rate of 12mm/min was maintained throughout the test and all specimens were compressed to a maximum strain value of 87.5% due to equipment limitations. It is important to highlight that no permanent deformation/failure was observed at peak load and specimen reverted back to its original shape on removing the load. The elastic modulus was calculated using Hooke’s law up to linear region at strain value of 40%, as shown in Figure 4-6(b). The properties of recycled tyre crumb obtained from both tests are presented in Table 4-5.

Table 4-5 Mechanical properties of recycled tyre crumb in uniaxial compressive and tensile testing

Properties	Crumb
Density (kg/m ³)	564.12
Average compression strength (MPa)	59.70
Elastic modulus (MPa)	1.92
Average tensile rupture strength (MPa)	0.307
Average elongation at break (%)	59.87



(a)



(b)

Figure 4-6 Recycled tyre crumb properties (a) Compressive strength (b) Stress-strain in uniaxial compression

Reinforcement

For finding reinforcement properties, tensile test was performed on three samples each for 8mm diameter deformed bars and 6mm diameter shear connectors to measure yield stress, ultimate stress and plastic strain using Shimadzu 300 kN universal testing machine. The properties of steel rebars and shear connectors are presented in Table 4-6.

Table 4-6 Properties of steel reinforcement and shear connector

Properties	Reinforcement	Shear connector
Diameter (mm)	08	06
Density (kg/m ³)	7900	7700
Avg Yield Stress (MPa)	530.33	658.14
Avg Ultimate Stress (MPa)	560.54	764.24
Avg Ultimate Strain (MPa)	0.088	0.0907
Elastic Modulus (MPa)	207010	215800
Poisson ratio	0.3	0.3

4.3.2 Formwork and Panel Casting

The formwork was constructed using structural timber plywood sheets and secured by screwing evenly on both faces and at bottom. Before pouring fresh concrete, silicone sealant was applied on all inner corners of the formwork to prevent any leakage of material/water and left for drying. The steel reinforcement mesh was attached on either face of core and connected through shear connectors before placing inside the formwork as shown in Figure 4-7(a). In order to ensure the core is located in the centre, plastic tipped wire chairs of 25mm and 20mm height were used at regular intervals for SCP, FSP and CRSP respectively. The formwork was positioned on a level surface to ensure equal distribution of concrete in formwork and fresh SCC was poured as shown in Figure 4-7(b). During the casting phase, recommended flow tests were performed, and cylinder samples were prepared for material testing. The formwork was protected by placing jute fabric cloth and was regularly water to prevent moisture loss.



Figure 4-7 (a) Timber formwork and location of core material (b) Final finish after pouring SCC

4.3.3 Instrumentation

The deformations were recorded using Linear Voltage Differential Transducers (LVDT) and strain gauges. LVDT with stroke length of 100mm was used to measure vertical deflections, whereas strain variation on concrete surfaces and in steel reinforcement were measured and recorded using 60mm and 2mm long strain gauges with gauge factor of 118.5 ± 0.5 and resistance of 120Ω . A total of five LVDTs were used along the span, in which two LVDTs were placed at each support (LD1 and LD2), one LVDT under each load (LD3 and LD5) and one LVDT at mid-span (LD4).

Figure 4-8 illustrates the location of all LVDTs along the specimen span. Two strain gauges were used for each specimen of SCP and attached to top and bottom concrete surface at mid-span. For each specimen of FSP and CRSP, a total of six strain gauges were used, SG1 and SG2 were placed on concrete surfaces of top and bottom wythe whereas, SG3 to SG6 were positioned on steel reinforcement in both directions. The detail positioning of all strain gauges is further demonstrated in Figure 4-9. In each case, the steel reinforcement surface was prepared by grinding and flattening curve surface before placing strain gauges and firmly secured using cyanoacrylate (CN) adhesive. Also, 3mm thick SB tape was placed on all strain gauges of steel reinforcement in order to prevent moisture penetration. The working of all strain gauges was checked using standard *Q1126* multimeter before pouring concrete.

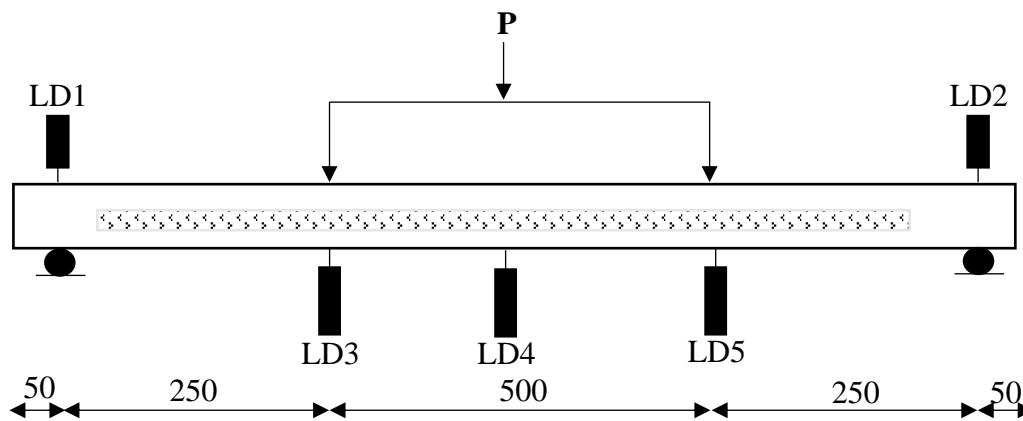


Figure 4-8 Instrumentation: Arrangement of LVDTs for specimen

4.3.4 Test setup

The test setup was assembled at centreline of reaction frame using steel hinge, 200kN load cell, hydraulic jack (SPX RD5518), spreader beam, 100mm thick rotating plates and rigid steel support. The top end of load cell was secured to steel hinge and hydraulic jack was attached to

the bottom. The load was transferred on specimen using spreader beam attached with two line loads by a distance of 500mm apart. Fresh plaster of Paris was applied onto rotating plates before placing specimen. These plates were simply supported at each end and allowed to rotate only about z -axis. The plates were secured on rigid steel support by intermittent welds evenly placed along length. In the end, the rigid steel supports were firmly anchored to ground in order to restrict movement. The detail arrangement of four-point bending is demonstrated in Figure 4-10.

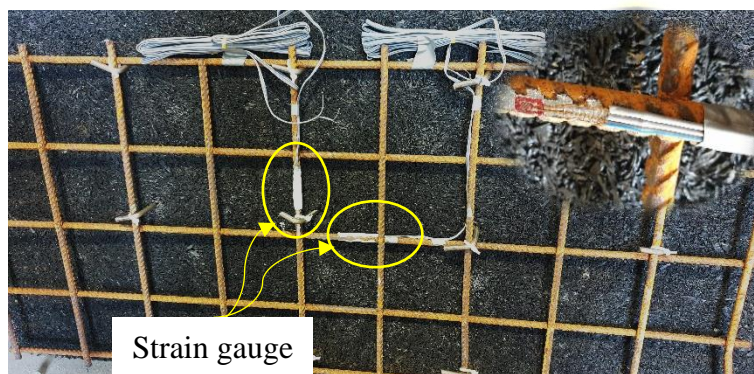
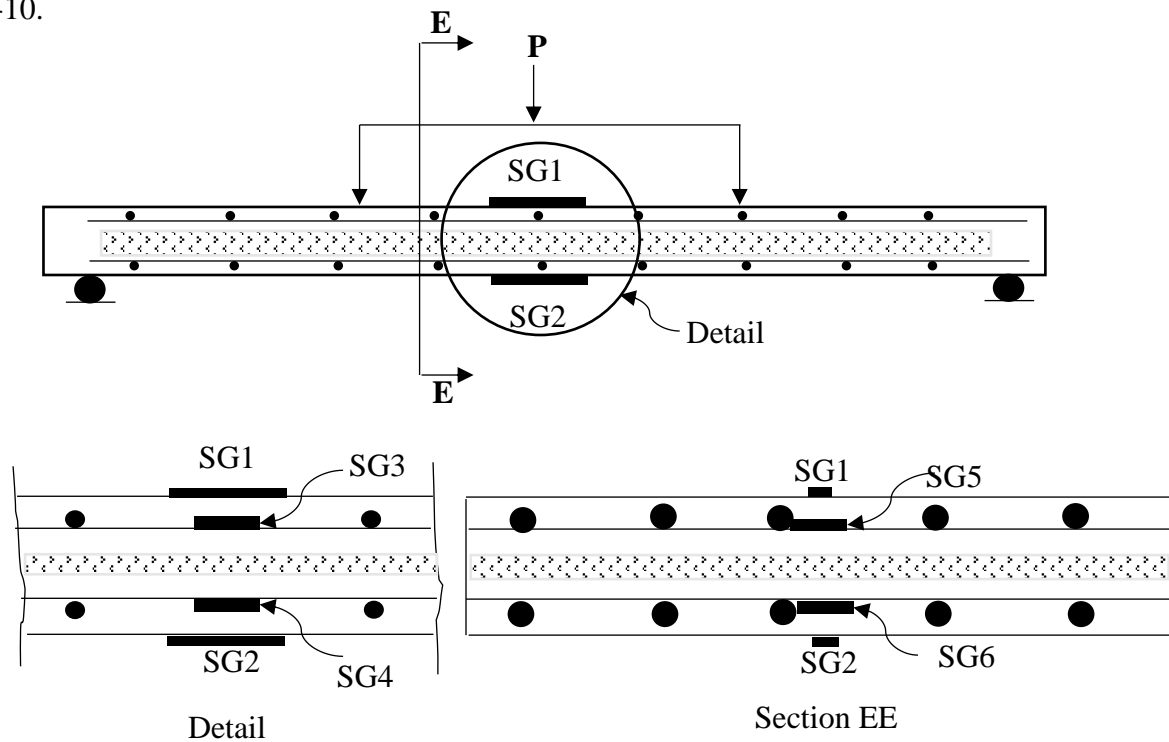


Figure 4-9 Instrumentation: Arrangement of strain gauges on concrete surface and reinforcement

After positioning the specimen in centre, all gauging sensors were attached to data acquisition system (HBM – Quantum X) for storing data at each 0.1 second increment. An initial testing load of 5kN was applied to inspect working of attached devices and Catman DAQ software. The sensors were calibrated back to zero after initial testing and afterwards, the load was gradually increased till failure. All six specimen were tested in a horizontal position. During testing, all crack patterns were marked on the specimen with cracking load. The test was terminated each time on appearance of excessive cracking in the bottom wythe.

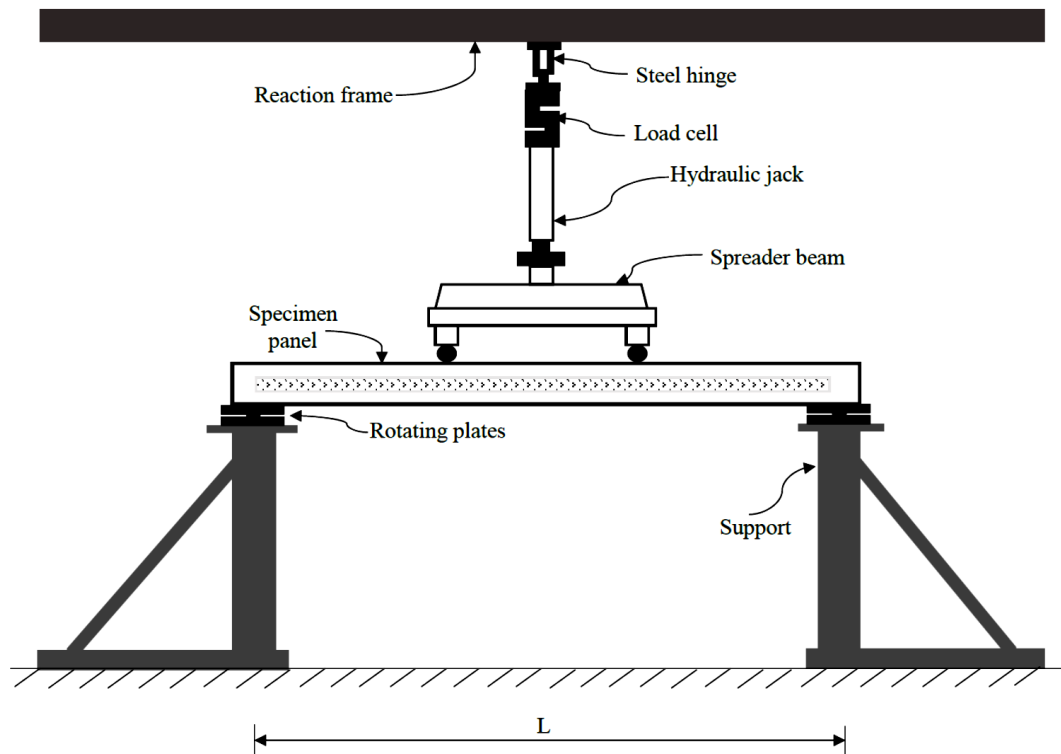


Figure 4-10 Test setup: Arrangement of four-point bending for all specimen

4.4 Results and discussion

The result of experimental work is analysed in terms of ultimate load, deflections, strain variations in concrete surfaces and reinforcement, crack pattern and composite behaviour of sandwich panels.

4.4.1 Load-deflection at mid-span (LD-4)

Figure 4-11 presents the load deflection behaviour of all specimens, in which the plotted load is the total externally applied load i.e. “P”. At initial phase of loading, all specimens are deflected linear elastically and followed Hooke’s law before appearance of first crack. In this region, the applied load is directly proportional to the deflection measured at mid-span of all

panels. The initial crack load for SCP and CRSP is higher as compared to FSP. The maximum initial cracking load of 36 kN was recorded in SCP-II as expected whereas, FSP-I recorded the lowest load of 19.78 kN. CRSP were initially able to resist 73% of maximum applied load as compared to SCP. On comparing the structural behaviour of two sandwich panels with different core material confirms that CRSP offered better resistance to deformation due to flexible nature by taking an additional 36% load at initial phase. It is also worth stating that the first crack in all specimens appeared in bottom concrete wythe. Furthermore, maximum deflection of 1.35mm was recorded in SCP-II and minimum deflection of 0.99mm in FSP-I near first crack.

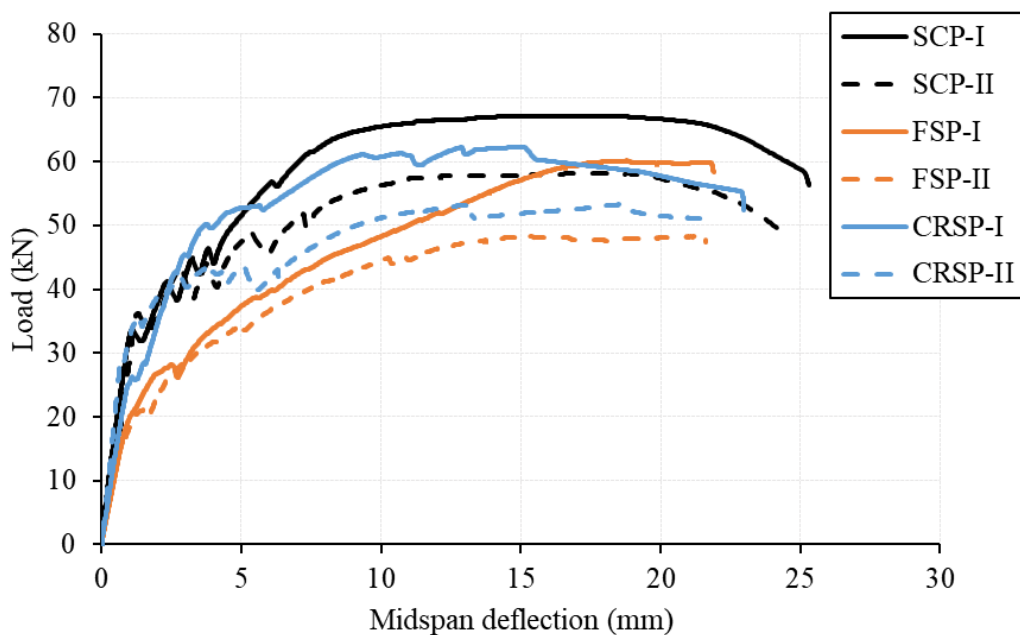


Figure 4-11 Load-deflection at mid-span (LD-4)

Subsequently, on increasing the load beyond elastic phase, all specimens started to behave non-linearly and produced large deflections till failure. In plastic phase, both SCP specimens deflected in a similar way with slight variations in resisting the applied load. Similarly, deviation in load deflection relation was witnessed in all specimens of sandwich panels in plastic region and these deviations begin to increase on approaching failure. The plausible reason for deviation could be the unintended change in initial alignment of core during pouring of fresh SCC, which may have altered the concrete wythe's thickness and therefore, influenced the structural performance of sandwich panels. The failure load, maximum deflection and moment recorded during each test is reported in Table 4-7. The average ultimate load of CRSP is 57.75 kN, which is approximately 92.15% than SCP.

Table 4-7 Summary of experimental test results in terms of load, moment and deflection

Specimen	Initial cracking load (kN)	Mean	Initial deflection (mm)	Initial cracking moment (kN-m)	Maxi load (kN)	Mean	Maxi deflection (mm)	Maxi moment (kN-m)
SCP-I	33.04	34.52	1.13	4.54	67.13	62.67	25.31	9.23
SCP-II	36		1.35	4.95	58.21		24.43	8.00
FSP-I	19.78	19.90	0.994	2.72	60.11	54.20	21.89	8.26
FSP-II	20.03		1.09	2.76	48.28		21.60	6.65
CRSP-I	25.85	27.09	1.17	3.55	62.30	57.75	22.98	8.57
CRSP-II	28.33		1.06	3.90	53.21		21.40	7.31

Figure 4-12 shows the deflections of panel CRSP-II under each load (LD-3 and LD-5) and at mid-span (LD-4). A maximum deflection of 21.40mm was recorded at mid-span before failure. In the end, it is concluded that the type and stiffness of core material effect the ultimate load capacity of the panels. However, the comparable structural behaviour of CRSP highlights the potential of recycling waste tyres and using it as alternate core material in sandwich panel. Consequently, the research study achieves its objective of providing another way to dispose off waste tyres.

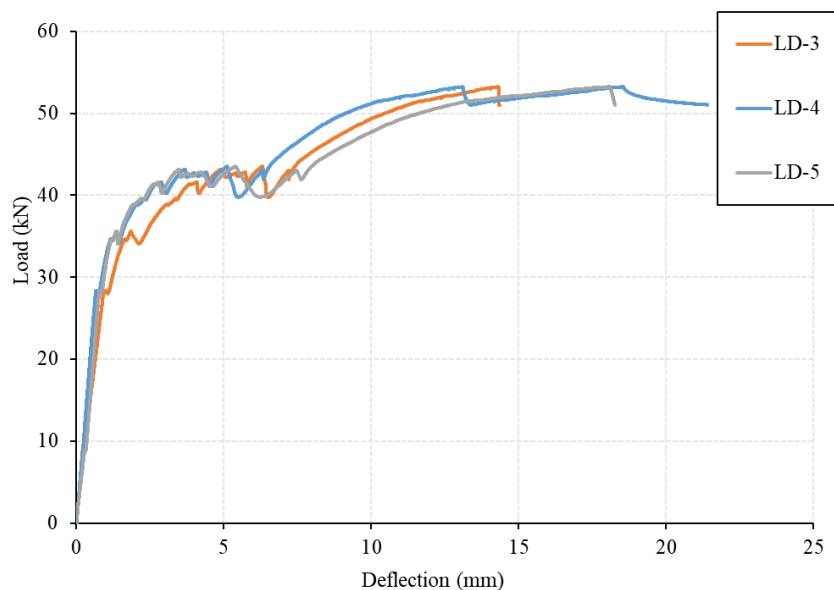


Figure 4-12 Load versus vertical deflection along the span for CRSP-II

4.4.2 Strain distribution

This section discusses the strain distribution at top and bottom concrete surfaces and reinforcements for SCP-I, FSP-II and CRSP-II. Figure 4-13 shows typical strain variation in concrete top (SG-1) and bottom surfaces (SG-2) of SCP-I. At initial stage of loading, the strain

increases proportionally on increasing the applied load and presents an ideal strain distribution curve. However, on appearance of first crack at 33.04 kN, the strain increases nonlinearly till failure. The maximum compression (SG1) and tension strain (SG2) recorded is 0.00125 and

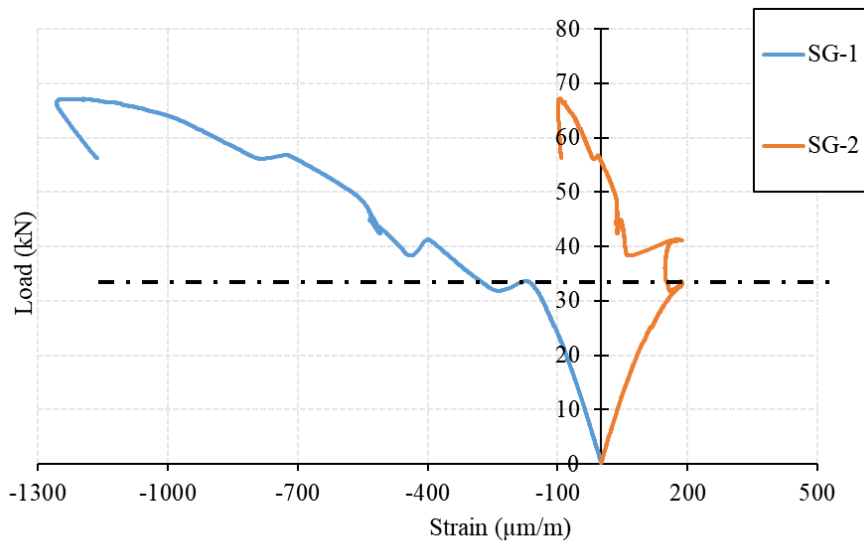


Figure 4-13 Strain distribution at mid-span in concrete top surface (SG1) and bottom surface (SG2) in SCP-I

0.000186 respectively.

Figure 4-14 presents the strain variations in concrete top and bottom surfaces and reinforcements in panel FSP-II. The specimen displayed linear distribution of strain, similar to SCP before initiation of crack, where top concrete wythe is in pure compression and bottom concrete wythe is in tension. However, on appearance of cracks in bottom wythe, the strain reaches the maximum value of 0.000120, lower than the maximum strain recorded in SCP-I. The top concrete wythe remains in compression even after extensive cracking in bottom

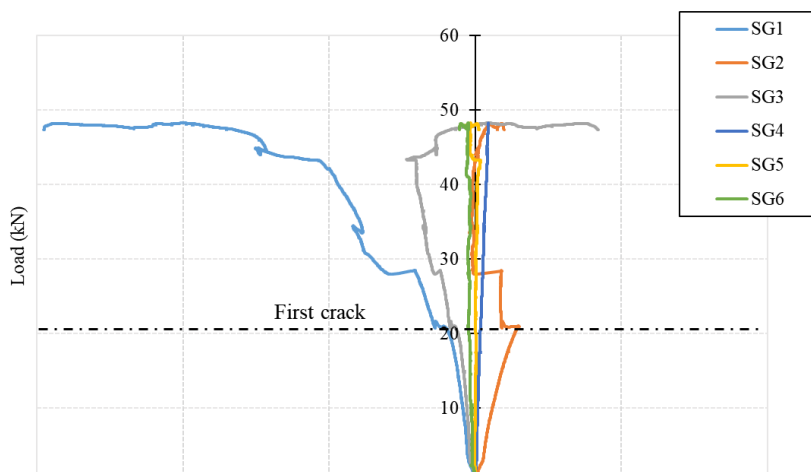


Figure 4-14 Strain distribution at mid-span in concrete wyth and reinforcement in FSP-II

concrete wythe. The strain (SG3 to SG6) recorded in reinforcement is insignificant and much lower than the yielding strain.

Figure 4-15 shows typical behaviour of CRSP-II till failure during testing. At first, the specimen followed a linear elastic relation and displayed partial composite behaviour before occurrence of first crack in the specimen, similar to SCP and FSP. The strain remained proportional to the applied load post initial cracking phase till 32.70 kN. The tensile strain (SG2) recorded in bottom concrete wythe at time of cracking is 0.000143, higher than the maximum strain in FSP. The post cracking behaviour of specimen exhibited nonlinear increase in strain till extensive cracking which ultimately led to complete failure. The data recorded in all strain gauges (SG3 to SG6) showed no sign of yielding in both longitudinal and transverse reinforcements. Furthermore, the compression strain recorded in all testing specimens remained below 0.002 which indicated no sign of crushing of top concrete wythes.

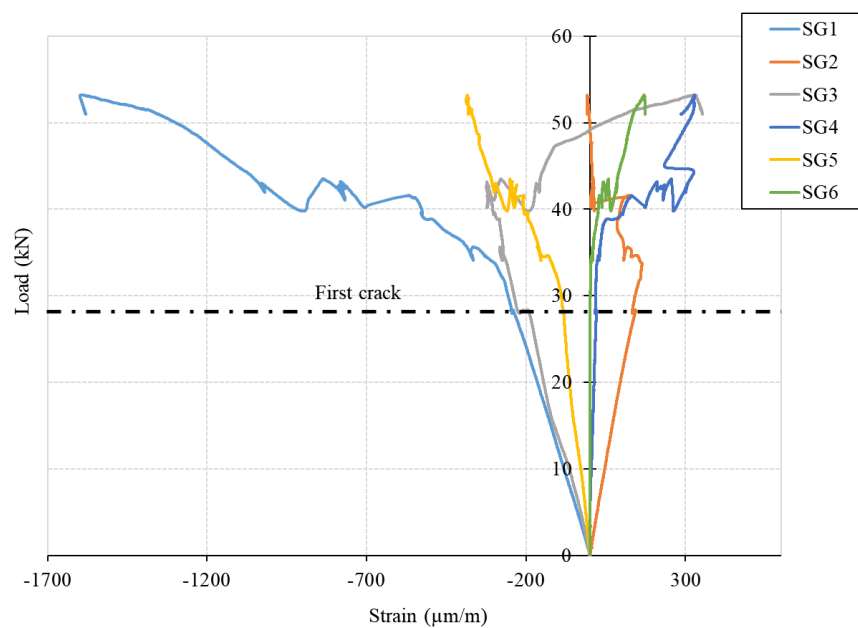


Figure 4-15 Strain distribution at mid-span in concrete wythe and reinforcement in CRSP-II

Figure 4-16 shows the strain variations of CRSP-II along panel thickness at different loading points. The neutral axis is marked at centre of panel depth and pattern filled section represents core thickness. The section above the core denotes top concrete wythe whereas, lowest part is the bottom concrete wythe. The negative sign indicate compression, while tension is displayed in positive sign. At initial stage of loading, the strain recorded in all attached sensors were fairly low. The strain variations in top and bottom concrete wythes are non-uniform and have slight discontinuity. Furthermore, the top concrete wythe and top reinforcement mesh was in pure

compression, while the bottom concrete wythe and reinforcement mesh was in pure tension throughout the loading, however, large discontinuity in strain was witnessed moments before the failure. The strain in top concrete wythe increased steadily on increasing the load and

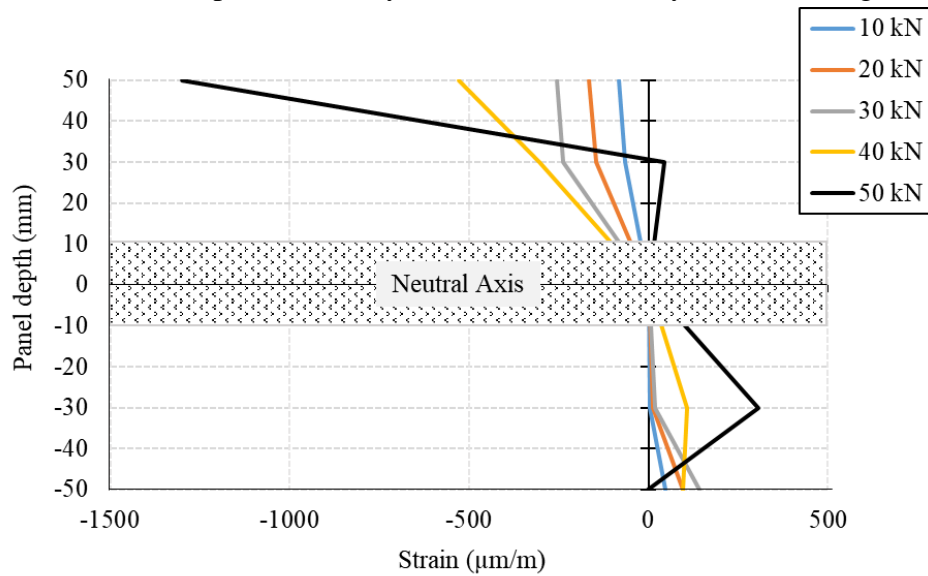


Figure 4-16 Strain variation along panel thickness in CRSP-II at different loading points

reached a maximum compression strain of 0.00129 whereas the strain in bottom concrete wythe increased till 30 kN i.e. 0.000142 and dropped near the failure.

4.4.3 Composite behaviour of sandwich panels

The degree of composite action of all sandwich panels were investigated by two approaches; (a) at elastic stage by calculating initial stiffness and (b) at failure by evaluating ultimate strength.

The initial stiffness method is proposed by Pessiki (Pessiki & Mlynarczyk, 2003) and later used by researchers to investigate the degree of composite action in precast concrete sandwich panels. In this method, the experimental moment of inertia (I_E), theoretical moment of inertia of composite (I_C) and non-composite (I_{NC}) behaviour of panels are calculated and compared using Equation (1)

$$K_1 = \frac{I_E - I_{NC}}{I_C - I_{NC}} \quad (1)$$

where, I_E is calculated using Equation (2) for four-point loading.

$$I_E = \frac{Pa}{24E_C\Delta} (3L^2 - 4a^2) \quad (2)$$

Benayoune et al. (Benayoune et al., 2008) suggested ultimate strength method to calculate the percentage of composite action (K_2) for either fully composite (100%) or non-composite (0%) panel. In composite action as shown in Figure 4-17(a), the whole panel is considered as one structural member to resist the externally applied load and ultimate moment is used to determine P_C , whereas for non-composite action, the two concrete wythes are assumed as two independent members as shown in Figure 4-17(b) and ultimate moment is evaluated separately

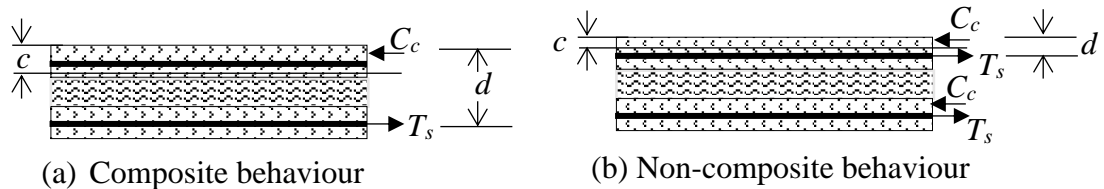


Figure 4-17 Ultimate strength approach to gauge degree of composition in sandwich panels for each wythe to define P_{NC} . The theoretical load calculated for fully composite and non-composite action is 79.53kN and 37.41kN, respectively. The following section elaborates on estimation of theoretical load calculations.

Fully composite action

When percentage of composite action is considered as 100%, the panel will behave as a solid concrete slab, where the internal force acting on the section are calculated using following procedure;

$$C_c = 0.85 * f'_c * b * a$$

$$T_s = A_s * f_y$$

where,

f'_c = compressive strength of concrete

b = width of stress block

c = depth of neutral axis from extreme compression face at ultimate stage

a = depth of equivalent stress

A_s = area of steel reinforcement

f_y = yield stress of steel reinforcement

$$C_c = 0.85 * 50 * 1000 * a = 42500a$$

$$T_s = 5 * 50.26 * 560 = 133189 \text{ N}$$

At internal equilibrium, $C_c = T_s$ therefore, $a = 3.13\text{mm}$

$$d = 100 - 20 = 80\text{mm}$$

The ultimate moment capacity will be calculated using, $M_u = T_s (d-a/2) = 10.44 \text{ kN-m}$

Ultimate load capacity per 1000mm length = $P_u = 8.M_u / l^2 = 75.75 \text{ kN/m}$

Hence, theoretical load capacity of composite panel = $P_c = 79.53 \text{ kN}$

Non-composite action

In this case, theoretical ultimate load capacity of panel is calculated by considering each wyth separately.

The ultimate moment capacity of one wyth, $M_u = T_s (d-a/2) = 2.45 \text{ kN-m}$

where, $d = 20\text{mm}$ (each wythe independently)

Therefore, the total moment capacity of panel is, $M_u = 2.45*2 = 4.91 \text{ kN-m}$

The ultimate load capacity per 1000 mm length = $P_u = 8.M_u / l^2 = 35.63 \text{ kN/m}$

Hence, theoretical load capacity of non-composite panel = $P_{NC} = 37.41 \text{ kN}$

Equation (3) is used to estimate the percentage of composite action (K_2) at ultimate loading stage.

$$K_2 = \frac{P_E - P_{NC}}{P_C - P_{NC}} \quad (3)$$

Table 4-8 shows the summary of percentage of composite action at elastic stage in relation to initial stiffness and at failure in context of ultimate strength for all concrete sandwich panels. All specimen displayed nearly same percentage of composite action in initial stiffness method and changes for each panel on approaching the failure. The analysis further illustrates that all sandwich panels behaved as partially composite panels after initiation of first crack and composite action significantly reduced on reaching ultimate capacity. CRSP-I displayed maximum composite behaviour of 59% in ultimate strength method. However, the composite behaviour can be improved, if desired, by employing the latest techniques like single or double steel truss shear connectors, glass fibre reinforced polyester shear grids etc.

Table 4-8 Composite action of all sandwich panels at elastic and ultimate stage

Specimen	Initial stiffness			Ultimate strength	
	Deflection (mm)	I_E (10^6 mm^4)	K_1 (%)	Ultimate load (kN)	K_2 (%)
FSP-I	0.545	20.76	81.91	60.11	53.89
FSP-II	0.395	22.03	82.21	48.28	25.80
CRSP-I	0.712	23.05	81.97	62.30	59.09
CRSP-II	0.78	27.88	82.04	53.21	37.5

4.4.4 Formation of cracks

During the experimental testing, all specimens were carefully observed for visible cracks and marked. The respective crack loads were noted and marked besides the crack lines. It is observed that all specimen ultimately failed in a similar way by developing flexural cracks in constant moment region. The cracks initially appeared in bottom concrete wythe as expected and propagated vertically towards the core depicting a flexure failure. On reaching the failure load, these cracks further travelled through the core towards top concrete wythe. Moreover, few angular cracks appeared near the end of supports, which resulted in shear failure. The typical failure mode and crack pattern of all specimens is illustrated in Figure 4-18. To summarise, the failure mode was initially governed by tensile failure of bottom concrete wythe and ultimately, by combine shear and bending failure. The test was terminated when large deformations were observed in relation to the applied load.

The CRSP showed promising results in terms of ductility and resisting the externally applied load. Owing to flexible nature of crumb rubber, no visible damage was witnessed in the core. This indicates that recycled tyre crumb core in panels can be recycled when sandwich panel reaches its service life by replacing the concrete wythes.



(a)



(b)



(c)

Figure 4-18 Failure and crack pattern at end of test (a) SCP (b) FSP (c) CRSP

4.5 Finite Element Analysis

In order to simulate structural behaviour of CRSP specimen, finite element analysis was conducted in “ABAQUS/CAE 6.14-5” (6.14, 2018) with standard/explicit model. The study aimed at numerical simulation of flexural test based on non-linear static analysis. It was primarily developed as a tool for future to perform parametric studies including the factors effecting the flexural strength, concrete damage and to investigate the influence of punching shear load. The material properties, assembly of parts, element types, load and boundary conditions are discussed in detail in following section.

4.5.1 Material Properties

The material behaviour of SCC was defined in terms of elastic and plastic properties. The linear elastic behaviour was described using Young’s modulus of 28 GPa and Poisson ratio of 0.3. For non-linear plastic behaviour, material models like concrete damage plasticity (CDP) and concrete smeared cracking are available in the software. However, CDP is commonly used to simulate damage in concrete using compressive and tensile behaviour. The constitutive parameters used in this study were dilation angle, eccentricity, uniaxial/biaxial ratio, the shape of the deviatoric cross section and viscosity. The values were obtained from Abrishambaf’s (Abrishambaf et al., 2015) study on SCC and are presented in Table 4-9. The material parameters for defining concrete compressive and tensile behaviour depend on crushing or cracking strains are presented in Table 4-10.

Table 4-9 Concrete Damage Parameters of 50MPa SCC used in FEA

Dilation Angle (ψ)	Eccentricity (ϵ)	Initial biaxial/uniaxial ratio (f_{b0}/f_{c0})	K_c	Viscosity parameter (μ)
40°	0.1	1.16	0.667	0.0001

The linear elastic and non-linear plastic behaviour was implemented to identify mechanical properties for 8mm and 6mm reinforcing bars. The elastic modulus and Poisson's ratio dictate linear elastic behaviour of material whereas, the plastic behaviour was specified in terms of yield stress, plastic stress and ultimate strain and is previously mentioned in Table 4-6. The material properties used for crumb rubber were elastic modulus and Poisson's ratio ($\mu=0.4$) only, since no plastic deformation was witnessed in core during material testing and four-point bending.

Table 4-10 Material properties for concrete compression and tension behaviour

Concrete compressive behaviour		Concrete compression damage	
Yield stress (MPa)	Inelastic strain	Damage parameter	Inelastic strain
20	0	0	0
30	7.38E-05	0	7.38E-05
35	5.13E-04	0	5.13E-04
40	0.000167	0	0.000167
45	0.000232	0	0.000232
48	0.000355	0	0.000355
49.5	0.000472	0	0.000472
50	0.000678	0	0.000678
49.5	0.000872	0.01	0.000872
48	0.001155	0.04	0.001155
45	0.001421	0.09	0.001421
40	0.001784	0.16	0.001784
35	0.002133	0.25	0.002133
30	0.002578	0.36	0.002578
20	0.0030	0.49	0.0030
15	0.00322	0.64	0.00322
10	0.00388	0.81	0.00388
Concrete tensile behaviour		Concrete tension damage	
Yield stress (MPa)	Cracking strain	Damage parameter	Cracking strain
4.07	0	0	0
0.04	0.001932	0.99	0.001932

4.5.2 Assembly and Interaction properties

The three-dimensional numerical model consists of two concrete wythes, crumb rubber, longitudinal and transverse reinforcement, shear connectors, supports and loading pins. All

parts of models were built separately as 3D deformable type and later, joined together using available techniques in assembly section. The sandwich panel is discretised using eight-noded reduced integration brick element (C3D8R) for both concrete wyth and core, whereas two-node 3D deformable truss element (T3D2) is used for defining reinforcement.

In interaction section, tie technique was used to connect the surfaces of both concrete wythes to the core in order to provide adhesive bonding between two solid surfaces. The 8mm and 6mm diameter steel reinforcement mesh was connected with solid elements to constrain and provide appropriate bonding using embedded region method. The contact between steel supports and bottom concrete wythe was defined by surface-to-surface contact (standard) using tangential ($\mu=0.45$) and normal behaviour, whereas, the contact between top concrete wythe and loading pins was established by tie contact technique. In analysis, supports and loading pins were defined as rigid bodies and were assigned reference point (RP) to apply constraints and extract significant data.

4.5.3 Loading and boundary conditions

The step part consists of initial and static, general with automatic increment type. The displacement/rotation option was applied in mechanical category to allow rotation about z-axis only ($U_x=U_y=U_z=U_{RX}=U_{RY}=0$) in order to simulate simply support conditions. Subsequently, constant displacement ($U_x=U_z=U_{RX}=U_{RY}=U_{RZ}=0$) was applied in y-axis through both loading pins onto the top concrete wyth till failure. The failure/fracture in concrete wythes were

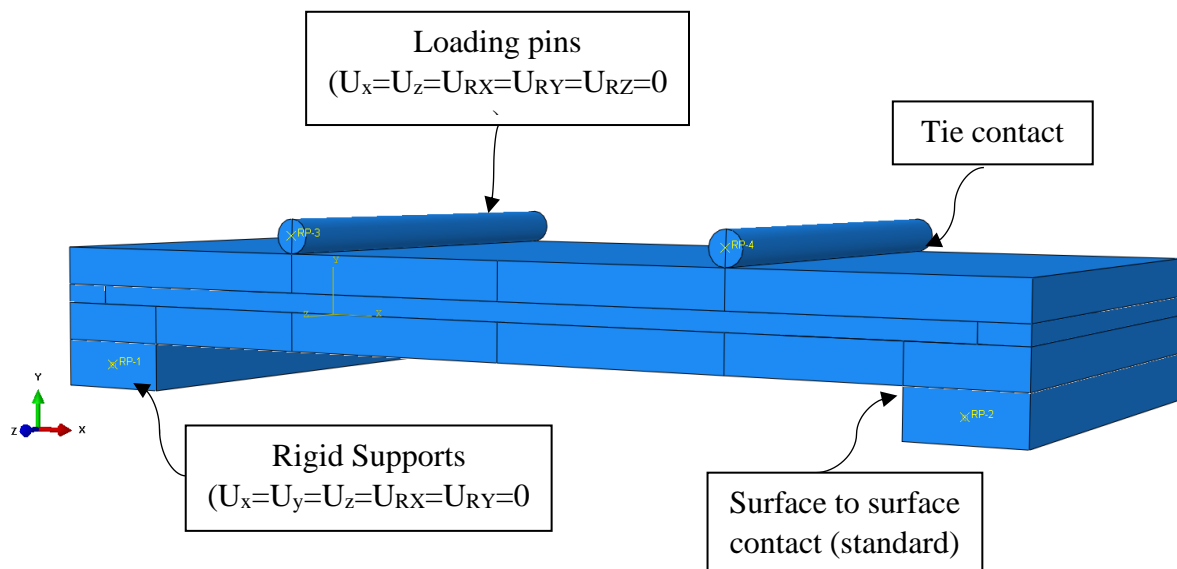


Figure 4-19 Numerical model of CRSP showing loading and boundary conditions

identified through field output in compressive (DAMAGEC), tensile (DAMAGET) damage and plastic strain (PE). Finally, the distortion in finite elements were critically analysed to delete any errors in the model. Figure 4-19 illustrates the numerical model of CRSP with relevant details.

4.5.4 Validation of model

Initially, various mesh sizes were applied and studied on FE model to obtain convergence of results with logical precision. However, an appropriate mesh size of 10mm was finally obtained for concrete wythe and core that gives accurate results in a reasonable time period. The validation of FE model was checked with experimental test result on CRSP and also, the efficiency of model in predicting structural behaviour of CRSP was analysed in terms of load-deflection curve and tensile failure in bottom concrete wythe. Table 4-11 shows convergence results by comparing the ultimate load and deflection for CRSP between experimental test and analysis.

Table 4-11 Comparison of ultimate load for experimental and FEA

Experimental	FEA	$\% = \frac{P_{FEA} - P_{EXP}}{P_{EXP}} \times 100$
Ultimate load (kN)		
62.30	69.85	12.11 %

4.5.5 FE Analysis Discussion

Figure 4-20 presents a comparison of load-deflection relationship for experimental testing and FEM analysis. At initial stage of loading, the proposed FE model showed a stiffer behaviour and initial crack appeared at around 30.89 kN, which is higher than the experimental cracking load. Later on, the relationship begins to converge as the load enters the plastic region. The

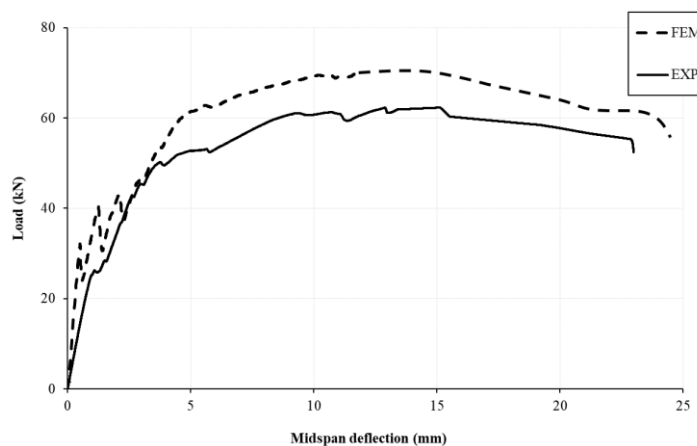


Figure 4-20 Load versus vertical deflection at mid-span for CRSP

initial cracks appeared exactly below the loading pins in bottom concrete wythe and propagated vertically towards core similar to experimentation. Several flexural cracks appeared in the bottom concrete wythe and ultimately, caused the failure. The analysis was finally terminated after the load-deflection relation became horizontal i.e. large deflections with negligible increase in load.

Figure 4-21 (a) and (b) depicts 3D and 2D failure pattern developed at ultimate collapse. The final deflected shape of CRSP is presented in Figure 4-22, where maximum deflection is measured at mid-span. The ultimate load obtained from FE model is 69.85 kN, close to experimental peak load. Both longitudinal and transverse reinforcement showed no sign of yielding during the analysis.

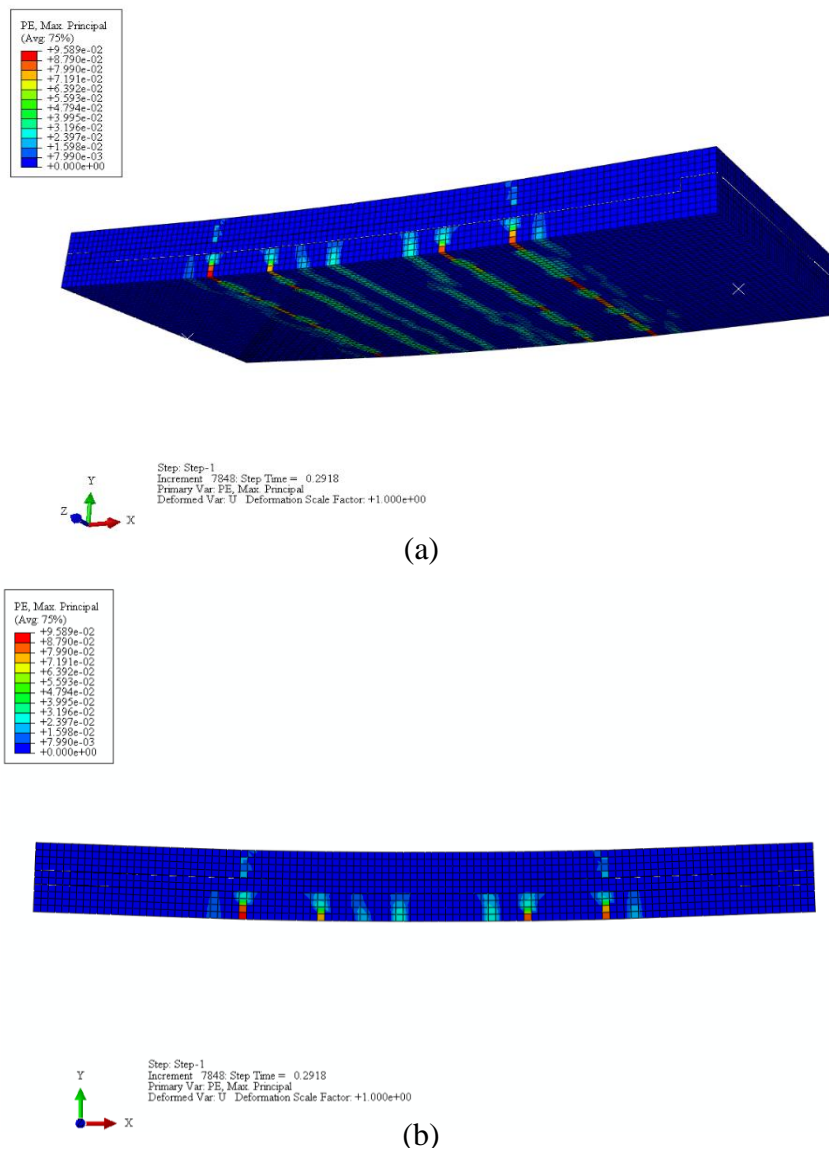


Figure 4-21 Concrete damage (a) 3D crack pattern on the bottom concrete wythe of CRSP at ultimate load (b) 2D crack pattern of CRSP at ultimate load

It can be observed that FE model has slightly exaggerated the load-deflection response of CRSP and overestimated the stiffness of the testing specimen. The possible reason could be the precise alignment of core in the centre of FE model as compared to testing specimen. As already discussed in load-deflection section that during pouring of fresh concrete in the formwork, deliberate attention was paid to keep the core exactly in the centre of the panel. But it was difficult to keep it perfectly aligned due to crumb rubber's flexibility. However, the analytical model is still capable of simulating the structural behaviour of CRSP in flexural bending in terms of ultimate load, vertical deflection at mid-span and concrete failure with reasonable accuracy when compared with experimental results.

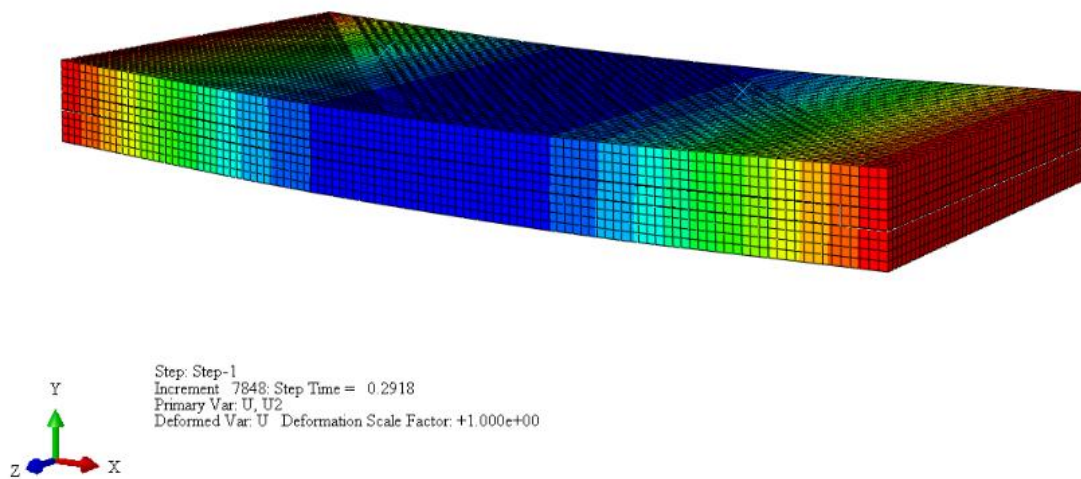


Figure 4-22 Deformed shape of numerical model of CRSP at ultimate load

4.6 Conclusion

This study basically explored the structural behaviour of an innovative precast concrete sandwich panel, in which recycle tyres are used for the first time as crumb rubber core. Three types of specimens i.e. SCP, FSP and CRSP were casted using SCC and tested in flexural bending. The structural behaviour of CRSP was studied along with SCP and FSP in terms of failure load, ultimate deflection, strain variation, degree of composite action and crack patterns. The vertical deflection and strain variations were examined at mid-span of all specimens. The degree of composite action was assessed in terms of initial stiffness and ultimate strength. A partial composite behaviour was observed in all sandwich panels by implementing both approaches. However, the percentage of composite action can be improved by employing latest techniques available in literature. During the experimental testing, all visible cracks were observed and marked with the respective cracking loads. The failure in all sandwich panels

occurred with initiation of vertical cracks between applied loads and propagated towards the core. This was followed by angular cracks appeared between the end support and applied load region and eventually, led to combine shear and flexural failure. All specimen produced large deflections and exhibited a ductile failure. CRSP-I resisted maximum load of 62.30kN, while FSP-II exhibited lowest strength of 48.28kN among all sandwich panels. In addition, the average ultimate strength of CRSP is nearly 6.54% higher than FSP in resisting the applied load. The research also proposed a 3D FE model for CRSP to study the analytical behaviour in bending. CDP model was implemented to simulate concrete damage in compression and tension. The validation of model was performed using the experimental data and a good agreement between the test and analysis was found. The model accurately predicted concrete damage in bending and could be used for further studies on proposed CRSP.

This study accomplished substantial finding which highlights that CRSP are efficient in terms of structural performance when compared with traditional precast concrete panels i.e. SCP and FSP. Therefore, the proposed sandwich panel offers a realistic alternative to reuse/recycle waste tyre as core material in sandwich panels, which will eventually help in reducing the harmful environmental impacts. In addition, these innovative panels may be employed as structural members in buildings, where traditional precast concrete panels are typically used. In the end, it is proposed in future, to investigate the structural behaviour of CRSP in resisting axial and impact loading.

4.7 Reference

- 6.14, Abaqus. (2018). ABAQUS Documentation', Dassault Systèmes, Providence, RI, USA. In
- Abrishambaf, A., Barros, J. A. O., & Cunha, V. M. C. F. (2015). Tensile stress–crack width law for steel fibre reinforced self-compacting concrete obtained from indirect (splitting) tensile tests. *Cement and Concrete Composites*, 57, 153-165.
- Alsaif, A., Koutas, L., Bernal, S. A., Guadagnini, M., & Pilakoutas, K. (2018). Mechanical performance of steel fibre reinforced rubberised concrete for flexible concrete pavements. *Construction and Building Materials*, 172, 533-543.
- Balcioğlu, H. (2018). Flexural behaviors of sandwich composites produced using recycled and natural material.
- Benayoune, A., Samad, A. A. A., Abang Ali, A. A., & Trikha, D. N. (2007). Response of pre-cast reinforced composite sandwich panels to axial loading. *Construction and Building Materials*, 21(3), 677-685.
- Benayoune, A., Samad, A. A. A., Trikha, D. N., Abang Ali, A. A., & Ashrabov, A. A. (2006). Structural behaviour of eccentrically loaded precast sandwich panels. *Construction and Building Materials*, 20(9), 713-724.
- Benayoune, A., Samad, A. A. A., Trikha, D. N., Ali, A. A. A., & Ellinna, S. H. M. (2008). Flexural behaviour of pre-cast concrete sandwich composite panel – Experimental and theoretical investigations. *Construction and Building Materials*, 22(4), 580-592.
- Bida, S. M., Aziz, F. N. A. A., Jaafar, M. S., Hejazi, F., & Nabilah, A. B. (2018). Advances in Precast Concrete Sandwich Panels toward Energy Efficient Structural Buildings.
- Carroll, J. C., & Helminger, N. (2016). Fresh and Hardened Properties of Fiber-Reinforced Rubber Concrete. *Journal of Materials in Civil Engineering*, 28(7), 04016027.
- Colombo, I. G., Colombo, M., & di Prisco, M. (2015). Bending behaviour of Textile Reinforced Concrete sandwich beams. *Construction and Building Materials*, 95, 675-685.
- Corredor-Bedoya, A. C., Zoppi, R. A., & Serpa, A. L. (2017). Composites of scrap tire rubber particles and adhesive mortar – Noise insulation potential. *Cement and Concrete Composites*, 82, 45-66.
- da Silva, F. M., Gachet Barbosa, L. A., Lintz, R. C. C., & Jacintho, A. E. P. G. A. (2015). Investigation on the properties of concrete tactile paving blocks made with recycled tire rubber. *Construction and Building Materials*, 91, 71-79.
- Dębska, B., Lichołai, L., & Miąsik, P. (2019). Assessment of the Applicability of Sustainable Epoxy Composites Containing Waste Rubber Aggregates in Buildings. *Buildings*, 9(2), 31.
- Ekenel, M. (2014). Testing and Acceptance Criteria for Fiber-Reinforced Composite Grid Connectors Used in Concrete Sandwich Panels. *Journal of Materials in Civil Engineering*, 26(6).
- Elchalakani, M. (2015). High strength rubberized concrete containing silica fume for the construction of sustainable road side barriers. *Structures*, 1, 20-38.

- Fernández-Ruiz, M. A., Gil-Martín, L. M., Carbonell-Márquez, J. F., & Hernández-Montes, E. (2018). Epoxy resin and ground tyre rubber replacement for cement in concrete: Compressive behaviour and durability properties. *Construction and Building Materials*, 173, 49-57.
- Fraile-Garcia, E., Ferreiro-Cabello, J., Mendivil-Giro, M., & Vicente-Navarro, A. S. (2018). Thermal behaviour of hollow blocks and bricks made of concrete doped with waste tyre rubber. *Construction and Building Materials*, 176, 193-200.
- Gara, F., Ragni, L., Roia, D., & Dezi, L. (2012). Experimental tests and numerical modelling of wall sandwich panels. *Engineering Structures*, 37, 193-204.
- Gheni, A. A., Alghazali, H. H., ElGawady, M. A., Myers, J. J., & Feys, D. (2019). Durability properties of cleaner cement mortar with by-products of tire recycling. *Journal of Cleaner Production*, 213, 1135-1146.
- Girskas, G., & Nagrockienė, D. (2017). Crushed rubber waste impact of concrete basic properties. *Construction and Building Materials*, 140, 36-42.
- Han, Wang Y-H, Xu J, & Y, X. (2016). Fatigue behavior of stud shear connectors in steel and recycled tyre rubber-filled concrete composite beams. *Steel and Composite Structures*, 22(2), 353-368.
- Han, Z., Chunsheng, L., Kombe, T., & Thong-On, N. (2008). Crumb rubber blends in noise absorption study. *Materials and Structures*, 41(2), 383-390.
- Handbook, P. (2007). *Precast and Prestressed Concrete* (6th ed.).
- Hesami, S., Salehi Hikouei, I., & Emadi, S. A. A. (2016). Mechanical behavior of self-compacting concrete pavements incorporating recycled tire rubber crumb and reinforced with polypropylene fiber. *Journal of Cleaner Production*, 133, 228-234.
- Huntsman. (2021). Rubber Crumb Polyurethane Adhesive System. Retrieved 16 Feb from <https://www.industrysearch.com.au/rubber-crumb-polyurethane-adhesive-systems/p/35965>
- I. Goh, W., Mohamad, N., Abdullah, R., & A. Samad, A. A. (2016). Finite Element Analysis of Precast Lightweight Foamed Concrete Sandwich Panel Subjected to Axial Compression. *Journal of Computer Science & Computational Mathematics*, 6(1), 1-9.
- Ismail, M. K., Hassan, A. A. A., & Hussein, A. A. (2017). Structural behaviour of reinforced concrete beams containing crumb rubber and steel fibres. *Magazine of Concrete Research*, 69(18), 939-953.
- Jokar, F., Khorram, M., Karimi, G., & Hataf, N. (2019). Experimental investigation of mechanical properties of crumbed rubber concrete containing natural zeolite. *Construction and Building Materials*, 208, 651-658.
- Joseph, J. D. R., Prabakar, J., & Alagusundaramoorthy, P. (2017). Precast concrete sandwich one-way slabs under flexural loading. *Engineering Structures*, 138, 447-457.
- Khalil, A., Abdul Samad, A., & Goh, W. (2014). Structural Behavior of Precast Lightweight Foam Concrete Sandwich Panel with Double Shear Truss Connectors under Flexural Load. *ISRN Civil Engineering*, 2014(1).
- Ma, M., JE. (2014). Structural performance of composite panels filled with light-weight crumb rubber concrete.

- Mishra, M., & Panda, K. C. (2015, 2015//). Influence of Rubber on Mechanical Properties of Conventional and Self Compacting Concrete. *Advances in Structural Engineering*, New Delhi.
- Mohamad, N., Goh, W. I., Abdullah, R., Samad, A. A. A., Mendis, P., & Sofi, M. (2017). Structural performance of FCS wall subjected to axial load. *Construction and Building Materials*, 134, 185-198.
- Mohammed, B. S., & Adamu, M. (2018). Mechanical performance of roller compacted concrete pavement containing crumb rubber and nano silica. *Construction and Building Materials*, 159, 234-251.
- Mugahed Amran, Y. H., Abang Ali, A. A., Rashid, R. S. M., Hejazi, F., & Safiee, N. A. (2016). Structural behavior of axially loaded precast foamed concrete sandwich panels. *Construction and Building Materials*, 107, 307-320.
- Murugan, Natarajan, & C. (2015, 2015//). Investigation of the Behaviour of Concrete Containing Waste Tire Crumb Rubber. *Advances in Structural Engineering*, New Delhi.
- Naito, C., Hoemann, J., Beacraft, M., & Bewick, B. (2012). Performance and Characterization of Shear Ties for Use in Insulated Precast Concrete Sandwich Wall Panels. *Journal of Structural Engineering*, 138(1), 52-61.
- Pessiki, S., & Mlynarczyk, A. (2003). Experimental evaluation of the composite behavior of precast concrete sandwich wall panels. *PCI journal*, 48(2), 54-+.
- Raffoul, S., Garcia, R., Pilakoutas, K., Guadagnini, M., & Medina, N. F. (2016). Optimisation of rubberised concrete with high rubber content: An experimental investigation. *Construction and Building Materials*, 124, 391-404.
- Rivas-Vázquez, L. P., Suárez-Orduña, R., Hernández-Torres, J., & Aquino-Bolaños, E. (2015). Effect of the surface treatment of recycled rubber on the mechanical strength of composite concrete/rubber. *Materials and Structures*, 48(9), 2809-2814.
- Sukontasukkul, P. (2009). Use of crumb rubber to improve thermal and sound properties of pre-cast concrete panel. *Construction and Building Materials*, 23(2), 1084-1092.
- Winter, M. G., Reid, M., & Johnson, P. E. (2005). Construction of road foundations on soft ground using lightweight tyre bales.
- Xu, J., Fu, Z., Han, Q., Lacidogna, G., & Carpinteri, A. (2018). Micro-cracking monitoring and fracture evaluation for crumb rubber concrete based on acoustic emission techniques. *Structural Health Monitoring*, 17(4), 946-958.
- Xu, J., Yao, Z., Yang, G., & Han, Q. (2020). Research on crumb rubber concrete: From a multi-scale review. *Construction and Building Materials*, 232, 117282.
- Youssf, O., Hassanli, R., Mills, J. E., Skinner, W., Ma, X., Zhuge, Y., Roychand, R., & Gravina, R. (2019). Influence of Mixing Procedures, Rubber Treatment, and Fibre Additives on Rubcrete Performance. *Journal of Composites Science*, 3(2), 41.

CHAPTER 5 COMPRESSIVE BEHAVIOUR OF PRECAST CONCRETE SANDWICH PANELS CONTAINING RECYCLED TYRE CRUMB CORE

5.1 Abstract

This paper presents the structural behaviour of precast concrete sandwich panels (PCSPs) containing recycled tyre crumb core under uni-axial compression and compared with that containing commonly used expanded polystyrene (EPS) foam. A total of six panels were cast and tested. Two for each category of precast concrete panels i.e. solid concrete panel, recycled tyre crumb sandwich panel and foam sandwich panel. Results showed that the ultimate axial load of recycled tyre crumb sandwich panel was found to be 91% of solid concrete panel and also exhibited higher structural response in comparison to foam sandwich panel. It was observed that all panels failed in a similar manner by crushing of concrete at ultimate load. Moreover, a finite element model was developed in ABAQUS using in-built model of concrete plasticity damage to simulate the ultimate axial capacity of recycled tyre crumb rubber concrete sandwich panel and its failure in uniaxial compression. Analysis showed that the FEM slightly overestimated the experimental results. Furthermore, the experimental test results showed that the recycled tyre crumb can be utilized as an alternate core material in PCSPs without substantially compromising the ultimate strength or any change in structural response.

5.2 Introduction

Global warming is one of the characteristics of climate change, which is caused by non-renewable fuel consumption, deforestation and mismanagement of land. It is stated that the surface temperature of the earth has increased by about 1 degree Celsius since 1980 and is currently rising by 0.2 degrees Celsius every ten years (NOAA, 2020). The development of infrastructure adversely affected the environment as it involved the extensive use of natural resources like extraction of raw material. In order to deal with growing environmental issues, research scientists around the globe are looking for viable options to recycle and reuse waste materials in order to conserve natural resources and offer sustainable solutions.

Discarded tyres are a major source of ecological hazard and currently, one of the biggest challenges is to recycle/reuse discarded tyres. The sale of tyres reached a significant figure of approximately 3.66 billion in 2018 (Statista, 2021). Similarly, around 48 million tyres complete their service life each year in Australia and merely 16% were locally recycled (Brindley et al., 2012). This alarms that the remaining percentage will end up in landfills causing environmental

and health issues. Therefore, there is a dire need to find alternate solutions to recycle/reuse waste tyres. Previously, various research studies have been conducted to incorporate waste tyres in civil engineering applications like tyre bales for soil reinforcement and erosion control (Awan & Shaikh, 2021), backfill material for bridges (Cecich et al., 1996), use of crumb rubber in replacement of fine aggregate (Batayneh et al., 2008; Mohammed et al., 2012) and in road asphalt mixing (Norambuena-Contreras et al., 2021; Vishnu & Lakshman Singh, 2021). It is pertinent to report that the use of crumb rubber in concrete improved the properties such as crack resistance (Ho et al., 2012), impermeability (Wang et al., 2019), toughness (Noaman et al., 2016), freeze-thaw resistance (Gesoglu et al., 2014) and damping ratio (Zheng et al., 2008), (Xue & Shinozuka, 2013) whereas, it significantly decreased the compressive strength, modulus of elasticity, bond strength, tensile and flexural strength (Pacheco-Torgal et al., 2012; Rashad, 2016; Roychand et al., 2020; Siddique & Naik, 2004; Strukar et al., 2019). However, it is encouraging to report that the use of rubberized concrete instead of traditional concrete improved the dynamic response of the structural member in terms of ductility, energy absorption and loss of stiffness, which therefore makes it suitable to be used in structural applications subjected to dynamic loads (Eltayeb et al., 2021).

Sandwich panels are widely used in the manufacturing of automotive, aerospace and concrete structures. In the construction industry, a typical sandwich panel consists of two outer wythes and a core. A wyth is usually made up of reinforced concrete or steel sheet whereas core is an insulation material like foam, balsa wood or corrugated sheet. Previously, numerous research studies have been carried out to explore the possibility of using different core materials like corrugated sheets (Rejab & Cantwell, 2013; Wadley et al., 2013; Zhang et al., 2016), honeycomb cores (Davalos et al., 2001; Qi et al., 2017; Xie et al., 2020), foam concrete core (Flores-Johnson & Li, 2012), truss core (Kazemahvazi et al., 2009; Kazemahvazi & Zenkert, 2009) and foam (Amran, Raizal, et al., 2016; Amran, Rashid, et al., 2016; Benayoune et al., 2006; Benayoune et al., 2008; Gara et al., 2012; Khalil et al., 2014; Metelli et al., 2011; Mohamad et al., 2017; Mugahed Amran et al., 2016). It is also learnt from the literature that the option of using recycled tyre crumb as core material in PCSP has never been explored. However, the use of recycled tyre crumb in sandwich panels is expected to add advantages like low thermal conductivity, high sound insulation, high impact resistance, elimination of low compressive strength problems and low energy utilization. Furthermore, the building industry contributes nearly one-third of all greenhouse gas emissions and recycling huge quantities of

discarded tyres in the form of core material in PCSPs could significantly reduce emissions and alleviate environmental hazards.

As discussed earlier, the existing research studies only focused on using the recycled tyre crumb as a partial replacement of fine aggregate in concrete mix and hardly any researcher explored the efficiency of PCSPs containing recycled tyre crumb as a core. Therefore, the structural performance of recycled tyre crumb sandwich panel in uni-axial compression loading was investigated in this research study. For this purpose, three types of precast concrete panels i.e. solid concrete panel, recycled tyre crumb sandwich panel and foam sandwich panel were manufactured and tested under axial loading for comparative analysis. The research also evaluated the ultimate axial load capacity, vertical deflection, lateral displacement, strain pattern in concrete and in reinforcement and mode of failure. A finite element model of recycled tyre crumb panel was also developed in ABAQUS to simulate the ultimate axial capacity. The validation of FE model was conducted with the experimental test data and later, the proposed FE model was used to predict the ultimate load capacity and concrete damage in compression. In the end, the ultimate axial load of PCSPs i.e. foam sandwich panel and recycled tyre crumb sandwich panel were computed through the empirical formulas proposed by the previous researchers. These equations provided conservative values for the design axial load and therefore, it was deduced that these equations can safely be applied.

5.3 Experimental work

In order to investigate and compare the structural performance of precast concrete sandwich panels under axial loading, three type of specimens i.e. solid concrete panel, foam (polystyrene) sandwich panel and recycled tyre crumb sandwich panel were tested. Two specimens were cast for each type. All specimens were 1100 mm high, 500 mm wide and 100mm thick. For composite panels, a standard thickness of 20mm and 40mm was selected for the core and concrete wythe, respectively.

5.3.1 Geometric details of specimen

Self-compacting concrete (SCC) was used to cast all the panels. In solid precast concrete panel, 8mm diameter deformed bars with centre-to-centre spacing of 100 mm were used in the form of a mesh. A minimum concrete cover of 40mm was maintained for the steel reinforcement (Figure 5-1). The precast concrete sandwich panels were made up of two outer reinforced concrete wythes and a core (insulation). Both concrete wythes were 40mm thick and reinforced

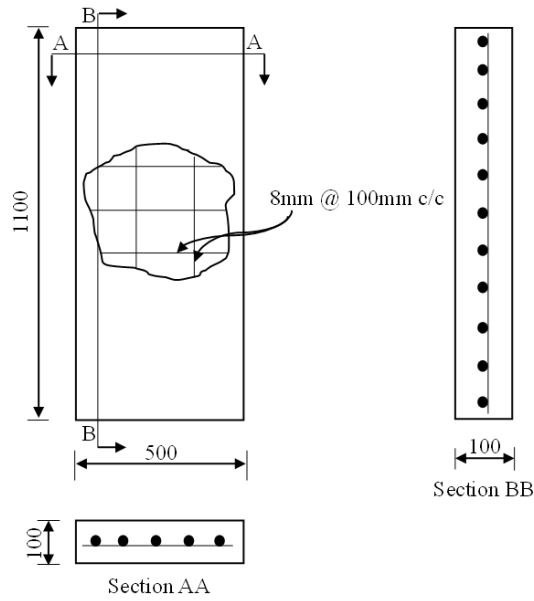


Figure 5-1 Geometric details of solid concrete panel (All dimensions are in mm)

with 8mm diameter deformed bars mesh with a spacing of 100mm centre-to-centre. The steel meshes embedded in each concrete wythes were connected through 6mm diameter shear connectors as shown in Figure 5-2, with a minimum concrete cover of 20mm.

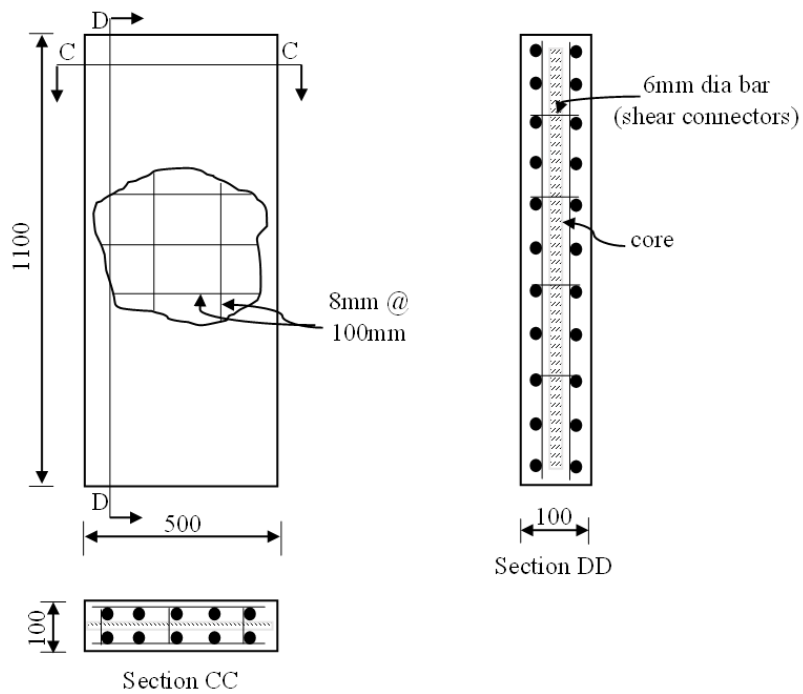


Figure 5-2 Geometric details of precast concrete sandwich panels (All dimensions are in mm)

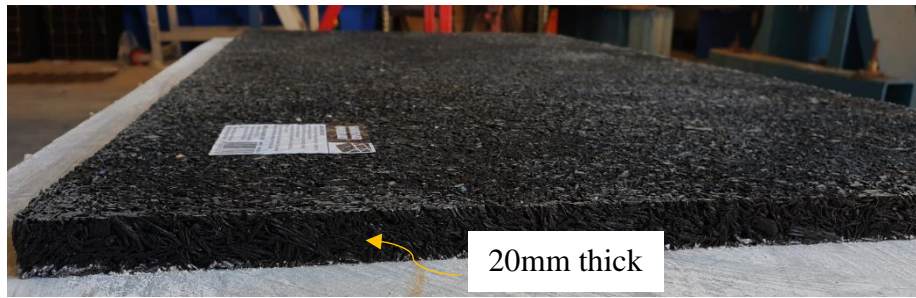


Figure 5-3 Recycle tyre crumb sheet

A core thickness of 20mm was designed for all sandwich panels. Two types of insulation material were selected for the construction of sandwich panels; (a) foam and (b) recycled tyre crumb rubber. Foam (polystyrene) is commonly used in the construction of PCSPs due to its low cost and easy availability whereas, recycled tyre crumb rubber is the new insulation material introduced in this research study. Both insulation materials are generally available in the form of sheets and can be cut into the required sizes. Figure 5-3 shows a typical crumb rubber sheet which were locally obtained. The assembling of steel mesh (SL81) with recycled



Figure 5-4 Steel mesh (SL81) and recycle tyre crumb rubber sheet with reinforcement details

tyre crumb rubber and shear connectors are presented in Figure 5-4. The mechanical properties of insulation materials are discussed in the following sections.

5.3.2 Casting of specimen

The design of formwork for concrete panels was a challenging task, especially for 40mm thick concrete wythes. In order to cast panels, the formwork was designed in a way to allow smooth pouring of SCC. For this purpose, the formwork was laid horizontally on the ground surface along the height and concrete was poured from the top. This procedure eliminated the chances of segregation of concrete and also ensured equal distribution of concrete volume. The formwork was primarily built using waterproof timber sheets and was secured using threaded screws all around. All corners and edges of the formwork were sealed from inside using silicone. The formwork was left in the open air to dry for one day before pouring the concrete.

All components of sandwich panels like core, steel meshes and shear connectors were assembled externally and were placed inside the formwork afterwards. The formwork was levelled before pouring the concrete. The SCC was poured directly from the concrete mixer into the formwork through a chute. Figure 5-5 illustrates the pouring of fresh SCC and the completion phase of the casting of all panels. To ensure the consistency of SCC, various lab tests like slump flow test, T_{500} , V-funnel test, J-ring and U-box test were performed at the time of pouring fresh concrete. In addition, concrete cylinder specimens of 200mm x 100mm were taken for material testing. The panels were left for air drying and were later covered in wet jute fabric for curing. All panels were regularly cured for 28 days.



Figure 5-5 Formwork and casting of all concrete panels

5.3.3 Material properties

Self-compacting concrete (SCC)

In order to attain better compaction and smooth flow, a maximum aggregate size of 10 mm was selected for the mix design. Table 5-1 presents the main constituents and their proportions used for designing 50 MPa SCC. The detail of lab investigations performed to check the consistency of SCC is presented in Table 5-2.

Table 5-1 Mix proportion of SCC

Mix Constituent	Proportion
Cement Type GP, kg/m ³	291
Cement Type LH, GGBS, kg/m ³	194
Aggregate, 10mm, kg/m ³	788
Dust, kg/m ³	207
Coarse Sand, kg/m ³	307
Fine Sand, kg/m ³	419
Admixture-1 Retarder N (Type Re Retarder), ml/m ³	728
Admixture-2 Viscocrete10 (Type HWRRe), ml/m ³	2910
Admixture-3 Flow 15 (Type HWRRe), ml/m ³	970
Water, L/m ³	190

It is evident from the test results that all the parameters measured at the time of pouring SCC lies within the standard limits. In order to measure the mechanical properties of SCC, all cylinder specimens were cured in a water tank for 28 days and dried before testing. Uniaxial compression and split tensile test were performed on a universal testing machine (MCC8) as per ASTM C39 and C496 standards. Table 5-3 shows the material properties of SCC.

Table 5-2 Consistency tests for SCC and results

Test	Unit	Values	Acceptable range
Slump flow	mm	750	650-800
T ₅₀₀ slump flow	sec	5	2-5
V-funnel	sec	8	6-12
J-ring	mm	8	0-10
U-box (h ₂ -h ₁)	mm	1	0-30

Table 5-3 Material properties of SCC

Properties	
Density (kg/m ³)	2506
f _c ' (MPa)	50
f _t (MPa)	4.07
Modulus of elasticity (MPa)	28000
Poisson's ratio(ν)	0.3

Steel mesh (SL81) and shear connector

Tensile test was conducted on Shimadzu 300 kN universal testing machine on three samples each for 8mm diameter deformed bars and 6 mm diameter shear connectors to determine yield stress, ultimate stress and strain according to ASTM A370 standard. The material properties of SL81 mesh and shear connectors are reported in Table 5-4.

Table 5-4 Material properties of steel mesh (SL81) and shear connectors

Properties	SL81 mesh	Shear connector
Diameter (mm)	08	06
Density (kg/m ³)	7900	7700
Avg Yield Stress (MPa)	530.33	658.14
Avg Ultimate Stress (MPa)	560.54	764.24
Avg Ultimate Strain (MPa)	0.088	0.0907
Elastic Modulus (MPa)	207010	215800
Poisson ratio	0.3	0.3

Core material

The typical material properties of polystyrene include density (28 – 45 kg/m³), modulus of elasticity (1090 – 2900 MPa) and Poisson's ratio (0.2 – 0.4). These properties were provided by the manufacturer. For recycled tyre crumb core, the complete process of preparation can be accessed on the web (Huntsman, 2021). In order to bind the crumb together, a methyl based harmless product i.e. Methylene diphenyl diisocyanate (MDI) polyurethane was used as a binder. Since recycled tyre crumb is a new material and the relevant properties were unavailable with the manufacturer. Therefore, the important material properties were fully investigated in the lab by carrying out (a) uniaxial tensile test and (b) uniaxial compression test.

Uniaxial tensile test was performed using a universal testing machine (Schimadzu, 50 kN) as per ASTM D412 standard on a specimen size of 200mm x 50mm x 20mm at a rate of 500 mm/min. A total of five specimens were tested, however, one specimen was rejected being an outlier. Figures 5-6 and 5-7 display the tensile strength and ductile performance of four specimens of crumb core, respectively.

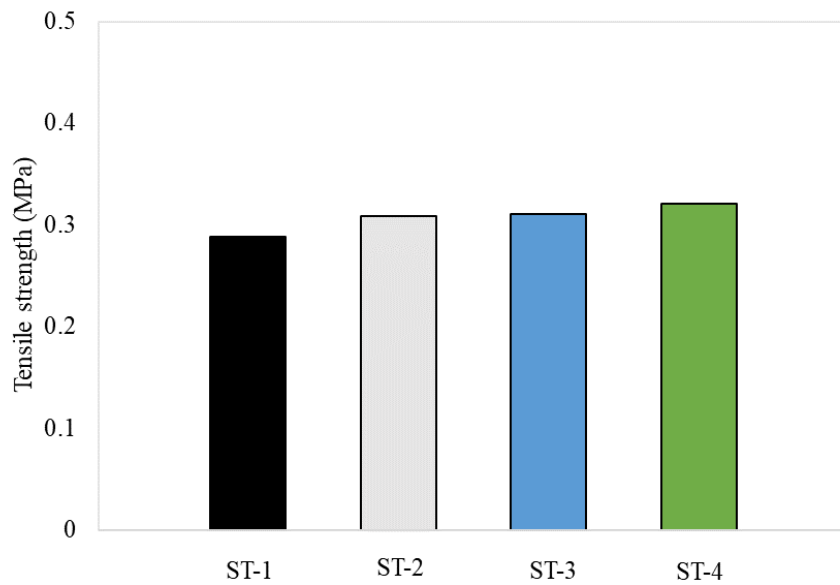


Figure 5-6 Ultimate tensile strength of four specimen of recycle tyre crumb core

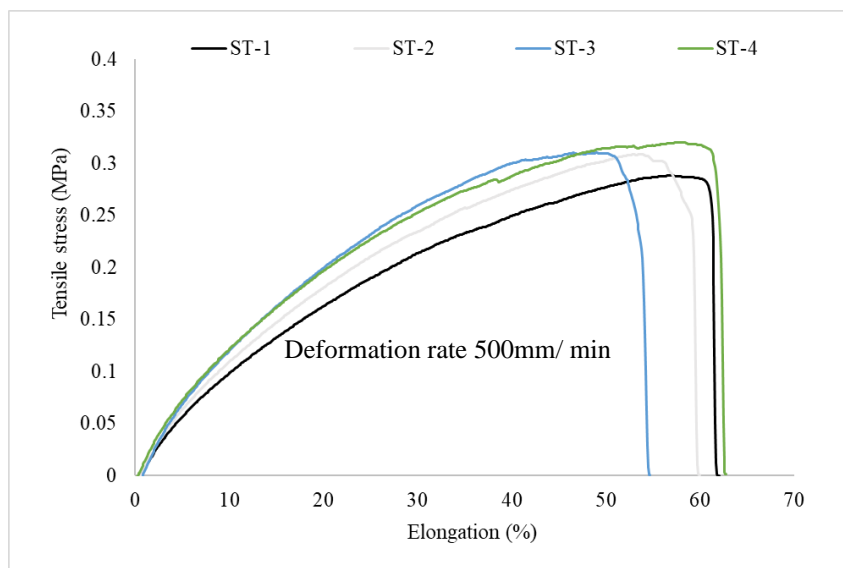


Figure 5-7 Tensile behaviour of recycle tyre crumb core

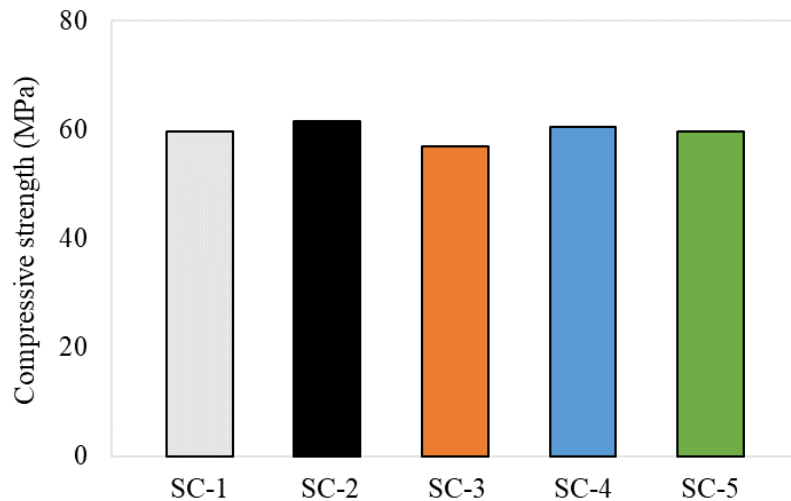


Figure 5-8 Compressive strength of five specimen of recycle tyre crumb core at strain value of 87.5%

Uniaxial compression test was also conducted on a universal testing machine (Schimadzu, 50kN) in accordance with ASTM D575 standard on a specimen thickness of 20 mm at a rate of 12mm/min. A total of five specimens were compressed to the maximum value of 17.5mm in order to avoid damage to the machine plates as they got too close. Therefore, the test was stopped at 17.5mm. Figure 5-8 exhibits the compressive strength of all specimens recorded only at a strain value of 87.5%. The maximum applied load was unable to produce any plastic deformation in all five specimens as shown in Figure 5-9. The material properties of recycled tyre crumb rubber are listed in Table 5-5.

Table 5-5 Material properties of recycle tyre crumb rubber

Properties	
Density (kg/m ³)	564.12
Average compression strength (MPa)	59.70
Elastic modulus (MPa)	1.92
Average tensile rupture strength (MPa)	0.307
Average elongation at break (%)	59.87

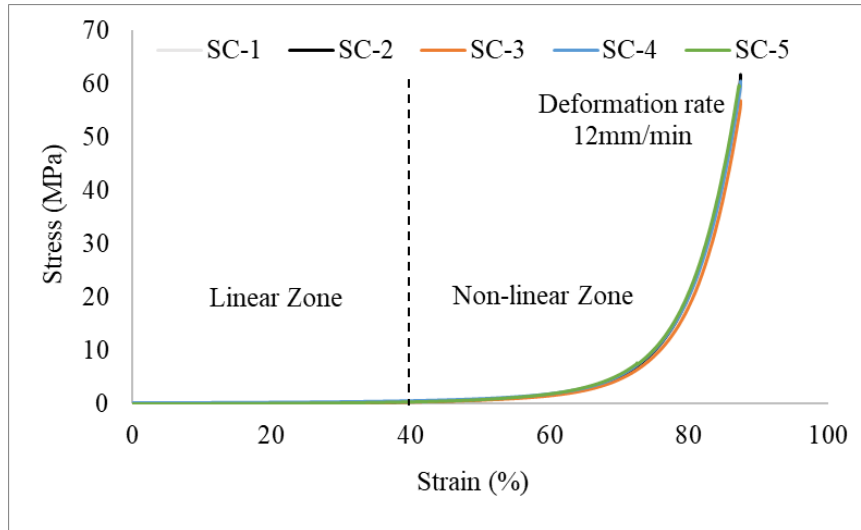


Figure 5-9 Compressive behaviour of recycle tyre crumb core

5.3.4 Instrumentation

The deformations were measured in terms of lateral and vertical deflection, strain variations on the concrete surface and steel reinforcement. Therefore, two types of sensors were employed to record these deformations (a) Linear Voltage Differential Transducers (LVDT) and (b) electrical strain gauges. For vertical and lateral displacement, LVDT with a maximum stroke length of 100 mm was used. Whereas for evaluation of strain, electrical strain gauges of 60 mm long with a gauge factor of 118.5 ± 0.5 and resistance of 120Ω were used. A total of seven LVDTs were used along the height of the panel, in which six LVDTs (LV1 – LV6) were placed horizontally and one LVDT (LV7) was placed vertically on the bottom flange of the load spreader. The graphical arrangement of all LVDTs is shown in Figure 5-10.

Similarly, four strain gauges (S1 to S4) were used on the concrete surface while another four strain gauges (S5 to S8) were positioned on steel reinforcement. S1 and S3 were placed at the centre along the height in vertical direction whereas S2 and S4 were used horizontally on concrete surfaces of front and back wythes (Figure 5-11). In addition, S5 and S7 were placed on steel reinforcement in the horizontal direction and S6 and S8 were placed vertically along the specimen height. Figure 5-12 demonstrates the detailed arrangement of all electrical strain gauges. Before placing the sensors on the concrete surface, the respective area was thoroughly cleaned using acetone and was sanded using silicon-carbide paper to even the surface. A similar procedure was adapted for placing strain gauges on steel reinforcement, in which the steel surface was slightly grinded and was made flat. Afterwards, all sensors were firmly secured using cyanoacrylate (CN and CN-E) adhesive. To stop moisture infiltration in electrical

strain gauges of steel reinforcement, a 3mm thick SB tape was placed on all strain gauges. In the end, a standard *Q1126* multimeter was employed to determine the serviceability of all electrical strain gauges.

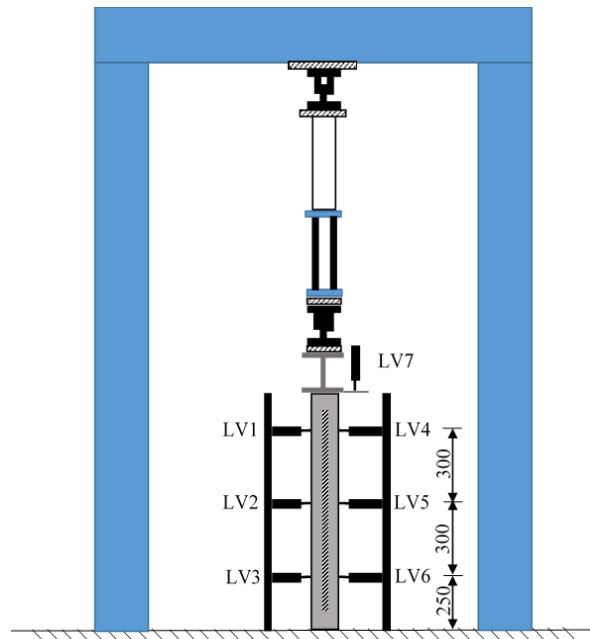


Figure 5-10 Instrumentation - Positioning of LVDTs - side elevation (all dimensions are in mm)

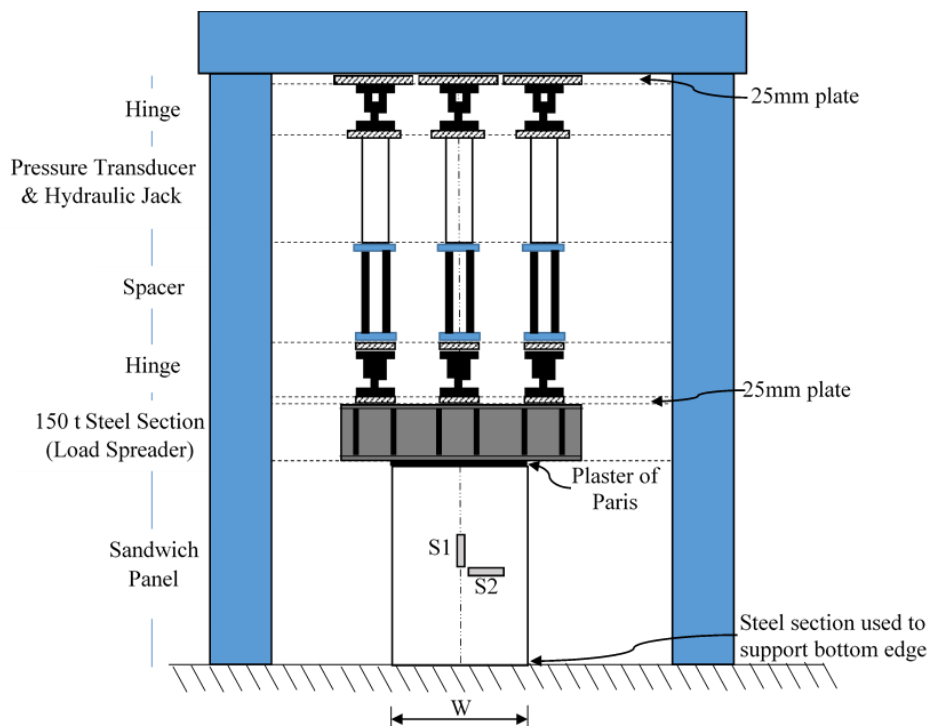


Figure 5-11 Instrumentation and test configuration – strain gauges on back side of concrete wythe (front elevation)

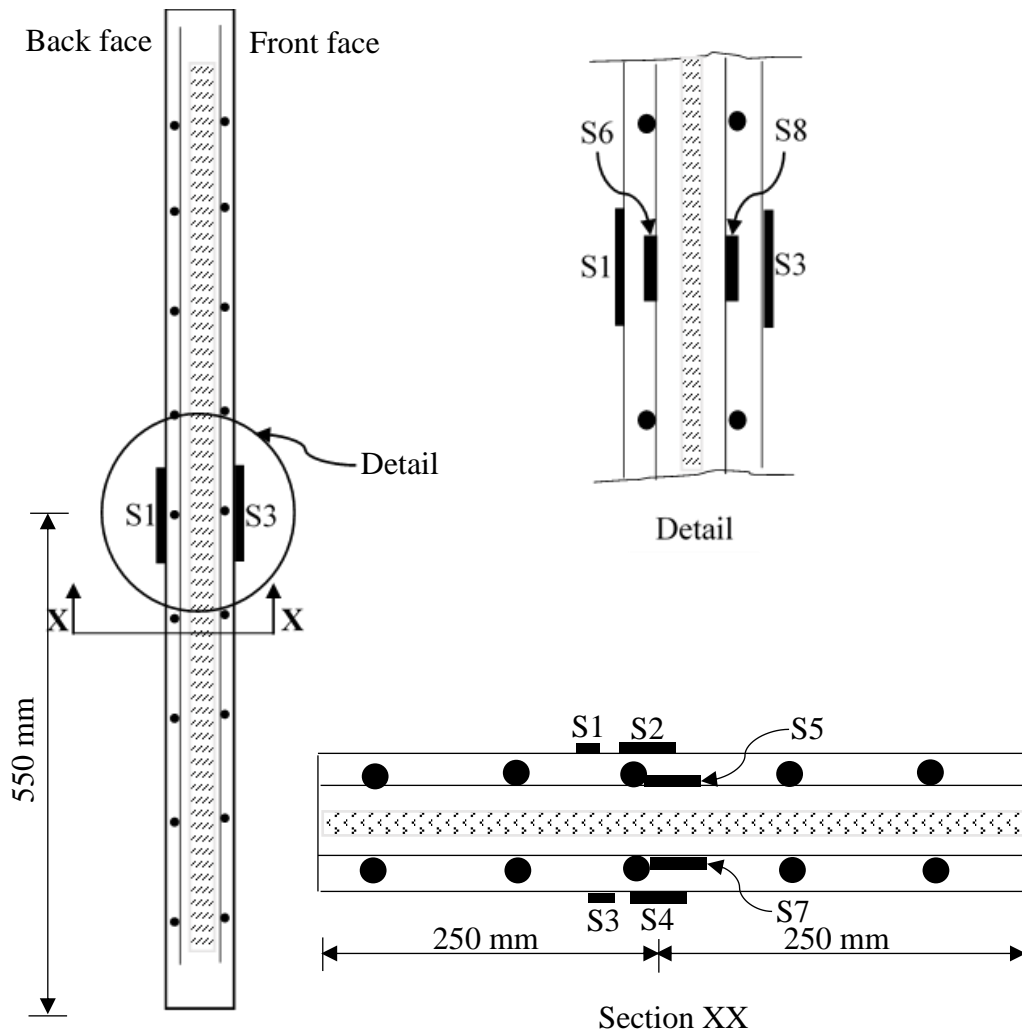


Figure 5-12 Strain gauges positioning on concrete surface at back and front face and on reinforcement mesh

5.3.5 Assembly of test setup

The structural test setup comprised of 25mm thick steel plates, 500 kN steel hinge, 720mm long spacers, 550 kN hydraulic jacks (SPX-RD5518) double-acting, hydraulic electric pump and 1500 kN load spreader. The test setup was designed to apply a compression load of 1500 kN with the help of three hydraulic jacks. The system was built on a reaction frame, in which three hydraulic jacks were separately attached to three steel hinges and steel plates at the top end, while the bottom end was attached to three spacers and steel hinges. The load spreader was connected to this assembly at three points and working of all three hydraulic jacks was checked before the placement of specimen and application of actual load. In order to ensure equal distribution of load and to obtain a flat surface, plaster of Paris was applied to the top surface of all specimens. Initially, a test load of 50 kN was applied to examine the performance of all equipment and attached devices. The bottom part of testing specimen was fixed against

any translation. In addition, the load spreader was centrally aligned with specimen and steel frames were used to ensure that the load is directly applied to the centre of specimen and hence, avoided creating any eccentricity. The first panel was tested by applying the compression load on the entire width of the specimen, however, no failure load was achieved. Therefore, due to the limited capacity of the test frame, it was decided to apply the load to 250mm width to achieve failure. All specimens were tested vertically under pure compression loading.

5.4 Results and discussion

5.4.1 Load – deflection behaviour

The load-deflection relationship of all specimens is presented in Figure 5-13, in which the load 'P' is the total compression load in kN applied through three hydraulic jacks and the vertical deflection is measured at the centre of specimen through LV7. The structural performance of precast concrete panels can be discussed into two phases; (a) elastic phase and (b) plastic phase. In the elastic phase, all specimens followed Hook's law and the change in vertical deflection was directly proportional to the applied load. In this phase, no permanent deformation in terms of cracks was observed. The initial average cracking load recorded for SPN (solid panel), FPN (foamed panel) and CRPN (crumb panel) was 1460 kN, 1121 kN and 1082 kN, respectively. A significant difference in terms of stiffness was witnessed between solid concrete panels and sandwich panels before the initial cracking. During the plastic phase, an increase in compression load resulted in significant deformations, ultimately reaching the peak load and failed due to concrete crushing. The maximum failure load i.e. 1579 kN was measured in SPN-II, while FPN-I resisted a compression load of 1300.99 kN. The maximum ultimate axial capacity of CRPN-II was 1440 kN. A maximum deflection of 2.42 mm was noted in CRPN-I while the lowest value of deflection i.e. 2.07 mm was measured in SPN-I. As anticipated, SPN illustrated a higher stiffness in the plastic zone and better axial resistance than PCSPs. A brittle failure was witnessed in SPN, whereas, both types of PCSPs showed slightly ductile failure. A summary of the initial cracking load and ultimate load of all the panels are shown in table 5-6.

It is significant to highlight that the structural performance of CRPN in compression is comparable when evaluated against traditional precast concrete panels. Furthermore, it can be observed from the experimental data that CRPN resisted 91.2% of SPN's ultimate failure load. The deformation in CRPN in terms of maximum deflection is 16.91% and 12.56% more than SPN and FPN. This highlights that CRPN may be used as an alternative structural member in

the construction of buildings by replacing the old traditional precast concrete panels without compromising the ultimate axial strength.

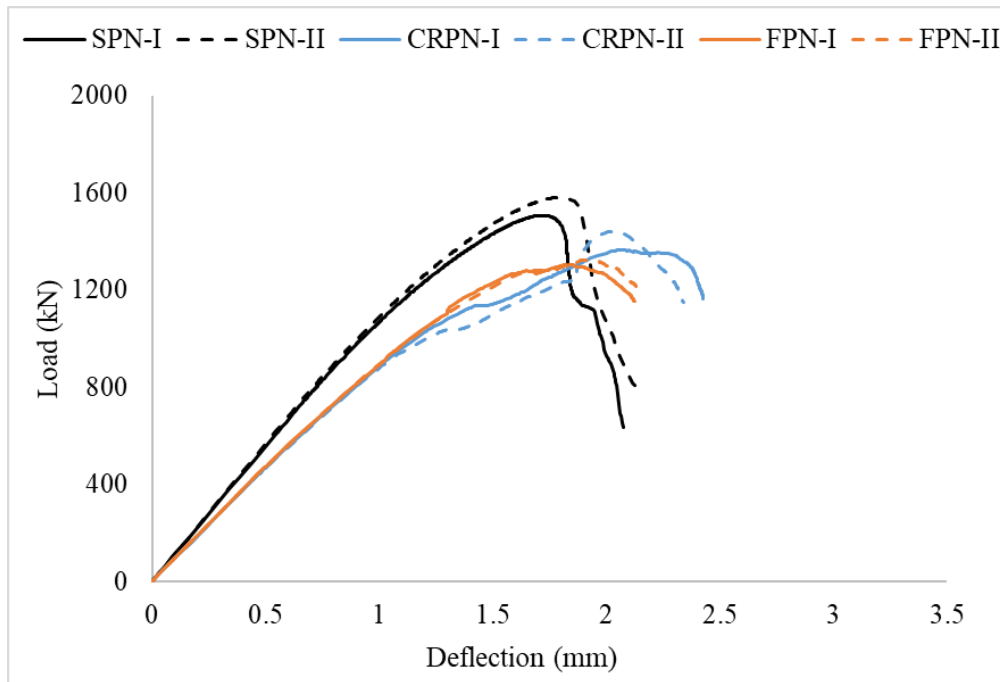


Figure 5-13 Structural performance of all precast concrete panels - load vs vertical deflection (LV-7).

5.4.2 Lateral displacement

In order to study the structural response of precast concrete panels, lateral displacements were measured through three horizontal LVDTs at each side along the panel height at three locations (a) bottom (b) mid-height and (c) top. The lateral displacement (LV3 and LV6) recorded at 250mm from the bottom support produced negligible deflections, which indicated that there was no lateral translation at the bottom end.

Table 5-6 Summary of experimental test results in terms of initial cracking and ultimate load

Specimen	Initial cracking load (kN)	Mean (kN)	Maxi load (kN)	Mean (kN)
SPN-I	1450.92	1460.22	1507.16	1543.55
SPN-II	1469.52		1579.94	
FPN-I	1103.09	1121.78	1300.99	1312.33
FPN-II	1140.48		1323.68	
CRPN-I	1127	1082.20	1365.58	1402.81
CRPN-II	1037.41		1440.05	

Furthermore, insignificant data was also reported for the lateral displacement (LV2 and LV5), recorded at 550 mm from the bottom, which confirmed the fact that there was no buckling in any of the panels. It is also due to the reason that the slenderness ratio ($h/d=11$) of all panels was comparatively low to cause any bending in the panels.

The lateral displacement (LV1 and LV3) recorded at 250 mm from the top end is shown in Figure 5-14. The initial behaviour of all panels up to 200 kN was similar and deformed in a linear elastic way. However, this behaviour began to change as the load increased beyond 600 kN. Both SPN specimens showed stiff behaviour and failed in a brittle way by concrete crushing near the top. The lateral deformations recorded in both SPNs were lower than PCSPs. Moreover, the post initial cracking behaviour of all PCSPs was ductile and deformed in a similar way. No noticeable difference in FPN and CRPN structural performance were observed except FPN-II, which could be the result of material or geometric imperfections.

In addition, it was observed from the analysis of lateral displacement that the applied axial load did not initiate any buckling. A maximum lateral displacement of 5.00mm was recorded in CRPN-I, while FPN-I were laterally displaced up to 5.17mm. The comparable analysis of PCSPs in terms of lateral displacement again validated that crumb rubber can be used as a core material in the construction of precast concrete sandwich panels, which, therefore offered a novel way of recycling waste tyres.

The variation in lateral displacement (LV1 to LV6) along the height of the panel is demonstrated in Figure 5-15. The positive and negative values of displacement represent the front and backside of CRPN-I respectively. The lateral deflection was initially below 1mm and increased on increasing the applied load. However, as the applied load approached the peak value, the lateral displacement became large. It was also observed that the values of lateral displacement were relatively similar on both sides and approached zero towards the bottom end of the panel owing to fixed support conditions.

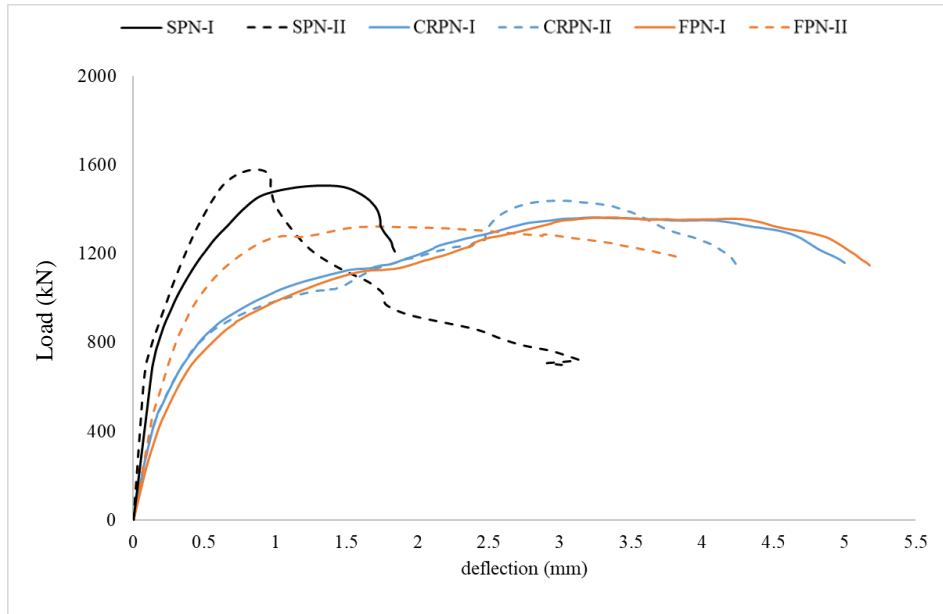


Figure 5-14 Structural performance of all precast concrete panels – load vs lateral deflection (LV-1)

5.4.3 Strain distribution in PCSPs

This section discusses the strain variations in both types of sandwich panels i.e. FPN and CRPN. The negative strain values indicate compression whereas, tension is presented in

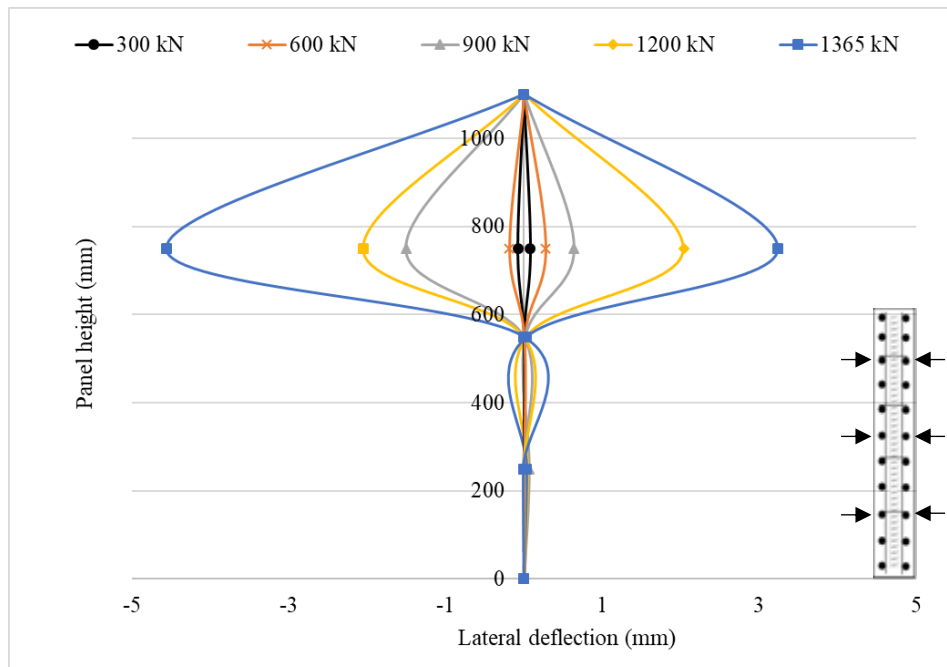


Figure 5-15 Lateral deflections (LV1 to LV6) along the height of the panel at different loading phases (CRPN-I)

positive values. Figure 5-16 shows the distribution of strain in FPN-I when the load was applied till failure. The electrical strain gauges (S1, S3, S6 and S8) along the height of the specimen illustrated that both front and backside of the test specimen was in pure compression, while the specimen experienced tension all along the width. This confirmed that the loading was applied exactly at the centre without causing any eccentricity. The maximum strain in compression was recorded in S1 i.e. 0.000998, whereas the maximum tensile strain was 0.000258, measured in S5. The strain in all steel reinforcement were below the yielding strain and therefore, no failure was observed in deformed bars.

The analysis of strain distribution in CRPN-I specimen is presented in Figure 5-17. It is evident from the strain data along the panel height that this CRPN-I specimen was also in pure compression. The strain variation (in all strain gauges) at the initial phase was linear before reaching a load of approximately 1127 kN and thereafter, continued to increase non-linearly till failure. Similarly, large increase in tensile strain (S5 and S7) was witnessed before the failure. In this scenario, the maximum compression strain was recorded in S1 i.e. 0.00144 while the maximum tensile strain of 0.000985 was measured in S5. It is vital to mention that the strain values recorded in CRPN specimen were higher than FPN and showed sufficient axial resistance against the applied loading before failure. However, no yielding strain was recorded in steel reinforcement.

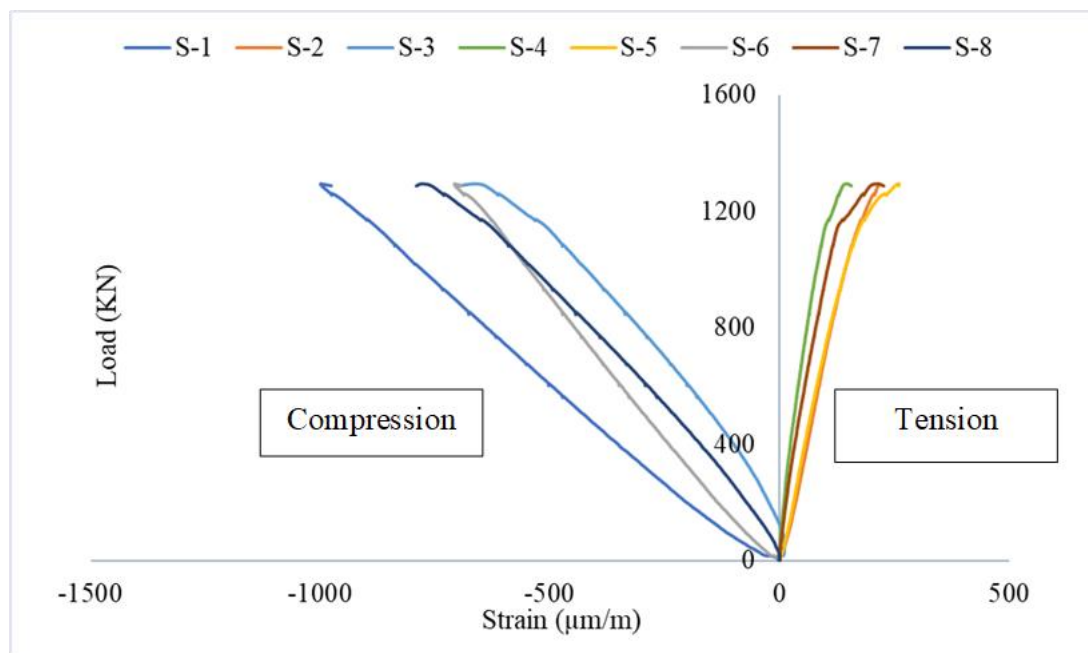


Figure 5-16 Strain distribution on concrete surfaces (S-1 to S-4) and in reinforcement (S-5 to S-8) in FPN-I

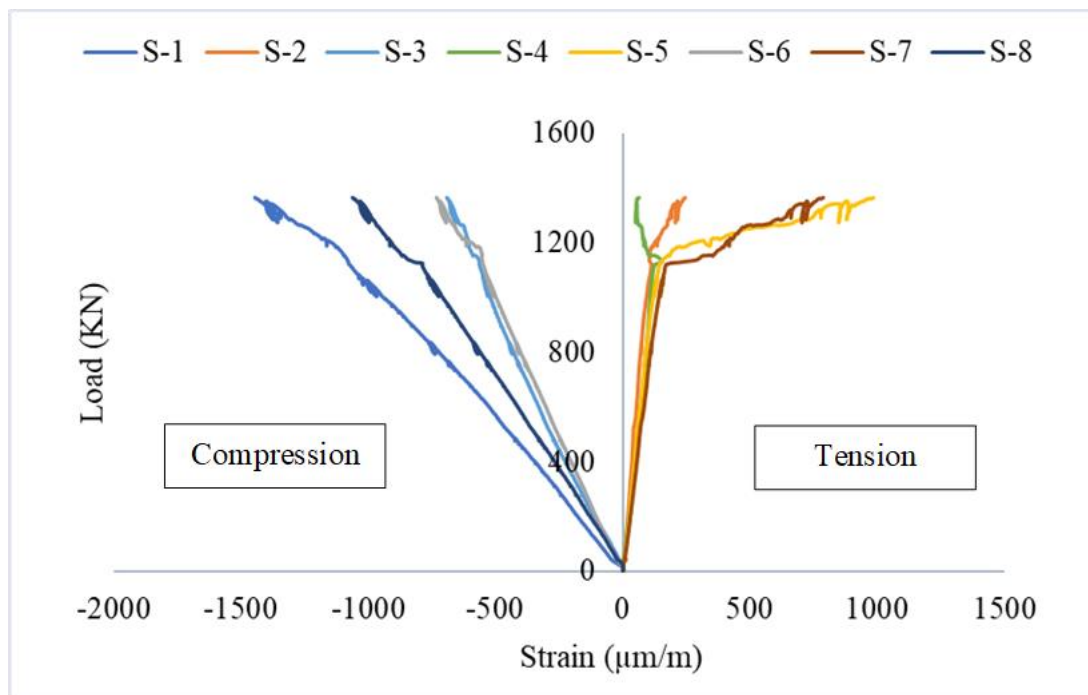


Figure 5-17 Strain distribution in CRPN-I on concrete surfaces (S-1 to S-4) and in reinforcement (S-5 to S-8)

The distribution of compressive strain (S1, S3, S6 and S8) along the thickness of CRPN-I at 550mm height at different loadings is shown in figure 5-18. Both (front and back) concrete wythes resisted maximum strain as compared to steel reinforcement. The initial strain distribution looked similar across the panel's thickness, which started to change significantly on reaching the peak load. The maximum strain of 0.00144 was recorded on backside, which specified that the concrete damage under compression was different in both concrete wythes. However, a similar mode of failure was observed in all other panels. These types of failures were also reported by previous research studies on the axial behaviour of PCSPs.

In order to assess the composite action of PCSPs under compression load, Amran (Mugahed Amran et al., 2016) and Mohamad (Mohamad et al., 2017) reported strain variation across the thickness of the panel at mid-height. Therefore, the distribution of strain plotted in figure 18 was considered to report the composite behaviour of CRPN. The symmetric distribution of strain at an early stage of loading in both wythes showed that the initial behaviour of the panel was fully composite. It was also noticed that even on increasing the applied load, the strain in longitudinal steel reinforcement didn't show any significant variations. However, after the propagation of initial crack at 1127 kN, the vertical strain on both concrete surfaces increased unsymmetrically, which resulted in loss of compositeness. It was also witnessed during the

experimental testing that the failure was conspicuous in one concrete wyth than the other. Typically, at failure all PCSPs show similar response in terms of composite behaviour under compression.

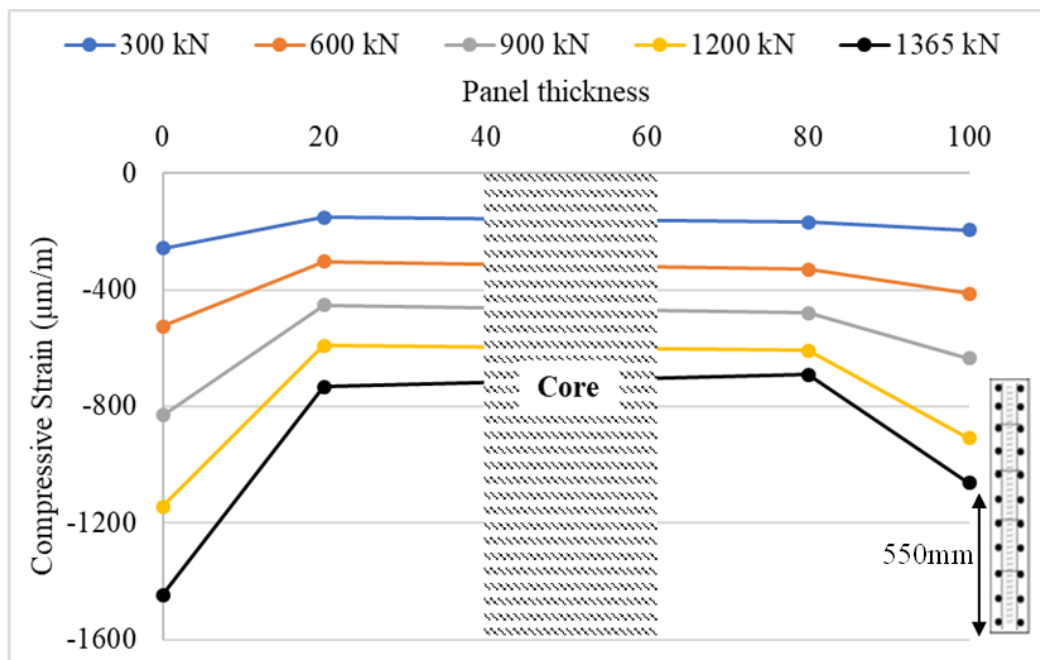


Figure 5-18 Strain variations along the thickness of panel (CRPN-I) at 550mm height at different phases of loading

5.4.4 Concrete damage pattern

All specimens were checked for any visible cracks before the testing and no damage was found in any of the specimens. During the experimentation, the pattern of all cracks was carefully observed and recorded. During the test, it was found that the initial cracking in PCSPs started right below the edges of the loading plate and travelled vertically along the panel height. These hairline cracks also travelled across the width of the panel and were originally small in size. Afterwards, these cracks started to widen up, once the load was increased beyond the elastic limit. Few oblique cracks also emerged under the loading plate and travelled diagonally towards both sides. It was noticed that the full cross-sectional area of the specimen contributed in resisting the axial stress. The failure region of the sandwich panel was restricted to 250mm distance from the top end. All sandwich panels eventually failed from crushing of concrete at the top and bending of few longitudinal deformed bars were also noticed.

The crack pattern of SPN was found to be different from both sandwich panels, in which a huge crack travelled, under one edge of the loading plate, vertically along the complete height of the specimen. The damaged area, in this case, was spread to 550mm from the top end. In

addition, the specimen failed in a brittle way with a sudden loud noise at the end of the test. The crushing of concrete was also witnessed at the top. Figure 5-19 shows failure in different panels before the removal of specimens.



(a)



(b)



(c)

Figure 5-19 Final failure modes in panels (a) Solid concrete panel (b) Crumb sandwich panel (c) Foam sandwich panel

5.5 Finite Element Analysis (FEA)

As previously discussed in the test setup section that due to limited loading capacity of the lab equipment, it was unworkable to carry out the axial test on an entire cross-section of the specimen therefore, finite element analysis was conducted to determine the ultimate capacity of CRPN. This numerical study was conducted in “ABAQUS/CAE 6.14-5” with standard/explicit model. The subsequent sections describe the key features of finite element modeling (FEM) and associated parameters.

5.5.1 Material properties

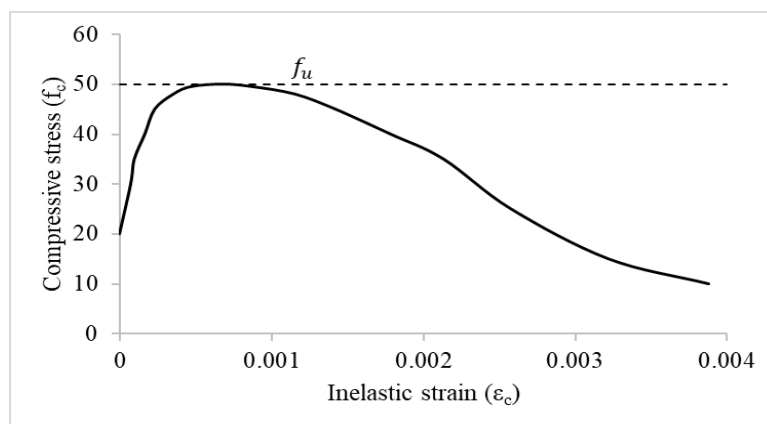
In order to perform the simulation in ABAQUS, different mechanical properties are required to define the material behaviour. In this instance, the properties for SCC, steel reinforcement, shear connectors and crumb rubber were identified. The material behaviour of respective components was classified in two steps; (a) elastic behaviour and (b) plastic behaviour. For SCC, the elastic behaviour was established using elastic modulus (E) and Poisson’s ratio (μ).

In order to define plasticity, few inbuilt concrete models are available in the program. In this study, concrete damage plasticity model (CDP) was selected to describe the plastic behaviour. The input parameters presented in Table 5-7 like shape factor (K_c), stress ratio (f_{b0}/f_{c0}) and eccentricity (ϵ) were the default values used in the model. Whereas, dilation angle (ψ) was selected after conducting a thorough literature review (Abrishambaf et al., 2015). Similarly, viscosity parameter (μ) was established through a sensitivity analysis in order to reduce iterations and achieve convergence. All input parameters correlated well with the experimental results.

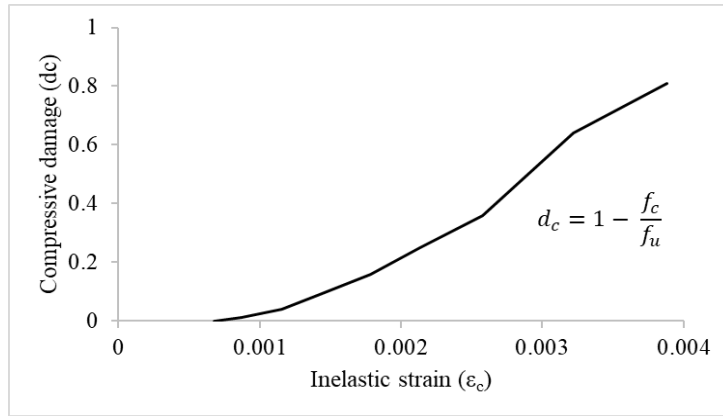
Table 5-7 Concrete damage parameters for SCC

Dilation Angle (ψ)	Eccentricity (ϵ)	Initial biaxial/uniaxial ratio (f_{b0}/f_{c0})	K_c	Viscosity parameter (μ)
40°	0.1	1.16	0.667	0.0001

Figures 5-20 and 5-21 shows the concrete compressive and tensile behaviour along with associated damage parameters. To define elastic behaviour in steel mesh (8mm diameter) and shear connectors (6mm diameter), a similar approach (i.e. elasticity and Poisson's ratio) was adopted, while plastic behaviour was established using properties like yield stress, plastic stress and ultimate strain. For describing the elastic behaviour of crumb rubber in compression, properties such as Young's modulus and Poisson's ratio ($\mu=0.4$) were used as crumb rubber hardly experienced any plastic deformation during the uniaxial compression testing. Moreover, the author followed the same approach in simulating the elastic behaviour of tyre-bale (Awan & Shaikh, 2021).

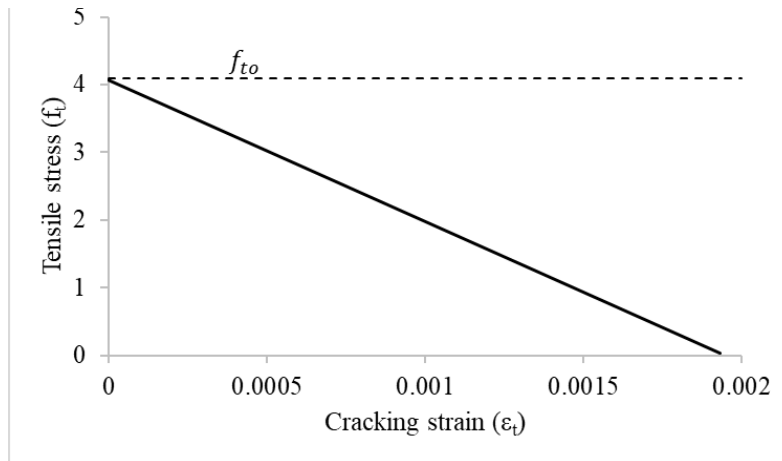


(a)

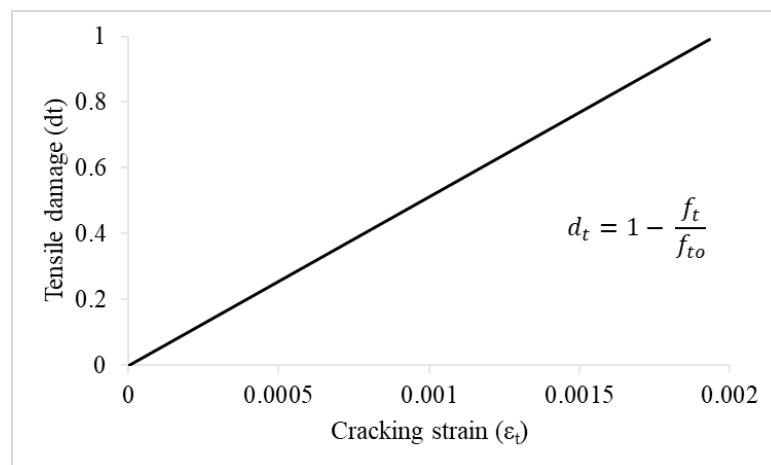


(b)

Figure 5-20 Concrete compressive behaviour (a) Stress-inelastic strain relationship (b) Compressive damage parameters



(a)



(b)

Figure 5-21 Concrete tensile behaviour (a) Tensile stress-cracking strain relationship (b) tensile damage parameters

5.5.2 Assembly method and interaction techniques

A 3D model of CRPN was built in standard/explicit model. It consisted of two outer concrete wythes, core, deformed bars, shear connectors and loading plate. All components of the sandwich panel were independently built and later, connected together. The concrete wythe, core and loading plate were discretised through eight-node reduced integration (C3D8R) brick element, while a two-node 3D deformable truss element (T3D2) was used for deformed bars and shear connectors.

Both concrete wythes and crumb rubber core were bonded together through interaction technique by identifying the relevant surfaces with reference to master and slave surfaces. The technique was used to join both concrete wythes (master surface) and core (slave surface). The deformed bars and shear connectors were constrained in solid elements through an embedded region approach. Lastly, the loading plate and the top surface of the FE model was connected through surface-to-surface contact (standard) via tangential ($\mu=0.45$) and normal behaviour. In addition, this loading plate was assigned a reference point (RP) at the centre and defined as a rigid body for the application of displacement.

5.5.3 Model constraints

The step consisted of initial and static, general with automatic increment type. For defining boundary conditions, the bottom end of the model was constrained against any kind of translation ($U_X=U_Y=U_Z=0$) and was only allowed to rotate about the x-axis ($U_{RY}=U_{RZ}=0$). Similarly, constant displacement ($U_X=U_Z=U_{RX}=U_{RY}=U_{RZ}=0$) was applied in the y-axis through the reference point of the loading plate until the failure. Finally, the output options like (DAMAGEC), tensile (DAMAGET) damage and plastic strain (PE) were utilized to establish the failure in concrete wythes. Figure 5-22 illustrates a 3D model of CRPN showing displacement load, important reference points and constraints.

5.5.4 Validation of FE model

The verification of the FE model for CRPN specimen was performed using the experimental data. In this study, the sensitivity analysis was conducted to determine the appropriate mesh size that provided precise results in a reasonable time with the least errors. Consequently, a mesh size of 20mm was selected for concrete wythe and core to perform the numerical analysis. In order to assess the structural efficiency of FE model, the load-deflection (LV7) curves and

concrete damage in compression from experimental data and numerical simulation were compared.

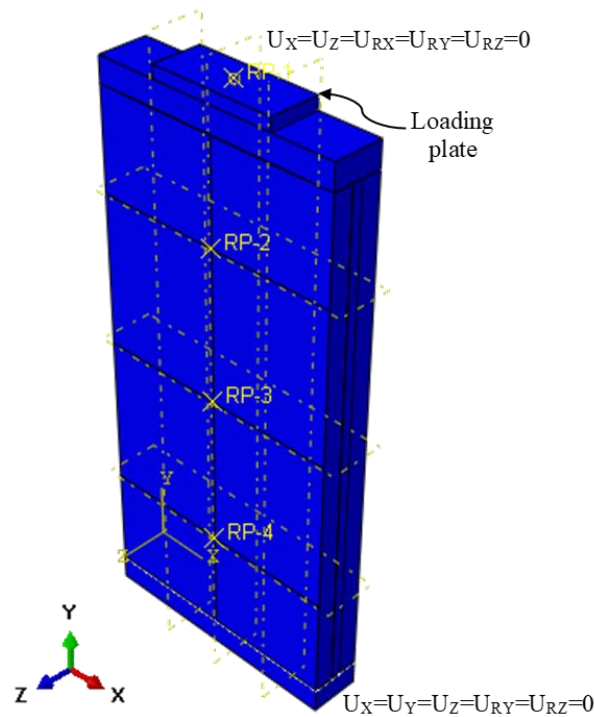


Figure 5-22 3D FE model of CRPN with constraints

5.5.5 Discussion on FE model

During the analysis, it was found that the FE model successfully captured the compression failure mode and predicted the ultimate strength with an error of 4% as calculated in Table 5-8. Figure 5-23 compiled the results of load-deflection curve from the experimental test and FE analysis. The elastic behaviour of the numerical model over-predicted the stiffness right from the starting point. Even after the initiation of early cracks, the model continues to demonstrate high strength in resisting the applied axial load. In the plastic region, the model finally reached the peak load and began to collapse. The compression damage region was symmetric and spread slightly beyond 250mm from the top end as illustrated in Figure 5-24.

Table 5-8 Comparison of ultimate load for experimental and FEA (CRPN)

Experimental	FEA	$\% = \frac{P_{FEA} - P_{EXP}}{P_{EXP}} \times 100$
Ultimate load (kN)		
1402.81	1460.21	4.0 %

The error in FE model may be attributed to different reasons such as unintended eccentricity of experimental load and difficulty in achieving perfect alignment of crumb rubber sheets due to its flexible nature during the casting phase. However, it is still encouraging to notice that the concrete damage in compression was identical to experimental failure. The cracks initially propagated under the loading plate and travelled vertically towards the centre before the ultimate failure by concrete crushing.

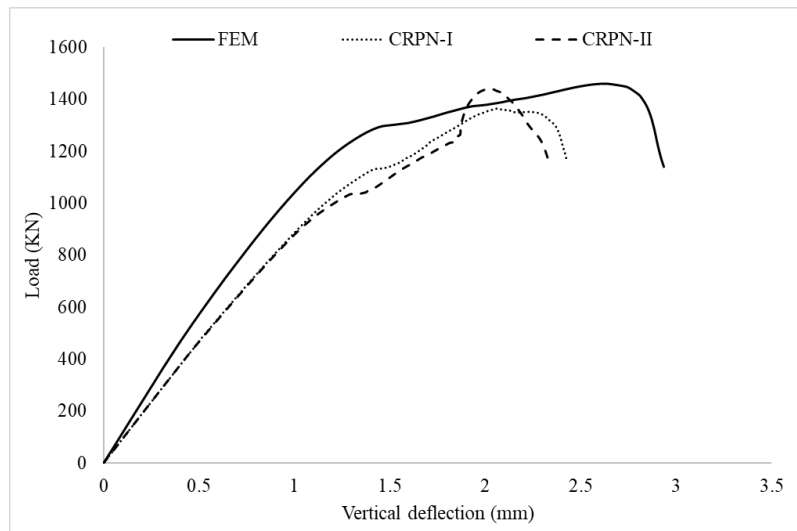


Figure 5-23 Axial performance of FEM and experimental test of CRPN

In the next stage of the numerical study, the axial load was applied on full width of the FE model to determine the ultimate capacity and failure mode in compression. During the analysis,

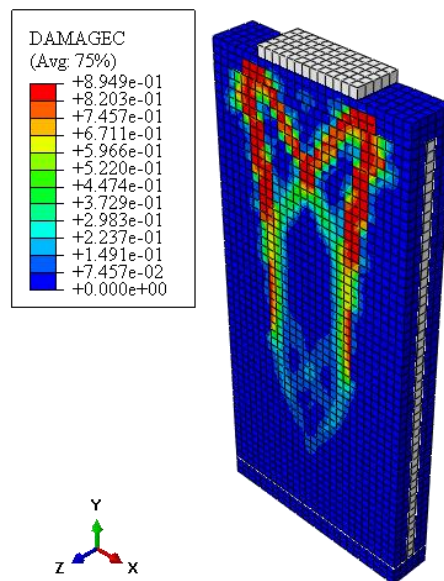


Figure 5-24 Concrete failure mechanism in compression in CRPN (uniaxial load on 250mm)

it was observed that CRPN failed in a similar way by crushing of concrete at the top end. The failure region was spread fully along the width and whole cross-sectional area contributed in resisting the applied load. The ultimate axial strength of 2880.8kN was measured at the time of failure, after which the load started to drop. Figure 5-25 shows the ultimate failure mode in CRPN predicted by FEA.

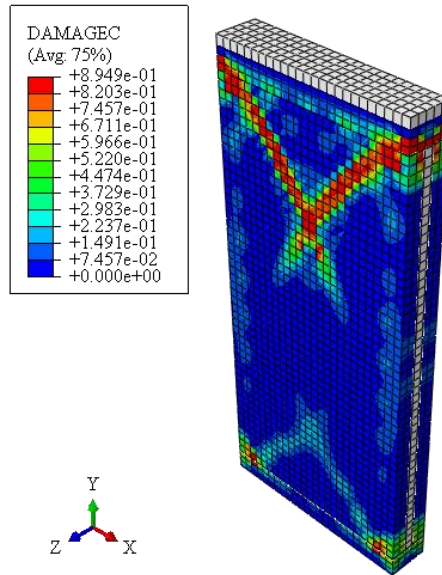


Figure 5-25 Concrete failure in compression predicted by FEA in CRPN (uniaxial load on full panel)

5.6 Design axial capacity of precast concrete panels

This section presents the existing empirical equations developed to estimate the ultimate axial capacity of precast concrete sandwich panels. Few researchers have developed empirical equations to estimate the axial strength of PCSPs. Benayoune (Benayoune et al., 2007) modified ACI equation and developed the following semi-empirical formula for sandwich panels by adding the reinforcement effect. The equation is only relevant to panels with a slenderness ratio less than 25 and subjected to concentric axial loading,

$$P_u = 0.4 \Phi f_{cu} A_c [1 - (kH/40t)^2] + 0.67f_y A_s \text{ -----Equation 1}$$

Where,

P_u = ultimate strength of sandwich panel

f_{cu} = concrete compressive strength

A_c = gross area of the section

K = effective height factor (0.8 for restrained walls and 1 for unrestrained walls against rotation)

H = the effective height of sandwich panel

t = total thickness of sandwich panel

f_y = yielding strength of steel

A_s = total area of longitudinal reinforcement

Mohamad (Mohamad, 2010) developed an empirical formula for lightweight foam concrete sandwich panels. The changes were addition of eccentricity effect and reducing the reinforcement contribution.

$$P_u = 0.4 \Phi f_{cu} A_c [1 - (kH/40(t-t/20))^2] + 0.6f_y A_s \text{ -----Equation 2}$$

In a recent research on sandwich panels, Amran (Mugahed Amran et al., 2016) suggested changes in ACI equation by reducing the concrete strength contribution to 37%. The equation also include limitation on slenderness ratio and concentric loading with maximum eccentricity limited to $t/6$.

$$P_u = 0.37 f_{cu} A_c [1 - (kH/32t)^2] + 0.67f_y A_s \text{ -----Equation 3}$$

Table 5-9 presents the comparison of axial design load for PCSPs. It is noticed that the axial strength predicted by the above models was lower than the experimental values. As all previous researchers generally modified the existing ACI equation by revising the contribution of three key elements in the equation (a) concrete compressive strength (b) slenderness and (c) steel reinforcement. Therefore, these safety factors incorporated substantially reduced the axial resistance of PCSPs and the values obtained from these expressions were conservative. However, it is also observed that the equations predicted close values of experimental failure load when the factor of safety was omitted in all equations.

Table 5-9 Design axial load (kN) of PCSPs calculated by existing equations

Panel	Avg Exp	Benayoune	Mohamad	Amran
CRPN	1402.8	675	508	586
FPN	1312.3			

5.7 Conclusions

This study explored the use of recycled tyre crumb rubber as a new core material in PCSPs and the structural efficiency in uni-axial compression of recycled tyre crumb rubber sandwich panel has been investigated. The study compared the structural performance of commonly used precast concrete panels like solid concrete panel and foam (expanded polystyrene) sandwich panel with recycled tyre crumb rubber sandwich panel in terms of axial load capacity, deflections, strain distribution and mode of failure. Based on experimental results, numerical and analytical models the following conclusion can be made:

- a. Among all PCSPs, the crumb rubber panel resisted a maximum axial load of 1440kN, which was 93% of the average ultimate axial load of solid concrete panel. Moreover, maximum vertical and lateral displacement of 2.42 mm and 5.00 mm, respectively was recorded in CRPN-I along with a maximum value of compression strain of 0.00144. It is important to mention that the deformation in CRPN in terms of maximum vertical deflection was 16.91% and 12.56% more than SPN and FPN. Due to the low slenderness ratio ($h/t=11$), the failure was governed by the crushing of concrete under the loading plate in all panels. No deformation such as yielding of steel reinforcement was noticed in any of the specimens.
- b. A finite element study was also successfully conducted to determine the axial capacity of the proposed sandwich panel when the load was applied on the complete panel with an error of 4.0% and FEA predicted an ultimate axial strength of 2880kN in CRPN. In the end, the existing empirical formulas for sandwich panels were used to evaluate the design axial load. The conservative values of design load dictated that these equations can safely be used to estimate the design axial load of the new proposed sandwich panel.
- c. The results from the experimental test indicated that there is a sustainable prospective to recycle/reuse waste tyres as a new core material in PCSPs, which will also help in alleviating the environmental hazards generated by the dumping of waste tyres. During the analysis, the recycled tyre crumb rubber sandwich panel demonstrated sufficient structural proficiency in terms of ultimate axial capacity and concrete damage in compression, which therefore makes it suitable to be used as a compression member in civil structures. The performance of the proposed sandwich panel under dynamic loading is planned to be undertaken in the next phase of research.

5.8 References

- Abrishambaf, A., Barros, J. A. O., & Cunha, V. M. C. F. (2015). Tensile stress–crack width law for steel fibre reinforced self-compacting concrete obtained from indirect (splitting) tensile tests. *Cement and Concrete Composites*, 57, 153-165.
- Amran, Y. H. M., Raizal, S. M. R., Farzad, H., Nor Azizi, S., & Ali, A. A. A. (2016). Structural Behavior Of Precast Foamed Concrete Sandwich Panel Subjected To Vertical In-Plane Shear Loading. In: Zenodo.
- Amran, Y. H. M., Rashid, R. S. M., Hejazi, F., Safiee, N. A., & Ali, A. A. A. (2016). Response of precast foamed concrete sandwich panels to flexural loading. *Journal of Building Engineering*, 7, 143-158.
- Awan, A. B., & Shaikh, F. U. A. (2021). Structural behaviour of tyre-bale sandwich wall under axial load. *Structures*, 31, 792-804.
- Batayneh, M. K., Marie, I., & Asi, I. (2008). Promoting the use of crumb rubber concrete in developing countries. *Waste Management*, 28(11), 2171-2176.
- Benayoune, A., Samad, A. A. A., Abang Ali, A. A., & Trikha, D. N. (2007). Response of pre-cast reinforced composite sandwich panels to axial loading. *Construction and Building Materials*, 21(3), 677-685.
- Benayoune, A., Samad, A. A. A., Trikha, D. N., Abang Ali, A. A., & Ashrabov, A. A. (2006). Structural behaviour of eccentrically loaded precast sandwich panels. *Construction and Building Materials*, 20(9), 713-724.
- Benayoune, A., Samad, A. A. A., Trikha, D. N., Ali, A. A. A., & Ellinna, S. H. M. (2008). Flexural behaviour of pre-cast concrete sandwich composite panel – Experimental and theoretical investigations. *Construction and Building Materials*, 22(4), 580-592.
- Brindley, Mountjoy, & Mountjoy. (2012). Study into domestic and international fate of end-of-life tyres [Report].
- Cecich, V., Gonzales, L., Høisaeter, A., Williams, J., & Reddy, K. (1996). USE OF SHREDDED TIRES AS LIGHTWEIGHT BACKFILL MATERIAL FOR RETAINING STRUCTURES. *Waste Management & Research*, 14(5), 433-451.
- Davalos, J. F., Qiao, P., Frank Xu, X., Robinson, J., & Barth, K. E. (2001). Modeling and characterization of fiber-reinforced plastic honeycomb sandwich panels for highway bridge applications. *Composite Structures*, 52(3), 441-452.
- Eltayeb, E., Ma, X., Zhuge, Y., Xiao, J., & Youssf, O. (2021). Dynamic performance of rubberised concrete and its structural applications – An overview. *Engineering Structures*, 234, 111990.
- Flores-Johnson, E. A., & Li, Q. M. (2012). Structural behaviour of composite sandwich panels with plain and fibre-reinforced foamed concrete cores and corrugated steel faces. *Composite Structures*, 94(5), 1555-1563.
- Gara, F., Ragni, L., Roia, D., & Dezi, L. (2012). Experimental tests and numerical modelling of wall sandwich panels. *Engineering Structures*, 37, 193-204.

- Gesoğlu, M., Güneyisi, E., Khoshnaw, G., & İpek, S. (2014). Abrasion and freezing–thawing resistance of pervious concretes containing waste rubbers. *Construction and Building Materials*, 73, 19-24.
- Ho, A. C., Turatsinze, A., Hameed, R., & Vu, D. C. (2012). Effects of rubber aggregates from grinded used tyres on the concrete resistance to cracking. *Journal of Cleaner Production*, 23(1), 209-215.
- Huntsman. (2021). Rubber Crumb Polyurethane Adhesive System. Retrieved 16 Feb from <https://www.industrysearch.com.au/rubber-crumb-polyurethane-adhesive-systems/p/35965>
- Kazemahvazi, S., Tanner, D., & Zenkert, D. (2009). Corrugated all-composite sandwich structures. Part 2: Failure mechanisms and experimental programme. *Composites Science and Technology*, 69(7), 920-925.
- Kazemahvazi, S., & Zenkert, D. (2009). Corrugated all-composite sandwich structures. Part 1: Modeling. *Composites Science and Technology*, 69(7), 913-919.
- Khalil, A., Abdul Samad, A., & Goh, W. (2014). Structural Behavior of Precast Lightweight Foam Concrete Sandwich Panel with Double Shear Truss Connectors under Flexural Load. *ISRN Civil Engineering*, 2014(1).
- Metelli, G., Bettini, N., & Plizzari, G. (2011). Experimental and numerical studies on the behaviour of concrete sandwich panels. *European Journal of Environmental and Civil Engineering*, 15(10), 1465-1481.
- Mohamad, N. (2010). The structural behaviour of precast light foamed concrete sandwich panel as a load bearing wall [PhD, Universiti Teknologi]. Malaysia.
- Mohamad, N., Goh, W. I., Abdullah, R., Samad, A. A. A., Mendis, P., & Sofi, M. (2017). Structural performance of FCS wall subjected to axial load. *Construction and Building Materials*, 134, 185-198.
- Mohammed, B. S., Anwar Hossain, K. M., Eng Swee, J. T., Wong, G., & Abdullahi, M. (2012). Properties of crumb rubber hollow concrete block. *Journal of Cleaner Production*, 23(1), 57-67.
- Mugahed Amran, Y. H., Abang Ali, A. A., Rashid, R. S. M., Hejazi, F., & Safiee, N. A. (2016). Structural behavior of axially loaded precast foamed concrete sandwich panels. *Construction and Building Materials*, 107, 307-320.
- NOAA. (2020, January 2021). National Centers for Environmental Information, State of the Climate: Global Climate Report. Retrieved May 05 from <https://www.ncdc.noaa.gov/sotc/global/202013>
- Noaman, A. T., Abu Bakar, B. H., & Akil, H. M. (2016). Experimental investigation on compression toughness of rubberized steel fibre concrete. *Construction and Building Materials*, 115, 163-170.
- Norambuena-Contreras, J., Arteaga-Pérez, L. E., Concha, J. L., & Gonzalez-Torre, I. (2021). Pyrolytic oil from waste tyres as a promising encapsulated rejuvenator for the extrinsic self-healing of bituminous materials. *Road Materials and Pavement Design*, 22(sup1), S117-S133.

- Pacheco-Torgal, F., Ding, Y., & Jalali, S. (2012). Properties and durability of concrete containing polymeric wastes (tyre rubber and polyethylene terephthalate bottles): An overview. *Construction and Building Materials*, 30, 714-724.
- Qi, C., Remennikov, A., Pei, L.-Z., Yang, S., Yu, Z.-H., & Ngo, T. D. (2017). Impact and close-in blast response of auxetic honeycomb-cored sandwich panels: Experimental tests and numerical simulations. *Composite Structures*, 180, 161-178.
- Rashad, A. M. (2016). A comprehensive overview about recycling rubber as fine aggregate replacement in traditional cementitious materials. *International Journal of Sustainable Built Environment*, 5(1), 46-82.
- Rejab, M. R. M., & Cantwell, W. J. (2013). The mechanical behaviour of corrugated-core sandwich panels. *Composites Part B: Engineering*, 47, 267-277.
- Roychand, R., Gravina, R. J., Zhuge, Y., Ma, X., Youssf, O., & Mills, J. E. (2020). A comprehensive review on the mechanical properties of waste tire rubber concrete. *Construction and Building Materials*, 237, 117651.
- Siddique, R., & Naik, T. R. (2004). Properties of concrete containing scrap-tire rubber – an overview. *Waste Management*, 24(6), 563-569.
- Statista. (2021). Projected worldwide tire market volume from 2014 to 2018. Retrieved May 05 from <https://www.statista.com/statistics/625275/global-tire-market-volume/>
- Strukar, K., Kalman Šipoš, T., Miličević, I., & Bušić, R. (2019). Potential use of rubber as aggregate in structural reinforced concrete element – A review. *Engineering Structures*, 188, 452-468.
- Vishnu, T. B., & Lakshman Singh, K. (2021). Experimental Investigation on Fatigue Characteristics of Asphalt Mixes with Different Automobile Waste Tyres as Modifiers. *Iranian Journal of Science and Technology, Transactions of Civil Engineering*.
- Wadley, H. N. G., Dharmasena, K. P., O'Masta, M. R., & Wetzel, J. J. (2013). Impact response of aluminum corrugated core sandwich panels. *International Journal of Impact Engineering*, 62, 114-128.
- Wang, R., Gao, P., Tian, M., & Dai, Y. (2019). Experimental study on mechanical and waterproof performance of lightweight foamed concrete mixed with crumb rubber. *Construction and Building Materials*, 209, 655-664.
- Xie, S., Feng, Z., Zhou, H., & Wang, D. (2020). Three-point bending behavior of Nomex honeycomb sandwich panels: Experiment and simulation. *Mechanics of Advanced Materials and Structures*, 1-15.
- Xue, J., & Shinozuka, M. (2013). Rubberized concrete: A green structural material with enhanced energy-dissipation capability. *Construction and Building Materials*, 42, 196-204.
- Zhang, P., Cheng, Y., Liu, J., Li, Y., Zhang, C., Hou, H., & Wang, C. (2016). Experimental study on the dynamic response of foam-filled corrugated core sandwich panels subjected to air blast loading. *Composites Part B: Engineering*, 105, 67-81.
- Zheng, L., Sharon Huo, X., & Yuan, Y. (2008). Experimental investigation on dynamic properties of rubberized concrete. *Construction and Building Materials*, 22(5), 939-947.

CHAPTER 6 BEHAVIOUR OF RECYCLED TYRE CRUMB SANDWICH PANEL UNDER LOW-VELOCITY IMPACT TEST

6.1 Abstract

The objective of this study is to compare the structural response of recycled tyre crumb sandwich panel (CRSP) with solid concrete panel (SCP) and foam concrete sandwich panel (FSP) against low-velocity impact. A total of six specimens are tested and their findings are reported. The impact test is carried out by dropping 100kg weight from 2 m height to generate impact energy, which can cause ultimate failure in all specimens. The structural performance is discussed in detail including impact force time-history, deflection time-history, strain time-history variation, impact energy and failure modes. The findings of the study show that the type of core materials of sandwich panels affect their structural response. The sandwich panel containing recycled tyre crumb performed well in terms of rebound force, permanent deflections and damage behaviour by partially absorbing the impact energy. A percentage decrease of 70% in strain value from the first impact to permanent strain was recorded in CRSP. Moreover, due to the dissipation of impact energy by the core, the crack width in CRSP was reduced considerably in the tension face which produced low deflections and caused minimal damage to the panel. Thus, in precast concrete panels recycled tyre crumb rubber can be introduced as a new alternative to traditional core materials.

6.2 Introduction

The world is rapidly implementing sustainable practices to reduce environmental impacts and carbon footprints in order to prevent climate change (NOAA, 2020; UN, 2022). The reuse/recycling of waste material, in numerous ways, attracted researcher's attention to expand their investigations and suggest innovative techniques. The production of tyres increased with the improvement of transportation system and the rapid growth in the number of vehicles (Qaidi et al., 2021). If these tyres are not disposed of properly, at the end of design life, will create environmental hazards. Discarded tyres are considered as waste material and reused/recycled in a variety of ways (Siddique & Naik, 2004). A considerable fraction of waste tyres is also used in civil engineering applications in the construction of asphalt roads (Presti, 2013; Shu & Huang, 2014; Vishnu & Lakshman Singh, 2021), embankments (Hossain et al., 2000; W. & A., 2006; W. Prikryl et al., 2005; Winter et al., 2005) and concrete mixtures (Roychand et al., 2020; Segre & Joekes, 2000; Strukar et al., 2019; Tantala, 1996; Wang et al.,

2019). In Australia, recycling companies are developing novel solutions for end-of-life tyres to be reused as crumb rubber asphalt mix, permeable pavements, crumb rubber graphene composites and recycled tyre-bale sandwich wall (TSA, 2022).

The use of waste tyres in the form of recycled tyre-bales (Awan & Shaikh, 2021b, 2021d) and recycled tyre crumb (Awan & Shaikh, 2021a, 2021c) in the construction of precast concrete sandwich panels (PCSPs) has been recently investigated. The results from a series of experimental testings and numerical simulations provided technical information and engineering properties about the use of recyclable materials as a new alternative. Recycled tyre crumb rubber sandwich (CRSP) is a type of sandwich panel, which consists of two reinforced concrete wyth, shear connectors and recycled tyre crumb as a core material. This type of precast concrete sandwich panel was mainly developed to offer sustainable alternative for reusing/recycling the waste tyres. Due to low thermal conductivity, excellent damping properties and sound insulation of rubber, CRSP has previously been studied in flexural bending and uni-axial compression for use in structural applications in the construction of buildings. Subsequently, the investigations reported that the structural performance of CRSP is duly comparable in flexural bending and compression when evaluated against traditional precast concrete panels.

6.3 Research Significance

In the event of natural calamities such as cyclones/storms, the exterior of the buildings is usually subjected to flying debris therefore, it is imperative to understand the structural behaviour of the panel against impact. In the literature review (Benayoune et al., 2007; Benayoune et al., 2006; Benayoune et al., 2008; Hosur et al., 2007; Liew et al., 2009; Mohamad, 2010), it was found that the existing research conducted on concrete sandwich panels mainly focussed on the use of foam, polystyrene, or extended polystyrene as a core material against low-velocity impact testing, whereas PCSP containing recycled crumb as core material has never been tested against dynamic loads. There is a research gap with regard to the structural response of precast concrete sandwich panels containing recycled tyre crumb rubber against impact loading. It is also learnt from the literature that for all the structural members the deflections must remain within the allowable limits to resist the external static and dynamic loads. As, rubber offers excellent impact resistance, energy dissipation and damping properties therefore, it is expected that sandwich panels containing tyre crumb will perform exceptionally well against impact force.

To further increase the usage of recycled tyre crumb in sandwich panels, this study examines the structural behaviour of three different types of precast concrete panels against impact. The main objective of this investigation is to study the impact force time-history, deflection time-history, strain time-history variations, impact energy and concrete failure for all three types of specimens. Furthermore, it is expected that this research provides an in-depth analysis about the performance of recycled tyre crumb sandwich panels and therefore, make it a reliable option to be employed as structural member in the construction of buildings.

6.4 Experimental Program

6.4.1 Specimen and geometric details

In order to evaluate the structural response of PCSP, three different types of concrete panels were designed and constructed. The overall dimensions of panel are 1000mm (length), 500mm (width) and 100mm (thickness). The first type is a solid concrete panel without core, reinforced with 8mm diameter deformed bars at a spacing of 100mm centre-to-centre in both directions. The geometric details of the panel are illustrated in Figure 6-1.

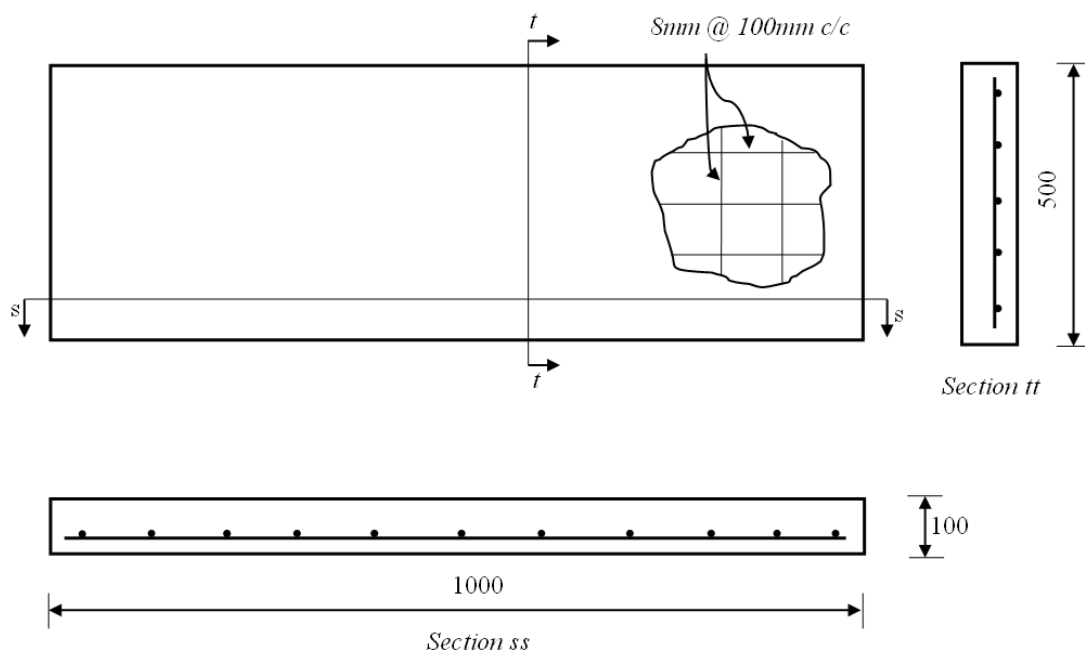


Figure 6-1 Geometric details of solid concrete panel (All dimensions are in mm)

The second type is a concrete sandwich panel containing 20mm thick polystyrene as core material. In this panel, each concrete wyth is 40mm thick and reinforced with 8mm diameter deformed bars in both directions. The two concrete wythes are connected to core material through 6mm diameter round bars. The third type is also a concrete sandwich panel containing 20mm thick recycled tyre crumb as core material. All other geometric details are similar to the second panel as shown in Figure 6-2. A minimum concrete cover of 25mm and 15mm is provided in solid concrete panel and sandwich panels respectively.

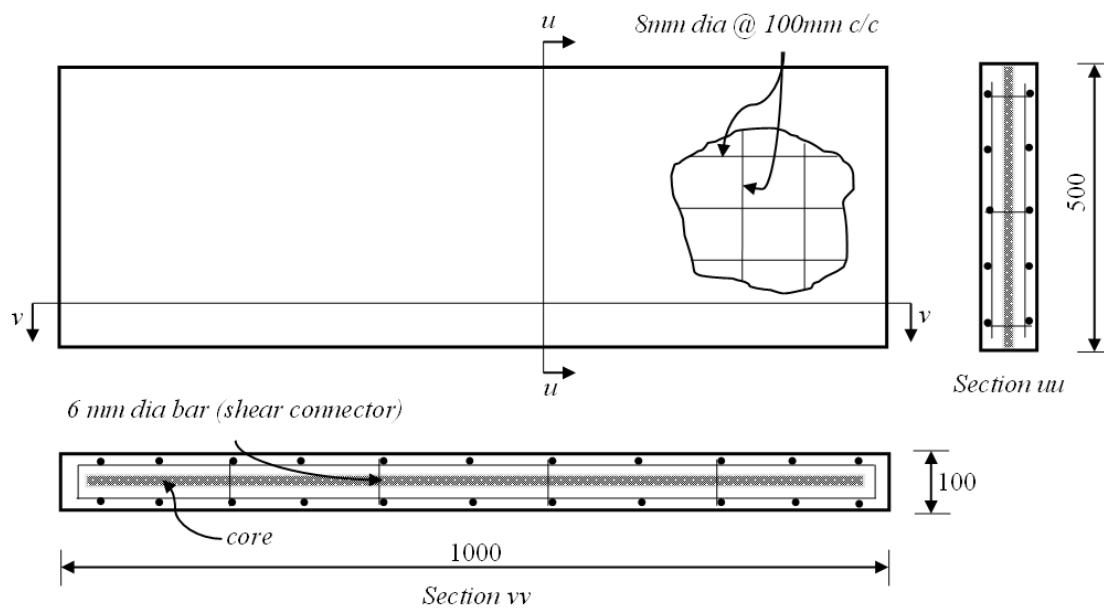


Figure 6-2 Geometric details of concrete sandwich panel (All dimensions are in mm)

6.4.2 Material details

In order to cast the concrete panel, self-compacting concrete with maximum aggregate size of 10mm and a compressive strength of 50 MPa was used for concrete wyth. The mix design of SCC is presented in Table 6-1. In addition, relevant field tests were performed to check the workability and acceptable ranges for SCC. The results obtained for each test are shown in Table 6-2. Three cylinders of 100mm x 200mm were tested to obtain uni-axial compressive strength of concrete. The properties obtained after material testing are presented in Table 6-3.

For material properties of 8mm and 6mm diameter steel, yield stress, plastic strain and elastic modulus were obtained through uni-axial tensile testing and are presented in Table 6-4. Similarly, the material properties of recycled tyre crumb in uniaxial compression and tension were investigated (Table 6-5) and discussed in detail in the reference (Awan & Shaikh, 2021a,

2021c). The material properties of polystyrene were provided by the manufacturer. Two specimens were cast for each type of concrete panel and cured for 28 days.

Table 6-1 Details of mix design and proportion for SCC of 50 MPa (Awan & Shaikh, 2021c)

Material description	Proportion
Cement Type GP, kg/m ³	291
Cement Type LH, GGBS, kg/m ³	194
Aggregate, 10mm, kg/m ³	788
Dust, kg/m ³	207
Coarse Sand, kg/m ³	307
Fine Sand, kg/m ³	419
Admixture-1 Retarder N (Type Re Retarder), ml/m ³	728
Admixture-2 Viscocrete10 (Type HWRRe), ml/m ³	2910
Admixture-3 Flow 15 (Type HWRRe), ml/m ³	970
Water, L/m ³	190

Table 6-2 Relevant test for SCC along with results and acceptable ranges (Awan & Shaikh, 2021c)

Test	Unit	Values	Acceptable range
Slump flow	mm	750	650-800
T ₅₀₀ slump flow	sec	5	2-5
V-funnel	sec	8	6-12
J-ring	mm	8	0-10
U-box (h ₂ -h ₁)	mm	1	0-30

Table 6-3 Properties of 50 MPa SCC (Awan & Shaikh, 2021c)

Properties	
Density (kg/m ³)	2506
f _c ' (MPa)	50
f _t (MPa)	4.07
Modulus of elasticity (MPa)	28000
Poisson's ratio(ν)	0.3

Table 6-4 Engineering properties of 8mm and 6mm diameter steel (Awan & Shaikh, 2021c)

Properties	SL81 mesh	Shear connectors
Diameter (mm)	08	06
Density (kg/m ³)	7900	7700
Avg Yield Stress (MPa)	530.33	658.14
Avg Ultimate Stress (MPa)	560.54	764.24
Avg Ultimate Strain (MPa)	0.088	0.0907
Elastic Modulus (MPa)	207010	215800
Poisson ratio	0.3	0.3

Table 6-5 Recycled tyre crumb properties in uni-axial compression and tension (Awan & Shaikh, 2021c)

Properties	
Density (kg/m ³)	564.12
Average compression strength (MPa)	59.70
Elastic modulus (MPa)	1.92
Average tensile rupture strength (MPa)	0.307
Average elongation at break (%)	59.87

6.4.3 Test setup

The concept of drop weight was implemented to perform the impact test. The setup for the impact testing comprised of 100 kg of weight, impact load cell, PVC shaft, steel plate, rotating plates, ultra-high-speed camera and steel supports. Two steel supports were initially positioned on ground and secured firmly with the help of high strength bolts. The rotating steel plates were placed on top of each support and welded intermittently to avoid displacement under impact. The strong reaction frame was used to hold PVC shaft and to ensure precise vertical alignment of the drop weight. The specimen was positioned horizontally before the testing and clamped at each end. A steel plate with a thickness of 50mm was attached to the midspan of the specimen and held together using steel clamps to apply a line load on the specimen. In next stage, a single load cell was placed on top of the steel plate to record the impact force. In the end, the weight was allowed to drop freely from a height of 2m onto the load cell. All specimens were tested in horizontal position. In addition, ultra-high speed FAST CAM SA-Z camera with a frequency of 21000 frames per second was used to record the high-resolution images and detect damage from beginning till ultimate failure under impact test. The circular tracing markers were also placed across the depth of the specimen at midspan to track the vertical deformation.

6.4.4 Instrumentation

In order to analyse the structural performance of all concrete panels, it is imperative to evaluate the externally applied load and deformations. For the applied load, an impact force-time history was generated through load cell. Similarly, the deformations were recorded through deflection time-history, strain variation time-history and failure mode. For this purpose, laser displacement sensors and strain gauges were used. Laser displacement sensor with a range of $\pm 300\text{mm}$ was placed at the midspan under the specimen. To eliminate the chances of errors, the sensor was carefully tested. A total of four strain gauges with a gauge length of 2mm were placed on steel reinforcements, in which one sensor was attached along the lateral direction and one was attached longitudinally along the specimen height on each mesh. Similarly, a 60mm long strain gauge was attached to the bottom side of the specimen. The surface was scrapped thoroughly with a sandpaper and cleaned before securing the strain gauge to the concrete surface. A digital multimeter was used to test the working of strain gauge. All the sensors were attached to the high-frequency data acquisition system to record the real-time data of the test. In this test, HBM – Quantum X was deployed to store the data at a rate of 5mHz. All specimens were checked for any cracks and damage before the testing. Figure 6-3 illustrates the details about the test setup, displacement sensor and strain gauge.

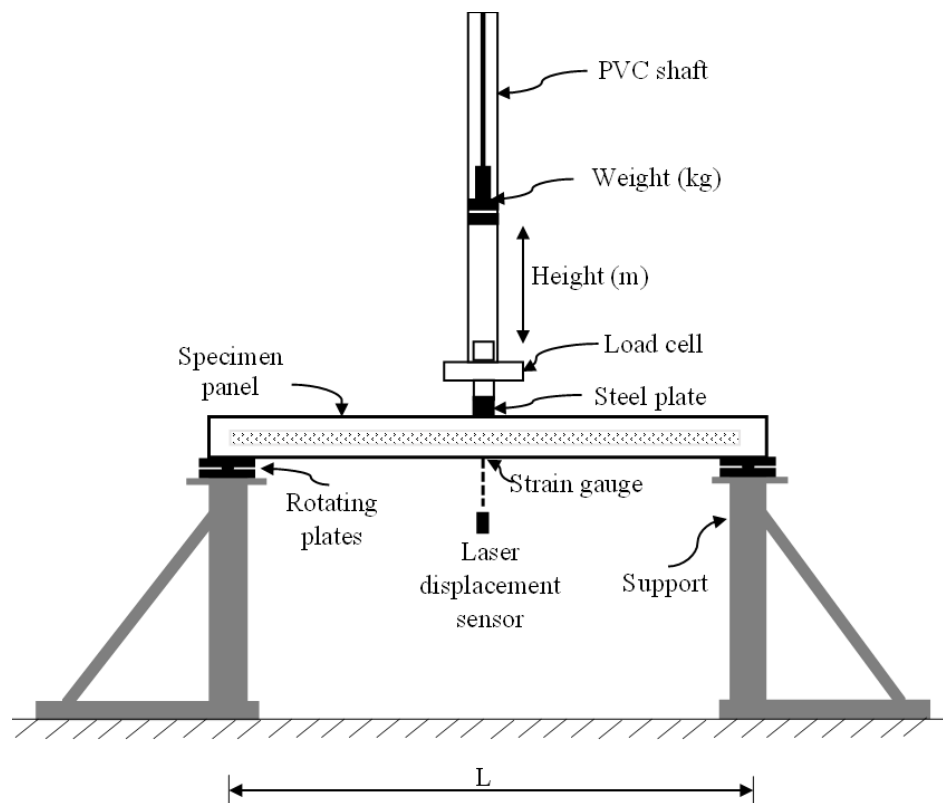


Figure 6-3 Impact test setup and instrumentation

6.5 Results and discussion

6.5.1 Impact force and deflection time-history

The impact force time-history of all six specimens is presented in Figure 6-4. It is important to mention that the velocity, drop weight, height and boundary conditions were same for all the specimens. However, the first impact force recorded by the load cell varies around 9.6%. Figure 4 shows the impact force time-history of all precast concrete panels, in which the first impact and rebound events are highlighted as “circle”. It can be seen that the first impact peaks look similar for all the specimen, while in case of rebounds during the free vibration period, the solid concrete panel was unable to show any resilience due to the ultimate collapse and therefore, no force was measured during the rebounding. In case of both sandwich panels, it is evident that the panels effectively resisted the impact and forced the weight to rebound. In the plastic region, total impact forces of 361 kN and 288 kN were measured in FSP, whereas total impact forces of 328 kN and 263 kN were recorded in CRSP. The average impact force measured in plastic region is comparatively less in CRSP than FSP. This is due to the fact that the impact was partially absorbed by the core containing recycle tyre and therefore, created a low rebound force.

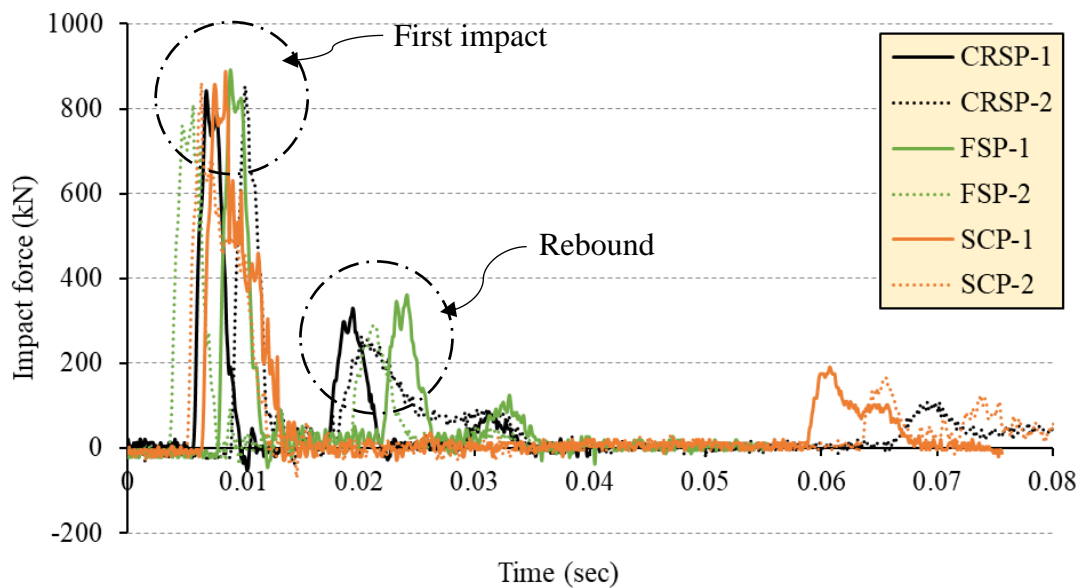


Figure 6-4 Impact force time-history of all panels

The displacement time-history of all specimens recorded at the midspan is presented in Figure 6-5. The vertical deflections of 37.9 mm and 36.38 mm were recorded in SCP while the deflection of 18.2 mm and 20.14 mm were measured in CRSP at the first impact. However, these deflections started to decline immediately after the impact, where lowest displacements were observed. Subsequently, after entering the plastic region, these displacements became permanent. In the plastic region, the highest and lowest permanent deflections were measured in SCP-1 (33.25 mm) and CRSP-2 (6.93 mm) respectively. The concrete panel containing recycled tyre crumb reduced the first impact deflection by 50% and the permanent deflections by 80% when compared with SCP. Similarly, on comparing with FSP, these deflections fell by 25% at first impact and 45% in the plastic region. Therefore, it can be stated that recycled tyre crumb can be used as an effective core material in concrete sandwich panels to dampen the impact forces. The detailed results including impact force and deflections of all concrete panels are summarized in Table 6-6.

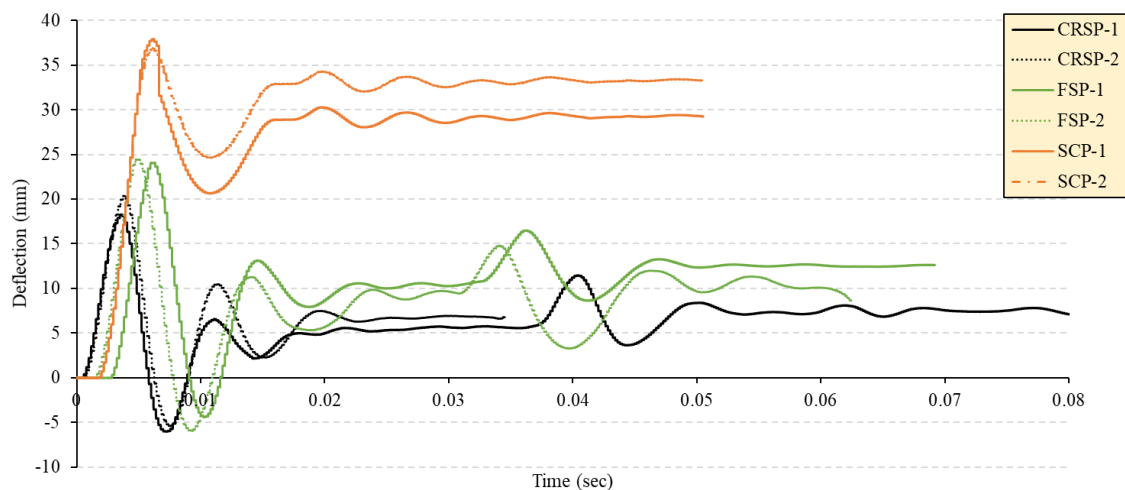


Figure 6-5 Displacement time-history of all panels at midspan

Table 6-6 Summary of impact forces and displacements of all panels

Panel	Initial impact force (kN)	Force in plastic region (kN)	Maximum deflection (mm)	Permanent deflection (mm)
SCP-1	887	-	37.89	33.25
SCP-2	859	-	36.38	29.24
FSP-1	889	361	24.08	12.55
FSP-2	809	288	23.92	11.32
CRSP-1	851	328	18.2	7.4
CRSP-2	841	263	20.14	6.93

6.5.2 Strain time-history variation

The variation in strain was recorded in bottom concrete wyth and in each steel mesh along longitudinal and lateral directions. During the impact, the strain gauge installed on the bottom concrete surface could not survive the impact and damaged, therefore no data is reported for strain time-history variation in concrete. Similarly, no significant data is obtained for the strain gauges installed on the reinforcement along the lateral direction.

Figures 6-6 and 6-7 show the strain time-history variation of longitudinal reinforcement in compression and tension wyths of FSP and CRSP. For FSP, the maximum strain of 0.013 was measured in tension whereas in compression a value of 0.0027 was recorded. Similarly, in case of CRSP, the maximum strain of 0.015 was recorded in tension while in compression it was 0.0089. For the same impact force, the maximum value of strain in tension is different. The strain recorded at the time of first impact is 15% higher in CRSP due to low stiffness of recycled tyre crumb and vice versa for FSP. However, after the first impact it can be observed in both sandwich panels that when strain enters the plastic region, the permanent strain decreases in both tension and compression and lowest tensile strain of 0.0044 is recorded in CRSP due to the damping properties of recycled tyre crumb. A percentage decrease of 27% and 70% in strain value from first impact to permanent strain was recorded for FSP and CRSP respectively. Therefore, it can be concluded that due to high damping ratio of recycled tyre crumb, the impact was partially absorbed by the core and lowest permanent strain was recorded in tension wyth of CRSP panel.

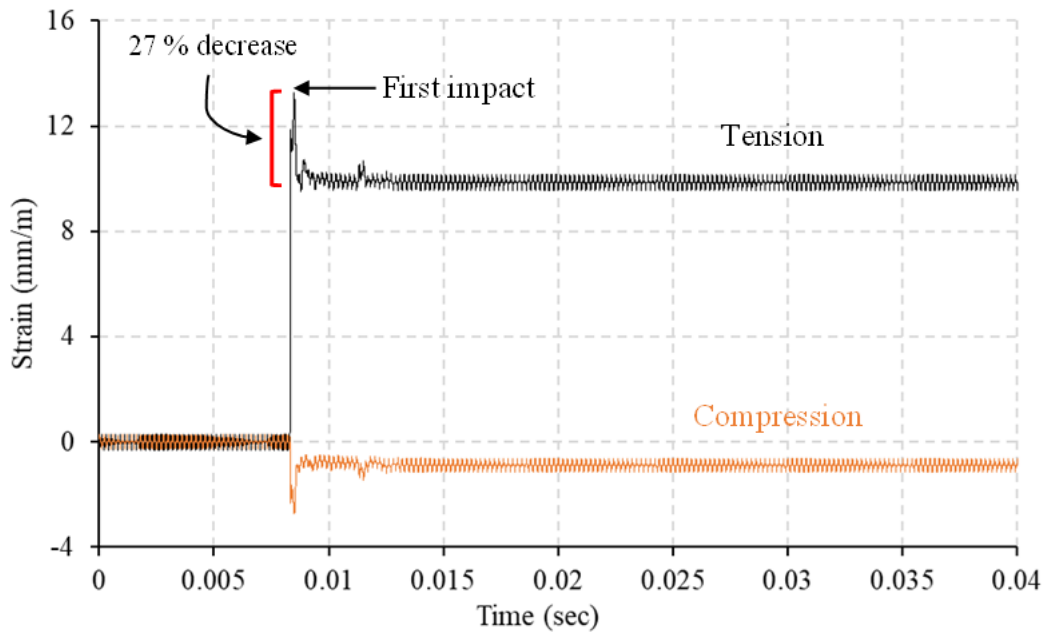


Figure 6-6 Strain distribution time-history of FSP

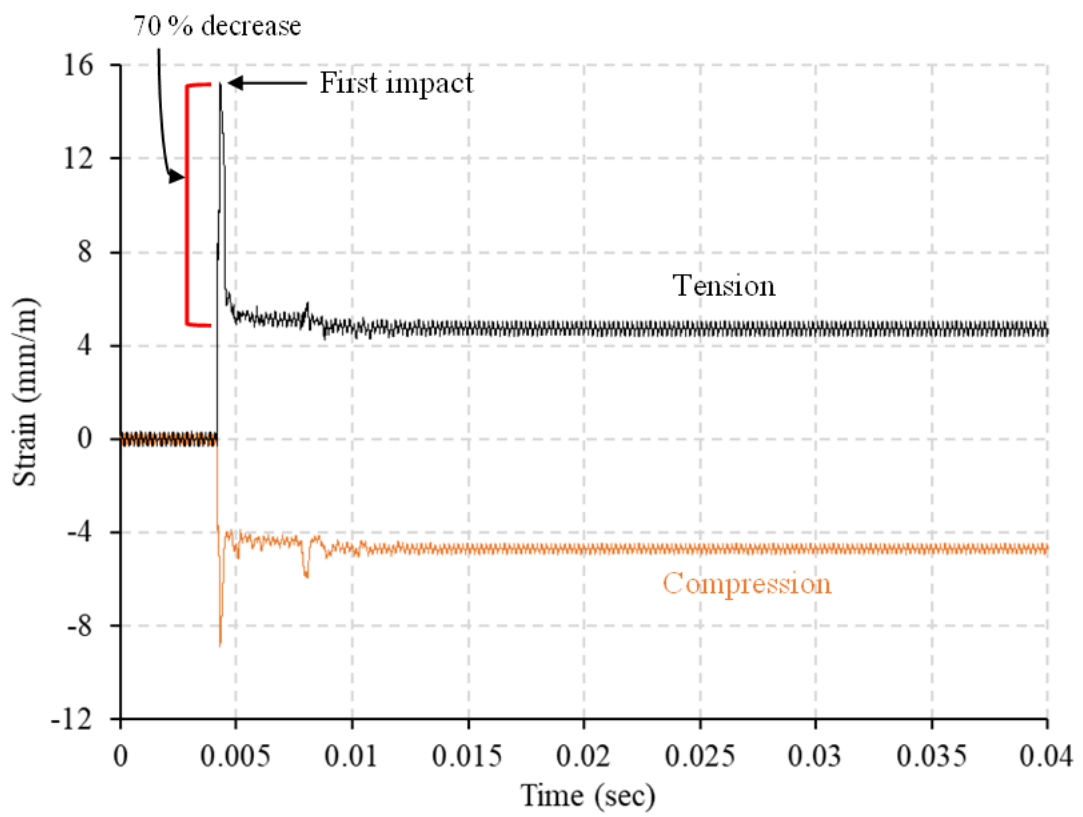


Figure 6-7 Strain distribution time-history of CRSP

6.5.3 Impact energy

The impact energy was estimated in term of absorbed energy (J) and specific absorbed energy (J/kg) for all concrete panels. Since the drop weight (kg) and drop height (m) remained same for all the panels, therefore the impact energy is similar for all panels. The following equation defines the energy just before the impact.

$$Energy (J) = \frac{1}{2}mv^2$$

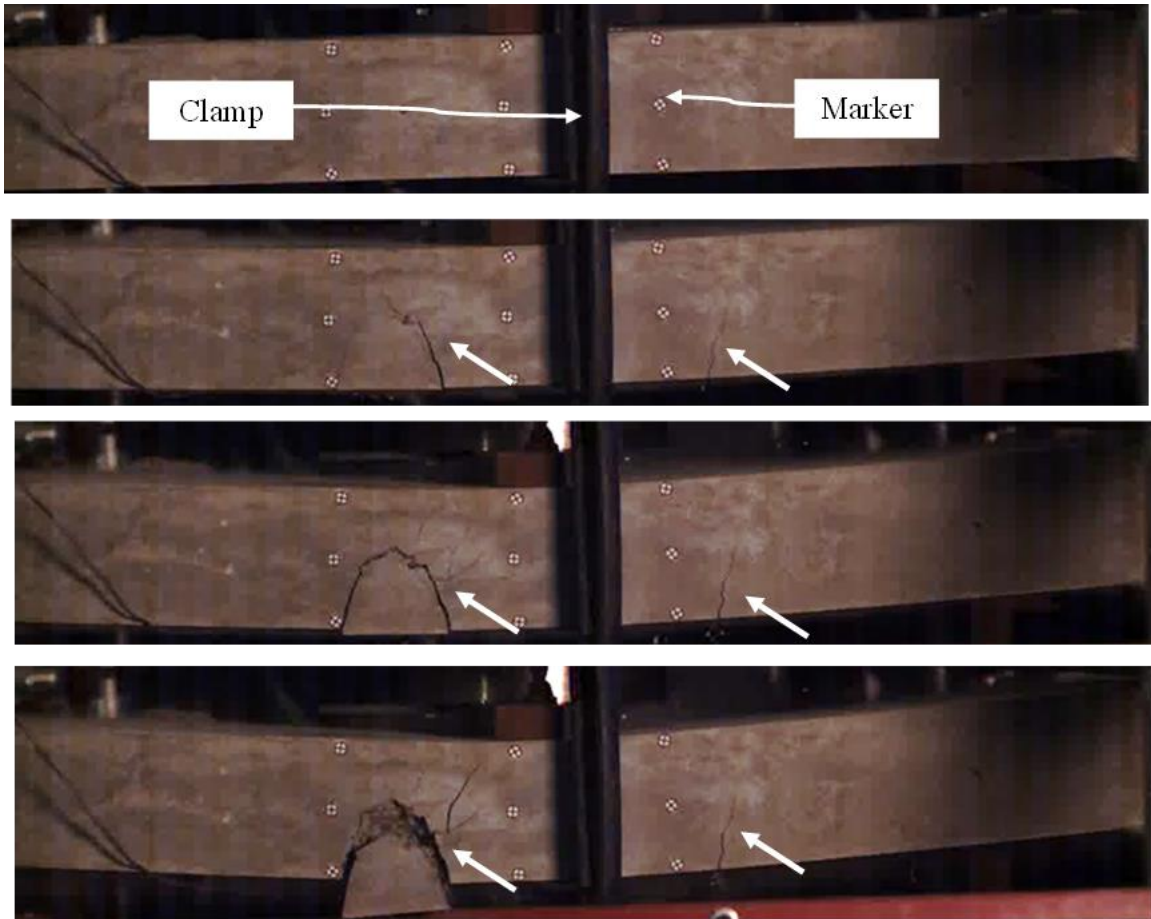
where, $v = \sqrt{2gh}$

In this case, the total absorbed energy measured is 1959.4 J, while the specific absorbed energy is 19.59 J/kg. However, solid concrete panel was unable to absorb any impact and therefore failed due to propagation of large cracks in tension. On the other hand, both sandwich panels absorbed this energy and developed minor cracks in tension wyth. It is also noticed that in order to study the effect of absorbed energy by the sandwich panel containing recycled tyre crumb, additional parametric research is required by varying the core thickness.

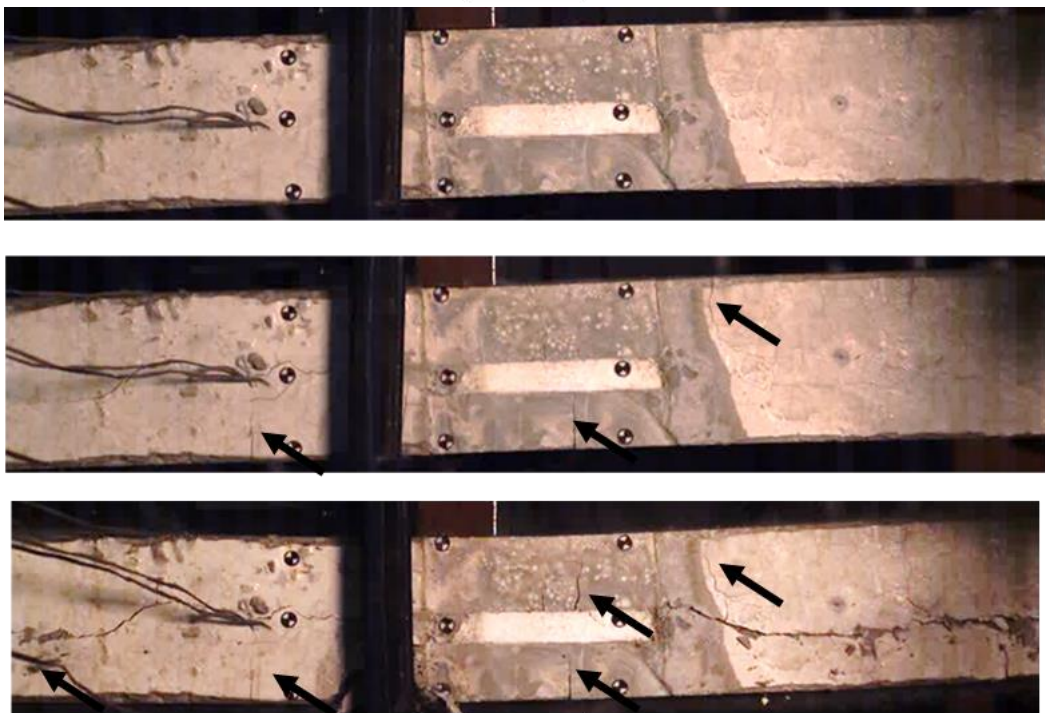
6.5.4 Damage behaviour

After the completion of impact test, the specimens were closely observed for all type of cracks before removing it. The crack patterns were recorded using ultra-high speed imaging system (FAST CAM) as mentioned earlier. In this test, a frame rate of 2000 frames per second was selected to obtain high resolution images under impact.

Figure 6-8 shows the crack pattern recorded at different intervals for all testing specimens. It can be observed that for the similar amount of absorbed energy, the large cracks took place in SCP at midspan which ultimately led to large permanent deflection in the panel. The flexural failure was dominant in the specimen where few small cracks originated from the tension face at the midspan and later, propagating through the depth of the panel. These cracks also travelled across the width of the panel and were asymmetric. In this scenario, the ultimate failure was a complete collapse of the panel. Since the impact force induced large strain in the panel, hence yielding of steel was seen in the longitudinal reinforcement bars.



(a)



(b)

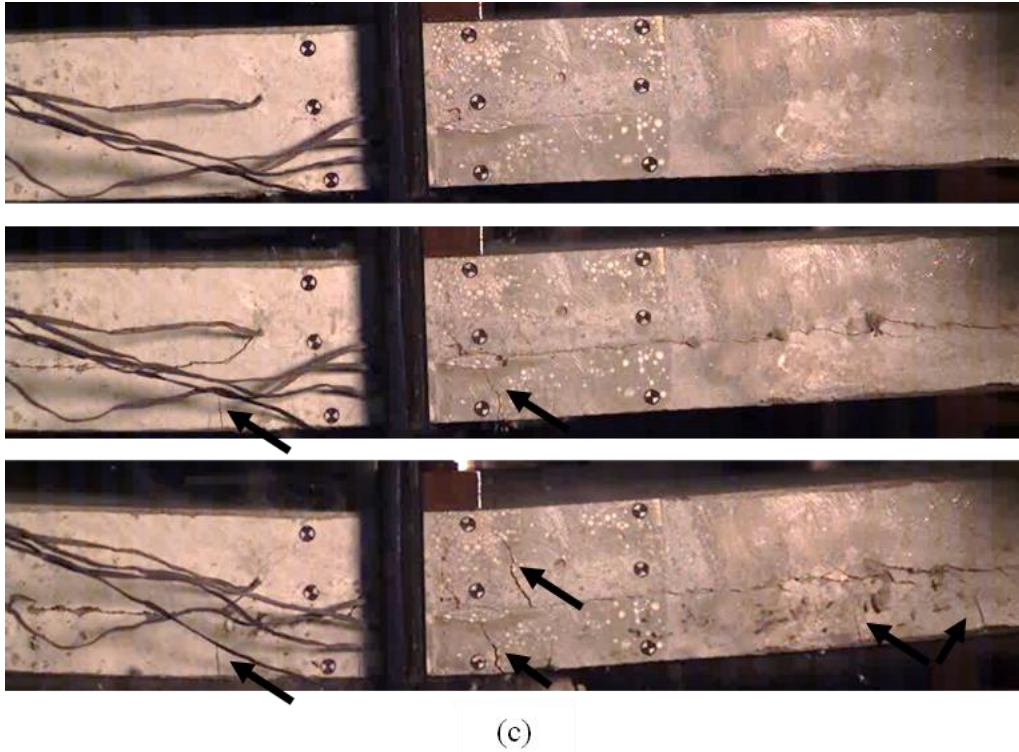
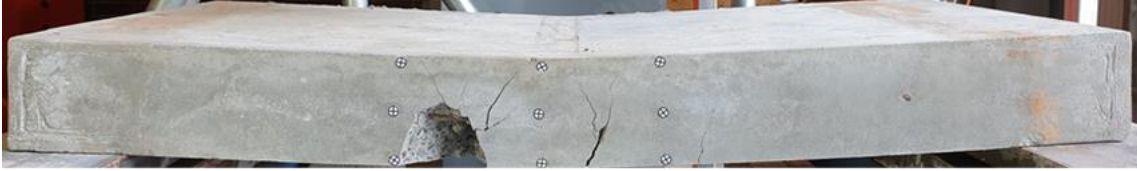


Figure 6-8 Failure mode against impact at different time intervals (a) SCP (b) FSP (c) CRSP

The impact behaviour of sandwich panels (FSP and CRSP) was different than SCP. In sandwich panels, the hairline flexural cracks initially developed in the tension wythe and propagated vertically towards core. However, no cracking was observed in both type of core material. These cracks further travelled towards the top wythe. In case of FSP, two medium-size cracks developed in the tension (bottom) wythe and travelled across the width of the panel. A continuous crack also developed on the face between the polystyrene core and concrete wythe however, it is hard to predict the actual bond behaviour and comment on whether this crack caused any debonding between the two surfaces. Similarly, in case of CRSP, the flexural cracks also developed in the bottom concrete wythe, however the width of cracks was less due to the fact that the impact energy was partly absorbed by the recycled tyre crumb core which eventually led to low permanent deflections in the panel. In addition, the spalling of concrete on the face were observed in both sandwich panels.

To conclude, it is evident from Figure 6-9 that the recycled tyre crumb sandwich panel developed least flexural cracks in tension wythe by absorbing the energy, produced low permanent deflections and displayed excellent resistance against impact.



(a)



(b)

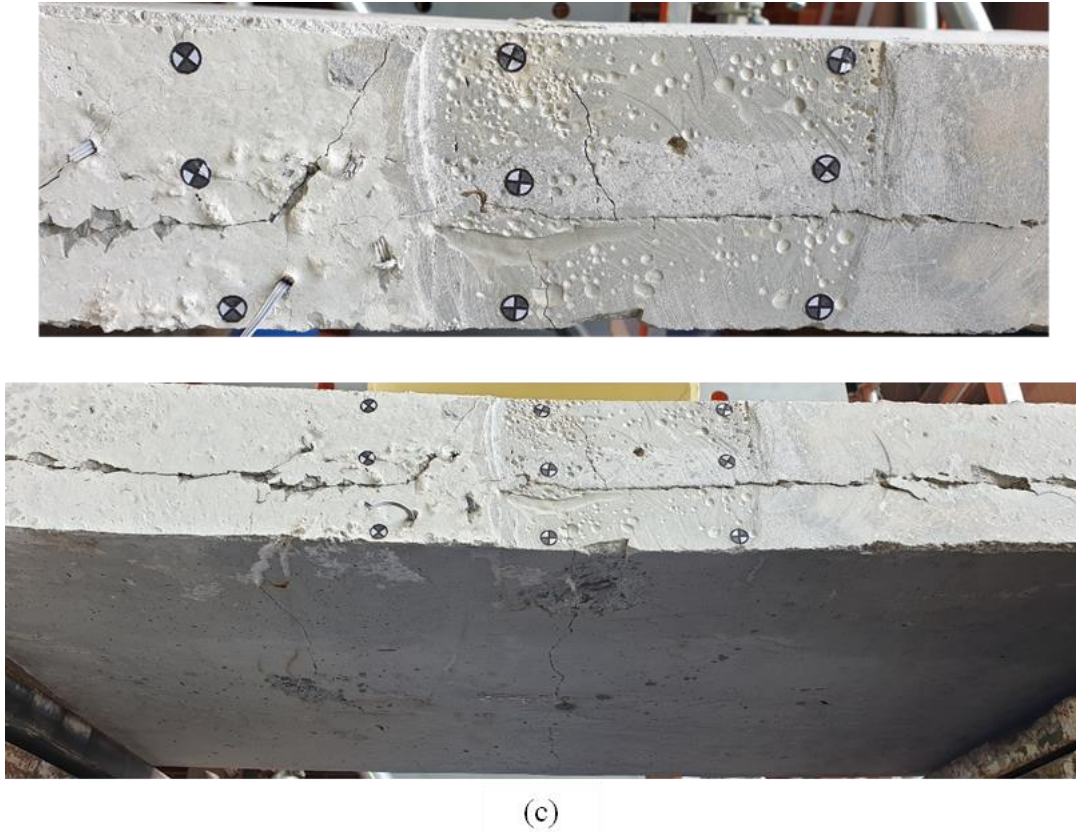


Figure 6-9 Ultimate failure against impact (a) SCP (b) FSP (c) CRSP

6.6 Conclusion

In this study, the structural response of recycled tyre crumb rubber sandwich panel against impact was investigated through the drop weight method. The test was conducted on three different types of precast concrete panels. During the experimental testing, two samples were tested for each type. The technical findings were discussed by analysing impact time-history, deflection time-history, strain time-history and damage behaviour for all specimens. During the assessment, it was evident that the structural performance of precast concrete panels against impact force was affected by the type and core material. In this study, CRSP partly absorbed the impact energy and produced minimum permanent deflection and strain. The further outcome of the analysis is summarized as followed:

- a. The first impact force fluctuated around 9.6% for all specimens. During the analysis, no rebounding force was recorded in SCP whereas, CRSP generated a low rebounding force of 263 kN in the plastic zone during the impact test and partially absorbed the impact.

- b. During the first impact, a maximum deflection of 37.89 mm was recorded in SCP whereas CRSP deflected to the lowest value of 18.2 mm. Similarly, the maximum permanent deflection of 33.25 mm and the minimum permanent deflection of 6.93 mm was measured in SCP and CRSP respectively. In a nutshell, the precast concrete panel containing recycled tyre crumb reduced the first impact deflection by 50% and the permanent deflections were decreased by 80% when compared with SCP. Similarly, on comparing with FSP, the deflections dropped by 25% at first impact and 45% in the plastic region.
- c. The strain recorded at the time of first impact is 15% higher in CRSP due to low stiffness of recycled tyre crumb and vice versa for FSP. However, after the first impact it was observed in both sandwich panels that the permanent strain decreased in tension as well as in compression. A percentage decrease of 27% and 70% in strain value from first impact to permanent strain was recorded for FSP and CRSP respectively.
- d. Severe concrete damage was witnessed in SCP in the form of large crack widths which ultimately led to large deflections and yielding of longitudinal deformed bars also occurred during the test. In case of CRSP, the crack width was fairly less since the impact was largely absorbed by the recycled tyre crumb core.
- e. To understand the effect of absorbed energy and specific absorbed energy for the sandwich panel containing recycled tyre crumb, additional parametric research is suggested by varying the core thickness.

6.7 References

- Awan, & Shaikh. (2021a). Compressive behavior of precast concrete sandwich panels containing recycled tyre crumb rubber core. *Structural Concrete*.
- Awan, & Shaikh. (2021b). Experimental and numerical study on structural behaviour of tyre-bale sandwich wall under different loading conditions. *Australian Journal of Structural Engineering*, 1-18.
- Awan, & Shaikh. (2021c). Structural behavior of recycled tire crumb rubber sandwich panel in flexural bending. *Structural Concrete*, 22(6), 3602-3619.
- Awan, & Shaikh. (2021d). Structural behaviour of tyre-bale sandwich wall under axial load. *Structures*, 31, 792-804.
- Benayoune, A., Samad, A. A. A., Abang Ali, A. A., & Trikha, D. N. (2007). Response of pre-cast reinforced composite sandwich panels to axial loading. *Construction and Building Materials*, 21(3), 677-685.
- Benayoune, A., Samad, A. A. A., Trikha, D. N., Abang Ali, A. A., & Ashrablov, A. A. (2006). Structural behaviour of eccentrically loaded precast sandwich panels. *Construction and Building Materials*, 20(9), 713-724.
- Benayoune, A., Samad, A. A. A., Trikha, D. N., Ali, A. A. A., & Ellinna, S. H. M. (2008). Flexural behaviour of pre-cast concrete sandwich composite panel – Experimental and theoretical investigations. *Construction and Building Materials*, 22(4), 580-592.
- Hossain, Priyantha W, & Jayawickrama. (2000). Use of whole Tyres in Earth retaining structures (0-1876).
- Hosur, M., Abdullah, M., & Jeelani, S. (2007). Dynamic compression behavior of integrated core sandwich composites. *Materials Science and Engineering A*, 445-446, 54-64.
- Liew, J. Y. R., Sohel, K. M. A., & Koh, C. G. (2009). Impact tests on steel–concrete–steel sandwich beams with lightweight concrete core. *Engineering Structures*, 31(9), 2045-2059.
- Mohamad, N. (2010). The structural behaviour of precast light foamed concrete sandwich panel as a load bearing wall [PhD, Universiti Teknologi]. Malaysia.
- NOAA. (2020, January 2021). National Centers for Environmental Information, State of the Climate: Global Climate Report. Retrieved May 05 from
- Presti, D. L. (2013). Recycled tyre rubber modified bitumens for road asphalt mixtures: A literature review. *Construction and Building Materials*, 49, 863-881.
- Qaidi, S. M. A., Dinkha, Y. Z., Haido, J. H., Ali, M. H., & Tayeh, B. A. (2021). Engineering properties of sustainable green concrete incorporating eco-friendly aggregate of crumb rubber: A review. *Journal of Cleaner Production*, 324, 129251.
- Roychand, R., Gravina, R. J., Zhuge, Y., Ma, X., Youssf, O., & Mills, J. E. (2020). A comprehensive review on the mechanical properties of waste tire rubber concrete. *Construction and Building Materials*, 237, 117651.
- Segre, N., & Joeques, I. (2000). Use of tire rubber particles as addition to cement paste. *Cement and Concrete Research*, 30(9), 1421-1425.

- Shu, X., & Huang, B. (2014). Recycling of waste tire rubber in asphalt and portland cement concrete: An overview. *Construction and Building Materials*, 67(PB), 217-224.
- Siddique, R., & Naik, T. R. (2004). Properties of concrete containing scrap-tire rubber – an overview. *Waste Management*, 24(6), 563-569.
- Strukar, K., Kalman Šipoš, T., Miličević, I., & Bušić, R. (2019). Potential use of rubber as aggregate in structural reinforced concrete element – A review. *Engineering Structures*, 188, 452-468.
- Tantala, M. W., J.A. Lepore, I. Zandi. (1996). Quasi-elastic behavior of rubber included concrete (RIC) using waste rubber tires. 12th International Conference on Solid Waste Technology and Management, Philadelphia, USA.
- TSA. (2022). Tyre Stewardship Australia. <https://www.tyrestewardship.org.au/>
- UN. (2022). Sustainable buildings. <https://www.unep.org/explore-topics/resource-efficiency/what-we-do/cities/sustainable-buildings>
- Vishnu, T. B., & Lakshman Singh, K. (2021). Experimental Investigation on Fatigue Characteristics of Asphalt Mixes with Different Automobile Waste Tyres as Modifiers. *Iranian Journal of Science and Technology, Transactions of Civil Engineering*.
- W., B. M., & A., Y. (2006). Use of waste tyre bales to construct a flood embankment. *Proceedings of the Institute of Civil Engineering*,
- W. Prikryl, and, R. W., & Winter, M. G. (2005). Slope failure repair using tyre bales at Interstate Highway 30, Tarrant County, Texas, USA. *Quarterly Journal of Engineering Geology and Hydrogeology*, 38, 377-386.
- Wang, J., Dai, Q., Guo, S., & Si, R. (2019). Mechanical and durability performance evaluation of crumb rubber-modified epoxy polymer concrete overlays. *Construction and Building Materials*, 203, 469-480.
- Winter, M. G., Reid, M., & Johnson, P. E. (2005). Construction of road foundations on soft ground using lightweight tyre bales.

CHAPTER 7 STRUCTURAL BEHAVIOUR OF STEEL FIBRES REINFORCED CONCRETE SANDWICH PANEL CONTAINING RECYCLED TYRE CRUMB CORE UNDER DIFFERENT LOADINGS

7.1 Abstract

Structural behaviour of precast concrete sandwich panels containing recycled tyre crumb core was evaluated in flexural bending and uni-axial compression. Each panel is 1000 mm long, 500 mm wide and 100 mm thick. Each sandwich panel consists of a 20 mm thick core and two 40 mm thick steel fibre reinforced concrete wythes. Two panels were tested for each test. The structural behaviour was discussed in relation to the ultimate strength capacity, deformations, strain variations in concrete and mode of failure. In addition, the degree of composite action was assessed in flexural bending through stiffness method in elastic stage. The concrete damage in terms of formation of cracks in tension concrete wyth was also compared to traditional precast concrete sandwich panels containing steel mesh. In flexural bending analysis, it was observed that the addition of steel fibres in concrete improved the post-cracking behaviour of the sandwich panels and resulted in less numbers of flexural cracks. For uni-axial compression, it followed a similar trend and failed by crushing of concrete occurred near the top end of the panel.

7.2 Introduction

Precast concrete sandwich panels (PCSPs) are widely used in the construction of low, medium and high rise industrial and residential buildings over the years (Seeber et al., 1997). Their use offers numerous benefits in context of quality control, efficient reinforcement detailing, fire resistance and durability (O'Hegarty & Kinnane, 2020). Typically, a sandwich panel consists of two concrete wythes, shear connectors and an insulation core. A variety of insulation materials including polystyrene foam (Benayoune et al., 2007; Benayoune et al., 2006; A. Benayoune et al., 2008; E. A. Flores-Johnson & Q. M. Li, 2012), foam concrete (E. A. Flores-Johnson & Q. M. Li, 2012), truss core (Kazemahvazi et al., 2009; Kazemahvazi & Zenkert, 2009), honeycomb core (Davalos et al., 2001; Qi et al., 2017) and corrugated core (Rejab & Cantwell, 2013; Wadley et al., 2013; Zhang et al., 2016) have been reported in the literature. Similarly, shear connectors are largely used to link the two outers concrete wythes together and to transfer lateral shear load. Different types of shear connectors like concrete connectors (I. Choi et al., 2015; Kim & You, 2015; Pessiki & Mlynarczyk, 2003), metallic connectors

(Abdelghani Benayoune et al., 2008; Bush & Stine, 1994; Salmon et al., 1997), fibre reinforced polymers (Chen et al., 2015; Naito et al., 2012), glass fibre reinforced polymers (Chen et al., 2015; K.-B. Choi et al., 2015), carbon fibre reinforced polymers (Bunn, 2011; Frankl, 2008; Sopal, 2013), basalt fibre reinforced polymers (Hodicky et al., 2013; Naito et al., 2012; Tomlinson et al., 2016) and concrete-insulation bond only (Hassan & Rizkalla, 2010; Kim & You, 2015; Naito et al., 2012; Pessiki & Mlynarczyk, 2003) have been reported in the literature. In a recent research study on PCSPs, the possibility of using recycled tyre crumb as a new core material has been thoroughly investigated in static loadings in terms of flexural bending (Awan & Shaikh, 2021b) and uni-axial compression (Awan & Shaikh, 2021a). The research focussed on the reuse/recycling of waste tyres to promote sustainability, reduce carbon footprints and eventually alleviate environmental impacts. The structural performance of the sandwich panel in flexural bending and compression when compared with traditional precast concrete panels remained significantly efficient. Due to its superior response to static loadings, the proposed panel was recommended to be used as a load bearing structural member in buildings.

In recent years, steel fibre reinforced concrete (SFRC) has extensively been used due to its excellent post-cracking behaviour against static and dynamic loadings. The addition of steel fibres in the concrete mixture improves the bonding between the matrix and fibre and therefore, increases the flexural strength, tensile strength and resistance against shear, spalling and abrasion (Xu et al., 2012). Furthermore, the use of steel fibres in slabs, beams and PCSPs has been investigated by various researchers under different static and dynamic loadings (E. Flores-Johnson & Q. Li, 2012; Lameiras et al., 2013; Lameiras et al., 2021; Lameiras et al., 2012; Wu et al., 2022). It was learnt from the literature that increasing the volume of steel fibres reduces the crack size, improve ductility and enhances the bearing capacity of the structural member (Wu et al., 2022).

During the manufacturing of PCSPs containing recycled tyre crumb, it was observed that the presence of deformed bars and connectors provided insufficient space for equal distribution of concrete mix and hence, the structural design was forced to compromise on reduced concrete cover. Also, it was hard to vibrate the concrete mix due to low thickness of concrete wyth. Therefore, in this study, SFRC was used in the construction of PCSPs without steel mesh. The benefits of using SFRC can be summarized as:

- a. Development of strong bond between recycled tyre crumb core and concrete mix because of addition of steel fibres.

- b. Provision of adequate space for pouring concrete mixture and better concrete cover to enhance fire and abrasion resistance.
- c. Easy vibration of concrete and therefore, equal distribution of concrete mixture in the panel.

In this study, the structural behaviour of precast steel fibre reinforced concrete sandwich (SFRC) panel containing recycled tyre crumb was examined under static loadings in context of flexural bending and uni-axial compression. A total of four specimens were manufactured using SFRC and two specimens were tested for each experiment. In this study, 60mm long and 0.9 mm diameter steel fibres with a density of 7800 kg/m³ were added in the concrete mix. The findings of the test were discussed in terms of ultimate strength capacity, deflections, strain variations and mode of failure. The damage behaviour including crack pattern of PCSPs containing recycled tyre crumb with and without steel fibres was compared.

7.3 Experimental Program

7.3.1 Geometric properties

In this study, the overall dimensions of the sandwich panel are 1000mm long, 500mm wide and 100mm thick. Each concrete wyth is 40mm thick and made up of SFRC, whereas the thickness of core is 20mm and contains recycled tyre crumb rubber. The geometric details of the panel are shown in Figure 7-1.

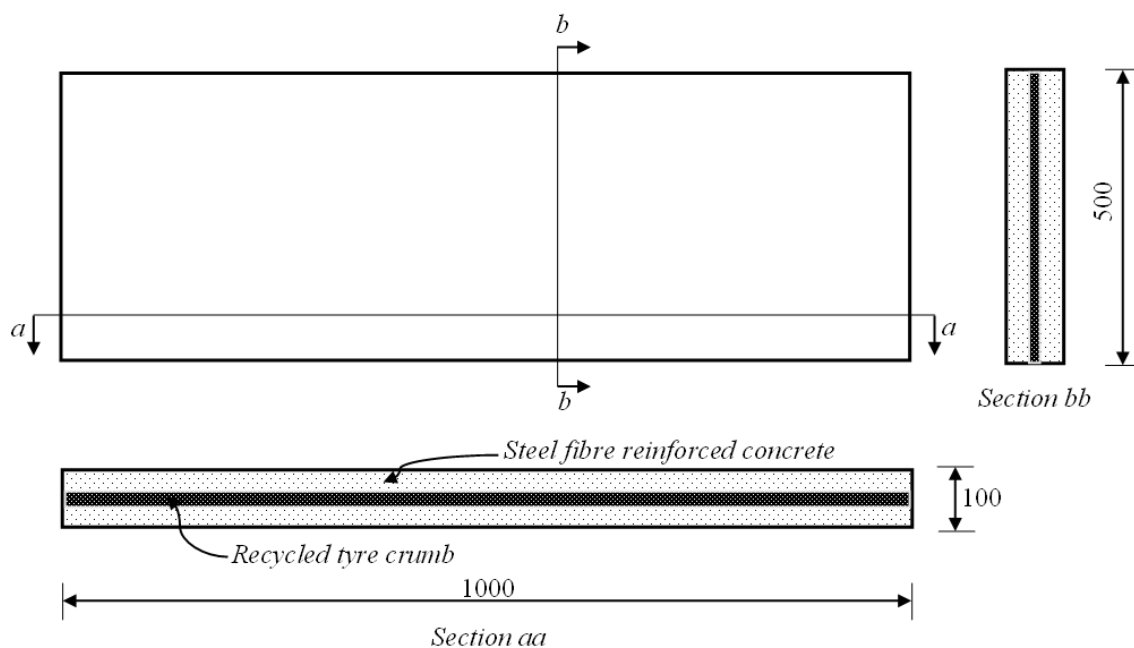


Figure 7-1 Geometric details of precast concrete sandwich panel (All dimensions are in mm)

7.3.2 Material properties

The concrete mix was prepared using 25 kg/m³ of steel fibres. Ordinary Portland cement and an aggregate size of 10 mm was used in the concrete mix. In addition, admixtures were added to improve the workability of the mix. The details of concrete mix design for SFRC are presented in Table 7-1. It is important to highlight that the steel fibres were added in regular intervals to prevent balling effect and to obtain reasonable distribution. During the casting of sandwich panels, the cylinder size of 100 mm x 200 mm was taken for the material testing as shown in Figure 7-2.

Table 7-1 Details of mix design and proportion for SFRC

Material description	Proportion
Cement (kg/m ³)	310
Aggregate - 10 mm (kg/m ³)	992
Dust (kg/m ³)	316
Natural sand (kg/m ³)	533
Steel fibre (kg/m ³)	25
Admixture (ml/m ³)	1194
Water (l/m ³)	179
Water-cement ratio	0.58

To determine the mechanical properties, uni-axial compression test and split tensile test were conducted as per ASTM C39 and C496 specifications on three samples using universal testing machine, MCC8 (Figure 7-3). The key material properties of SFRC are presented in Table 7-2.



Figure 7-2 Concrete cylinder of SFRC taken at time of casting



Figure 7-3 Material testing - concrete compressive strength

In concrete mixture, 60 mm long and 0.9 mm in diameter steel fibres (DRAMIX 3D) were used. The typical density of these fibres is 7800 kg/m^3 . The material properties of steel fibres, obtained from the manufacturer, are presented in Table 7-3.

Table 7-2 Properties of 35 MPa SFRC

Properties	
Density (kg/m^3)	2500
f_c' (MPa)	35
f_t (MPa)	3.6
Modulus of elasticity (MPa)	30000
Poisson's ratio(ν)	0.3

For the core, recycled tyre crumb rubber was locally procured. The material properties of recycled tyre crumb rubber in uni-axial compression and tension were previously investigated in the lab due to the absence of necessary data from the manufacturer. The material properties of recycled tyre crumb are provided in Table 7-4. Moreover, the details about manufacturing process and the results of material testing can be found in the reference (Awan & Shaikh, 2021b).

Table 7-3 Properties of steel fibres

Test	Unit	Values
Fibre type	steel	Dramix 3D
Density	kg/m^3	7800
Length	mm	60
Diameter	mm	0.9
Tensile strength	MPa	1160
Elastic modulus	GPa	210

Table 7-4 Recycled tyre crumb properties in uni-axial compression and tension

Properties	
Density (kg/m ³)	564.12
Average compression strength (MPa)	59.70
Elastic modulus (MPa)	1.92
Average tensile rupture strength (MPa)	0.307
Average elongation at break (%)	59.87

7.3.3 Specimen casting

All the specimens were cast in horizontal position. A total of four formworks were fabricated using timber and secured using steel screws at regular intervals along the length and width. The formwork was cleaned thoroughly and bonded at the corners using silicone to prevent leakage. In addition, a debonding agent was applied on the interior surfaces of the formwork to prevent concrete sticking and easy disassembly of the specimens. The formwork was initially placed on a level surface and first layer of SFRC was poured and vibrated thoroughly to ensure even distribution of concrete. In the next phase, the core was placed on top of first concrete layer and aligned properly. At the end, the last layer of concrete was poured and vibrated again as shown in Figure 7-4. During the casting of panel, it was noticed that the vibration of top layer of concrete was difficult owing the damping properties of recycled tyre crumb. The specimens were left in open to dry for a day and later placed under shaded area for 28 days curing.



Figure 7-4 Formwork and casting of panels

7.4 Flexural bending

7.4.1 Test setup

The test setup for flexural bending was built up using a strong steel reaction frame, 500 kN steel hinges, 550 kN hydraulic jack (SPX-RD5518), 200 kN load cell, 1500 kN load spreader, end plates and end supports. For the test setup, the steel hinge was initially bolted to the reaction frame at one end while load cell was attached to its other end. Afterwards, the load cell was connected to the hydraulic jack and load spreader beam to apply the line load at two points as shown in Figure 7-5.

To place the specimen in horizontal position, end supports were used at both ends. Subsequently, the rotating plates were installed on top of these end supports plates to allow rotation and restrain translation in any direction. Before the testing each specimen, the top surface of rotating plates was levelled by applying gypsum plaster. For the test, the length of pure bending region was 400 mm, whereas the length between end support and the applied load was 250mm. All panels were tested in horizontal position.

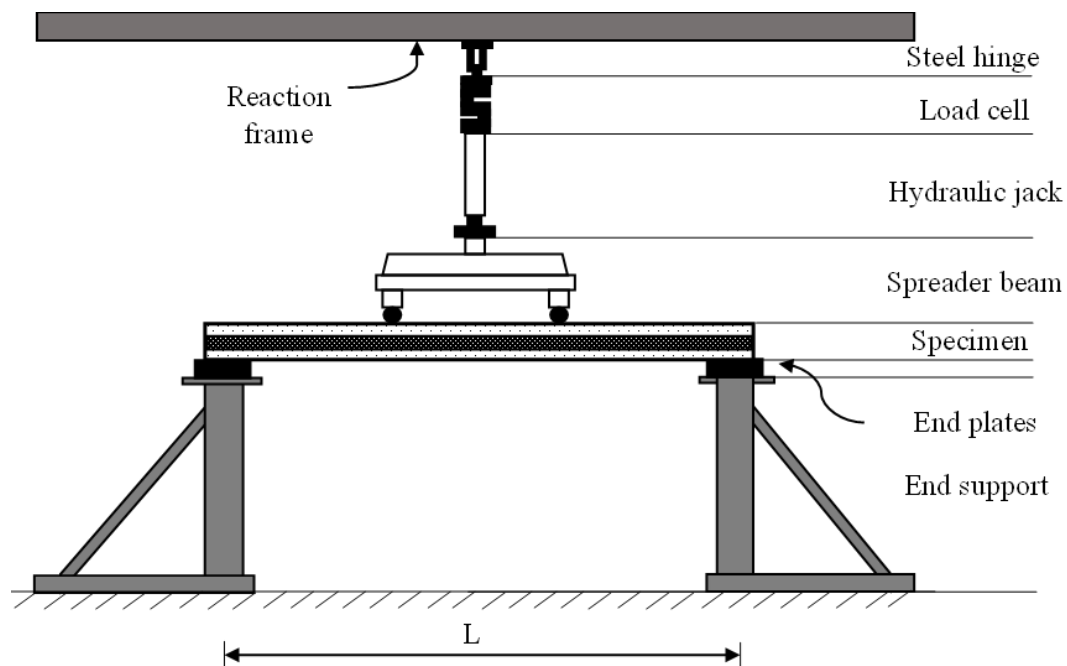


Figure 7-5 Flexural bending test setup

7.4.2 Instrumentation

To monitor deformations including displacements and variations in strain, linear variable displacement transducers (LVDTs) and strain gauges were installed on the panel. A total of five LVDTs were used, in which two LVDTs (L1 and L5) were placed on the end supports, two LVDTs (L2 and L4) were used under the applied load and the last LVDT (L3) was placed at midspan. Similarly, 60 mm long strain gauges with gauge resistance $120 \pm 0.3 \Omega$ and gauge factor of $2.13 \pm 1\%$ were installed at the top (S1) and bottom (S2) surface of the panel. The location of LVDTs and strain gauges is presented in Figure 7-6. Before the installation of strain gauges, the concrete surface was cleaned and levelled using a sandpaper. CN-E (concrete, mortar) adhesive was used to attach the sensors to the concrete surface. A data acquisition system (HBM Quantum X) was used to record and store the relevant data. All the sensors were checked thoroughly for accuracy before the test.

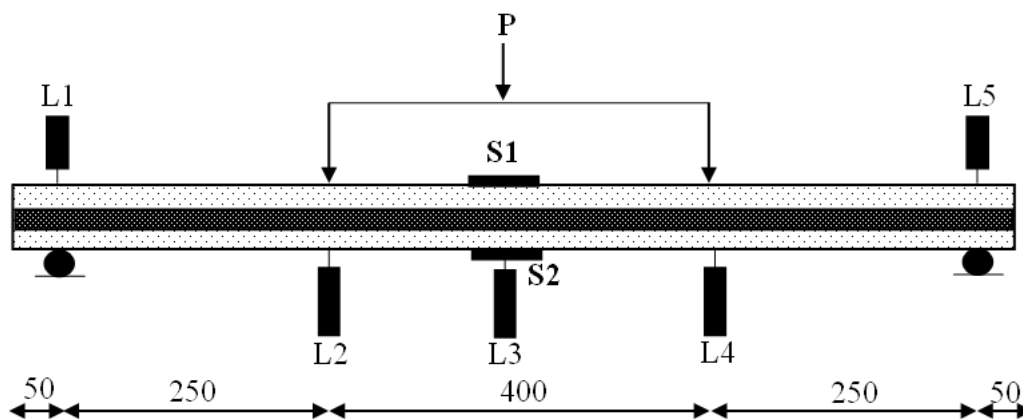


Figure 7-6 Instrumentation of flexural bending test – location of LVDTs and strain gauges

7.5 Uni-axial compression test

7.5.1 Test setup

The compression test setup consisted of 500 kN hinge, pressure transducer, 550 kN hydraulic jacks (SPX-RD5518), 720 mm long spacers and 1500 kN steel section. The setup was designed to apply a concentric load of 1000 kN and built on a strong steel reaction frame having a maximum capacity of 5000 kN. Initially, the top end of both hydraulic jacks was attached to the steel hinges and later, both elements were bolted to the reaction frame while the bottom end of jack was connected to the steel spacers. In the next stage, these spacers were connected to the load spreader through another set of steel hinges. The working of hydraulic jacks and

pressure transducer was monitored before the application of actual load. The specimen was positioned in vertical direction and the bottom end was constrained against translation. The gypsum plaster was applied evenly to the top surface of the specimen to create a level surface. An initial load of 50 kN was applied to examine the working of all instruments. Subsequently, the load was applied continuously in constant increments till failure. Before the test, all specimens were checked for any minor cracks. The test setup designed for uni-axial

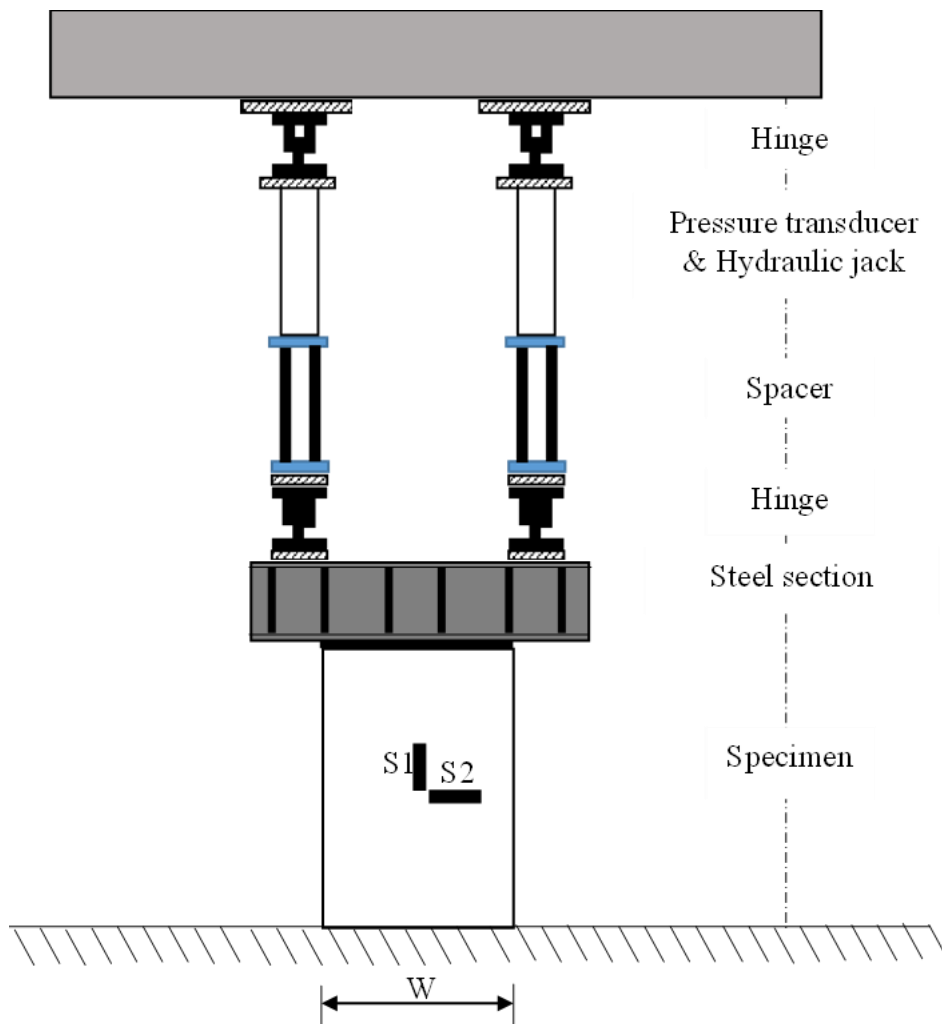


Figure 7-7 Uni-axial compression test setup

compression is illustrated in Figure 7-7.

7.5.2 Instrumentation

In this test, a total of seven LVDTs with a maximum stroke length of 100 mm were mounted to measure the out-of-plane and vertical displacements, in which three LVDTs (L1 to L3) were placed against the front face while other three LVDTs (L4 to L6) were placed against the rear face in horizontal direction. Lastly, one LVDT (L7) was set vertically at the top end of the

specimen. The first set of LVDTs L1 and L4 was placed at a height of 850 mm while the second set (L2 and L5) was placed at 550 mm from the bottom. In the end, the last set of LVDTs (L3 and L6) was arranged at 250 mm (Figure 7-8). Similarly, a total of four strain gauges were attached to the panel. Two strain gauges (S1 and S3) were attached along the height, while other two (S2 and S4) were attached across the width of the panel. All the strain gauges were placed at the centre of the panel (500 mm from the bottom end) as previously shown in Figure

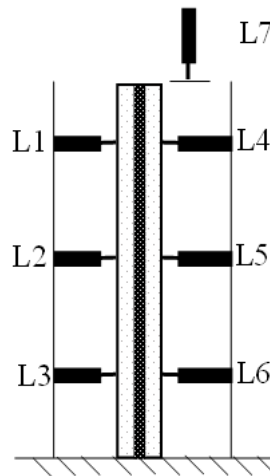


Figure 7-8 Instrumentation of compression test – location of LVDTs

7-7. A similar procedure, as mentioned earlier, was followed to install and connect the sensors to the data acquisition system for storing the data.

7.6 Results and discussions

7.6.1 Flexural bending - load-deflection behaviour

Figure 7-9 presents load-deflection behaviour of both panels at the midspan (L3), in which the load ‘P’ is the total applied force by the load cell. The initial behaviour of both panels was linear elastic, in which the increase in vertical deflection was directly proportional to the increase in applied load. This region follows Hooke’s law and no permanent deformations were observed. The initial stiffness of the panels showed similar trends without any significant variations. At this stage, the vertical midspan deflections recorded were 0.99 mm and 1.07 mm for panel-I and II. However, in the next phase, the structural behaviour of the specimens changed considerably when the initial cracking occurred at 71% of the ultimate load i.e. 14.13 kN and 12 kN for panel-I and II respectively. During this phase, the midspan deflections increased largely with a small increment in the applied load and eventually failed by the development of large flexural cracks in tension zone. The maximum failure loads recorded for

panel-I and II were 19.76 kN and 18.99 kN respectively. The maximum deflections of 11.78 mm and 11.81 mm were measured at the failure. The load-deflection response of panel-II along the span is reported in Figure 7-10 and it can be observed that the vertical deflections in pure

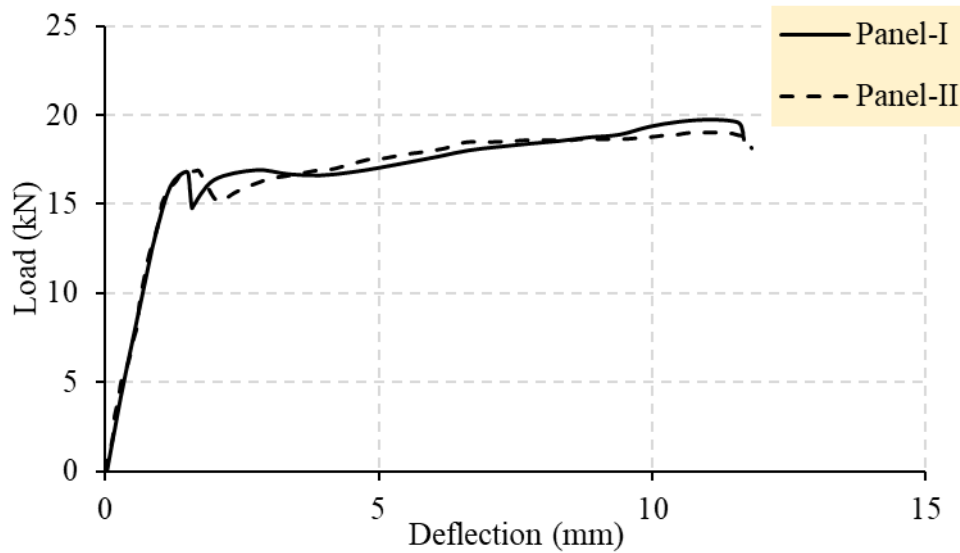


Figure 7-9 Load-deflection response of both panels at midspan (L3)

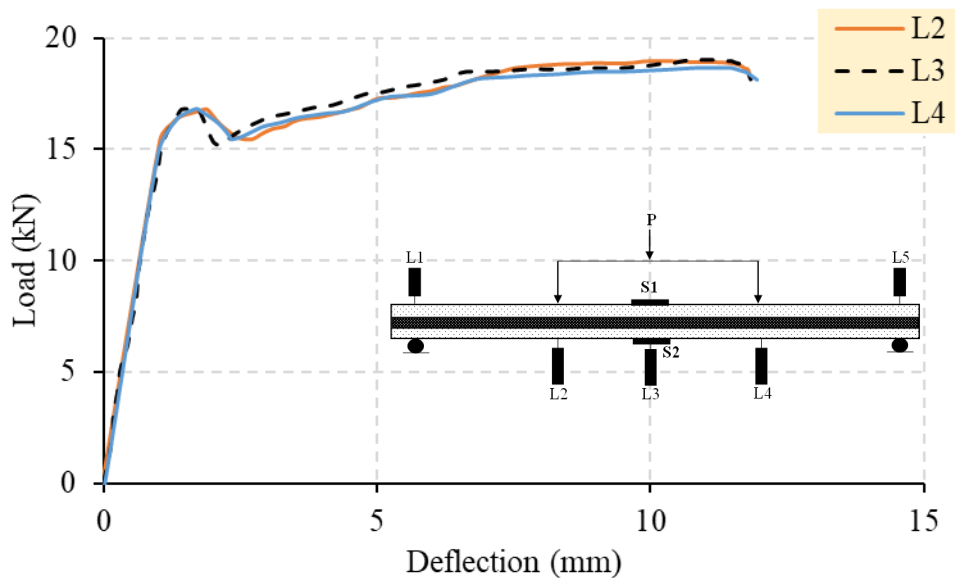


Figure 7-10 Load-deflection response of panel-II along the span

bending region along the span remained the same. The LVDTs (L1 and L5) mounted at each end support did not show any significant data and therefore, validated the fact that no displacement occurred during the test at the end supports.

7.6.2 Strain distribution

The change in strain recorded at the top face (S1) and at the bottom face (S2) of the specimen is presented in Figure 7-11. The strain reported in negative values represents the compression in top wyth, whereas tension in the bottom wyth is highlighted by the positive values of strain. The initial strain in linear elastic region was quite low and proportional to the applied load. In this region, no permanent deformations in terms of strain variation were observed in the panel. However, on further increasing the load, the first cracking occurred in the panel. The strain recorded in compression and tension wyths at the time of initial cracking was 0.000238 and 0.000142 respectively. In the plastic region, the permanent deformations continued with increase in the applied load. Therefore, a non-linear response in terms of strain variations was observed in both compression and tension wyths, which eventually led to the failure of the panel because of significant loss of stiffness. The maximum strain in tension wyth was

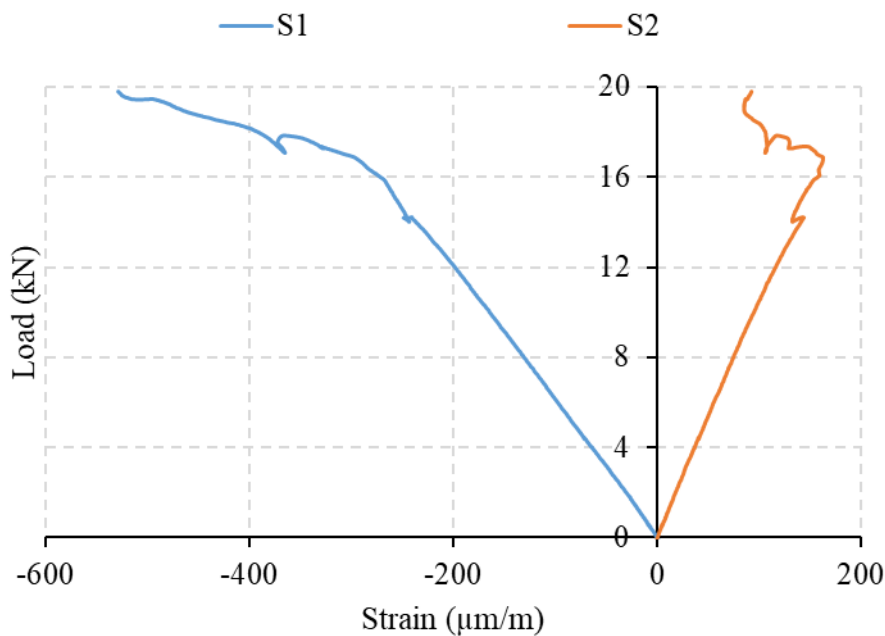


Figure 7-11 Strain variations in the panel at the top and bottom concrete surface

0.000162. Similarly, the maximum strain at the time of failure was 0.000528 (twice the strain at initial cracking) in compression which did not exceed the ultimate compression strain value of 0.0035 (Standards, 2007). Hence, no crushing of concrete was witnessed in the top concrete wyth.

7.6.3 Failure mode

All the panels were checked for any hairline cracks and damage before the test. During the experiment, flexural failure was dominant in pure bending region. The vertical cracks developed in the tension wyth under the applied load. Subsequently, these cracks propagated through the core and ultimately reached the compression wyth at failure. The initial width of these cracks was small but increased significantly on reaching the failure. During the test, it was noticed that the cracks also travelled across the entire width of the panel and were symmetric. Moreover, the entire depth of the panel contributed in resisting the applied load. Finally, the failure occurred due to the significant increase in crack widths as shown in Figure 7-12. It is important to point out that no crushing of concrete under the applied load was observed. The experiment was finally stopped when large deformations were observed on slight increase in the load.



Figure 7-12 Concrete damage - flexural failure in the panel

In a previously conducted study on flexural behaviour of precast concrete sandwich panels containing recycled tyre crumb, similar formation of cracks was observed in CRSP (Awan & Shaikh, 2021b). However, in this study few numbers of flexural crack developed because of using SFRC in concrete wyths. This is due to the fact that SFRC increased the structural integrity and also, improved the post-cracking behaviour of the member (Zhang et al., 2022). To conclude, both specimens failed due to the development of large cracks in the bottom

concrete wyth and flexural failure was dominant in CRSP. In addition, no deformation was observed in the core.

7.6.4 Degree of composite action

The degree of composite action is an important technique and categorized into two behaviours (a) composite behaviour and (b) non-composite behaviour. In composite behaviour, the member acts as a single section and allow complete transfer of shear between the two outer wyths, whereas in non-composite behaviour, the two outer wythes acts independently and there is no transfer of shear stresses. Any behaviour which lies between these two categories (0 – 100%) is known as partial composite behaviour.

Pessiki (Pessiki & Mlynarczyk, 2003) used equation I to gauge the degree of composite action (k%) in elastic region, in which experimental second moment of area (I_E) can be defined using initial cracking load (P), elastic modulus of concrete (E_c), length of panel (l), distance between support and load (a) and the relevant deflection (Δ). Equation II is used to estimate I_E in flexural bending.

$$k(\%) = \frac{I_E - I_{NC}}{I_C - I_{NC}} \quad - \quad \text{I}$$

$$I_E = \frac{P a}{24 E_c \Delta} \cdot (3l^2 - 4a^2) \quad - \quad \text{II}$$

In composite behaviour, the second moment of area (I_C) is calculated using the expression III.

$$I_C = \frac{bh_1^3}{12} + bh_1 \cdot \left(\frac{h-h_1}{2}\right)^2 + \frac{bh_2^3}{12} + bh_2 \cdot \left(\frac{h-h_2}{2}\right)^2 \quad - \quad \text{III}$$

Whereas in non-composite behaviour, the second moment of area (I_{NC}) is the sum of second moment of area of each wyth and can be estimated using the expression IV.

$$I_{NC} = \frac{bh_1^3}{12} + \frac{bh_2^3}{12} \quad - \quad \text{IV}$$

Figure 7-13 shows the dimensions required for the calculation of second moment of area. The degree of composite action for both panels is presented in Table 7-5, in which I_C is

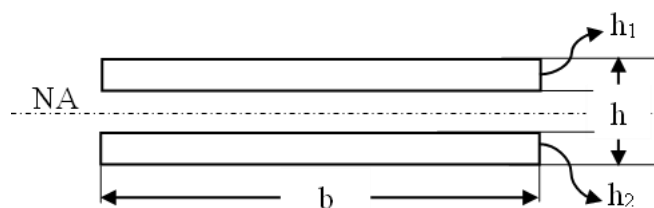


Figure 7-13 Degree of composite action – cross section of the panel

$38.67 \times 10^6 \text{ mm}^4$ and I_{NC} is $5.33 \times 10^6 \text{ mm}^4$. The composite behaviour ranges from 11% to 19% using recycled tyre crumb alone without shear connectors which in fact is better than Pessiki. In his research, a composite action of 5% was reported, when expanded polystyrene was used as a core material without shear connectors. To enhance the composite action of the sandwich panels, latest techniques can be implemented for complete transfer of shear load. One of the effective connectors developed are carbon fibre reinforced polymers and its use has sufficiently improved the composite action to a great extent (Frankl, 2008; Sennour et al., 2013).

Table 7-5 Degree of composite action at initial stiffness stage

Type	Load (kN)	Deflection (mm)	I_E ($\times 10^6 \text{ mm}^4$)	k (%)
Panel - I	14.13	0.99	11.66	19
Panel - II	12	1.07	9.16	11.5

7.7 Uni-axial compression

7.7.1 Load deflection behaviour

Figure 7-14 presents uni-axial compressive response of both panels in terms of axial load-deflection relationship. In this test, two panels were tested, in which the total applied load (kN) is denoted by 'P' and applied through two hydraulic jacks. Similarly, LVDT - L7 recorded the vertical deflection on top of the panel. In the preliminary phase of loading, the deflection was proportional to the compressive load and increased linearly. However, a slight variation in initial stiffness was observed in the members owing to the difficulty in achieving the precise alignment of recycled tyre crumb. Consequently, the difference in member's stiffness continued to increase after the appearance of first crack. On increasing the applied load, excessive cracking occurred near the top end of the panel and failed abruptly. Both panels resisted a maximum axial load of 799 kN. In this case, the maximum deflections of 4.76 mm and 5.11 mm was recorded in panel-I and II respectively at ultimate failure. Due to brittle failure of both panels, it was hard to exactly determine the first cracking load of both panels.

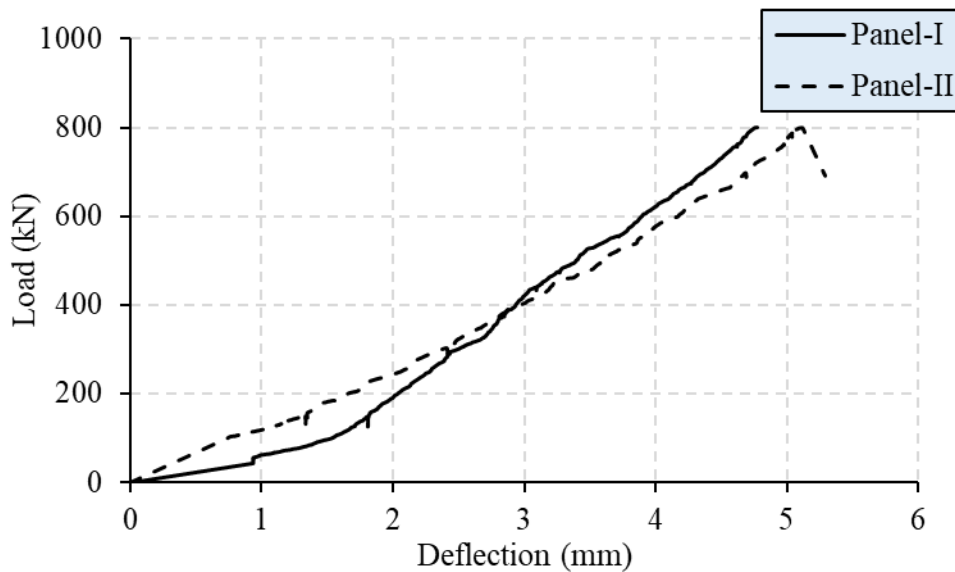


Figure 7-14 Load-deflection response of both panels in uni-axial compression (L7)

7.7.2 Out-of-plane displacement

The out-of-plane displacements were recorded at three locations along the height of the panel as shown in Figure 7-15. In this figure, the positive and negative signs denote the front and rear face of the panel. Similarly, each graph line represents out-of-plane displacements measured at different axial loads. The deflections (L3 and L6) measured near the bottom end of the panel were low throughout the test and clearly indicated that there was no translation near the bottom support. In the early stage of axial loading, the lateral displacements measured were below 0.5 mm at front face (L4) whereas rear face (L1) deflected more than 1 mm at a load of 400 kN. Therefore, it is apparent from the figure that these deflections were not symmetric owing to the alignment issue. A significant increase in lateral deflections were observed near the top end of the panel when load increased beyond 600 kN. At failure load of 799 kN, the maximum deflections of 1.46 mm and 1.43 mm were recorded at front and rear face of the panel. To summarize, both panels did not experience significant out-of-plane deflections when compared with the recent research study on recycled tyre crumb rubber sandwich panel (Awan & Shaikh, 2021a). The probable reason could be the short height of the panel and addition of steel fibres in concrete.

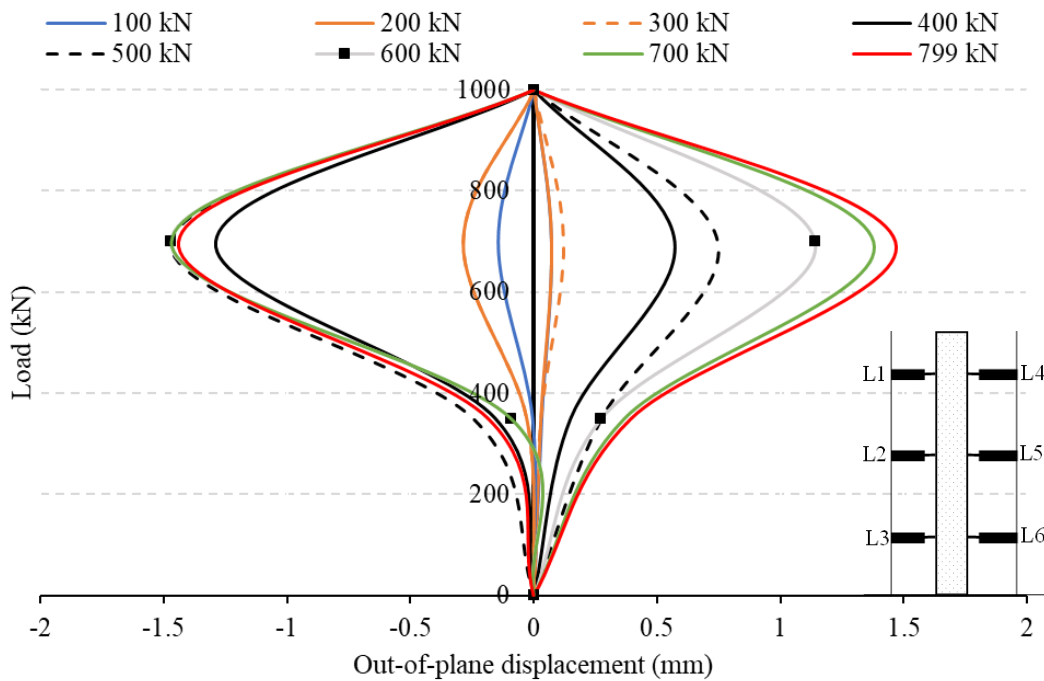


Figure 7-15 Out-of-plane displacement along the height of the panel

7.7.3 Strain distribution

The strain variations along the height (S1 and S3) and the width (S2 and S4) were measured at mid height of the panel. The compression and tension in the panel is defined by negative and positive values as demonstrated in Figure 7-16. It can be observed that all strain variations along the height were negative values which typically represented pure compression in the panel. A maximum compression strain of 0.000604 was recorded in S3 while S1 showed a minimum compression strain of 0.000144. Therefore, failure was conspicuous in one concrete wyth than the other due to the uneven distribution of compressive strain. Similarly, slight tensile strain was noticed across the width of the panel. In this case, the maximum values recorded by S2 and S4 were 0.000008 and 0.000092 respectively. Since the tensile strain is below the range of 0.0001 - 0.0002, hence no significant tensile cracking was witnessed at the centre of the panel.

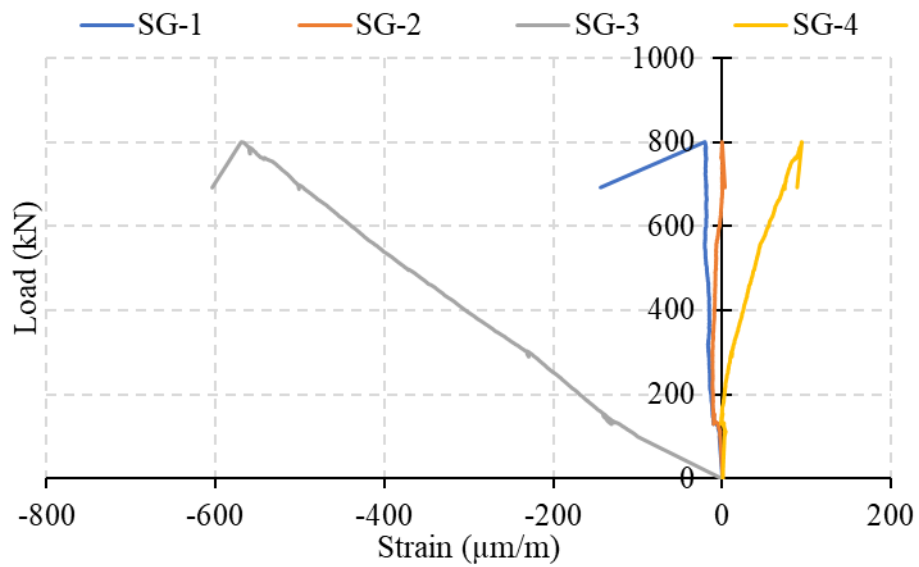


Figure 7-16 Strain variation in the panel under compression

7.7.4 Failure mode

During the test, all cracks and damages were clearly observed and recorded. Figure 7-17 illustrates the actual concrete damage in the panel at ultimate load. At early stage of loading, the panel behaviour was linear elastic thus no cracking was observed. However, the excessive



Figure 7-17 Concrete damage under compression at ultimate failure

cracking occurred near the top end of the panel when applied load reached the failure. The panel collapsed owing to the increase in compressive strain by concrete crushing. After the test, it was noticed that these cracks did not travel far along the height of the panel. However, the cracks propagated across the entire thickness of the panel which indicated that the full thickness of the panel provided resistance against the applied load. Also, no tensile cracking or crushing of concrete was witnessed near the bottom end of the panel. This type of failure in terms of formation of cracks is typical in all precast concrete sandwich panels.

7.8 Conclusion

This study presented the structural behaviour of precast steel fibre reinforced concrete sandwich panel containing recycled tyre crumb rubber as core. The specimens were tested under flexural bending and uni-axial compression. A total of four specimens were manufactured using 60mm long steel fibres and tested experimentally. The main objective of this investigation to study the failure mode of sandwich panels containing recycled tyre crumb when steel fibre reinforced concrete is used as compared to conventional concrete with steel mesh. In addition, the results were discussed in context of ultimate strength capacity, deflections, strain variations on concrete face and failure mode. The findings of the research are summarized as under:

Flexural bending

- a. In flexural bending, the initial cracking occurred at 71% of ultimate load i.e. 14.13 kN and 12 kN for panel-I and II respectively. Similarly, the maximum failure load recorded for panel-I and II is 19.76 kN and 18.99 kN respectively. In this test, the maximum deflections of 11.78 mm and 11.81 mm were measured at the failure.
- b. No crushing of concrete was observed in the top concrete wyth since the maximum compressive strain of 0.000528 is less than the failure strain of 0.0035. A significant increase in tensile strain in bottom concrete wyth caused the flexural cracking in pure bending region.
- c. Addition of steel fibres in concrete enhanced the structural integrity and improved the post-cracking behaviour of the sandwich panels and resulted in less numbers of flexural cracks.
- d. The degree of composite action at elastic stage was assessed through stiffness method and was estimated around 19% and 11.5%, which indicated a partial composite behaviour.

- e. A low intensity of applied load caused insignificant deformation in recycled tyre crumb core.

Uni-axial compression

- a. In uni-axial compression, the maximum load resisted by both panels is 799 kN. However, slight variation in initial stiffness of both panels was observed owing to difficulty in getting the precise alignment of the flexible core.
- b. The maximum out-of-plane deflections of 1.46 mm and 1.43 mm were recorded at the front and rear face of the panel near the top end of the panel.
- c. A maximum compression strain of 0.000604 was recorded in the rear face (S3) while front face (S1) showed minimum compressive strain of 0.000144. Hence, severe failure was observed in rear concrete wyth as a result of unequal distribution of compressive strain.
- d. The ultimate failure was witnessed near the top end of the panel due to the crushing of concrete. However, no tensile cracking and concrete crushing was observed near the bottom end of the panel.

7.9 Reference

- Awan, & Shaikh. (2021a). Compressive behavior of precast concrete sandwich panels containing recycled tyre crumb rubber core. *Structural Concrete*.
- Awan, & Shaikh. (2021b). Structural behavior of recycled tire crumb rubber sandwich panel in flexural bending. *Structural Concrete*, 22(6), 3602-3619.
- Benayoune, A., Samad, A. A., Trikha, D., Ali, A. A., & Ellinna, S. (2008). Flexural behaviour of pre-cast concrete sandwich composite panel—experimental and theoretical investigations. *Construction and Building Materials*, 22(4), 580-592.
- Benayoune, A., Samad, A. A. A., Abang Ali, A. A., & Trikha, D. N. (2007). Response of pre-cast reinforced composite sandwich panels to axial loading. *Construction and Building Materials*, 21(3), 677-685.
- Benayoune, A., Samad, A. A. A., Trikha, D. N., Abang Ali, A. A., & Ashrabov, A. A. (2006). Structural behaviour of eccentrically loaded precast sandwich panels. *Construction and Building Materials*, 20(9), 713-724.
- Benayoune, A., Samad, A. A. A., Trikha, D. N., Ali, A. A. A., & Ellinna, S. H. M. (2008). Flexural behaviour of pre-cast concrete sandwich composite panel – Experimental and theoretical investigations. *Construction and Building Materials*, 22(4), 580-592.
- Bunn, W. (2011). CFRP Grid/Rigid Foam Shear Transfer Mechanism for Precast. Prestressed Concrete Sandwich Wall Panels.
- Bush, T. D., & Stine, G. L. (1994). Flexural behavior of composite precast concrete sandwich panels with continuous truss connectors. *PCI journal*, 39(2), 112-121.
- Chen, A., Norris, T. G., Hopkins, P. M., & Yossef, M. (2015). Experimental investigation and finite element analysis of flexural behavior of insulated concrete sandwich panels with FRP plate shear connectors. *Engineering Structures*, 98, 95-108.
- Choi, I., Kim, J., & Kim, H.-R. (2015). Composite behavior of insulated concrete sandwich wall panels subjected to wind pressure and suction. *Materials*, 8(3), 1264-1282.
- Choi, K.-B., Choi, W.-C., Feo, L., Jang, S.-J., & Yun, H.-D. (2015). In-plane shear behavior of insulated precast concrete sandwich panels reinforced with corrugated GFRP shear connectors. *Composites Part B: Engineering*, 79, 419-429.
- Davalos, J. F., Qiao, P., Frank Xu, X., Robinson, J., & Barth, K. E. (2001). Modeling and characterization of fiber-reinforced plastic honeycomb sandwich panels for highway bridge applications. *Composite Structures*, 52(3), 441-452.
- Flores-Johnson, E., & Li, Q. (2012). Structural behaviour of composite sandwich panels with plain and fibre-reinforced foamed concrete cores and corrugated steel faces. *Composite Structures*, 94(5), 1555-1563.
- Flores-Johnson, E. A., & Li, Q. M. (2012). Structural behaviour of composite sandwich panels with plain and fibre-reinforced foamed concrete cores and corrugated steel faces. *Composite Structures*, 94(5), 1555-1563.
- Frankl, B. A. (2008). Structural Behavior of Precast Prestressed Concrete Sandwich Panels Reinforced with CFRP Grid.

- Hassan, T. K., & Rizkalla, S. H. (2010). Analysis and design guidelines of precast, prestressed concrete, composite load-bearing sandwich wall panels reinforced with CFRP grid. *PCI journal*, 55(2), 147.
- Hodicky, K., Hulin, T., Schmidt, J. W., & Stang, H. (2013). Structural performance of new thin-walled concrete sandwich panel system reinforced with BFRP shear connectors. *Proceedings of the 4th Asia-Pacific Conference on FRP in Structures*, Melbourne, Australia.
- Kazemahvazi, S., Tanner, D., & Zenkert, D. (2009). Corrugated all-composite sandwich structures. Part 2: Failure mechanisms and experimental programme. *Composites Science and Technology*, 69(7), 920-925.
- Kazemahvazi, S., & Zenkert, D. (2009). Corrugated all-composite sandwich structures. Part 1: Modeling. *Composites Science and Technology*, 69(7), 913-919.
- Kim, J., & You, Y.-C. (2015). Composite behavior of a novel insulated concrete sandwich wall panel reinforced with GFRP shear grids: effects of insulation types. *Materials*, 8(3), 899-913.
- Lameiras, R., Barros, J., Valente, I. B., & Azenha, M. (2013). Development of sandwich panels combining fibre reinforced concrete layers and fibre reinforced polymer connectors. Part I: Conception and pull-out tests. *Composite Structures*, 105, 446-459.
- Lameiras, R., Barros, J. A. O., Valente, I. B., Poletti, E., Azevedo, M., & Azenha, M. (2021). Seismic behaviour of precast sandwich wall panels of steel fibre reinforced concrete layers and fibre reinforced polymer connectors. *Engineering Structures*, 237, 112149.
- Lameiras, R. M., Valente, I., Barros, J. A., Azenha, M., & Ferreira, P. I. d. S. (2012). Fibre reinforced polymer (FRP) connectors for steel fibre reinforced self-compacting concrete (SFRSCC) sandwich panels.
- Naito, C., Hoemann, J., Beacraft, M., & Bewick, B. (2012). Performance and characterization of shear ties for use in insulated precast concrete sandwich wall panels. *Journal of Structural Engineering*, 138(1), 52-61.
- O'Hegarty, R., & Kinnane, O. (2020). Review of precast concrete sandwich panels and their innovations. *Construction and Building Materials*, 233, 117145.
- Pessiki, S., & Mlynarczyk, A. (2003). Experimental evaluation of the composite behavior of precast concrete sandwich wall panels. *PCI journal*, 48(2), 54-71.
- Qi, C., Remennikov, A., Pei, L.-Z., Yang, S., Yu, Z.-H., & Ngo, T. D. (2017). Impact and close-in blast response of auxetic honeycomb-cored sandwich panels: Experimental tests and numerical simulations. *Composite Structures*, 180, 161-178.
- Rejab, M. R. M., & Cantwell, W. J. (2013). The mechanical behaviour of corrugated-core sandwich panels. *Composites Part B: Engineering*, 47, 267-277.
- Salmon, D. C., Einea, A., Tadros, M. K., & Culp, T. D. (1997). Full scale testing of precast concrete sandwich panels. *Structural Journal*, 94(4), 354-362.
- Seeber, K., Andrews, R., Baty, J., Campbell, P. S., Dobbs, J., Force, G., Francies, S., Freedman, S., Gleich, H., & Goettsche, G. (1997). State-of-the-art of precast/prestressed sandwich wall panels. *PCI Committee Report*, 42(2), 33.

- Sennour, L., Lucier, G., & Rizkalla, S. (2013). Structurally Composite, Thermally Efficient Precast Concrete. *Concr Plant Int*.
- Sopal, G. J. (2013). Use of CFRP grid as shear transfer mechanism for precast concrete sandwich wall panels. North Carolina State University.
- Standards, B. (2007). *Structural Use of Concrete: Part 1: Code of Practice for Design and Construction*. British Standards Institution.
- Tomlinson, D. G., Teixeira, N., & Fam, A. (2016). New shear connector design for insulated concrete sandwich panels using basalt fiber-reinforced polymer bars. *Journal of Composites for Construction*, 20(4), 04016003.
- Wadley, H. N. G., Dharmasena, K. P., O'Masta, M. R., & Wetzel, J. J. (2013). Impact response of aluminum corrugated core sandwich panels. *International Journal of Impact Engineering*, 62, 114-128.
- Wu, K., Zhang, Y., Lin, S., Leng, F., & Xu, C. (2022). Experimental study on bearing capacity of steel and steel fiber reinforced concrete composite beams without rebar cages. *Structures*, 38, 1165-1179.
- Xu, Z., Hao, H., & Li, H. (2012). Mesoscale modelling of fibre reinforced concrete material under compressive impact loading. *Construction and Building Materials*, 26(1), 274-288.
- Zhang, J., Wu, Z., Yu, H., Ma, H., & Da, B. (2022). Mesoscopic Modeling Approach and Application for Steel Fiber Reinforced Concrete under Dynamic Loading: A Review. *Engineering*.
- Zhang, P., Cheng, Y., Liu, J., Li, Y., Zhang, C., Hou, H., & Wang, C. (2016). Experimental study on the dynamic response of foam-filled corrugated core sandwich panels subjected to air blast loading. *Composites Part B: Engineering*, 105, 67-81.

CHAPTER 8 CONCLUSIONS AND RECOMMENDATIONS

8.1 Summary

This thesis largely focused on the development of recycled tyre-bale and recycled tyre crumb rubber sandwich panels, in which waste tyres were used as a core material in two different ways. Whole waste tyres were used in the construction of recycled tyre-bale sandwich panels whereas recycled tyre crumb was used as core material in crumb rubber sandwich panels. The structural response of the precast concrete sandwich panels was studied through a series of lab experiments as well as finite element numerical models developed in ABAQUS using concrete damage plasticity model.

The research was divided into two phases. In first phase, the structural behavior of recycled tyre-bale sandwich panels was investigated under different loading conditions. In uni-axial compression, the compressibility of tyre-bale, effect of eccentric loading and severe corrosion conditions in tie-wires were evaluated, whereas in flexural bending the ultimate strength capacity, deformations, concrete failure modes were examined in four-point bending and punching shear load. In addition, the degree of composite action was estimated at elastic stage by initial stiffness method and at failure by ultimate strength approach in flexural bending. In second phase, a precast concrete sandwich panel containing recycled tyre crumb as core was investigated in uni-axial compression, flexural bending and low-velocity impact. Moreover, the mechanical properties of recycled tyre crumb rubber were fully investigated in compression and tension.

Based on the analysis of the results, the significant findings of this research on the development of recycled tyre-bale and recycled tyre crumb sandwich panels are summarized as followed:

8.2 Recycled tyre-bale sandwich panels

- In uni-axial compression and flexural bending, the tyre-bale behaved in non-linear elastic manner, showing no sign of stiffness degradation during the application and removal of load. This elastic response of tyre-bale highlights the significance of reusing/recycling the tyre-bale, when sandwich walls reach their designed service life.
- Steel tie-wires wrapped around the tyre-bale considerably influenced the axial resistance of sandwich panel. The strength capacity of the wall reduced significantly

when severe corrosion conditions were simulated. Hence, it is vital to employ conventional methods to shield steel tie-wires against any kind of corrosion.

- The undulating surface of tyre-bale significantly increased the bond strength between concrete wall and tyre-bale and stayed intact before the failure. Only a slight debonding was observed after the failure.
- In flexural bending, tyre-bale exhibited insignificant compressibility at low load. Subsequently, no failure or damage was observed in the tyre-bale and steel tie-wires.
- In flexural bending, the cracks developed between the applied loads and travelled through the depth and width of bottom concrete wall. The vertical deflection measured before the initiation of first crack was within the defined limits of span/250 as per Australian standards. But a significant increase in vertical deflection was recorded on reaching the failure load. However, no crack/ failure was witnessed in the top concrete wall.
- The structural response of tyre-bale sandwich panel under the punching shear load is similar to flexural bending and followed similar crack lines in transverse direction along width.
- The proposed finite element model can be used in determining the factors affecting the flexural and punching shear strength of the tyre-bale sandwich panel.
- The degree of composite action was poor at the elastic stage by initial stiffness and at the ultimate stage by the strength method. The analysis showed poor composite action. Therefore, it is recommended to employ the latest techniques to improve the degree of composite action in the tyre-bale sandwich wall.

8.3 Recycled tyre crumb sandwich panels

- The degree of composite action was assessed in terms of initial stiffness and ultimate strength. A partial composite behaviour was observed in all sandwich panels by

implementing both approaches. However, the percentage of composite action can be improved, if required, by employing latest techniques available in literature.

- In flexural bending, the failure in all sandwich panels occurred with initiation of vertical cracks between applied loads and propagated towards the core. This was followed by angular cracks appeared between the end support and applied load region and eventually, led to combine shear and flexural failure. All specimen produced large deflections and exhibited a ductile failure.
- In uni-axial compression, due to the low slenderness ratio ($h/t=11$), the failure was governed by the crushing of concrete under the loading plate in all panels. No deformation such as yielding of steel reinforcement was noticed in any of the specimens
- The validation of finite element model was performed using the experimental data and a good agreement between the test and analysis was found. The model accurately predicted concrete damage in bending and could be used for further studies.
- During the low-velocity impact force analysis, crumb rubber sandwich panel generated a low rebounding force in the plastic zone during the impact test and partially absorbed the impact.
- In the analysis of impact force, the precast concrete sandwich panel containing recycled tyre crumb core reduced the first impact deflection by 50% and the permanent deflections by 80%. Similarly, on comparing with foam sandwich panel, the deflections are dropped by 25% at first impact and 45% in the plastic region.
- The strain recorded at the time of first impact is 15% higher in recycled tyre crumb sandwich panel due to low stiffness of recycled tyre crumb core. However, after the first impact it was observed in sandwich panels that the permanent strain decreased in tension as well as in compression. A percentage decrease of 27% and 70% in strain value from first impact to permanent strain was recorded for foam sandwich panel and recycled tyre crumb sandwich panel respectively.

- Severe concrete damage against low-velocity impact was witnessed in solid concrete panel in the form of large crack widths which ultimately led to large deflections and yielding of longitudinal deformed bars also occurred during the test. In the case of crumb rubber panel, the crack width was fairly small since the impact was largely absorbed by the recycled tyre crumb core.
- f. Addition of steel fibres in concrete enhanced the structural integrity and improved the post-cracking behaviour of the sandwich panels and resulted in less numbers of cracks against flexural bending and uni-axial compression. In flexural bending, the degree of composite action at elastic stage was assessed through stiffness method and was estimated around 19% and 11.5%, which indicated a partial composite behaviour.
- The overall results from the research accomplished substantial finding which highlighted that recycled tyre crumb rubber sandwich panels are efficient in context of structural performance on comparing against traditional precast concrete panels. Hence, the proposed sandwich panel offers a realistic alternative to reuse/recycle waste tyre as core material in sandwich panels, which will eventually help in reducing the harmful environmental impacts. In addition, these panels may be employed as structural members in buildings, where traditional precast concrete panels are typically used.

8.4 Recommendation for Future Work

The thesis has discussed the development of recycled tyre-bale and recycled tyre crumb sandwich panels. The technical and engineering aspects about the structural performance of the sandwich panels have been provided in the context of ultimate strength capacity, deformations, strain variations, mode of failures and development of 3D finite elements models. The overall findings of the research exhibit excellent performance of the panels and strongly support the use of recycled tyre-bale and recycled tyre crumb sandwich panels in structural engineering applications. However, owing to the time constraints and limitation of lab equipment, few research topics could not be addressed that can be undertaken to further improve the understanding of sandwich panels under Australian conditions:

- Fire performance of sandwich panels is a vital parameter in the construction industry. The fire resistance of recycled tyre-bale and recycled tyre crumb sandwich panels needs

to be investigated in order to increase the confidence of designers and professional engineers.

- In this research, self-compacting and steel fiber reinforced concrete was used in the construction of concrete wythes. Additional studies can be undertaken by using high-strength rubberized concrete to further improve the impact resistance and structural efficiency of the panels.
- The thickness of the core containing recycled tyre crumb was constant in all the panels however, further research can be carried out by varying the thickness of the core and gauge the structural performance against static and dynamic loads.
- This research relied on existing empirical formulas for calculating the axial strength of the sandwich panels. Therefore, further research can be conducted to develop a theoretical design equation for recycled tyre-bale and recycled tyre crumb sandwich panels.
- The flexural performance of recycled tyre crumb rubber was investigated under four-point bending. In addition, the numerical model can be utilized to perform parametric analysis to determine the effect of different parameters. Similarly, further research can be carried out to study the structural behavior under punching shear load and against shear load.
- In order to promote the large-scale use of sandwich panels in structural engineering applications, further research can be undertaken to understand the thermal and acoustic properties of the panels.
- Another important aspect in the design of sandwich panels is the bond strength between the surfaces. Therefore, additional research can be undertaken to study the bond strength behavior between the core and wythes.

BIBLIOGRAPHY DISCLAIMER

Every reasonable effort has been made to acknowledge the owners of copyright material. I would be pleased to hear from any copyright owner who has been omitted or incorrectly acknowledged.

APPENDIX – I

**COPYRIGHT CLEARANCE AGREEMENTS BETWEEN THE
AUTHOR AND THE JOURNALS**

The appendix contains the permissions from the relevant journals to reuse the candidate's published research work presented in this thesis.

Chapter 2, Article: "Structural behaviour of tyre-bale sandwich wall under axial load in the Journal of Structures"



Structural behaviour of tyre-bale sandwich wall under axial load

Author: Abdul Basir Awan, Faiz Uddin Ahmed Shaikh

Publication: Structures

Publisher: Elsevier

Date: June 2021

© 2021 Institution of Structural Engineers. Published by Elsevier Ltd. All rights reserved.

Journal Author Rights

Please note that, as the author of this Elsevier article, you retain the right to include it in a thesis or dissertation, provided it is not published commercially. Permission is not required, but please ensure that you reference the journal as the original source. For more information on this and on your other retained rights, please visit: <https://www.elsevier.com/about/our-business/policies/copyright#Author-rights>

BACK

CLOSE WINDOW

Chapter 3, Article: “Experimental and numerical study on structural behaviour of tyre-bale sandwich wall under different loading conditions in the Australian Journal of Structural Engineering”

Taylor & Francis Journal Material:

'Abdul Awan & Faiz Shaikh (2021) Experimental and numerical study on structural behaviour of tyre-bale sandwich wall under different loading conditions, Australian Journal of Structural Engineering, 22:4, 299-316, DOI: 10.1080/13287982.2021.1970699'.

Permission to reproduce the above content from our Journal in your Doctoral Thesis to be posted on your University's repository is granted.

We will be pleased to grant permission to reproduce your 'Accepted/Original Manuscript' (please check the embargo: Open access cost finder - Author Services (taylorandfrancis.com) on the sole condition that you acknowledge the original source of publication.

This is an 'Accepted/Original Manuscript' of an article published by Taylor & Francis Group in [JOURNAL TITLE] on [DATE], available online: [https://www.tandfonline.com/\[Article DOI\]](https://www.tandfonline.com/[Article DOI])."

This permission does not cover any third party copyrighted work which may appear in the material requested. Please ensure you have checked all original source details for the rights holder.

Further permission will be required if your thesis is published. (Please see information for sharing your work <https://authorservices.taylorandfrancis.com/sharing-your-work/>)

Thank you for your interest in our Journal.

With best wishes,

Annabel

Annabel Flude | Permissions Administrator

Chapter 4, Article: “Structural behavior of recycled tire crumb rubber sandwich panel in flexural bending in the *Journal of Structural Concrete*”

JOHN WILEY AND SONS LICENSE
TERMS AND CONDITIONS

Apr 26, 2022

This Agreement between Mr. Abdul Awan ("You") and John Wiley and Sons ("John Wiley and Sons") consists of your license details and the terms and conditions provided by John Wiley and Sons and Copyright Clearance Center.

License Number	5291711077950
License date	Apr 18, 2022
Licensed Content Publisher	John Wiley and Sons
Licensed Content Publication	Structural Concrete
Licensed Content Title	Structural behavior of recycled tire crumb rubber sandwich panel in flexural bending
Licensed Content Author	Abdul Basir Awan, Faiz Uddin Ahmed Shaikh
Licensed Content Date	Oct 27, 2021
Licensed Content Volume	22
Licensed Content Issue	6
Licensed Content Pages	18
Type of Use	Dissertation/Thesis
Requestor type	Author of this Wiley article
Format	Electronic
Portion	Full article
Will you be translating?	No
Title	Development of recycled tyre-bale and tyre crumb sandwich panels
Institution name	Curtin University Australia
Expected presentation date	Apr 2022
Requestor Location	Mr. Abdul Awan U4 74 Preston Street Como, Western Australia 6152 Australia Attn: Mr. Abdul Awan
Publisher Tax ID	EU826007151
Total	0.00 AUD
Terms and Conditions	

TERMS AND CONDITIONS

This copyrighted material is owned by or exclusively licensed to John Wiley & Sons, Inc. or one of its group companies (each a "Wiley Company") or handled on behalf of a society with which a Wiley Company has exclusive publishing rights in relation to a particular work (collectively "WILEY"). By clicking "accept" in connection with completing this licensing transaction, you agree that the following terms and conditions apply to this transaction (along with the billing and payment terms and conditions established by the Copyright Clearance Center Inc., ("CCC's Billing and Payment terms and conditions"), at the time that you opened your RightsLink account (these are available at any time at <http://myaccount.copyright.com>).

Chapter 5, Article: “Compressive behavior of precast concrete sandwich panels containing recycled tyre crumb rubber core in the *Journal of Structural Concrete*”

JOHN WILEY AND SONS LICENSE
TERMS AND CONDITIONS

Apr 26, 2022

This Agreement between Mr. Abdul Awan ("You") and John Wiley and Sons ("John Wiley and Sons") consists of your license details and the terms and conditions provided by John Wiley and Sons and Copyright Clearance Center.

License Number	5291711235592
License date	Apr 18, 2022
Licensed Content Publisher	John Wiley and Sons
Licensed Content Publication	Structural Concrete
Licensed Content Title	Compressive behavior of precast concrete sandwich panels containing recycled tyre crumb rubber core
Licensed Content Author	Abdul Basir Awan, Faiz Uddin Ahmed Shaikh
Licensed Content Date	Nov 24, 2021
Licensed Content Volume	0
Licensed Content Issue	0
Licensed Content Pages	17
Type of Use	Dissertation/Thesis
Requestor type	Author of this Wiley article
Format	Electronic
Portion	Full article
Will you be translating?	No
Title	Development of recycled tyre-bale and tyre crumb sandwich panels
Institution name	Curtin University Australia
Expected presentation date	Apr 2022
Requestor Location	Mr. Abdul Awan U4 74 Preston Street Como, Western Australia 6152 Australia Attn: Mr. Abdul Awan
Publisher Tax ID	EU826007151
Total	0.00 AUD
Terms and Conditions	

TERMS AND CONDITIONS

This copyrighted material is owned by or exclusively licensed to John Wiley & Sons, Inc. or one of its group companies (each a "Wiley Company") or handled on behalf of a society with which a Wiley Company has exclusive publishing rights in relation to a particular work (collectively "WILEY"). By clicking "accept" in connection with completing this licensing transaction, you agree that the following terms and conditions apply to this transaction (along with the billing and payment terms and conditions established by the Copyright Clearance Center Inc., ("CCC's Billing and Payment terms and conditions"), at the time that you opened your RightsLink account (these are available at any time at <http://myaccount.copyright.com>).